2018

Agricultural Intensification in the Midwest: Impacts on Regional Surface Humidity

Andrew Hill
Minnesota State University, Mankato

Agricultural Intensification in the Midwest:

Impacts on Regional Surface Humidity

By

Andrew C. Hill

A Thesis Submitted in Partial Fulfillment of the Requirements for
the Degree of
Master of Science in Geography

Minnesota State University, Mankato
Mankato, Minnesota

May 2018

Date: ____4/3/2018____

Agricultural Intensification in the Midwest:

Impacts on Regional Surface Humidity

Andrew C. Hill

This Thesis has been examined and approved.

Examining Committee:

_____

Dr. Martin Mitchell, Chairperson

_____

Dr. Fei Yuan

_____

Dr. Christopher Ruhland

Acknowledgment

I would like to give acknowledgment to all who assisted in making this thesis possible, especially my wife Amanda for her patience and unyielding support throughout this project. You have always supported me full heartedly in all my efforts and this was paramount to my ability to stay focused. I would also like to thank my children Jack and Bailey, you both provided me with simple, yet essential relief during my studies and reminded me that a child's perspective is the purest view, free of bias and external influence. Thank you to my parents, Joan and Spencer, who have strongly supported my involvement with academics in many ways.

I also owe a great deal of my success to my academic committee, especially my advisor Martin Mitchell, who brings exceptionally rare insight to the discipline of geography through his unique personal experience and world views. Fei Yuan, who is very well trained in subjects I will likely never master. Her technical knowledge and practical approach to problem solving is exceptional. Christopher Ruhland, who brought strong domain knowledge of plant biology and provided me full use of his research lab and equipment. He also was an important influence on my academics during my undergraduate years and always urges his students to step out of their comfort zones, which is vital for future success.

Finally, I would like to thank all the geography faculty from whom I took my courses from and all my colleagues, for their instruction, lectures, and friendship provided me invaluable knowledge. Two faculty members in particular, Forrest Wilkerson and Ginger Schmid, deserve separate recognition for their personal support during my studies. If you had not encouraged me to consider pursuing a master's degree, it is doubtful I would be at this stage today. Thank you all!

Abstract

Agricultural Intensification in the Midwest: Impacts on Regional Surface Humidity

By: Andrew C Hill

Department of Geography

Minnesota State University, Mankato

2018

An overwhelming majority of anthropogenic climate change studies have placed emphasis on biogeochemical agents, chiefly carbon dioxide emissions, which operate on a global scale. Fewer studies focus on biophysical factors such as land use/ land cover which operate on a regional or local scale. The impact from biophysical factors will continue to be reinforced with a growing human population and expanding resource demands. Of these factors, agricultural land use represents one of the largest, most extensive, and vital land use allocations.

The U.S. Midwest, dominated by rain-fed corn and soybean agriculture, is a key agricultural region which is lacking in studies exploring climate impacts. Potential increases in soil moisture availability combined with modern agricultural practices has resulted in the anthropogenic elevation of surface humidity and dew point temperature within this region. Commensurate with this change is a modification of surface energy balances resulting in decreased daily temperature ranges from diurnal cooling and elevated nocturnal minimums. Increased atmospheric moisture also has a direct effect on human comfort through a decrease in evaporative cooling capacity.

An updated 61-year regional growing season climatology from 59 NWS first order stations of dew point temperature, minimum/maximum temperature, and vapor pressure deficit provides evidence of land use impacts on regional and local climate factors. Significant increases in dew point (1-2°F), focusing on the Midwest, have been identified. Further, these increases have not been found in the U.S. South which is the typical source region for advected atmospheric moisture into the Midwest, thus indicative of a localized moisture source. Examination of historic USDA agricultural statistics aids in the understanding of potential contributions from land use on surface humidity. Further, 2017 field work provides a current multi-level canopy model of transpiration rates for regionally grown corn and soybeans with considerations for several controlling environmental variables. This has allowed accurate up-scaling to field levels allowing prediction of overall atmospheric moisture contributions at determined mid-day transpiration maximums over the course of the 2017 growing season.

Table of Contents

Table of Figures

Chapter 1: Introduction

1.1 Introduction

The human population continues to grow at unprecedented rates, with global population presently standing at 7.4 billion people, up significantly from 2.5 billion in 1950, or 1.6 billion in 1900 (United Nations 2017). This vast increase in population has been supported by an intensified agricultural system, which in turn is reinforced by population growth in an auto-correlative manor. This has been especially true in the United States (U.S.) Midwest which is often geographically referred to as the Corn Belt, although soybean cultivation has become an important rotation crop which also defines the region. To reach such levels of intensification, the U.S. agricultural system has progressed from a labor-intensive industry employing over half of the population prior to 1890 to a streamlined system with marked mechanical, technological, and biological improvements resulting in incredible efficiency. Presently, only one percent of the population remains as farm workers (Lebergott 1966; USDA 2012). During this period of focused development, crop yields have matched the trend in increasing efficiency with national corn yields increasing nearly 400 percent and soybean yields increasing well over 1000 percent relative to the turn of the 20th century (USDA 2012). In 2012 the U.S. supplied 35.5 percent (313.95 million tons) of total global corn (883.54 million tons) and 35.3 percent (84.19 metric tons) of total global soybean (238.73 million tons) (USDA 2013).

Much of this development has centered on the U.S. Midwest Corn Belt (Figure 1.1) resulting in momentous changes in technology, production efficiency, and land use practices. This assertion is further supported by the fact that overall cultivated land has not increased more than ten percent in the last fifty years, indicating that cropland management practices have a larger effect than expansion (Lobell, Bala, and Duffy 2006). In many instances, land use changes have been often overlooked pursuant to regional and local climate factors.

Figure 1.1 Image of the Corn Belt in Southern Minnesota, note the frequently occurring midday fair weather cumulus formation, photo by author, taken on July 7th, 2017, corn pictured is at V10 growth stage.

Agricultural land use changes can act to modify the surface energy balance by altering albedo and the partitioning of latent and sensible heat resulting in potential

effects on temperature and humidity (Raddatz 2007). The Midwest Corn (and Soy) Belt, located within mid-continent North America, forms a battle ground between competing air masses, most notably maritime tropical (mT) vs continental polar (cP) during summer high-sun season. The region's overall summer climate is largely a result of this air mass competition. Agricultural land use practices in the region are likely impacting the resulting climate with intensified corn and soybean agriculture acting as a potential source of augmentation for local surface humidity. Specifically, corn and soybeans are contributing to increases in surface humidity through stomatal conductance of water vapor and subsequent transpiration into the lower atmospheric boundary layer, thus elevating the dew point and reinforcing a localized greenhouse effect.

1.2 Research Questions

To gain a better understanding of Midwest agricultural land use and its subsequent effects on local and regional surface humidity, a variety of different research questions are addressed:

- What spatial and temporal changes have occurred in observed growing season dew point temperatures across the Midwest to the Gulf Coast over the 61-year (1956-2016) study period?
- How have other associated climate variables changed during this time, including: growing season daily maximum temperature, daily minimum temperature, and atmospheric vapor pressure deficit?

- How has agricultural land use changed over the study period, including: overall yields, yields per acre (production efficiency), planting population rates, and technological advancements?
- Does a potential statistical relationship exist between elevated surface moisture variables and changes in agricultural practices and land use?
- How much moisture are typical corn and soybean fields contributing at midday to surface humidity via transpiration processes at different developmental stages (changing leaf area) throughout the 2017 growing season?
- What effects do environmental conditions have on overall transpiration rates?

1.3 Research Approach

This research has been carried out with a two-part approach with the first part consisting of meteorological data acquisition for a 61-year study period from regional National Weather Service (NWS) First Order Stations (FOS) and subsequent statistical analysis addressing any spatial and temporal changes in several climate variables. Specifically, data collection and analysis were focused on mean growing season dew point temperature, daily maximum temperature, daily minimum temperature, and atmospheric vapor pressure deficit. Moreover, USDA agricultural data were analyzed for relationships between land use, production efficiency, yields, planting populations, and technological advancements. Further statistical analysis was used to provide a possible link between changes in climate variables and agricultural factors.

The second part consists of field work survey measures completed throughout the 2017 growing season in two corn and two soybean production fields located in South

Central Minnesota (Nicollet County). This field work provides a quantification of potential midday contributions to regional boundary layer moisture for corn and soybean agriculture within the northwestern boundaries of the rainfed Midwest Corn Belt. Several variables were examined including overall photosynthetic rates, stomatal conductance, transpiration rates, soil moisture availability, leaf area index (LAI), sunlit vs. shaded canopy leaf fractions, vapor pressure deficit, and weather conditions at the time of survey measurements.

1.4 Study Region Selection

To improve understanding of regional agricultural land use on humidity in the lower atmosphere (boundary layer) and to distinguish these changes from transient air mass influences, two study regions were used (Figure 1.2).

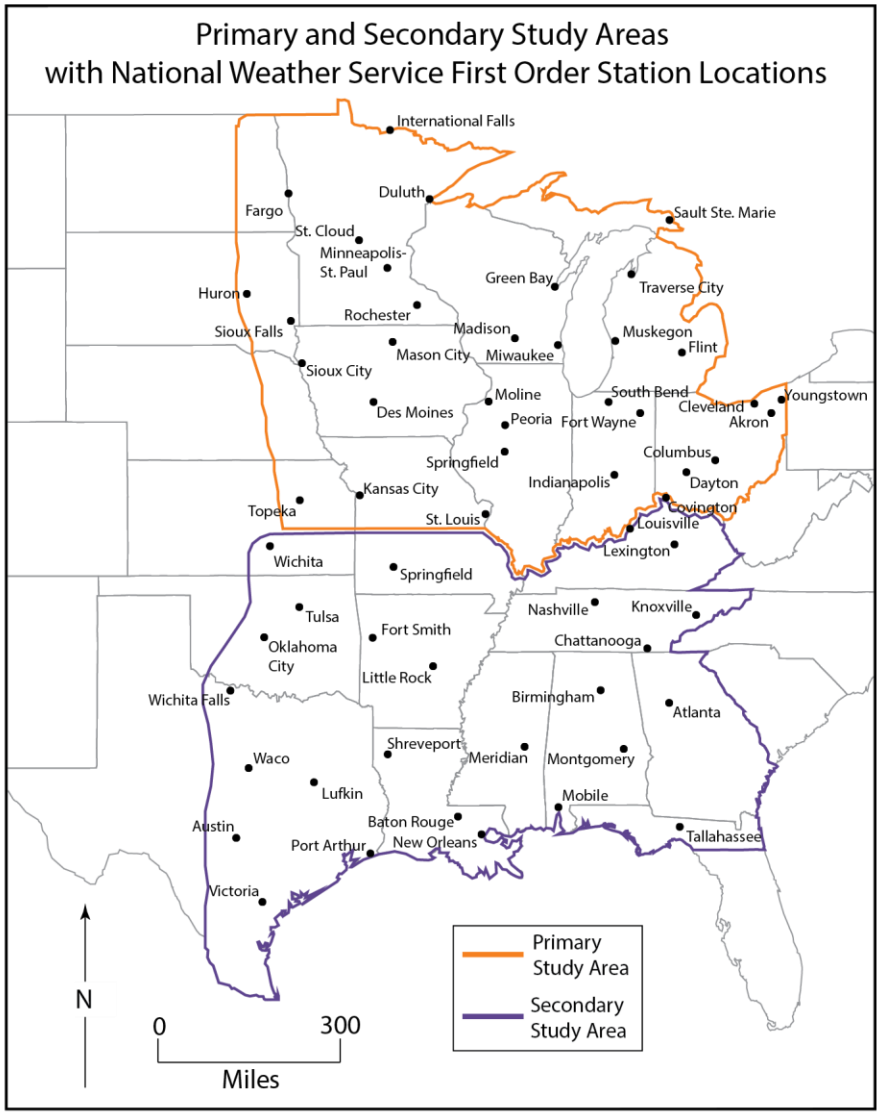

Figure 1.2 Primary and secondary study areas showing locations of National Weather Service (NWS) First Order Stations (FOS).

The primary study region is defined largely by the portion of the Midwest historically referred to as the Corn Belt, including only the portions receiving a majority of necessary water for crop growth from natural summertime precipitation patterns (Figure 1.3) (USGS 2010). This selection has purposefully excluded areas west of the midcontinent 100th meridian, which are often included in modern day definitions of the Corn Belt (Hudson 1994). These excluded areas rely heavily on irrigation practices

which provide a direct and well recognized anthropogenic source of soil moisture and absolute humidity within the boundary layer (Mahmood et al. 2008; Grassini, Yang, and Cassman 2009).

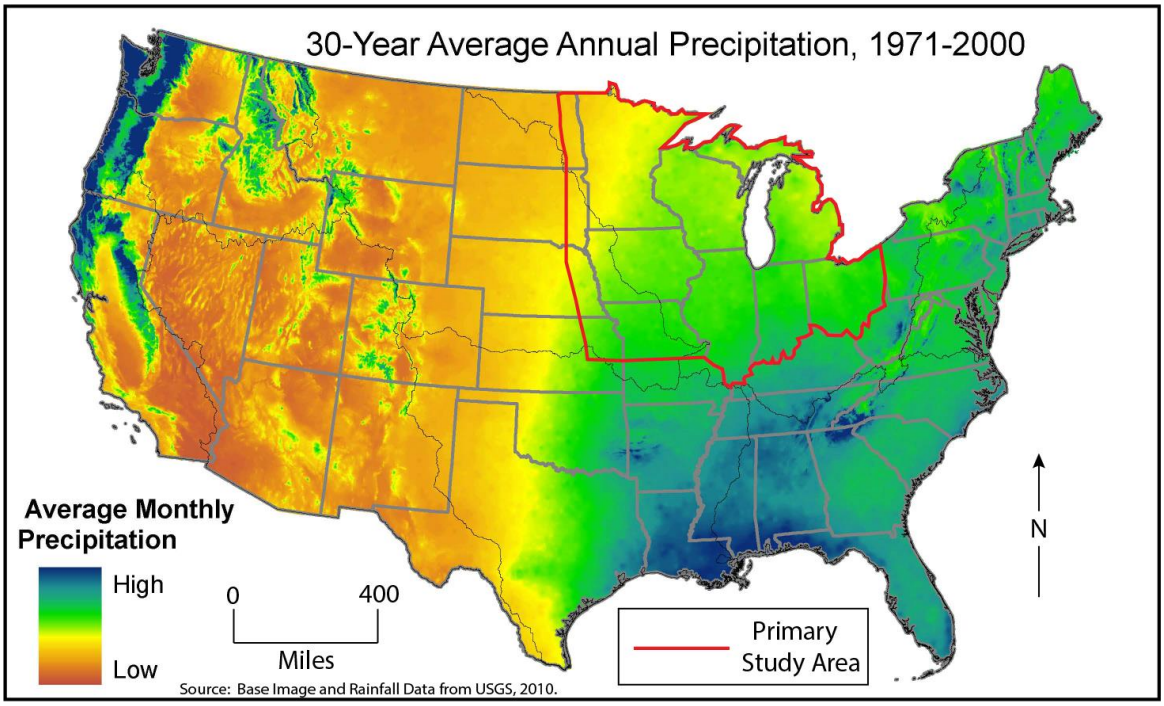

Figure 1.3 30-year precipitation average (1971-2000) within the contiguous United States showing location of primary study area (USGS 2010).

Consequently, this research is directed towards primarily rain-fed corn and soybean agriculture within the Central and Eastern Midwest Corn Belt to better gauge effects from changes in agricultural land use practices and changes in summertime precipitation patterns that may alter soil moisture availability for crop use and increased transpiration. The secondary study region, extending south from the rain-fed Corn Belt to the Gulf Coast, was chosen to gauge any effects from changes in maritime tropical

(mT) air mass humidity in a zone much closer to its source region, prior to its advection into the Corn Belt.

1.5 Conclusion

Examining spatial and temporal changes in dew point temperatures and meteorological variables related to surface moisture relative to changes in Midwest agriculture, provides an improved understanding of potential agricultural land use effects on surface humidity and the overall temperature regime. Field survey measures of corn and soybean transpiration processes during the 2017 growing season yield a clearer picture of potential lower atmospheric moisture contributions delivered directly from intensified Midwest agriculture. The following chapters provide a detailed analysis of these climatological effects within the boundary layer and investigates the evidence of Midwest agricultural practices, specifically the intensification of crop cultivation, serving as a source for a variety of causative climatic factors.

Chapter 2: Review of Literature

2.1 Introduction

People have modified the terrestrial environment with consequent effects encompassing the entire biosphere. One of the most drastic modifications to the natural world, an often-overlooked factor in climate studies, stems from land use change. Over the last 300 years these changes have reached a new maximum with 50 percent of the terrestrial biosphere now utilized for human settlement and agriculture (Ellis et al. 2010). The cause of this rapid expansion and land use change has been driven by human population growth. Population has been steadily rising since 1700 from around 600 million to around 6.3 billion by the turn of the 21st century due to drastic reductions in infant mortality, prolonged lifespans, and social-economic influences occurring in both developing and less developed countries, which have resulted in the unprecedented doubling of world population within a 40-year period (Turner 1990; Cohen 2003).

This situation forces increased demand for land products such as timber, settlement space, and crops, which encourages an intensification of commodity-based agriculture not only in support of basic human needs, but as a critical component of trade and commerce. For example, contemporary market demands for renewable fuel sources, chiefly ethanol, are expected to increase corn production within the Midwest (Wallander, Claassen, and Nickerson 2011). Developing countries continue to make economic improvements. Their increasing per capita income has elevated demand for meat products, requiring increased grain production for animal feeds (Edgerton 2009). As

demand for agricultural products increases, production goals may be met with two basic approaches: (1) either increased production on existing cropland or, (2) cropland expansion into other areas previously unsuitable or unused for agricultural production (Edgerton 2009; Alexander et al. 2015). The latter often has had more drastic ecological consequences (Secchi et al. 2009). A good example was the Soviet decision under Nikita Khrushchev to expand grain production into the virgin lands (Rowe 2011). More recently, the conversion of vast swaths of Amazon Rainforest into cropland or ranchland has gained attention.

The remainder of this chapter focuses on a literature review pertaining to agricultural history in the U.S. as applied to the Midwest, with a synopsis of modern agricultural technologies. Next, the impact of land use on climate is addressed followed by a separate review of literature pertaining to agricultural land use. Also included, is an overview of Midwest air masses and dewpoint climatologies, along with a summary of corn and soybean stomatal physiology and environmental response factors.

2.2 Agricultural History in the U.S. and Midwest

Origins of agriculture within the U.S. often mirror practices from old world Europe. Settlers used the same tools which they were familiar including draft animals, cultivation devices, and seed varieties (Conkin 2008). Until the 1880's, exports were non-existent on any large scale and farm products were used to supply local markets, often used as a trading commodity. During this early period (1790-1865), American agriculture was largely the center of normal everyday life with 90 percent of the population someway involved in the trade with an estimated 50 percent of all human

labor dedicated to food production (Conkin 2008). This represented an intensified agricultural system, at least within a cultural sense, and likely provided the initial motivations for later improvements to simplify crop production while freeing a dedicated segment of the labor force for other occupational pursuits in the growing industrial sector of the U.S. economy.

Following the initial agricultural practices of colonists and settlers, American agriculture became the focus of extensive policy development and education services. This began in 1862 with the passing of the *Homestead Act* and increased westward national expansion. The *Homestead Act* provided the most valuable agricultural necessity by providing 160-acre plots of land to any man over the age of 20 or 320 acres to a married couple in exchange for an agreement to occupy and cultivate the plot for at least a five-year period (Homestead Act 1862). The program had an instant attraction with over 1.5 million claim applications just nine months after the bills introduction, which eventually led to 270 million settled acres or roughly 10 percent of all modern-day U.S. land (Anderson 2011).

While agriculture had become one of the nation's largest interests, it remained without a major government department or bureau (Duemer 2007). This changed in 1862 with the initial steps taken for the creation of the United States Department of Agriculture (USDA). This legislation was enacted along with a long-sought educational land grant program known as the *Morrill College Act* which provided 17.4 million acres of research land to public universities (Morril College Act 1862; Loss 2012). This was also driven by the newly realized need that the nation's future largely depended upon the education

of its citizens, especially in areas of agriculture and mechanical arts, which at the time was limited to private East Coast institutions (Alan 2004). The system was especially effective in producing a high number of engineering graduates who later redefined the 20th century with their innovations with much of this directly supporting the technological needs of America's progressing agricultural industry (Nienkamp 2010). The land grant agriculture programs were particularly valuable to further development by their extensive experiments of new techniques, equipment, crop types, and varieties which would have been economically prohibitive and risky for the regular farm producer (Alan 2004). The success of the original *Morril Act* was further strengthened in 1980 with the passing of the second *Morril Act*, which provided increased federal funding and expanded education efforts (Brooks and Marcus 2015).

The invention of the steel plow earlier in the 19th century provided homesteaders a means of effectively clearing the tough prairie sod landscape. Tile drains and stream powered dredges allowed for extensive land drainage, particularly in the wet prairie areas of the Midwest, as they did for tole (bulrush) marshes found on the lower Sacramento and San Joaquin Rivers in California (Ingebritsen 2000). Later, engineering and mechanical progress led to the development of steam driven tractors in the 1890's, which were refined by the 1930's with more efficient and reliable gasoline engines. In 1921 there were around 300,000 tractors in use, by 1930 there were 1.2 million (Conkin 2008), and from 1950-1970, 1.7 million more modern tractors were sold (Clampitt 2015). From a regional perspective, tractors outnumbered draft horses in the U.S. Midwest by 1926, whereas in the U.S. South, tractors did not out number mules until 1954.

Other important early innovations include the creation and industrial-scale production of synthetic chemical fertilizers which were cost effective and dramatically increased yields. This was supported by the *National Defense Act of 1916* in which WWI munitions plants were salvaged and repurposed to produce nitrogen-based fertilizers from similar explosive manufacture technologies resulting in a doubling of fertilizer production in the 1940's and an impressive on-farm input application increase of 300 percent (National Defense Act of 1916 1916; Johnson 2016).

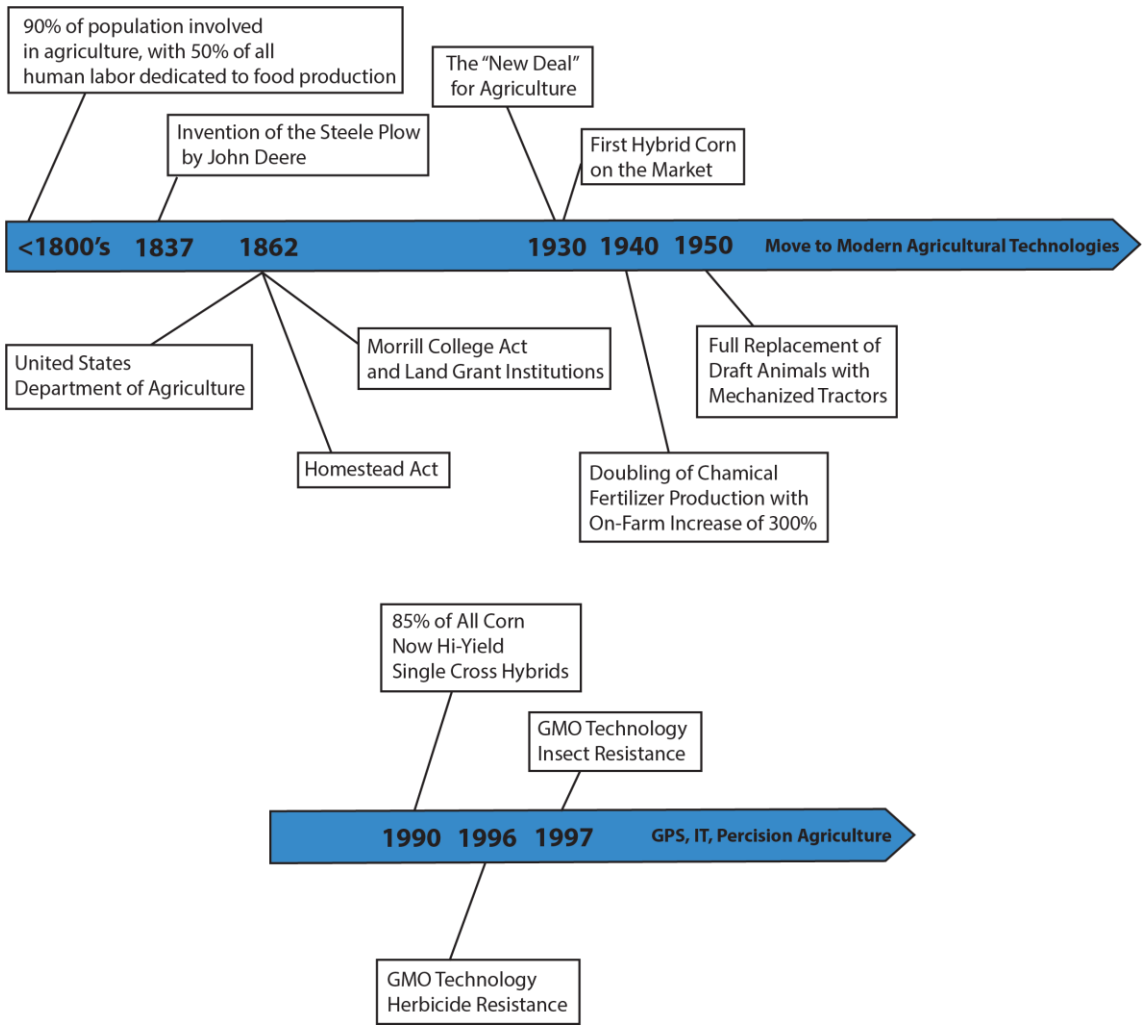

Figure 2.1 Timeline of important developments which supported agricultural intensification within the U.S.

Another necessary reform occurred following the great market crash of 1929, which sought to stabilize commodity market trade prices after agricultural overproduction caused dramatic drops in market shares. The "New Deal" which focused on stabilizing volatile agricultural markets began providing federal subsidies for producers who agreed to periodically take land out of production and kill off excessive livestock in order to reduce the large fluctuations in supply (Fishback, Horrace, and Kantor 2005). During this period, many smaller farms were unable to endure, which ultimately increased the average farm size. Collectively, these developments set the stage for further agricultural progress which became largely driven by private industry and scientific research (Figure 2.1).

2.3 Modern Agricultural Technologies

The incredible increases in production efficiency resulting in consistent and higher yields are the result of changes in both cultural practices and genomic modification through traditional selective breeding techniques and direct genetic manipulation. The former has been the result of extensive classical breeding efforts from both major and minor seed companies. Considering the phenotypic diversity of the domestic dog, classical selective breeding is indeed a powerful tool. These techniques have been the backbone of historical crop development and continue to play a vital role in mitigating negative pressures such as disease susceptibility (Eathington et al. 1993; Staskawicz et al. 1995), flood damage resistance (VanToai et al. 1994), and unfavorable soil conditions (Rao et al. 1993), while adding valuable traits such as reduced flower abortion (Sharma, Dybing, and Lay 1990), increased nitrogen fixation in soybean (Coale,

Meisinger, and Wiebold 1985; Keyser and Li 1992), and nutritional improvement (Ortiz-Monasterio et al. 2007), among countless other traits.

Historically, crop developments have been driven by open pollinated varieties, which lacked the vigor and yield potential of modern hybridized varieties. The first hybridized corn crops were produced in the early 20th century as double cross hybrids, which led to the selection of elite lines that have been further improved by single crossed hybrids, representing 85 percent of all U.S. corn production by 1990 (Bradshaw 2017). By the 1992 USDA *Census of Agriculture*, the collective production efficiency of corn within the Corn Belt states increased 118 percent from 57 to 124 bushels per acre since the 1959 census (USDA 2012). Soybeans, which are native to China, comprise a self-pollinating plant which has resulted in highly inbred lines and reduced overall genetic diversity. A major goal of current soybean breeding has been selection of varieties which have increased oil production traits compared to high protein production found in typical wild type varieties. Soybeans are the source of over half of all oilseed production (Zhou et al. 2015). Overall, soybeans have not seen as dramatic of a per acre yield increase as corn, which may be attributed to the narrow genetic base (Singh and Hymowitz 1999). For example, from 1959 to 1992 soybean yields increased 57 percent from 23 to 37 bushels per acre (USDA 2012).

One such trait, or rather crop culture characteristic, that has largely come about through classical breeding is selection of varieties which possess stress tolerance to increased planting densities. This has been especially true for the corn plant where per plant yield potential has not increased dramatically since the 1930's (Duvick 2005), yet

genetic improvements resulting in better resource allocation, reduced abiotic/biotic stress, and tolerance to higher plant populations has steadily increased corn plant density (Tokatlidis and Koutroubas 2004), resulting in greater yields and production efficiencies. Increasing corn density has been a consistent and linear trend with an average annual increase of around 320 plants/acre occurring each growing season (USDA 2017). This rate has been observed throughout the greater Corn Belt with most states reporting yearly population rates beginning in 1982, with the exception of Iowa, which has been reporting since 1963 (Figure 2.2) (USDA 2017).

This pattern has been less obvious with soybeans but is also increasing due to classical breeding efforts to reduce negative effects of high plant densities. Early studies on soybean plant density indicate a reduction in pod/seed counts in response to higher plant density (Weber, Shibles, and Byth 1966), an effect supported by modern varieties possessing more leaves than needed for maximum yield, thus decreasing lower canopy photosynthesis and lowering yield potentials (Srinivasan, Kumar, and Long 2017). Despite this drawback, pod counts have shown a linear increase of around 22 additional pods/18ft^2 each growing season since 1990 when survey reporting began (USDA 2017). Pod counts provide a proxy for soybean density, as population counts are not typically reported. This pattern has also been consistent throughout the greater Corn Belt (Figure 2.3). Another factor supporting an increase in soybean planting density is lower seed costs, which allows producers to "overplant" what is needed for maximum yield to ensure the best germination rates. Typically yield maximums for soybean are achievable with modest population rates of 101,000-141,000 plants/acre, however actual average rates are

often around 141,000-182,000 plants/acre (Grassini et al. 2014). These increases mark the dramatic improvements which were made possible largely through classic breeding and cultural improvements, prior to direct genetic modification with the commercial introduction of genetically modified organism (GMO) technology in 1996.

The first successful transgene plant was created in the early 1980's with vector mediated gene transfer that most often takes advantage of the naturally occurring soil bacterium *Agrobacterium tumefaciens*, which is responsible for crown gall disease in tree species resulting in large visible gall growths. The Agrobacterium mediated gene transfer has become the most effective plant gene transfer technique used in biotechnology applications along with other diverse bacteria mediated transfers (Guo et al. 2011).

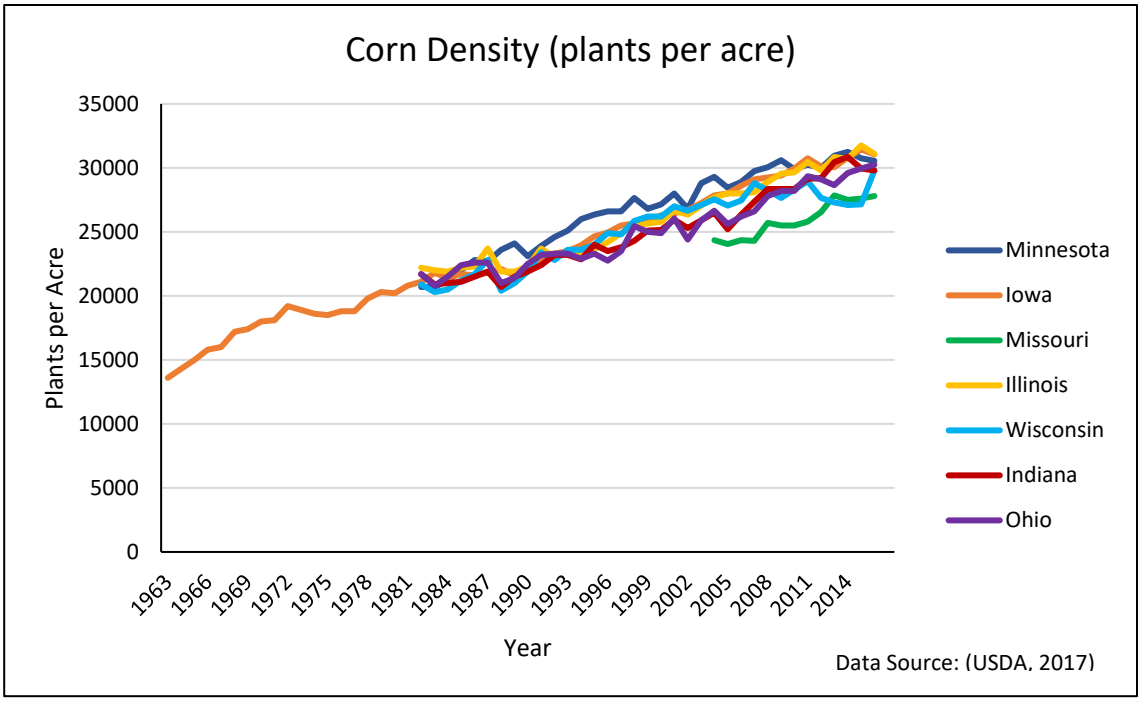

Figure 2.2 Reported corn density within U.S. Corn Belt states 1963-2016.

Many other techniques can be used including the physical method of particle bombardment or the "gene gun" where trait specific DNA coated heavy metals are fired into the cell penetrating the cell wall, resulting in genetic expression of the new traits (Broothaerts et al. 2005). In all cases, modern gene transfer techniques provide a new addition to plant breeding efforts, which seeks to express specific and often novel genetic traits thereby altering phenotypic expression.

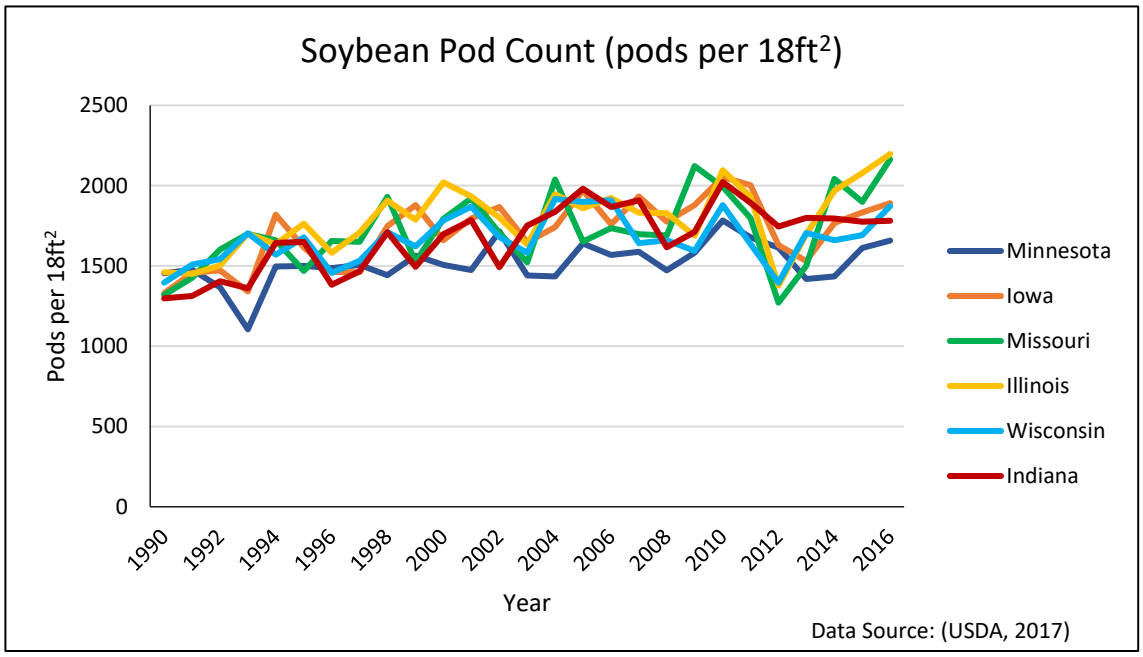

Figure 2.3 Reported soybean pod counts within U.S. Corn Belt states 1990-2016.

Commercially available GMO crop technology was realized with Monsanto's introduction of Round-Up (glyphosate herbicide) tolerant "Round-up Ready" soybeans in 1996 which were quickly adopted with the trait present in over half of all soybeans grown in the U.S. by 2001, and in 77 percent all of global soybean crops by 2009 (Halford

2011). Herbicide resistant corn and cotton followed in 1997, canola in 1999, and sugar beets in 2007 (Brookes 2014). At the time of initial introduction, genetically modified (GM) crops were grown on approximately 4.2 million acres in the U.S. Subsequent adoption of the technology soared globally to over 395 million acres in twenty-nine countries by 2006; making GM crops the fastest adopted agronomic technology in history (Khush 2012). This fast rate of adoption by producers demonstrates the need and value that the modern technology provides and also illustrates the contextual impact of improved global transportation and communication systems.

New traits continued to be developed, such as insect resistant *Bacillus thuringiensis* (Bt) corn varieties, which are geared towards systemic defense of destructive insects like corn borer, rootworm, and earworm (Mannion and Morse 2012). By 2010, Bt corn varieties accounted for sixty-three percent of all corn acres in the U.S., just thirteen years after its initial commercial introduction in 1997 (Fernandez-Cornejo and Wechsler 2012).

The introduction and widespread use of GM crops has indeed accounted for yield increases; however, this effect has been indirect and is largely due to reductions in crop stress pressures such as weed competition and insect damage, allowing for an optimization of crop performance. Producers using standard non-GM crops have also benefited from the "Halo Effect," i.e., an overall reduction in viable pest and weed populations from a lack of suitable agricultural habitat associated with the close spatial presence of other producer's resistant GM crops. This situation parallels success of human disease vaccination campaigns (Mannion and Morse 2012).

Many other improvements driven both by technological developments and continued classical breeding efforts have acted to improve on-farm efficiency and further elevate crop yields. Extensive modern-day breeding programs, which are widely distributed, offer specific varieties regionally adapted to local conditions, along with a hastened turnaround time from breeding program development to commercial availability have become more common. Such developments ensure up to date genetic performance for variable and changing environmental conditions. For example, within the U.S. Corn Belt, a typical turnaround time for a new corn hybrid is about six years with most new varieties only remaining in commercial use for three to four years before replacement, a practice in-part driven by the highly competitive U.S. seed market (Atlin, Cairns, and Das 2017). Other newly developing advances such as geo-spatial information technology and global positioning systems (GPS), form the backbone of precision agriculture, which further reinforces efficiency of production.

2.4 Land Use and Influences on Climate

It has long been recognized that weather and climate processes can have a profound impact on terrestrial ecosystems through variations in incoming solar radiation, temperature, and precipitation (Prentice et al. 1992). Recently, this topic has gained further attention with growing concerns over the potential influences of climate change (Jentsch and Beierkuhnlein 2008; Seddon et al. 2016). While climatic factors indeed play a significant role in both biological and physical earth processes, an often-overlooked question remains. What potential effects do altered ecosystems have on weather and climate processes? These effects can occur through biophysical (water, energy, leaf area

index, stomatal conductance, albedo) and biogeochemical (atmospheric composition) surface fluxes which can have far reaching global effects on circulation and thermodynamics (Foley et al. 2003; Mahmood et al. 2014). These surface fluxes operating on a short-term (biophysical) and long term (biogeochemical) scale, also have a significant impact on weather and climate processes (Pielke et al. 1998).

Anthropogenic land use, often for agriculture and/or settlement, comprises one such example of large-scale ecosystem alteration. In North America, large scale agricultural settlement and land use began relatively recently, around 1700, resulting in a large transformation on the East Coast by 1825, followed by a quickened pace of westward expansion, with land use transformation reaching a stabilized rate by 1930 (Ramankutty and Foley 1999).

Increasing trends in anthropogenic land usage can have important climate implications (Bonan 1997; Pielke et al. 1998; Kalnay and Cai 2003; Mahmood et al. 2014), which act on a regional and local scale (Bounoua et al. 2002; McPherson, Stensrud, and Crawford 2004; Feddema et al. 2005). These effects occur largely through a modification of the surface energy balance (Equation 2.1), which accounts for the fate of net absorbed solar radiation (Q*), derived largely from incoming solar radiation (K↓).

$$Q^* = Q_E + Q_H + Q_G \qquad \text{Eq. 2.1}$$

This Q* is ultimately channeled into three major energy fluxes, namely longwave thermal energy in the form of latent heat (Q_E), sensible heat (Q_H), and ground heat or ground conduction (Q_G). These three variables are flux values representing possible

partitions for net absorbed solar radiation (Q*), with the magnitude and direction determined by atmospheric and land cover conditions. The order of flux variables in the energy balance equation (Equation 2.1) indicates their order of preferred partitioning, given specific environmental conditions. For example, after a rainfall on a warm summer day, Q* loads will be largely transferred into Q_E to be later released during condensation in the upper atmosphere where energy loads are lower. Subsequently, as the surface dries and water is no longer available for evaporation, Q* becomes disproportionally transferred into Q_H which directly causes near surface air temperatures to rise and promotes convectional uplift of surface air parcels. As the surface continues to warm some degree of heat will also be transferred downward into the soil through conductive processes (Q_G), although this flux value is much less significant than Q_E and Q_H. Considering the insignificance of Q_G in boundary layer energy dynamics, Q_E and Q_H can be represented by the Bowen Ratio (Equation 2.2), which provides a quantification of the partitioning between Q_E and Q_H (Oke 1978).

$$\beta = Q_H/Q_E \qquad \text{Eq. 2.2}$$

Therefore, a Bowen's ratio of < 1 indicates a higher partitioning to latent heat which does not directly contribute to any surface warming but provides a source of increased lower atmospheric humidity (Oke 1978).

Other factors also play an important role in determining land use/cover effects on boundary layer climate by directly altering energy available at the surface including albedo and surface roughness (Foley et al. 2003). Any change in albedo will affect

energy available at the surface, alter the energy balance, and will have important effects on the resulting climate. Surfaces with a low albedo are capable of absorbing higher levels of incoming solar radiation, thus increasing available solar energy which is either partitioned into latent or sensible heat depending on surface qualities (non-vegetated vs. vegetated) and moisture availability (Feddema et al. 2005). Surface roughness or the roughness layer represents a disturbed air flow effect, resulting from the physical presence of objects on the surface (cropland, forest, buildings). This region typically extends one to three times the height of ground objects (Oke 1978), and affects the rate of convective heat transfer into the upper boundary layer. A reduction in surface roughness results in reduced sensible and latent heat fluxes and can increase ground heat conductance, whereas an increase in roughness can allow for faster latent and sensible heat flux movement (Wang and Wang 2015).

These land use effects on boundary layer climate can be summarized by Equations 2.3 and 2.4, which show the net radiative fluxes of the energy balance and the water balance, respectively (Pielke 2001). Newly introduced variables of Q_S represent solar insolation, A is albedo, $Q_{LW\downarrow}$ and $Q_{LW\uparrow}$ is down welling and up welling longwave radiation, P is precipitation, E is physical evaporation, T is biological transpiration, RO is run-off, and I is infiltration.

$$Q^* = Q_s\,(1\text{-}A) + Q_{LW\downarrow} - Q_{LW\uparrow} = Q_E + Q_H + Q_G \qquad \text{Eq. 2.3}$$

$$P = E + T + RO + I \qquad \text{Eq. 2.4}$$

It is important to realize that these equations are not independent of one another, but rather a change in one variable will have an effect on the others with the exception of incoming solar radiation which remains relatively constant (Pielke 2001), effected only by cloud cover or atmospheric scattering. For example, if run-off (RO) and infiltration (I) are reduced, more water will be available for evapotranspiration, although common field tile drains will accentuate run-off from heavy precipitation events. Considering a typical agricultural landscape dominated by vegetation, the majority of evapotranspiration contributions come from transpiration (T) (Schlesinger and Jasechko 2014), causing a shift within the energy balance resulting in a higher partitioning of latent heat (Q_E) with a reduction of both sensible heat (Q_H) and ground heat conductance (Q_G). Equations 2.3 and 2.4 can therefore be combined and re-written for a vegetated environment to (Equation 2.5):

$$Q_E = T = P - (RO + I) \qquad \text{Eq. 2.5}$$

Calculation of evapotranspiration may be carried out directly through gas exchange measurements or using a lysimeter, both methods require expensive equipment and multi-variant calculations. It is more common and often more convenient to use an indirect method which relies upon common meteorological data such as the Blaney-Criddle model which utilizes a crop specific co-efficient (K) and a consumptive use factor which accounts for average monthly temperature (t), and hours of monthly sunlight (p) (Equation 2.6).

$$ET = K\left(\frac{tp}{100}\right) \qquad \text{Eq. 2.6}$$

The crop coefficient is calculated from the difference in reference evapotranspiration (open pan evaporation) to the actual transpiration of a specific crop and is also dependent upon local climate, which can limit universal applications (Guerra, Ventura, and Snyder 2016).

Many modeling studies have addressed potential climate impacts stemming from changes in human land use. These studies show an overall cooling pattern associated with temperate latitude agricultural regions from changes in surface moisture and increased energy balance partitioning into latent heat (Bounoua et al. 2002; Feddema et al. 2005; Diffenbaugh 2009). Moreover, temperate latitudes also show increased winter and spring cooling resulting from higher snowpack albedo (Betts 2001). There is also an indication that more drastic changes will occur in tropical areas with deforestation effects and an expected increase in C4 vegetation, which completes normal carbon assimilation with greater water use efficiency, therefore reducing transpiration and increasing partitioning to sensible heat (Betts 2001; Defries, Bounoua, and Collatz 2002). It has been recognized that interactions between vegetation and the atmosphere are complex which severely limits the ability of models to accurately predict these interactions (Angelini et al. 2011).

Fewer direct observational studies exist addressing land use impacts on climate, with most papers focusing on a specific climate factor, such as moisture interactions between the surface and atmospheric boundary layer. Considering rural regions dominate the Midwest landscape, ample soil moisture conditions are especially important when considering possible atmospheric climatic influence (Frye and Mote 2010). These

conditions often do not have a direct effect on local precipitation because precipitation source and sinks often located hundreds of miles apart, transported by air mass advection processes (Brubaker, Entekhabi, and Eagleson 1993). However, increased lower atmospheric moisture supported by soil moisture sources impacts air temperature and daily temperature range through an increased regional greenhouse effect and general overall cloud cover (Trenberth 2004; Angelini et al. 2011)

Urban land use also imparts well recognized climate influence, although these effects are considerably more localized, often only effecting the urban center and small regions downwind (Mahmood et al. 2014). Potential climate impacts are a result of the built-up city structure which acts as a heat source, increases surface roughness from buildings, and provision of impermeable surfaces, which alters the surface water and energy balance. Heat formation, also known as the urban heat island, is the combined result of higher energy balance partitioning into sensible heating from a lack of vegetated surfaces, decreased surface albedo, and anthropogenic heat sources (exhaust, heating, and cooling waste), which causes increased convective uplift and can lead to increased thunderstorm development (Bornstein and Lin 2000; Dixon and Mote 2003). Surface roughness affects mixing abilities, delaying dispersion of heat, aerosols, and other pollutants into the upper boundary layer (Arnfield 2003). The water balance is affected by both the lack of vegetation and plentiful surface impermeability which reduces potential water storage, evapotranspiration, and leads to increased run-off (Grimmond and Oke 1986).

These studies, among others, show that land use factors indeed play a significant role in the resulting local/regional climate. The relationship between land use and climate is dynamic with each exerting potential influence among one another. It is a likely assertion that over the long term (millennia) climate and global circulation patterns play a larger role in land use determination, while over the short term (decades) anthropogenic land use may play a major role in modifying climate at the local/regional scale. The largest portion of anthropogenic land use is agriculture (McPherson and Stensrud 2005), which often requires: (1) drastic land use change from existing native vegetation; and (2) large expanses of acreage to support growing market and economical demands. Globally around 36 percent of the terrestrial non-glaciated earth is used for managed cropland or pasture (Desjardins, Sivakumar, and de Kimpe 2007). It is likely that within these regions dominated by vegetation or agriculture that soil moisture and vegetative/crop transpiration plays a significant role in potential atmospheric influence, especially when extremal airmass influences are at a minimum or when the regional landscape can arrest the temperature and/or moisture characteristics with an advected external air mass.

2.5 Agricultural Land Use and Climate Effects

Agricultural land use represents a system in which surface-atmosphere interactions take place primarily through vegetation. Many present day agricultural regions were historically dominated by natural vegetation which adapted to local conditions over many thousands of years. These historic vegetation-atmosphere interactions were not hastened by human progress, but possessed the requisite time scales

for mutual adaption to one another. The influence of anthropogenic agricultural land use, on the other hand, represents an abrupt transition in land surface properties with technological advances allowing for extensive spatial expansion.

Conversion from natural pre-settlement vegetation often results in overall cooling with an increase in surface albedo from short, homogeneous crops (Bounoua et al. 2002), and an energy balance dominated by latent heat which has a direct impact on humidity (Raddatz 2007). This cooling effect is strengthened by upper atmosphere reflectance (K↑) from increased cloud formation (Trenberth 2004), with clouds over agricultural regions forming earlier and persisting longer than with other conjoining land use types or border areas (Adegoke, Pielke Sr, and Carleton 2007). This parallels findings of Yuan and Michell (2014) with later growing season (September-October) temperatures clearly reflecting higher cloud cover, although cloud cover data was not available for this study (Yuan and Mitchell 2014).

Increased partitioning into latent heat through the evapotranspiration of water is responsible for a reduction in overall surface heating. Within highly vegetated systems the bulk of evapotranspiration finds its source from biological transpiration, at a minimum, accounting for two thirds of overall land-atmosphere moisture flux (Jasechko et al. 2013; Schlesinger and Jasechko 2014), although this contribution can be much greater depending on moisture availability and vegetation types. The degree and direction of this flux partitioning relates to soil moisture availability, dominate wind patterns, and incoming solar radiation loads. This effect is often more pronounced over agricultural cropland, thus leading to reduced diurnal cooling and a suppression of daily

temperature range (DTR) (Bonan 2001; Lobell, Bala, and Duffy 2006; McPherson, Stensrud, and Crawford 2004; McPherson and Stensrud 2005; Yuan and Mitchell 2014).

Increases in nocturnal minimum temperatures (Yuan and Mitchell 2014), also fits with a pattern of enhanced greenhouse warming by water vapor within the boundary layer, albeit increased cloud cover aloft (a form of water vapor) also factors into this trend (Dai and Trenberth 1999; Karl et al. 1993). In either case, nocturnal radiative losses are minimized. This overall trend of increased latent heat partitioning occurs over many other parts of the U.S. experiencing increased atmospheric moisture (Dai and Trenberth 1999; Kalnay and Cai 2003), with the agriculturally intensive Midwest being no exception (Bonan 1997; Bounoua et al. 2002; Diffenbaugh 2009). An increase in latent heat flux can have a significant impact on atmospheric energy sources which can act to fuel convection and precipitation events and has a direct effect on surface humidity and dew point temperatures (Tsvetsinskaya, Mearns, and Easterling 2001; Raddatz 2007). Increases in atmospheric water vapor can have other important climate implications since water vapor is the most potent/dominate greenhouse gas (Held and Soden 2000; Cess 2005), which absorbs infrared radiation over a much broader range than CO_2 and represents a strongly positive feedback mechanism (Seinfeld 2011).

These climatic effects are most pronounced during the summer growing season in agriculturally rich regions such as California's Central Valley, the Great Plains Wheat Belt, and the Midwest Corn Belt. Of these regions, the Midwest Corn (and soy) Belt is located within a zone of typically ample soil moisture because of summertime precipitation events associated with frontal systems and/or convective uplift. The region

has been the focus of extensive agricultural improvement beginning with early advances during the Green Revolution such as the selection of locally adapted hybrids, university extension services, and technological advancements in mechanization. When combined with more modern developments such as increased planting populations, GMO technology, nutrient management, and data processing, overall production and yields have increased markedly. Midwestern agricultural expansion and subsequent intensification of corn and soybean crops has resulted in a likely anthropogenic increase in regional and local dew point temperatures as a direct result of crop transpiration.

2.6 Midwest Airmass and Dewpoint Climatology

The general pattern of humidity throughout the U.S. has been established as seasonally dependent upon the dominance of a particular air mass (Dodd and Dodd 1965; Robinson 1998; Gaffen and Ross 1999). For example, a decreasing gradient is produced from the warm, sub-tropical Gulf Coast to the intermountain region. This warm, humid maritime tropical (mT) air source influences areas east of the Rockies by advection from the low-level jet and is most pronounced during summer (Figure 2.4) with a more defined and spatially limited gradient in winter (Figure 2.5).

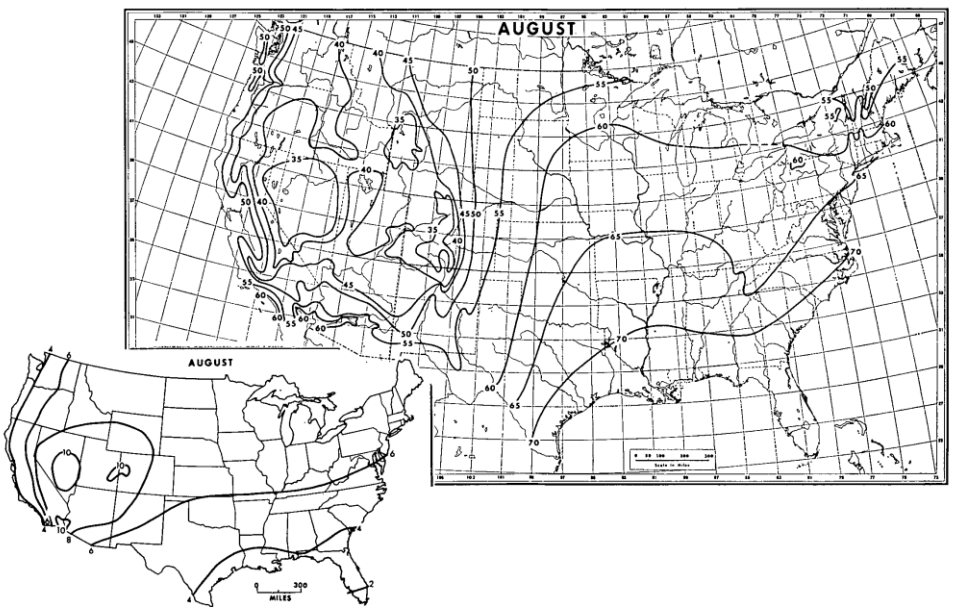

Figure 2.4 General pattern of humidity over the contiguous U.S. in summer (Dodd and Dodd 1965).

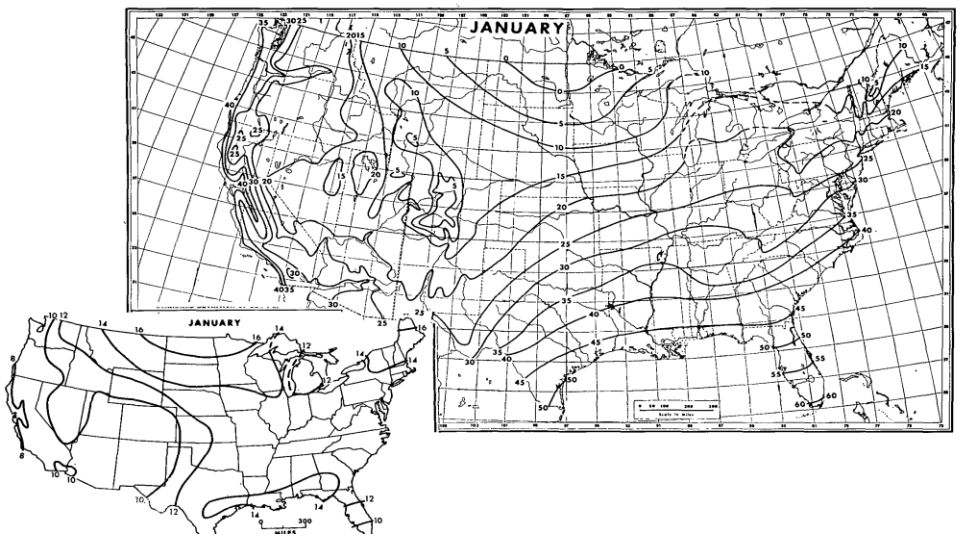

Figure 2.5 General pattern of humidity over the contiguous U.S. in winter (Dodd and Dodd 1965).

Meanwhile, regions west of the Rockies are influenced by modified maritime polar (mP) or maritime tropical (mT) air masses originating over the Pacific Ocean, that occasionally transit into the U.S. Midwest. Finally, continental polar (cP) air masses originating in Central Canada which are characteristically dry, cold and stable in winter, yet warm, modestly humid and neutral in summer completes the list of potential air masses entering the region east of the Rockies. The U.S. Midwest is typically a battle ground between air masses originating in these source regions (Hart and Ziegler 2008).

Among climatic factors influenced by human land use is a modification of lower atmospheric surface moisture resulting in elevated humidity. Surface humidity is directly related to the physical amount of water vapor in the atmosphere, therefore readily available dew point temperature (air temperature at which saturation occurs) provides a convenient proxy measure of atmospheric boundary layer moisture (Sandstrom, Lauritsen, and Changnon 2004). In addition, dew point relates to human comfort, especially when combined with ambient air temperature (Brown and DeGaetano 2013).

The overall pattern of surface humidity within the U.S. is supported by the general air mass climatology with elevated dew point temperatures characteristic of advected mT air. During the summer, growing season dew points are greatest within the immediate mT source region with a diminishing gradient extending northward (Figure 2.6).

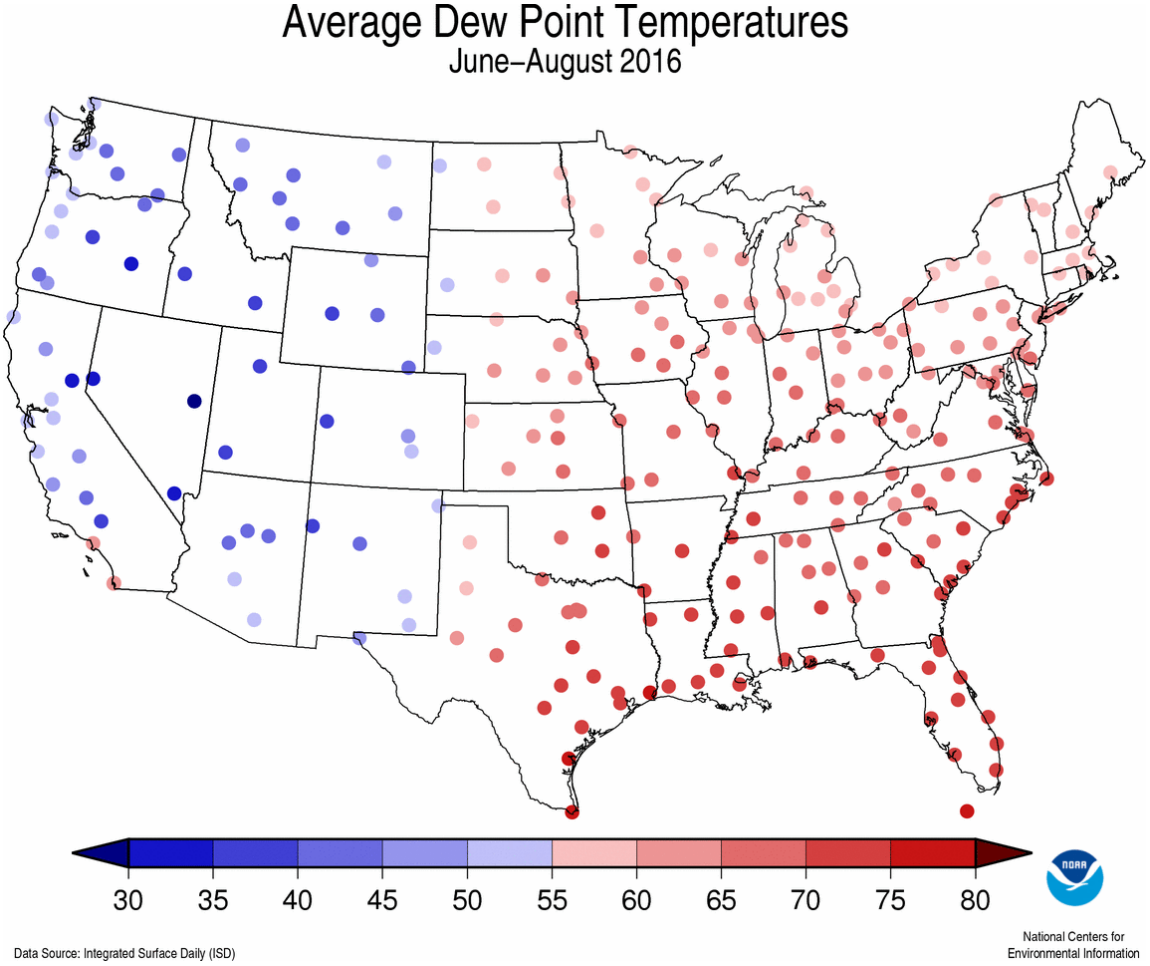

Figure 2.6 Average reported dewpoint temperatures in the contiguous U.S. during summer 2016 (NOAA 2017a).

Regions from the Rockies extending to the Pacific coast are characteristically moderated due to a lack of available surface moisture and cool, coastal conditions influenced by dominate offshore winds. For example, sea surface temperatures off the California or Oregon Coasts average 58°F in summer, a sharp contrast to the 78°F reading in the Gulf of Mexico (NOAA 2017c). During winter months, overall dew points are less significant with lower temperatures unsupportive of considerable moisture holding capacities.

Through the work of several dew point climatologies which examine temporal trends, there has been a significant increase identified (Knappenberger, Michaels, and Schwartzman 1996; Schwartzman, Michaels, and Knappenberger 1998; Gaffen and Ross 1999; Brown and DeGaetano 2013). Several other dew point climatologies have focused on the occurrence of extreme dew point events fitting specific parameters, often dew point temperatures ≥ 21-22°C (70-72°F) over a period of several days (Sparks, Changnon, and Starke 2002; Sandstrom, Lauritsen, and Changnon 2004; Changnon, Sandstrom, and Bentley 2006), while others have focused on dew point trends during heat wave events (Kunkel and Changnon 1996; Changnon, Sandstrom, and Schaffer 2003; Vanos, Kalkstein, and Sanford 2015). These studies also show an increase in overall occurrence of extreme dew point events in the latter portion of the study periods, which generally occur post 1980. Finally, Yuan and Mitchell (2014) found that rural Minnesota experienced significant changes in precipitation and nocturnal minimum temperatures which indicated an increase in water vapor in the earth-atmosphere system (Yuan and Mitchell 2014).

Within this collection of climatologies and among others there is speculation of influence from agricultural land use on increasing surface moisture and dew point trends (Kunkel and Changnon 1996; Bentley and Stallins 2008; Brown and DeGaetano 2013; Yuan and Mitchell 2014), with only three observational studies directly addressing this possible contribution from non-irrigated agriculture (Changnon, Sandstrom, and Schaffer 2003; McPherson, Stensrud, and Crawford 2004; Sandstrom, Lauritsen, and Changnon 2004). These studies all focus on historical dew point data sets and include studies on

winter wheat for a portion of Oklahoma (McPherson, Stensrud, and Crawford 2004), periods of high heat in the Chicago metro (Changnon, Sandstrom, and Schaffer 2003), and extreme events in the Central U.S. (Sandstrom, Lauritsen, and Changnon 2004), making clear the need for expanded studies focusing on the entire Midwest, defined by the Corn/Soybean Belt where water balance surpluses generally occur during most of the growing season. There is also evidence that elevated dew point temperatures observed within the Midwestern region are not being significantly influenced due to strengthened maritime tropical air mass incursions and are likely due to a more localized, regional source (Kunkel and Changnon 1996; Sandstrom, Lauritsen, and Changnon 2004; Bentley and Stallins 2008; Brown and DeGaetano 2013).

Enhanced local and reginal dew point temperatures can have a variety of negative impacts including effects on human health and comfort (Gaffen and Ross 1998; Davis et al. 2003; Schwartz, Samet, and Patz 2004; Gao et al. 2014), livestock welfare (Bishop-Williams et al. 2015; Wegner et al. 2016), reduction in evaporative cooling system (AC) efficiency and performance (Sparks, Changnon, and Starke 2002; Changnon, Sandstrom, and Bentley 2006), and an increase in conditions favorable for development of crop and plant disease (Granke and Hausbeck 2010; Clarkson et al. 2014; Xin et al. 2016).

2.7 Corn and Soybean Stomatal Physiology and Environmental Response

Plants have evolved various mechanisms to deal with moisture deficits and arid environments, most notably is the formation of a waxy cuticle which composes the epidermal layer of most leaves. Since plant biochemical processes utilize CO_2 and O_2,

they must still be able to perform some degree of gas exchange. The ultimate pathway for this gas exchange and transpired water vapor out of plant tissue is through pore-like openings located on leaves, referred to as stomata. Stomatal location (adaxial vs. abaxial) and distribution (scattered vs. uniform) varies with a particular plant species. The mechanical functioning is controlled by closely associated guard cells which have a direct control on stomata aperture. This is accomplished, in simple terms, by the guard cells ability to respond to different environmental conditions, swelling and opening during periods of ample moisture associated with high turgor pressure. Likewise, during periods of water stress, these guard cells contract and close stomata in an effort to conserve dwindling water supplies, to prevent desiccation and permanent wilting point, ultimately resulting in plant death. Stomata serve as the connection between the plant and atmosphere, critical for the diffusion of CO_2 into actively photosynthesizing organelles.

There also exists a tradeoff between CO_2 diffusion and water loss to the atmosphere when stomata are open. This loss of water vapor is largely driven by both soil moisture availability and the atmospheric vapor pressure deficit. The former being controlled by precipitation patterns, soil types, and characteristics of vegetative cover. The latter being controlled by pressure gradients from the surface to upper atmosphere, temperature, and boundary layer humidity (Bunce 1997; McAdam and Brodribb 2015).

2.7.1 Carbon Fixation of the C3 and C4 pathways and Response to Ambient CO_2

Corn and soybean stomatal anatomy and physiology have distinct differences. While both corn and soybeans belong to the taxonomic group of angiosperms (flowering plants), corn belongs to the monocot class, *Liliopsida,* while soybeans belong to the dicot

class, *Magnoliopsida.* The corn plant has stomatal openings evenly distributed on both sides of the leaf and contains the novel C4 carbon fixing pathway. Soybean stomatal distribution is skewed such that abaxial (lower) leaf surfaces contain a higher frequency of stomata, with carbon fixation carried out through the more common C3 (Calvin Cycle) pathway. The spatial and biochemical differences between these pathways affect photosynthetic efficiency and overall stomatal response.

The ancient C3 pathway utilized by soybeans likely first evolved from the Cyanobacteria during a geologic time consisting of relatively high atmospheric CO_2 and low O_2 (Shih 2013). The pathway is also very common with 85-90 percent off all plant species exclusively utilizing this cycle (Gerhart and Ward 2010). Under these past atmospheric conditions of high CO_2 and low O_2, the C3 pathway performed very efficiently at carbon fixation, however in response to the decreasing CO_2 and increasing O_2 during the onset of the Cretaceous this efficiency was greatly reduced (Ehleringer et al. 1991; Beerling 2005). The problem arises with the primary catalyzing enzyme rubisco carboxylase/oxygenase. It is important to consider that rubisco is not very selective in the C3 cycle and will just as readily bind atmospheric O_2 instead of CO_2. The enzyme acts as both a carboxylase (carbon fixing) and an oxygenase (oxygen fixing). When O_2 is present along with CO_2 there is a considerable reduction in photosynthetic efficiency as some of the intermediates produced in the C3 cycle are removed when rubisco fixes O_2 instead of CO_2.

This problem is compounded by basic leaf morphology and an environment of hot and dry conditions (plants preform gas exchange by diffusion through stomatal pores

which are physiologically controlled in response to variable environmental conditions). During hot/arid conditions or a reduction in water availability, plants typically close stomata to conserve water loss to the atmosphere through transpiration. Although this conserves water it also confines what atmospheric gases are present within intracellular spaces. As stomata are closed and available CO_2 (and O_2) are used up in the carbon fixation reactions, oxygen is also produced as a photosynthetic byproduct. Consequently, additional O_2 becomes available for rubisco to fix resulting in photorespiration (rubisco acts as an oxygenase) and carbon fixation efficiency dramatically decreases. Some estimates indicate that C3 efficiency dropped by as much as 60-80 percent during atmospheric increases of O_2, placing great physiological stress on this group of plants and likely contributed to forcing the evolution of the novel C4 pathway (Beerling 2005).

The C4 pathway present in corn has been shown to have independently arisen around sixty-six times in response to these conditions through evolutionary processes (Sage, Sage, and Kocacinar 2012). The C4 pathway is able to perform with higher efficiency than the more common C3 pathway under conditions of high heat stress, especially in environments with high solar insolation (K↓) (Still et al. 2003). Although only 2-3 percent of all higher plants possess the C4 pathway its ecological importance is profound accounting for 20-30 percent of all global primary productivity (Ehleringer 2005). It is important to realize that the C4 pathways do not replace the C3 pathway or Calvin Cycle. C4 plants still contain and utilize the C3 pathway for carbon fixation, however the difference comes from the appearance of a new carbon fixing pathway (C4) and a spatial separation between the new C4 and the existing C3.

Significant anatomical difference exists in the leaves of C4 plants (Kranz anatomy), which allows them to concentrate CO_2 into deeper cells, which are not exposed to atmospheric O_2. The C4 pathway is located within cells near the leaf surface (mesophyll cells), that are near the stomatal openings. These cells are exposed to normal atmospheric air consisting of both CO_2 and O_2 (Hopkins and Huner 2004). In the C4 pathway, CO_2 is first fixed by a different enzyme known as phosphoenolpyruvate carboxylase or PEPc. This enzyme has an incredible selective affinity for CO_2 and unlike rubisco in the C3 cycle it will only fix CO_2 even in environments which contain considerable O_2. The first carbon compound produced is a 4-carbon acid molecule known as oxaloacetate. After the production of oxaloacetate from atmospheric CO_2 and PEPc, there is another conversation to 4-carbon malate, which is subsequently transferred from the exterior mesophyll cells into bundle sheath cells located deeper in the leaf. Surprisingly, once malate is in the bundle sheath cells it is converted back into CO_2 and then enters the C3 pathway producing the same products as C3 exclusive plants (Hopkins and Huner 2004).

Consequently, the C3 cycle is now located in an environment with very little or no O_2 present. This situation greatly increases photosynthetic efficiency at higher temperatures as restrictive photorespiration will no longer occur. The C4 system effectiveness at moving CO_2 into the bundle sheath cells containing the C3 cycle results in CO_2 concentrations 10-60 times higher than in the mesophyll cells of a C3 excusive plant (Eldra P. Solomon 2005). Thus, allowing higher photosynthetic efficiency with restricted stomatal apertures resulting from moisture deficits and water stress. Increasing

atmospheric CO_2 reduces stomatal conductance and leads to lower rates of transpiration and overall reduced water use for both C3 and C4 vegetation (Field, Jackson, and Mooney 1995).

2.7.2 Response to Water Status and Light

Plant water status and light levels are of significant importance to stomatal response. Stomatal action represents a feedback mechanism which is directly related to water loss and active photosynthesis. This process is also a "trade-off", as plants diffuse CO_2 to intercellular spaces for carbon fixation reactions, water vapor diffuses out of these same spaces into the ambient atmosphere. Stomatal response to reduced plant water potentials is not as dramatic as restrictions imposed on photosynthetic rate, as other non-stomatal factors seem to carry a greater weight (Zhou et al. 2013). Nonetheless, plant water status and soil moisture availability play a critical role in determining overall conductance potential. The diffusion of water vapor out of stomatal pores is also greater than CO_2 at similar conductance values due to the greater concentration gradient between intercellular (H_2O saturated) values and that of the atmosphere (Hetherington and Woodward 2003; McAusland et al. 2016). Ambient humidity is another important water variable that: (1) plays a role in overall atmospheric demand or vapor pressure deficit (VPD), and (2) impacts the transpiration rate by reducing conductance associated with low humidity or higher VPD (Lange et al. 1971; Bunce 1997).

Stomatal response to light or variable levels of irradiance provides the most often characterized stomatal environmental response which occurs in almost all plant species. The physiological mechanism of stomatal opening relates to the accumulation of

potassium ions and sugars in the flanking guard cells (increasing turgor pressure), which is largely driven by light activated signals (Shimazaki et al. 2007). There is a degree of variability in stomatal action with light activated opening occurring much slower as opposed to shade induced closing. These response rates can also be hastened by a reduction in overall plant water status (Jones 2014). The regulation of the stomatal aperture is likely a result of multiple signaling pathways (Hetherington and Woodward 2003), with the strongest environmental influences being irradiance levels, water status, humidity or VPD, and ambient CO_2 availability.

It should also be noted that stomatal response to environmental changes and recovery to a post response state occur at different rates. Initial response to changes in light, water availability, and humidity occur rapidly, often within seconds, while subsequent recovery is much longer, often on the order of hours, regarding changes in light or humidity, and days regarding changes in water availability.

2.8 Conclusion

Agricultural land use remains a valid explanation for this apparent source of regional moisture. Overall, more water is available in the earth-atmosphere system indicating an intensified hydrologic cycle (Ross and Elliott 1996; Ross and Elliott 2001; Elliott and Angell 1997; Willett et al. 2007). This can act to supplement soil moisture through additional precipitation, which has been found to be occurring within the Midwest (Hest 2014; Yuan and Mitchell 2014). These findings support the assertion that more water vapor exists within the earth/atmosphere system, with much of this potential contribution directly from plant transpiration, as this biological source typically accounts

for 60-80 percent of total evapotranspiration (Jasechko et al. 2013; Schlesinger and Jasechko 2014). Other agricultural practices can also have a potential positive impact on surface moisture include: (1) modern hybrid selection geared towards drought tolerance, which can prove more effective at extracting soil moisture at greater depths and (2) the steady increase in plant populations per acre in all parts of the Midwest driven by higher yield potentials and genetic improvements (Widdicombe and Thelen 2002; Cox and Cherney 2011; Hao et al. 2015)

A clear need remains for reanalysis of the potential effects of agricultural intensification in the Midwest on the modification of regional and local surface moisture as expressed by dew points. Past studies either focused on a localized region or extreme event occurrences. These studies would benefit from extending current data sets into the 21st century, and extending coverage to a larger region, namely the Midwest Corn and Soybean Belt. Moreover, the inclusion of a region bordering the Gulf Coast offers an additional advantage. Since the region is contiguous to the southern bounds of the Midwest, any statistically significant increases in dew point here would indicate a stronger advection of maritime tropical (mT) air from its source region. Meanwhile, the lack of change in dew point or change in dew points along the peripheral boundary of the Midwest, would point to a regional source within the Midwest, assuming increases in dew points are widespread. This study aims to answer this situation.

Chapter 3: Data Acquisition and Methodology

3.1 Introduction

The data collection and methods for this project were divided into two corresponding sections. Part one consisted of meteorological data collected over a historic time series across a large region of the Central and Eastern contiguous U.S. for statistical analysis, supplemented by agricultural census data collected from the Midwest Corn Belt states to gauge major changes in agricultural land use. Part two was based on field data obtained throughout the 2017 corn/soybean growing season within the far northwestern boundary of the rain-fed Corn Belt located in central Nicollet County, southern Minnesota. These field observations were used to construct a model to accurately up-scale individual leaf transpiration rates to represent whole canopy flux values occurring within typical corn/soybean production fields. Overall, the survey measures sought to provide a quantification of lower atmospheric moisture contributions from Midwest agricultural land use while addressing main environmental factors influencing changes and driving moisture flux rates.

3.2 Meteorological and Midwest Agricultural Data Acquisition

Meteorological data were obtained from 59 weather stations distributed within both the primary and secondary study regions (Figure 1.2). 32 stations were located within the U.S. Corn Belt, representing the primary study region and 27 stations located within the Southeastern U.S. extending south to the Gulf Coast, representing the secondary study region. These selections provided a well distributed coverage of the

study regions. Records were collected over a 61-year study period beginning in 1956 and continuing through 2016. This study period was further partitioned into two separate climatic periods consisting of an early (1956-1985) (30 year) and late (1986-2016) (31 year) period. This was done to complete statistical change detection and to provide a means for detecting any temporal changes occurring across the study regions.

One key aspect of the present study was a focus on station selections which were minimally affected by changes in instrumentation, recording procedures, and/or station relocations over the 61-year time series. Several dew point sensing instrument changes have occurred at these stations including a switch from sling psychrometers to lithium chloride hygrothermometers in the 1960's, followed by chilled-mirror hygrothermometers in the late 1970's to mid-1980's, and finally to the modified chilled-mirror devices during conversion to the present day Automated Surface Observing System (ASOS) during the 1990's (Sandstrom, Lauritsen, and Changnon 2004). This resulted in selecting only National Weather Service (NWS) First Order Stations (FOS), where several studies have confirmed data integrity and consistency at these stations through metadata analysis (D. Changnon, personal communication, January 11, 2017) (Gaffen and Ross 1999; Robinson 2000; Sandstrom, Lauritsen, and Changnon 2004).

The primary meteorological data record used to represent boundary layer moisture was dew point temperature, which serves as a good proxy for absolute humidity and therefore provides a direct quantification of near-surface boundary layer moisture. Using Microsoft Access spreadsheet processing, hourly dew point readings spanning a 24-hour period were converted to daily averages, which were subsequently used to calculate an

overall annual growing season average. It was important to consider an entire 24-hour period for average calculations due to climate implications for elevated dew points occurring both day and night. Considering the USDA growing season definition of daily minimum average surface temperatures above 32°F, a five-month growing season (153 days) was used as the data collection period for the Midwest Corn Belt states spanning May through September (USDA-NRCS 2017b). Other meteorological data collected from these NWS FOS included daily maximum and minimum temperature which has a link to near surface atmospheric moisture. The temperature data were also used to calculate an overall annual growing season daily maximum and minimum temperature average. Finally, vapor pressure deficit (VPD) was calculated as an overall annual growing season average utilizing daily average temperature and dew point data based off Teten's Formula (Equations 3.1-3.3) (Murray 1966). Terms within these equations represent actual vapor pressure (ea) and saturation vapor pressure (es).

$$ea = 6.1078^{(17.269 * Tdew) / (237.3 + Tdew)} \qquad \text{Eq. 3.1}$$

$$es = 6.1078^{(17.269 * Tair) / (237.3 + Tair)} \qquad \text{Eq. 3.2}$$

$$VPD = es - ea \qquad \text{Eq. 3.3}$$

VPD is the difference (deficit) between the amount of moisture in the air and how much moisture the air can hold when it reaches saturation (temperature dependent).

When air becomes saturated, water will condense out to form dew or clouds. As the VPD increases, plants essentially draw more water from roots. VPD was calculated to gauge any potential changes in atmospheric demand for water occurring over the study period, thus influencing typical rates of evapotranspiration by creating a larger gradient between the saturated air inside a plant leaf and external ambient atmospheric air. Typically, VPD has a linear relationship to the rate of evapotranspiration. It should be noted that VPD in this study was generated from empirical equations which were created from prior observation-based studies and not derived from physical scientific theory.

Agricultural data were obtained for the selected eight-state U.S. Corn Belt through the USDA *Census of Agriculture*, which is released every four to five years. Records were collected for all twelve census years available within the study period beginning in 1959 and continuing through 2012. Several pertinent records were obtained at the state and county levels, including: total cropland acreage harvested, corn acreage harvested, soybean acreage harvested, corn yield, soybean yield, and calculated yield per acre production efficiencies for both corn and soybean. In Southern Minnesota, where the 2017 growing season field-work took place, these data were collected at the county level (totaling thirty-four counties) for a more detailed examination of temporal changes occurring within the far northwestern boundaries of the rain-fed Corn Belt from the early and late portions of the study period.

3.3 Meteorological and Agricultural Data Analysis

To ascertain any statistically significant changes occurring in near surface humidity within the Eastern half of the contiguous U.S., including the Midwest Corn

Belt, all selected 59 NWS FOS were used for dew point temperature analysis. These data were downloaded from the Midwest Regional Climate Center (MRCC) at University of Illinois, Urbana-Champaign, through the online cli-MATE system. Data management and organization was paramount when working with these inherently large datasets as a typical station carried around 500,000 hourly dew point readings and 44,000 daily minimum/maximum temperature readings for the 61-year study period. Downloaded as a csv file, raw data were stored in Microsoft Excel. Using Microsoft Access, hourly data were processed to calculate daily averages which were then used to derive monthly averages and ultimately an annual growing season average for each station spanning the 61-year study period. This same procedure was used to obtain and edit daily maximum and minimum temperature data. A total of 55 stations with complete records were used.

In all cases, data were processed to arrive at an overall growing season average for dew point temperature, maximum temperature, and minimum temperature. These data sets were then tested by a Shapiro-Wilk analysis to ascertain normality. Once normality was confirmed, the parametric students t-test was applied to the data in IBM SPSS. These growing season averages were then statistically analyzed over the study period time series by applying independent t-tests in IBM SPSS statistical software package. All the dew point and temperature data were used in these analyses including calculated VPD, differentiated between an early (1956-1985) and late (1986-2016) study period with the null hypothesis that no difference would be found between the two study periods. This was done on a per station bases, applying the t-test to each station's record independently.

Stations which were used for dew point data collection were also individually analyzed with the change point software package for the open-source R statistics program (Killick and Eckley 2014). Within the change point package, the pruned exact linear time (PELT) algorithm was used because it has been optimized for fast computation through optimal partitioning and pruning, while maintaining overall accuracy. The change point analysis was applied to the 61-year dataset as one continuous unit, which complemented the t-test that examines the time frame from the perspective of the two distinct periods. This change point analysis provided a graphical display of the dew point time series data indicating specific years of significant change occurring in season-averaged dew point temperature, thus allowing improved and more targeted comparison for any changes occurring within station observed dew points. Stations were also combined in the Midwest Corn Belt (primary study area) to arrive at overall individual state averages for the eight-state region. These were used in a separate change point analysis to directly compare any changes occurring within USDA agricultural statistics data, specifically production efficiencies (yield per acre), which may have coincided with any significant changes in dew point temperature. In addition, USDA agricultural data was used as a visual comparative analysis tool in the construction of several choropleth images. The use of this data was to aid in the overall understanding of how changes in agricultural practices and land use occurring within existing corn and soybean cropland may support an increasing trend in regional near surface humidity.

3.4 GIS Spatial Analysis of Meteorological Variables

To improve meteorological data analysis and interpretation across a wide spatial region, a geographic information system (GIS) can be a valuable tool for geostatistical and visual comparative analysis of these variables. One useful tool for climate/meteorological data analysis is spatial interpolation. A variety of mathematical and statistical functions are used to create a continuous raster surface based on known variables at vector-based point locations (Burrough 1986). Point locations of known measured variables may be sparse, evenly distributed, or randomly distributed thought-out the area of interest/analysis and different interpolation techniques can have distinctive advantages over others for these situations (Li and Heap 2014). The types of variables being measured will also have pros and cons associated with various interpolation methods. In all instances, the final interpolated data product provides a continuous raster surface which contains data for very cell within the interpolation envelope or the defined processing extent.

Many interpolation techniques exist, and novel methods are continuously being developed based on customized or applied research needs. Interpolation methods most commonly used for meteorological/climate data include: inverse distance weighted (IDW), splines, and various kriging approaches (Hancock and Hutchinson 2006; Aalto et al. 2013; Pereira, Oliva, and Misiune 2016; Tanır Kayıkçı and Zengin Kazancı 2016). All of these approaches seek to provide climate data in regions with sparse or non-existent meteorological networks, areas where more frequent spatial data collection is limited, or to define climate parameters between observing station point locations. Since

climate variables such as temperature, humidity, and dew point are continuous across space and time, being traditionally recorded at point locations (weather observing stations), spatial interpolation techniques can be a valuable tool for extending data readings within observing networks across a wide regional surface. This can be critical for agricultural suitability assessments and provides a continuous raster surface required for many climatological analysis methods and improved monitoring.

Of the commonly used interpolation methods, Kriging techniques represent a large variety of interpolation methods which are based on geostatistical approaches which consider the statistical relationship across all data points (global trend) and among the known or measured points. Since these methods are statistics based, an error estimate can be generated, providing an indication of how well the predicted (interpolated) values fit the actual data (Samanta et al. 2012). The prediction method works by calculating the spatial autocorrelation within the data which conforms to the principal that nearer things are more related than distant things. Semi-variograms are produced showing the average differences between points plotted against distance between these points and a model is fit to represent how dramatically changes in the variables are affected by distance changes. In other words, points which are located farther apart likely have a greater range in values than points that would be located near one another. The method not only accounts for weighted distance between data points but considers the overall spatial arrangements of the points within the larger expanse of the study region which can improve interpolation results in data which shows spatial variability.

The meteorological data obtained from the 59 NWS FOS was organized in a general Microsoft Excel spreadsheet and up-loaded into ArcMap 10.5 as a csv file. Since data management and storage is important in any GIS study a file geodatabase was created and used to store and query all data as a flat file geo-relational data model. A base map of the U.S. showing state boundaries provided an accurate representation of the entire study region; downloaded from the U.S. Census Bureau within the on-line TIGER GIS database (Cencus-Bureau 2017). This map was uploaded to ArcMap as a shapefile and was subsequently converted to a new map layer before being imported to the file geodatabase as a feature class. Spatial data contained on the csv file consisted of decimal degrees representing each station's latitude and longitude using the 1983 geographic coordinate system (GCS) with WGS 84 Datum. When importing the table, the WGS 84 Datum was changed to NAD 83 in order to match the U.S. base map. The table was then used to display (x, y) points prior to being converted to a new layer and geodatabase storage. Since the base map consisted of the entire U.S. a clip tool was used to select only the area of interest while masking out features beyond the clip boundary.

A series of interpolated raster maps were created from two 30-year datasets of annual growing season averaged dew point temperatures using basic ordinary kriging. This was also done for both maximum and minimum 30-year growing season averaged temperature datasets and for vapor pressure deficit calculated from the temperature and dew point data. The final analysis involved creating an image difference comparison between the early and late 30-year climate periods for all meteorological variables. This

was completed using a raster calculator and simply subtracting the late period rasters from the early period rasters.

3.5 Corn and Soybean Flux Survey Data Collection and Model Variables

To obtain a better understanding of potentially significant moisture contributions directly from corn and soybean agriculture a multi-variable model has been created based off several key factors affecting overall plant transpiration and stomatal conductance rates. This work also sought to gauge the importance of these factors in influencing actual transpiration rates to provide a more accurate quantification of moisture contributions from the leaf level, scaled up to a per acre estimate or whole canopy scale. In addition, a total regional flux estimate was calculated for the entire eight state Corn Belt based off total 2017 acreage of corn and soybeans. Measured variables included: field capacity, soil moisture, per acre plant population, and leaf-stem/petiole angle. Measured meteorological variables included: air temperature, dew point temperature, relative humidity, atmospheric pressure, percent sky cover, wind speed, and direction. Calculated variables included: plant leaf area, leaf area index (LAI), solar angle, vapor pressure deficit (VPD), fraction of sunlit and shaded leaves, stomatal conductance, photosynthetic rate, and transpiration rate.

During the 2017 growing season a series of survey measures were taken with the Li-6400 infrared gas analyzer (IRGA), Theta soil moisture probe, and HH-2 moisture meter in conjunction with several meteorological variables collected from the nearest municipal airport (New Ulm, MN KULM) at time of survey measures. These survey

measures were completed every 7-10 days or as clear weather allowed. The goal of the field work was to create a multi-variable mechanistic model which sought to quantify plant transpiration rates to gauge corn and soybean crop contributions to atmospheric boundary layer humidity.

Since one of the more important variables in determining potential transpiritive flux rates is soil moisture availability, current volumetric soil moisture was recorded each measurement day to insure crops were not under water stress, thus reducing potential moisture contributions through decreased stomatal conductance.

3.5.1 Flux Rate Measurements

Calculated values of photosynthetic rate, stomatal conductance, and transpiration were carried out with the Li-6400 Infrared Gas Analyzer (IRGA) from Li-Core Biosciences (Lincoln, NE) (Figure 3.1). The Li-6400 is an open exchange instrument which utilizes sensitive gas analyzers capable of parts per million (ppm) resolution needed for accurate plant gas exchange measurements. Actively growing leaf material is lightly clamped within a neoprene sealed chamber with a transparent top. The instrument monitors active air exchange, allowing for photosynthesis and conductance to continue while being measured in real time by the analyzers (Figure 3.2). In an open system, such as the Li-6400, air within the leaf sample chamber is replaced at a steady rate which allows quantification of CO_2 and water vapor based of the calculated difference in gas concentration in the outgoing and incoming air streams. The instrument also allows for

manipulation of the incoming air stream to gauge responses to variable CO_2 and water vapor concentrations.

Figure 3.1 The Li-6400 from Li-Core Biosciences, photo taken by author during early season flux measurements (6/15/2017).

Since the main goal of this portion of the study was to quantify actual plant transpiration rates based off near-ambient conditions, the Li-6400 was configured to supply chamber air with ambient humidity levels, which were achieved through a complete by-pass of the Drierite® desiccant chemical scrub tube. In the event of excessively humid days, which triggered high humidity alerts on the IRGA, slight scrubbing of water vapor was applied to reach acceptable humidity levels, which remained near ambient. Considering the IRGA's high sensitivity to CO_2, errors

associated with animal respiration (field work requires one to still breath) were eliminated by scrubbing all incoming air of CO_2 through the soda lime chemical tube.

Figure 3.2 Flux readings being taken with the Li-6400 on a shaded corn leaf, photo taken during late season measurements (9/4/2017).

This CO_2 free air was then resupplied with CO_2 at the observed ambient on-site concentration of 400 ppm utilizing the inline CO_2 mixer and external CO_2 cartridge assembly.

3.5.2 Field Capacity, Permanent Wilting Point, and Available Soil Moisture

Early in the growing season, prior to cultivation and planting, a series of soil core samples were obtained from the four study fields. Used for laboratory field capacity determination, these samples were placed in aluminum trays containing drainage openings and thoroughly saturated with tap water. The trays were allowed to drain freely under gravity for a 24-hour period, after which the trays were weighed and dried in an oven at 221°F (105°C) for 24 hours. After cooling, the sample trays were weighed to

Figure 3.3 Soil samples awaiting analyses for field capacity determination (4/18/2017).

determine total volumetric water content or field capacity based off the change in weights and the known density of water (Figure 3.3). Soil types were determined using the USDA soil test guidelines (Thien 1979; USDA-NRCS 2017a), and were used to estimate permanent wilting point based off a specified percentage of total calculated field capacity.

Measured values of soil moisture were carried out with the Delta-T Devices type ML2X Theta soil probe in conjunction with the HH-2 moisture meter which provides a volumetric quantification of soil moisture. A series of soil moisture readings were taken in each field at the time of survey measurements. These readings were used to compare deviations from field capacity and permanent wilting point to ascertain any unfavorable conditions due to excess or lack of soil moisture which could impact moisture flux readings or transpiration rates.

3.5.3 Other Measured and Calculated Variables

Plant leaf area was calculated by removing all leaves from a representative plant sample, placing/taping the leaves flat to a large poster board without overlap and photographed with a 16.0-megapixel resolution digital camera (Nikon Coolpix L840) (Figure 3.4). The photos were subsequently uploaded to Adobe Photoshop which allowed for pixel counting and area calculation based on a known pixel size (Chen et al. 2010), and reference pixel count based on a $5cm^2$ section of color paper (Figure 3.5). This process provided a whole plant leaf area, which was subsequently used to arrive at leaf area index (LAI) based off plant population counts and field sizes.

Figure 3.4 Soybean leaves photographed for subsequent leaf area analysis, note the 5cm² reference square (9/3/2017).

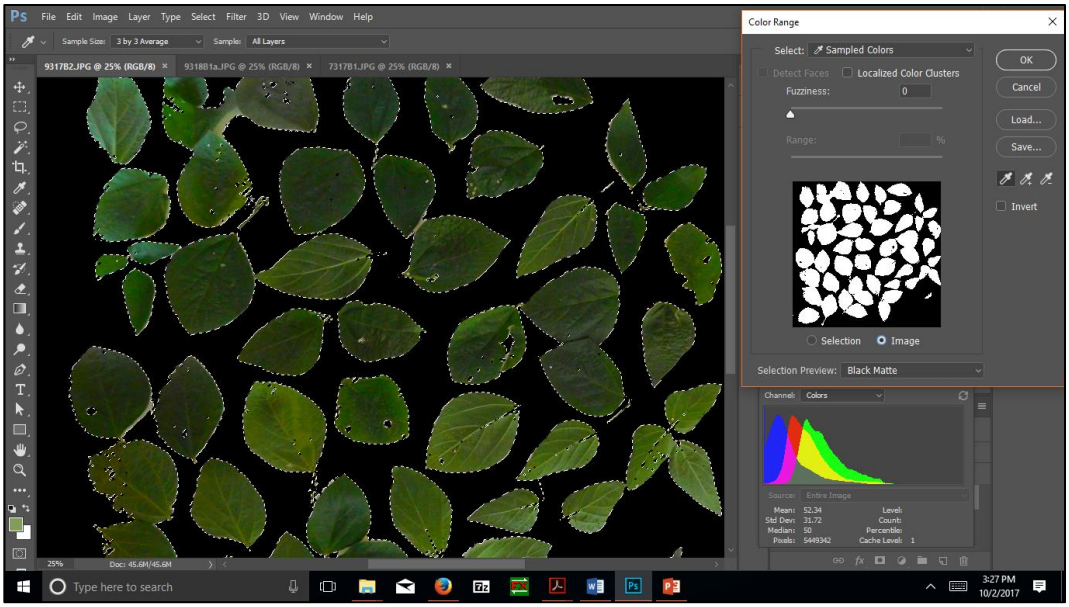

Figure 3.5 Leaf area analysis in Adobe Photoshop.

Plant population counts were completed early in the growing season and again later in the season to arrive at actual plant counts. A length of row representing 1/1000th acre was determined by row spacing and several surveys were completed throughout each field that were averaged and scaled to a per acre population rate. Finally, leaf angle was measured once during peak growing season (August) as a series of readings in each field utilizing a smartphone compass application (Escribano-Rocafort et al. 2014). Also collected at the time of survey measures were meteorological variables of air temperature, dewpoint, relative humidity, atmospheric pressure, wind speed, and direction from the nearest municipal airport weather observation station (KULM, located in New Ulm, MN) approximately twelve miles from the field study sites.

Calculated values of vapor pressure deficit or atmospheric demand for water vapor were achieved by applying equations 3.1-3.3, using measured ambient station conditions of air temperature for saturation vapor pressure and dew point temperature for vapor pressure. Solar zenith angle was calculated by using NOAA's online solar position calculator which considers the local lat/long geographic position coordinate, time zone, day of the year, and time of day (NOAA 2017b). Sunlit and shaded leaf fractions within the canopy were calculated using equations from a similar study which modeled canopy level gas exchange fluxes (Equations 3.4 and 3.5) (Dai, Dickinson, and Wang 2004).

Eq. 3.4 $f_{Sun}(x) = e^{-k_b x}$

Eq. 3.5 $f_{Shade} = 1 - f_{Sun}$

x = current leaf area index (LAI)

k_b = $G(\mu) / \mu$

$G(\mu)$ = $\theta_1 + \theta_2\mu$

θ_1 = $0.5 - 0.633X - 0.33X^2$

θ_2 = $0.877(1-2\theta_1)$

μ = cosine of zenith solar angle

X = empirical parameter for leaf angle, ranging from 1 to -1, (1 representing horizontal leaves 0°, -1 representing vertical leaves 90°)

Transpiration rates were calculated automatically from Li-6400 IRGA software based upon the following variables (Equation 3.6) (Li-Cor 1999).

Eq. 3.6

$$E = \frac{F(w_s - w_r)}{100s(1000 - w_s)}$$

E = Transpirations Rate (mmol/H_2O/m^2/sec)

F = $(\mu_i)(10^6)$

W_s = $(w_o)(10^3)$

W_r = $(w_i)(10^3)$

S = leaf area of sample ($6cm^2$)

μ_i = incoming air flow rate (mol/s)

μ_o = outgoing air flow rate (mol/s)

w_i = incoming H_2O mol fraction (mol H_2O/mol air)

w_o = outgoing H_2O mol fraction (mol H_2O/mol air)

3.6 Field Sampling Data Analysis and Modeling Strategy

Survey measures were carried out every seven to ten days, or as weather conditions allowed, throughout the 2017 growing season within four production fields located in Nicollet County, Minnesota, consisting of two corn and two soybean fields. Due to the inherent sensitivity of the IRGA combined with long equilibrium times for stomatal conductance in response to various environmental conditions, chiefly variable solar insolation levels, measurements were only carried out on clear days with minimal cloud cover. One measurement day was carried out during overcast conditions to observe how values were affected by a large insolation reduction with increased diffuse radiation. On measurement days, readings were taken during a diurnal period representing maximum potential conductance and transpiration rates, typically occurring for a two-three hour period beginning at local solar noon (Reicosky, Kaspar, and Taylor 1982; Leakey et al. 2004).

IRGA readings were taken a minimum of twelve rows into a field, from the field boundary, as a series of eight upper canopy sunlit leaves, followed by eight lower canopy shaded leaves. Each reading occurring at the individual leaf level was given sufficient time to reach a stomatal equilibrium state from slight environmental changes within the IRGA chamber. In addition, steps were taken to ensure as close to ambient conditions as possible, thus reducing stomatal equilibrium times and providing a more accurate representation of actual stomatal flux values. Active monitoring was accomplished using the “Graph-It” program in the IRGA software which provided a real time visual graphical display of flux values. Readings were logged when flux curves reached a near zero

slope, with typical equilibrium times ranging from 30 seconds to 1 minute. The sampling interval was no less than every eight to ten plants down a selected row with around 60 row feet covered each measurement series.

The first key variable in arriving at accurate canopy level fluxes involved calculating a leaf area index (LAI), defined by the one-sided green leaf area per unit of ground area. Per acre plant population counts were used in conjunction with individual plant leaf area determined by destructive leaf area sampling with digital photography and subsequent pixel counts within photo processing software (Equation 3.7).

$$\text{Eq. 3.7} \qquad \frac{(\text{Individual Plant Leaf Area}) \times (\text{Per Acre Population})}{4046.86\ \text{m}^2} = \text{LAI}$$

The calculated LAI was then used with the cosine of the zenith solar angle and measured leaf angle (leaf to stem angle) to calculate the fraction of sunlit and shaded leaves by applying equations 3.4 and 3.5. Next, utilizing the designated proportions of sunlit and shaded leaves, the per plant measured leaf area was divided into an upper and lower canopy portion representing total area of sunlit and shaded leaves, respectively. These calculated upper and lower canopy leaf areas were then combined with the averaged IRGA readings taken both for sunlit and shaded leaves, yielding a total overall plant flux rate, which was then up-scaled using the per acre plant population counts. For a more convenient interpretation of transpiration flux values, the reported mmolar H_2O rates were covered to milliliters H_2O per acre, per unit of time, thus providing an

understandable quantification of typical midday transpiration rates occurring at various growth stages throughout the 2017 growing season.

Aside from the ultimate flux value of interest for this study (transpiration), values of stomatal conductance and overall photosynthetic rate were also recorded. Stomatal conductance is a representation of the degree of stomatal aperture which is affected by several environmental conditions previously discussed. Since this value can vary greatly in different conditions and across the plant as a whole (different leaf-level stomatal distributions), transpiration was focused upon as this process represents the actual flux of water vapor out of the leaves into the lower atmospheric boundary layer. For example, a plant may experience a high value of conductance within a protective closed canopy environment (microclimate), but actual water movement out of the plants (transpiration) is reduced due to factors such as low VPD, high humidity, low temperatures, etc. Values of conductance were recorded to compare the relationship between transpiration and influencing environmental factors.

Photosynthetic rate is a measure of CO_2 assimilation by the C3 of C4 carbon fixation reaction pathways. In C3 plants such as soybean, this rate is largely dependent upon stomatal conductance values as this can have a restrictive effect on the amount of available CO_2 for rubisco mediated fixation and/or increased inefficient photorespiration with O_2. With C4 plants such as corn, the rate of carbon assimilation is not as greatly affected by reduced conductance with a CO_2 concentrating mechanism present involving a spatial separation between the C4 and C3 pathways. In either case, the photosynthetic rate was also recorded to gauge effects of other environmental factors on overall carbon

fixing rates, how this rate was related to overall transpiration, and as a comparison to confirm whether measured values were within ranges reported by other literature.

3.7 Remote Sensing Crop Health Comparison

To insure the study site fields were representative of those within a larger area in terms of health and overall crop performance, a remote sensing monitoring approach was applied. A wide variety of vegetation indices have been developed utilizing specific electromagnetic band combination from available satellite platform sensors. These bands extend into areas of infrared (.8-3um) which is strongly reflected by healthy vegetation. The normalized difference vegetation index (NDVI) (Equation 3.8), was introduced in 1974 (Rouse Jr et al. 1974), and has been the dominate index in remote sensing studies of vegetation (Gao 1996). There have also been steady developments with other unique indices which utilize other band combinations. Of these, the normalized difference water index (NDWI) (Equation 3.9) (Gao 1996) has shown to be useful for many applications including quantification of vegetation water content by utilizing a near infrared band (NIR) centered at 0.86um and short wave infrared band (SWIR) centered at 1.24um, which is effective at water absorption.

A radius extending approximately ten miles from center of the study sites was used to compare corn and soybean fields of south central Minnesota (Nicollet County), to monitor crop health, vegetation water content, and determine temporal changes throughout the 2017 growing season (May-September). Images were obtained for the 2017 growing season that included Nicollet County from the USGS site Earth Explorer. Pre-processing was completed to identify images which were acceptable for further

analysis that contained minimal cloud cover and/or atmospheric interference. This resulted in five images ranging from May 22^{ed} to September 11th. Images were further processed to stack all required layers and an area extending ten miles from the field study sites was extracted as a subset image.

This analysis includes vegetation water content derived from numerous field verification studies (Jackson et al. 2004; Chen, Huang, and Jackson 2005; Yilmaz, Hunt, and Jackson 2008; Huang, Chen, and Cosh 2009), and will utilize NDWI as an indicator correlating to actual water volume. NDVI will also be directly analyzed for the same images to gauge any apparent differences in assessing overall vegetation health and LAI. Gaining a better understanding of vegetation water content at different periods within a growing season is important for drought monitoring, irrigation management, yield predictions, and climate model applications considering lower atmospheric moisture sources.

Data acquisition and extraction was completed utilizing Landsat-8 OLI images from the 2017 growing season and was subsequently analyzed with Erdas Imagine 2015 software. Landsat-8 was chosen due to its moderate pixel resolution of 30 meters, which provides an accurate spatial representation of common agricultural field sizes while being able to cover an entire county. The temporal resolution of 16 days provides an acceptable image sampling interval for general growth stage health and water quantification, however improved temporal resolution may be necessary or desired for studies requiring more frequent monitoring. Landsat-8 also has the desired spectral resolutions, providing a near infrared (NIR) band centered at 0.865um (band 5) and a shortwave infrared

(SWIR) band centered at 1.609um (band 6) which works well for both standard NDVI and NDWI.

After processing to arrive at subset images, both NDVI and NDWI were applied which produced greyscale images with normalized pixel values ranging from -1 to 1. Since greyscale images are less useful for visualization, pseudo color images were created for NDVI results to aid in visualization and image comparison. To apply crop specific water volume content (WVC) equations to the same image, corn and soybean field types must be known. An unsupervised image classification with thirty iterations was performed on the September 11th image which contained good crop differentiation characteristics as corn fields had apparent tasseling present while most bean fields were essentially dark green. This was used to produce a basic land classification map identifying corn and soybean field locations. These combined products were used to apply crop specific equations for both corn and soybean to the same image. This was done utilizing NDWI, as this specialized index is reported as a superior indicator of accurate WVC.

3.8 Summary of the Methods

By collecting meteorological data on dew point temperature, minimum/maximum temperature, and calculated VPD from NWS FOS, with proven consistent and reliable data records, a clearer picture of any spatial and temporal changes will be achieved though statistical and visual comparative analysis. Application of the independent t-test to individual stations provides a measure of statistically significant temporal change from the early (1956-1985) to late (1986-2016) portions of the study period. While visual

comparative analysis though graphical display of this data provides an indication of any spatial changes occurring. Further, change point analysis of dew point records has provided significant years in which these changes took place. By comparing changes occurring in agricultural census data with state averaged changes in dew point temperature, a possible link will be established.

Raster surface maps, based on the kriging spatial interpolation method, show the changes in the analyzed meteorological variables. Since these variables are continuous through space, but are traditionally collected at a limited number of station point locations, these images can provide extended estimates to where spatial and temporal changes have taken place. Since this technique can only consider the point data that is available, this can limit accurate results within areas possessing relatively sparse data collection networks and results must be considered with these limitations in mind.

Field data collected during the 2017 growing season were used to create a model to accurately up-scale individual leaf level flux rates to canopy level, providing a quantification of transpiration rates and potential midday contributions to lower atmospheric humidity. Several important environmental variables, which can have a dramatic impact on potential transpiration rates, was also included for analysis. Remote sensing was used to monitor overall crop health through NDVI and vegetation water volume content (WVC) utilizing NDWI throughout the growing season to confirm whether the field-based readings occurred in settings that were representative of the surrounding area.

Chapter 4: Results and Discussion

4.1 Metrological Data Analysis Results

The primary study region (Midwest Corn Belt) contained 33 stations while the secondary study region (Southern U.S. to Gulf Coast) contained 26. Overall, both regions experienced some degree of increasing dewpoint temperature, however a greater increase was found within the primary study region and many of the smaller increases within the secondary region were statistically insignificant.

Of the 33 stations located within the primary region, 76 percent experienced an average increase of ≥ 1°F in dew point temperature between the early and late climatic periods. A one degree rise in dew point occurring between 68-72°F, translates into a three and a half degree rise in saturation vapor pressure. Of the 26 stations located in the secondary region only 19 percent experienced an increase of this magnitude. Results from the independent t-test showed that all increases > 1°F were significant at the 99 percent confidence level (a=.01). Clearly, a higher magnitude of dew point increase was supported by a higher statistically significant confidence interval indicating a more definitive increase associated with the lower alpha.

Results from the independent t-test of dew point temperature between climate periods over the five-month growing season (May-September) are summarized cartographically for improved visualization (Figure 4.1). T-test results for all stations are

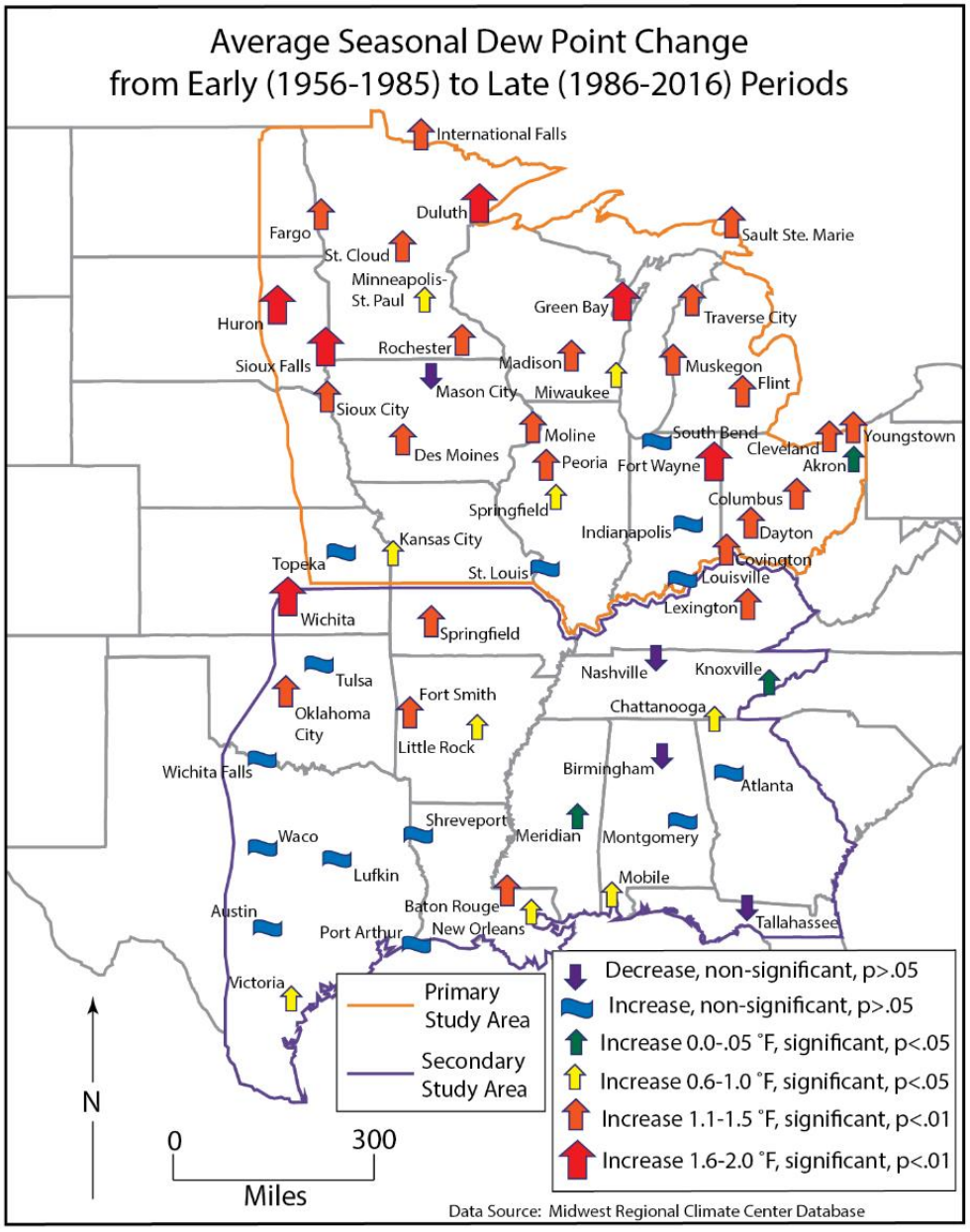

Figure 4.1 Results from independent t-test comparing early (1956-1985) and late (1986-2016) climate periods for dew point temperature over the five-month growing season (May-September).

tabulated for reference within Appendix A. From this systematic per station analysis it can be determined that a greater overall increase in atmospheric boundary layer (ABL) moisture is occurring throughout the Midwest Corn Belt region.

Further, this magnitude of increase has not occurred within the Southern portion of the U.S. This region accounted for three of the four decreases and 85 percent of the stations that had an increase of < 1°F, with half of these increases testing statistically insignificant at the 95% level (a=.05). Since this Southern region extends to the Gulf Coast and is the primary source region for advected maritime tropical (mT) air mass humidity into the Corn Belt, it can be inferred that some other mechanism outside the source region is providing an increased localized moisture source.

Increases in atmospheric moisture can have effects on other meteorological variables such as daily minimum and maximum temperature. Consequently, these were used in a similar independent t-test analysis to gauge any associated changes within these variables. The same parameters were used for temperature change analysis which covered the same early and late climate periods and the five-month growing season average. Results are summarized visually for maximum temperature (Figure 4.2) and minimum temperature (Figure 4.3) with tabulated results in Appendix A.

Daily maximum temperature averages occurring over the summer growing season have increased at a similar magnitude across both study regions, something that fits with global warming pursuant to enhanced planetary CO_2 concentrations ranging from 315 to over 400 ppm during the study period. This is a typical pattern occurring in many regions and this increase in daily temperature maximum can act to increase the VPD or

evaporating potential of the atmosphere, thus acting to increase transpiration or evaporation rates across the board. Of the 54 stations included in the maximum temperature analysis roughly half of the records tested statistically insignificant at the 95

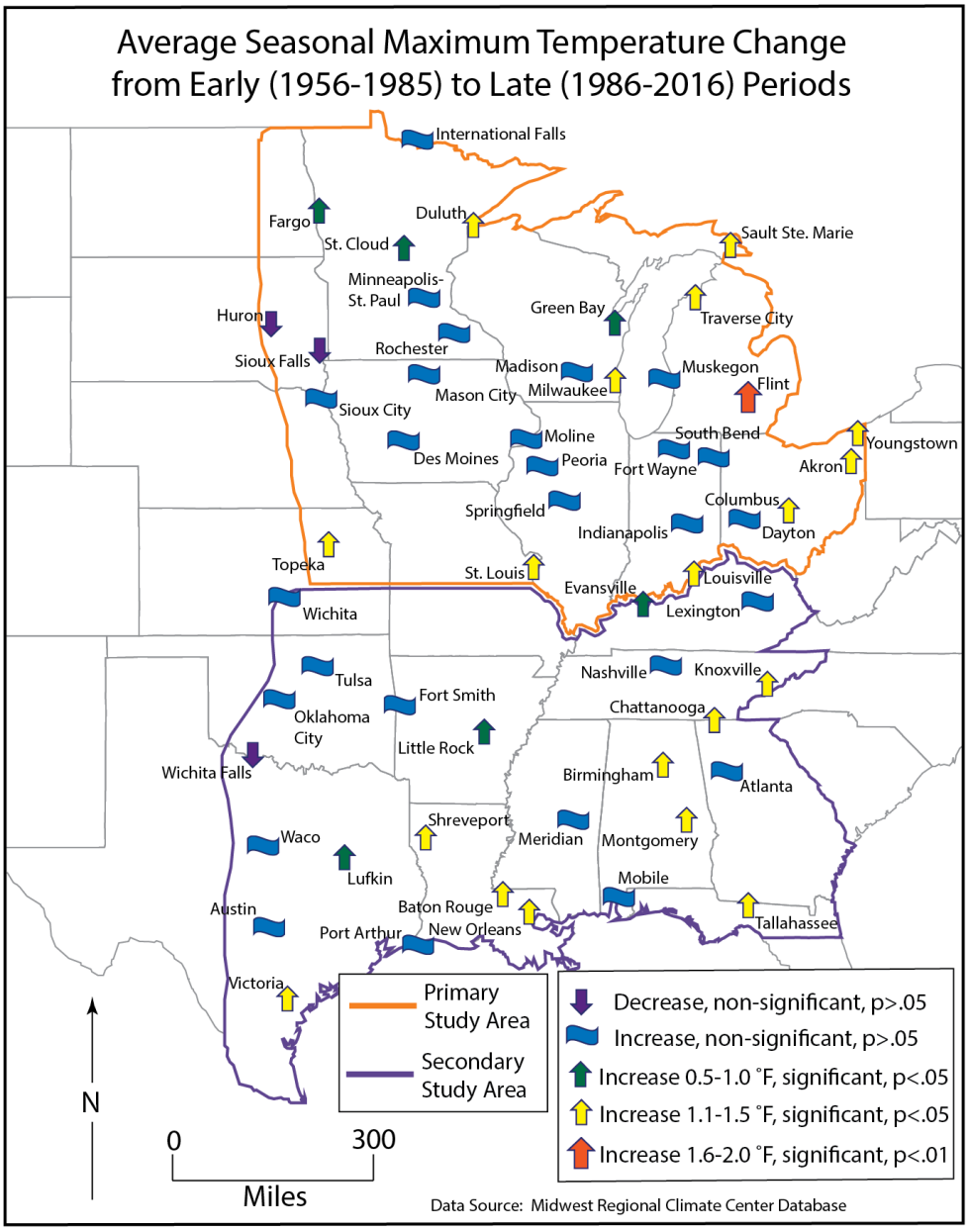

Figure 4.2 Results from independent t-test comparing early (1956-1985) and late (1986-2016) climate periods for daily maximum temperature over the five-month growing season (May-September).

percent confidence level (a=.05). The increase in daily maximum averaged 0.83°F with a standard deviation of around 0.50°F indicating a relatively uniform increase. However, within the core region of the Midwest Corn Belt stations had a lower average increase indicating some degree of suppressed daily maximum, an indicator of increased latent heat partitioning and reduced sensible surface heating.

Daily minimum temperature averages over the same summer growing season have increased at a greater magnitude than the daily maximums. This situation indicates increased atmospheric moisture, which acts to blanket heat near the surface, resulting in reduced rates of nocturnal cooling. Increases of the greatest magnitude have again occurred within the Midwest Corn Belt region with roughly half of these stations experiencing an increase ≥ 1.6°F and all testing statistically significant at the 99 percent confidence level (a=.01). Only three stations within the Southern region experienced similar patterns indicating much more pronounced increases occurring mainly within the Midwest.

VPD was also included in the t-test analysis to ascertain whether an increase in VPD may be responsible for increasing lower atmospheric moisture within the Midwest or if changes in agricultural land use practices are potentially playing the larger role in humidity increases. VPD was calculated as a percent change between the early and late climate periods and results are again presented visually (Figure 4.4) and tabulated within Appendix A. Within the southern and eastern portions of the study regions the overall trend is an increase in VPD which is supported by higher daily maximum temperatures. It is interesting to note that ten stations located within the core region of the Corn Belt

have experienced a decrease in VPD. Since VPD considers both surface temperature (increase in surface temperature = increase in VPD) and dew point temperature (increase in humidity = decrease in VPD), these lowered readings in the Corn Belt point towards a link to increases in atmospheric moisture.

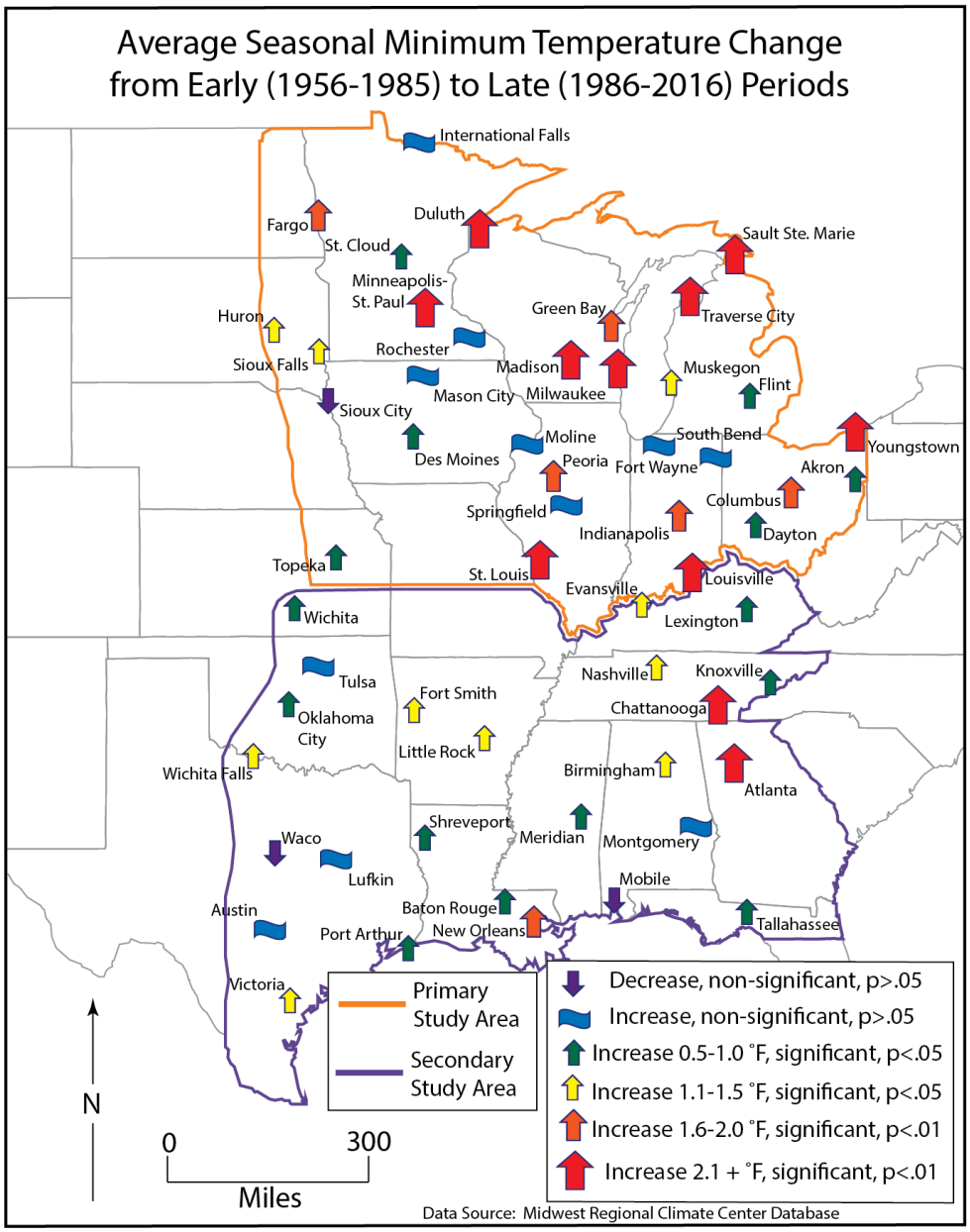

Figure 4.3 Results from independent t-test comparing early (1956-1985) and late (1986-2016) climate periods for daily minimum temperature over the five-month growing season (May-September).

Only 26 percent of stations tested statistically significant for this VPD increase with these stations representing the largest category of increase (> six percent increase between climate periods). These 14 stations are mainly located within the eastern half of both study regions.

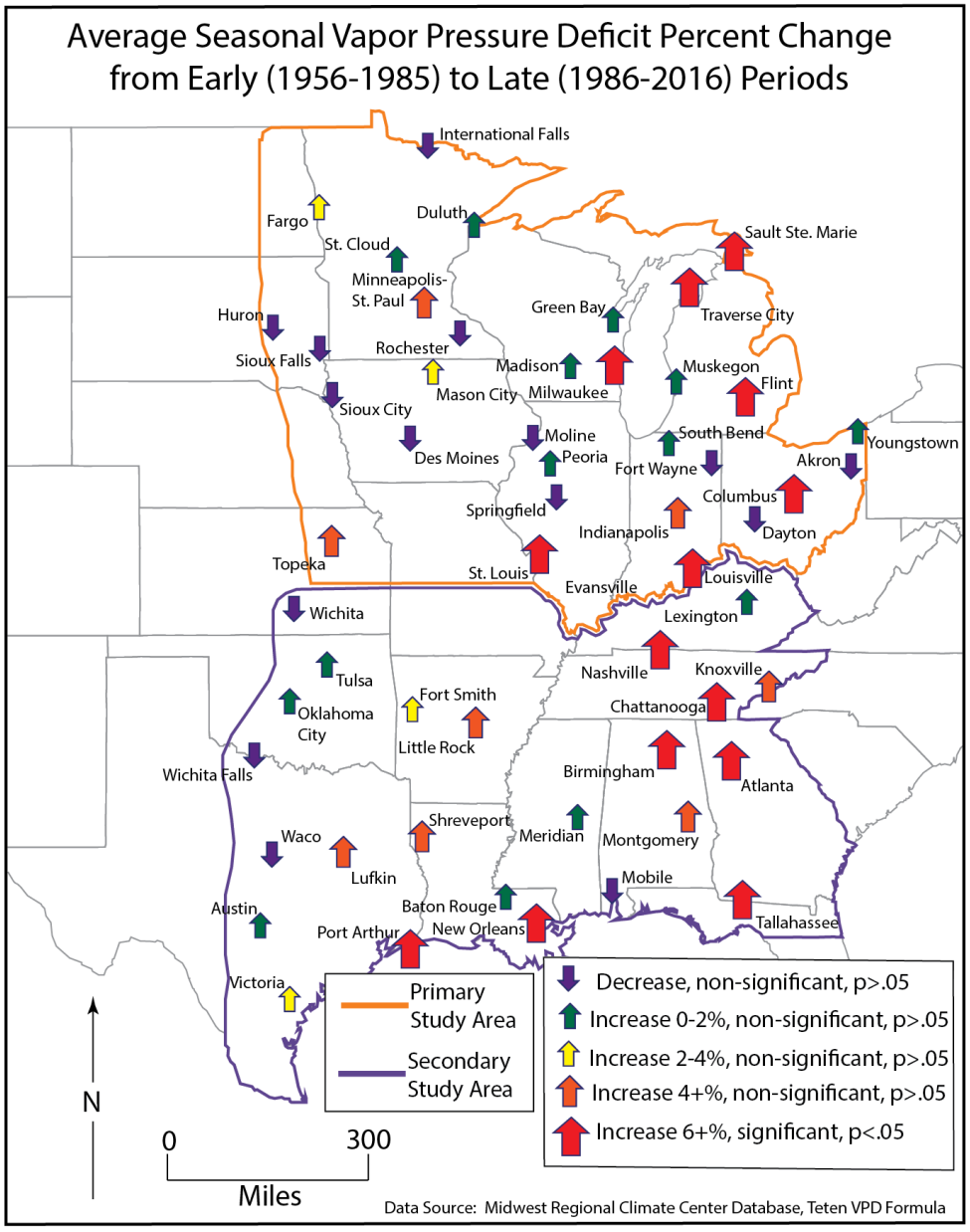

Figure 4.4 Results from independent t-test comparing early (1956-1985) and late (1986-2016) climate periods for vapor pressure deficit over the five-month growing season (May-September).

The change point analysis over the 61-year span calculates regions within the data where before and after change point means are different, providing specific years in the timeseries where statistically significant changes took place. A manual penalty value was assigned based on visual examination of graphical change point results, choosing a value in which the number of change points best fit intuitive visual changes within the data series. The penalty values in the PELT algorithm essentially modify the sensitivity to change point break detection with larger penalty values generating a lower frequency of change points. This was completed individually for all stations used for dew point records within both study regions resulting in 59 total change point graphs. The results for all stations can be found within Appendix B.

Considering all fifty-nine graphical results, an overall increasing trend in dew point temperature is apparent with 82 percent of primary study region stations experiencing a clear, often linear increase and no stations experiencing a steady or decreasing trend. Within the secondary study region stations, 62 percent have steady average dew point temperatures over the timeseries and another 46 percent experiencing some degree of increase. Several representative stations from the primary and secondary study region are presented here (Figures 4.5 and 4.6).

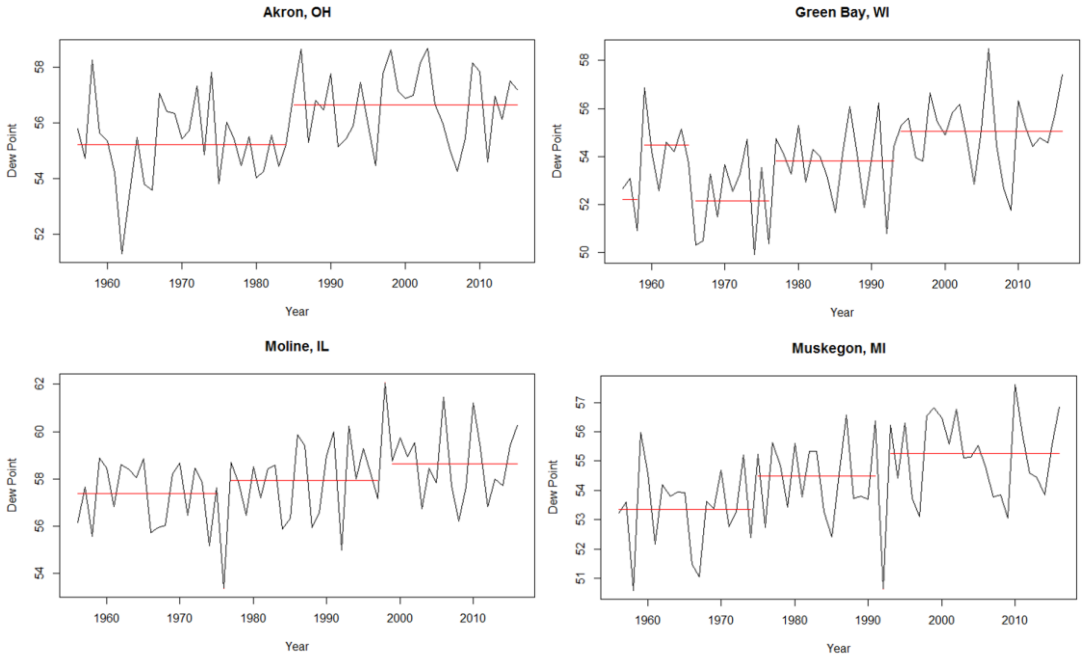

Figure 4.5 Sample of change point results from stations within the primary study region representing typical increase patterns.

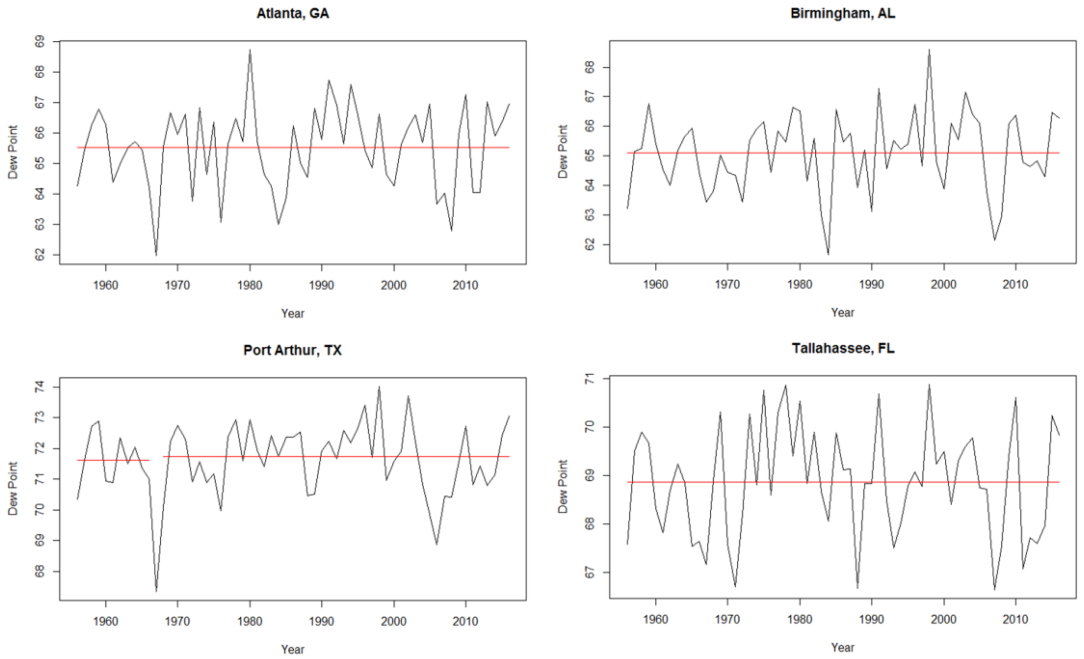

Figure 4.6 Sample of change point results from stations within the secondary study region representing typical steady dew point patterns.

Years in which change points occurred were also recorded to determine any temporal pattern or commonalities between stations or common change point years (Figure 4.7). Clearly, years representing the most common change points across all study regions occur in 1977, 1986, and 2010. Study region specific change points indicating number of increases vs. decreases are also included for a more complete picture of spatial and temporal changes (Figures 4.8 and 4.9).

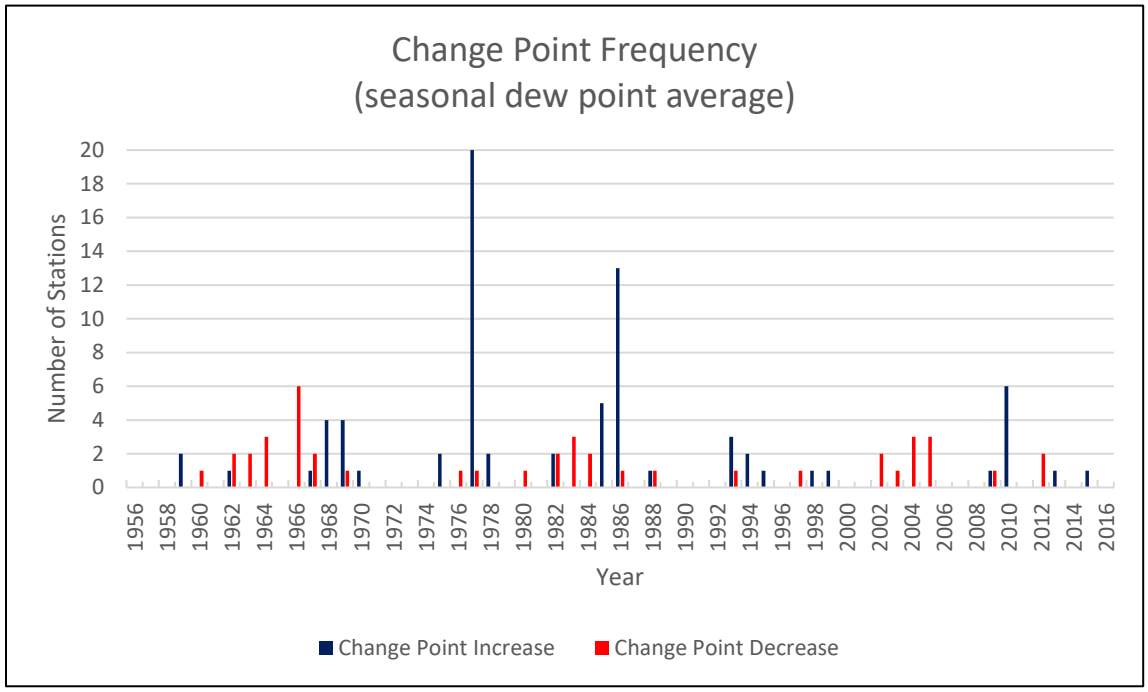

Figure 4.7 Change point station frequency increases and decreases for dew point temperature across both study regions.

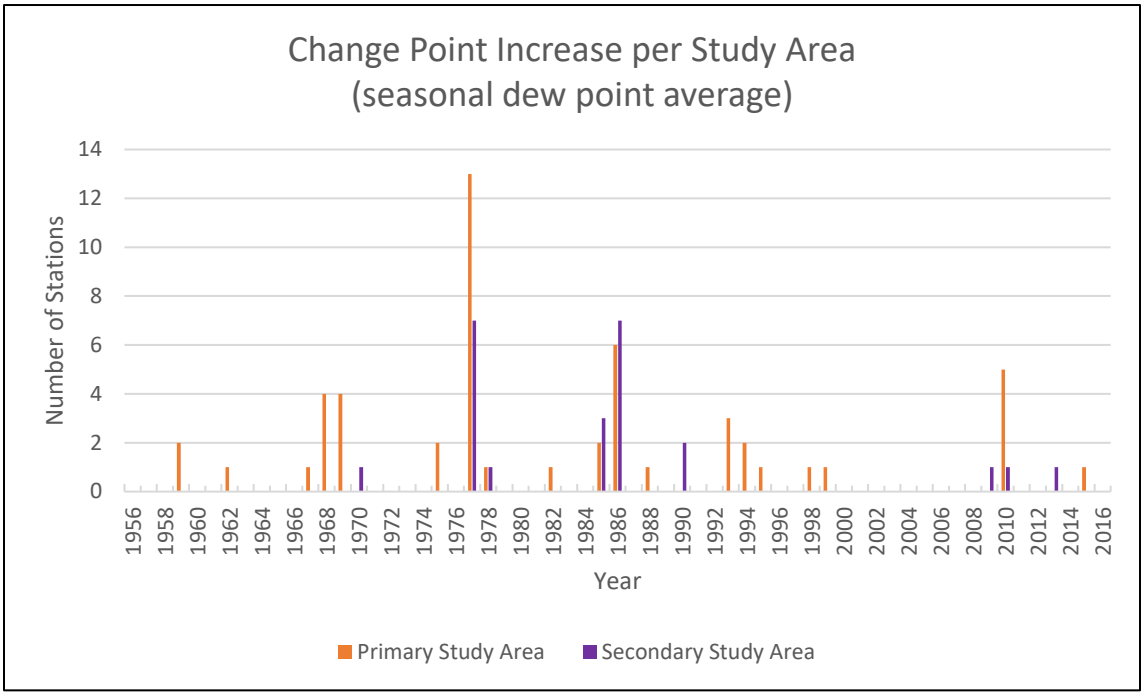

Figure 4.8 Change point station frequency increases only for dew point temperature across both study regions.

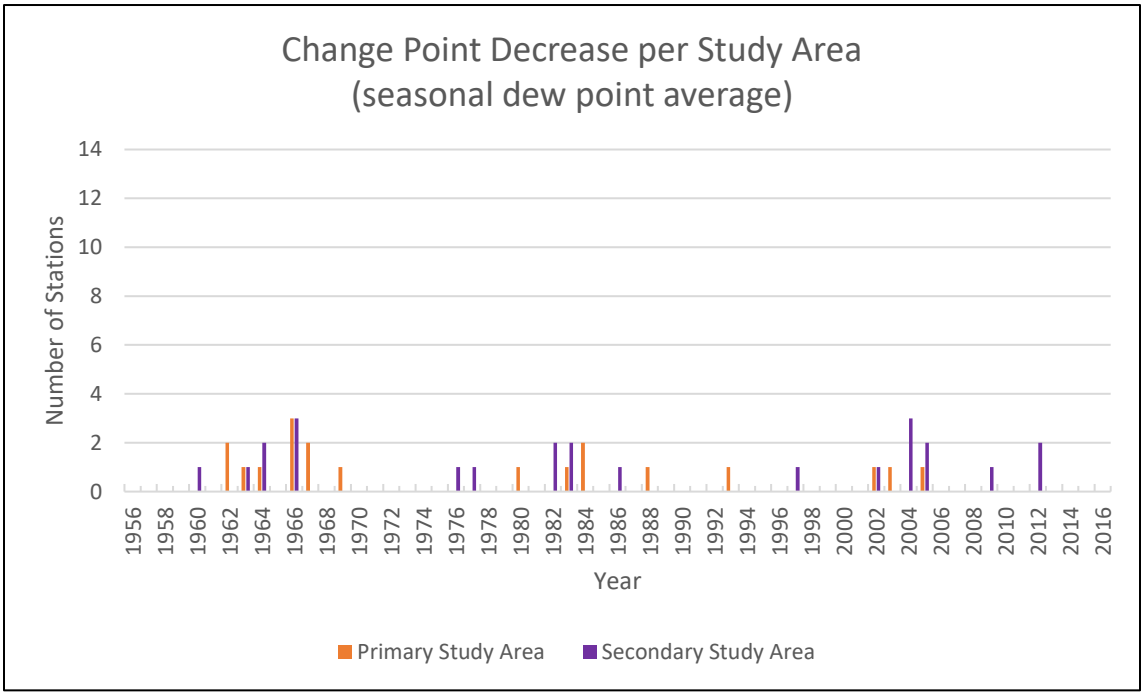

Figure 4.9 Change point stations frequency decreases only for dew point temperature across both study regions.

Results from GIS interpolation provide a complete spatial view of changes occurring in a continuous environmental variable (dewpoint, temperature, and VPD). The interpolation images based on kriging are listed for reference within Appendix C. From these images raster difference images were created for each of the four climate variables comparing changes from the early to late climate period interpolations using the raster calculator resulting in four new images (Figures 4.10-4.13).

Results for yearly growing season averaged dew point temperature show that increases are rather widespread between periods, however more drastic increases are apparent throughout the Midwest, on the order of a 1-2°F compared to the Southern U.S. which has seen a 0-1°F increase. Variables of maximum and minimum temperature show a variety of changes. Maximum temperature is more erratic with less of a definitive spatial pattern, while minimum temperature has increased in the central and northern areas of the study region on the order of 1-3°F. The final variable consisting of vapor pressure deficit indicates an increase in the southeastern region of the study area with slight decreases apparent in the western and northern portions, including the Midwest. While these interpolation techniques provide a convenient way of estimating variables across space and make sense for such continuous environmental data as temperature, they certainly have limitations and such interpretations should be made cautiously. Overall, the results obtained from these various interpolations support an increasing trend in atmospheric boundary layer moisture occurring within the Midwest Corn Belt.

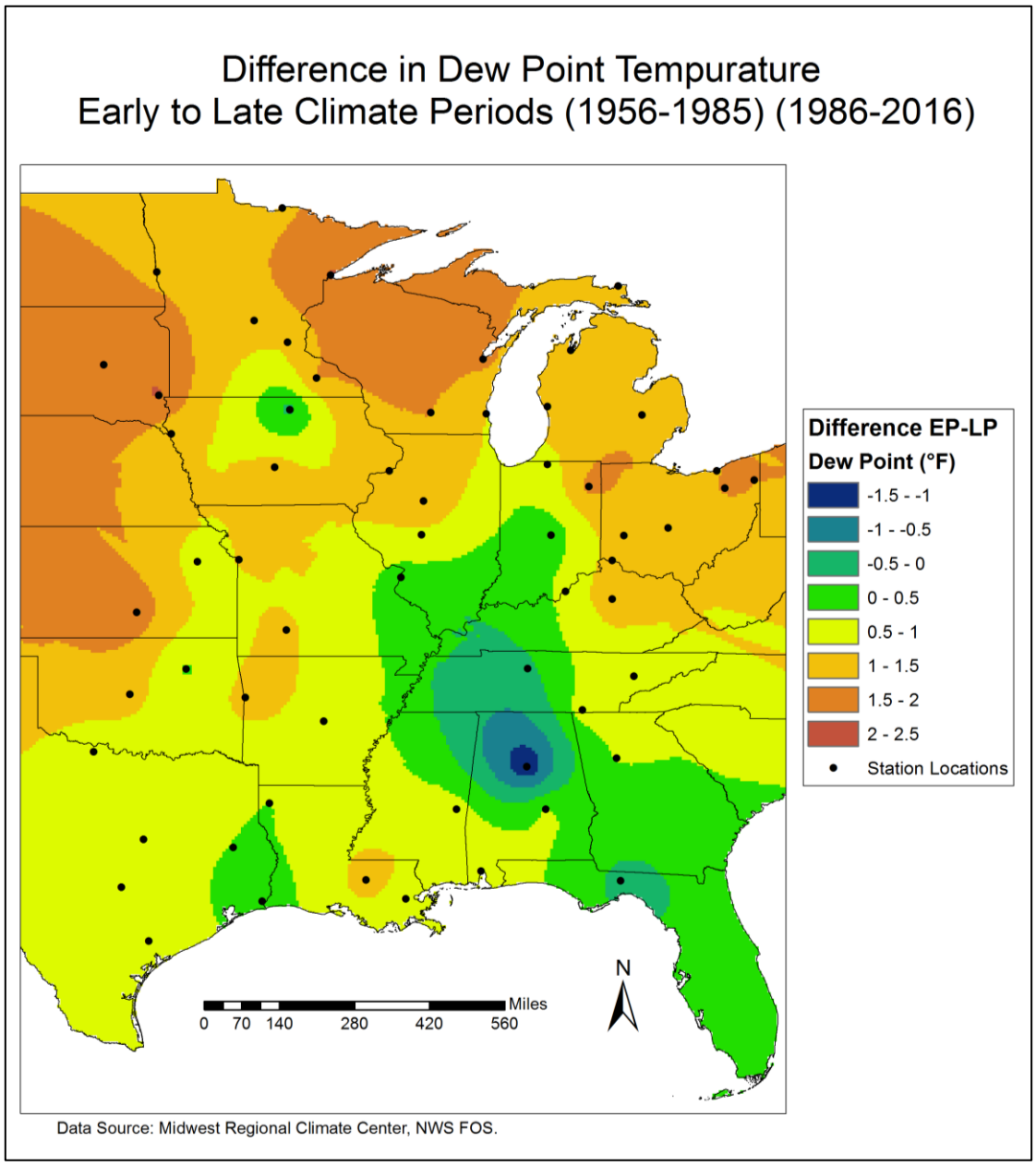

Figure 4.10 Interpolated dew point temperature difference between early and late climate periods

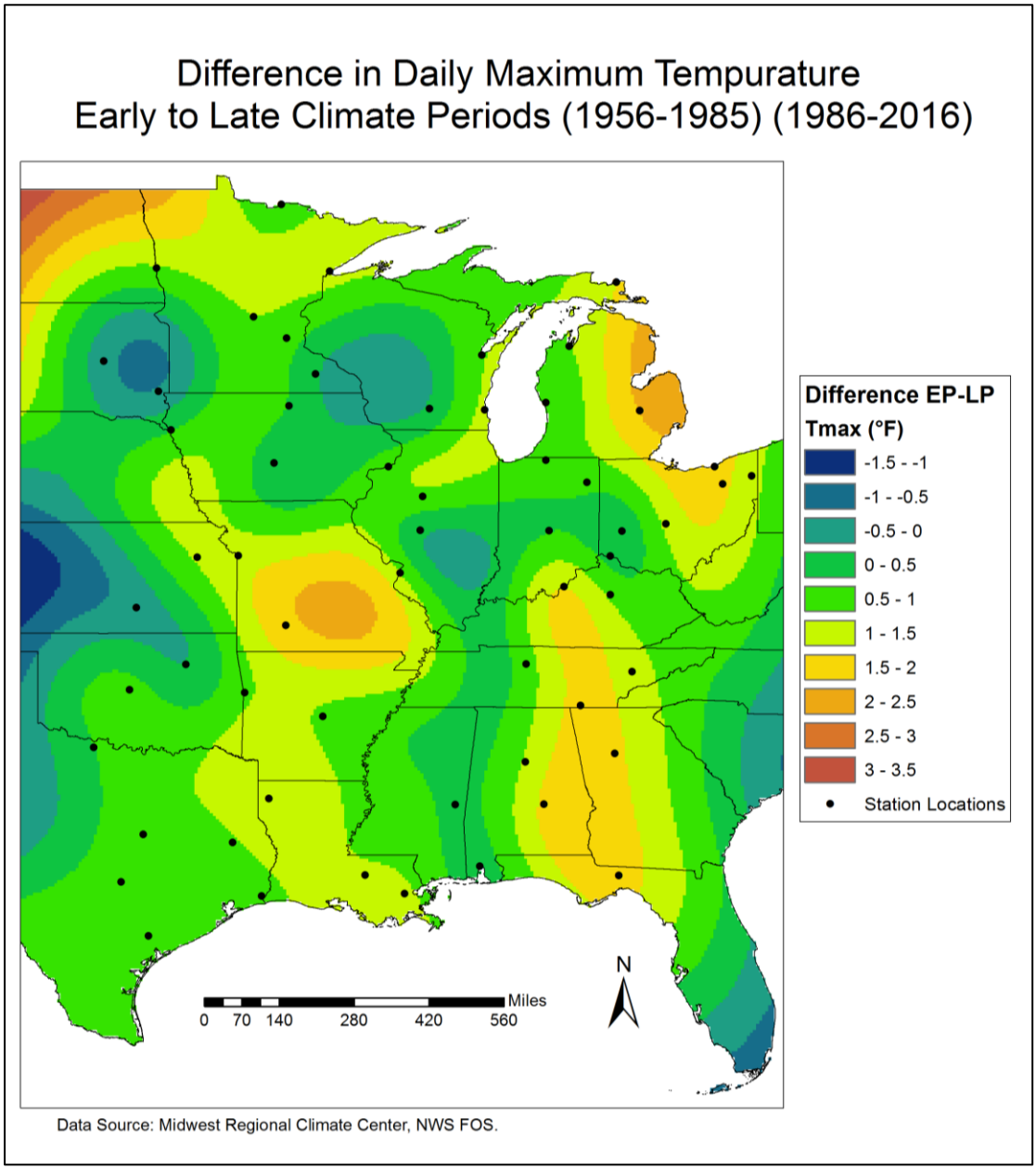

Figure 4. 11 Interpolated daily maximum temperature difference between early and late climate periods

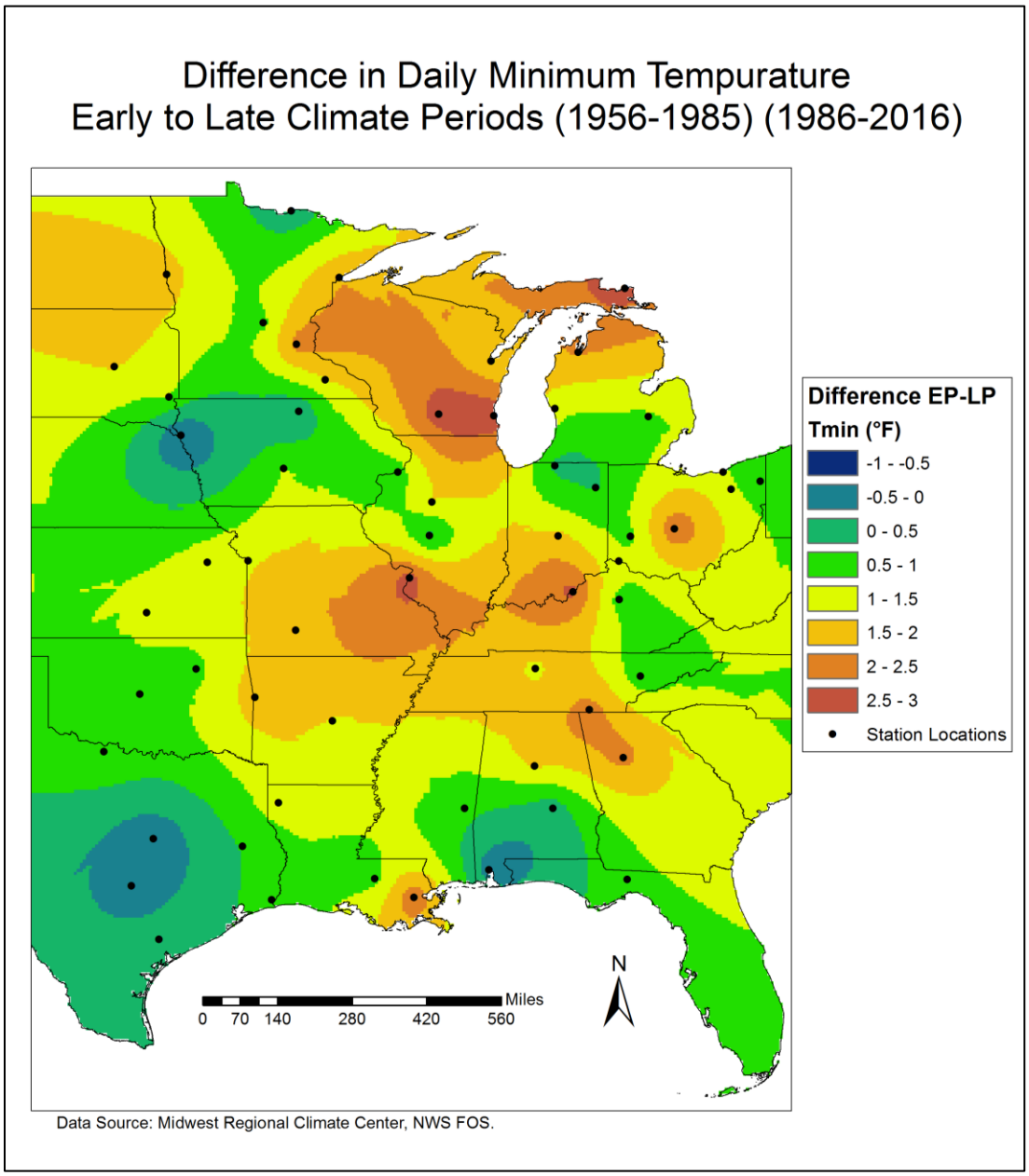

Figure 4.12 Interpolated minimum temperature difference between early and late climate periods

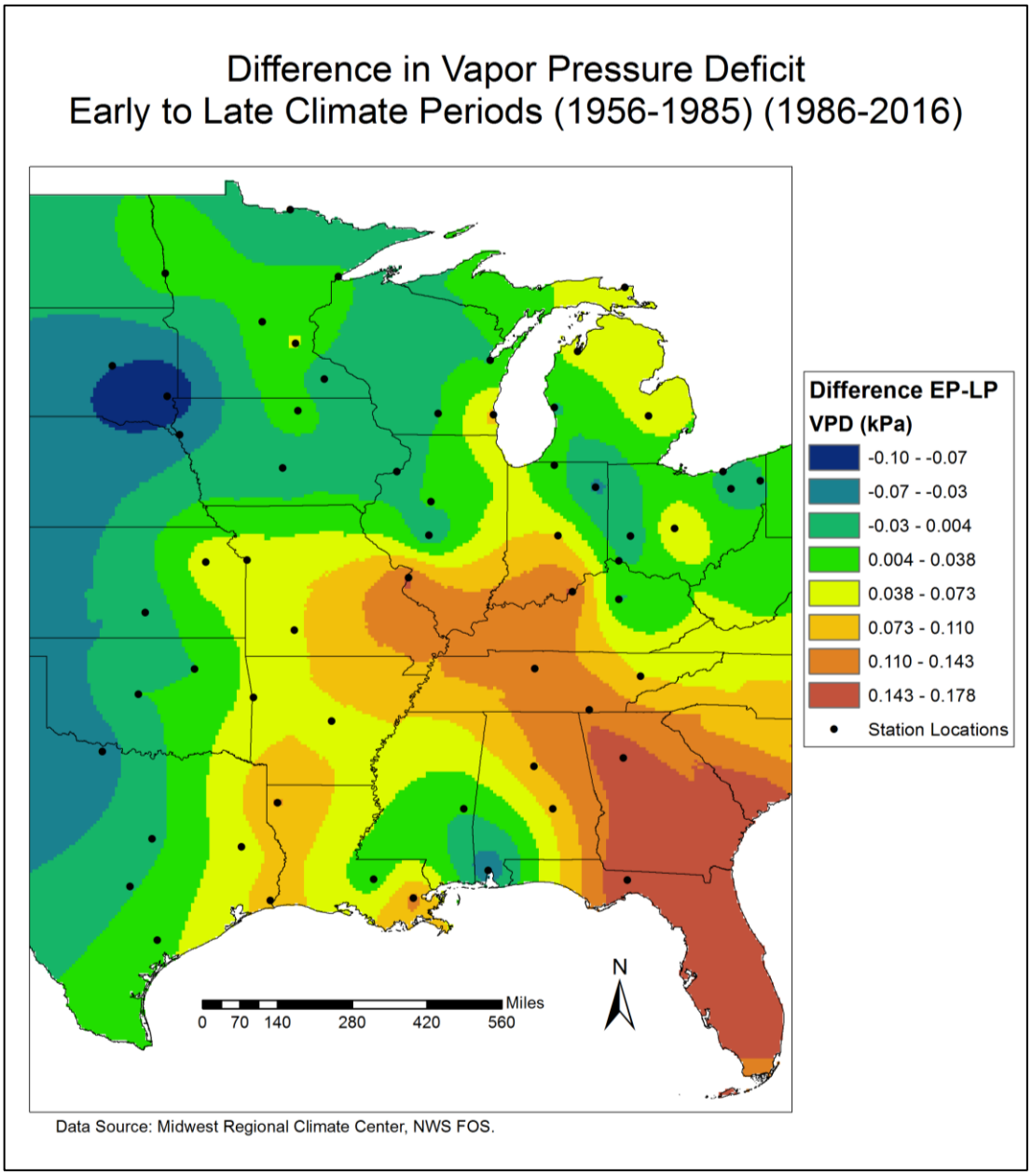

Figure 4.13 Interpolated vapor pressure deficit difference between early and late climate periods

4.3 USDA Agricultural Data Results and Discussion

Statistical analysis of meteorological records and assembly of growing season averaged dew point, maximum/minimum temperature, and VPD has indicated what spatial and temporal changes have taken place and has provided an updated regional climatology of these variables. Since the goal of this study is to link possible changes in agricultural intensification within the Midwest Corn Belt to changes occurring in regional near surface humidity, several agricultural statistics have been collected from the USDA *Census of Agriculture* for the eight-state rain-fed portion of the Corn Belt. The eight states selected include Minnesota, Iowa, Missouri, Illinois, Wisconsin, Indiana, Michigan, and Ohio. Not all of these states are top producers of corn and soybean crops, however they are all located within close spatial proximity to the core of the Corn Belt (Southern Minnesota, Iowa, Illinois, Indiana) as defined by total production bushels (Figures 4.14 and 4.15). Any changes in climatic variables from intensification will likely have influence that will be observable within all eight of these states.

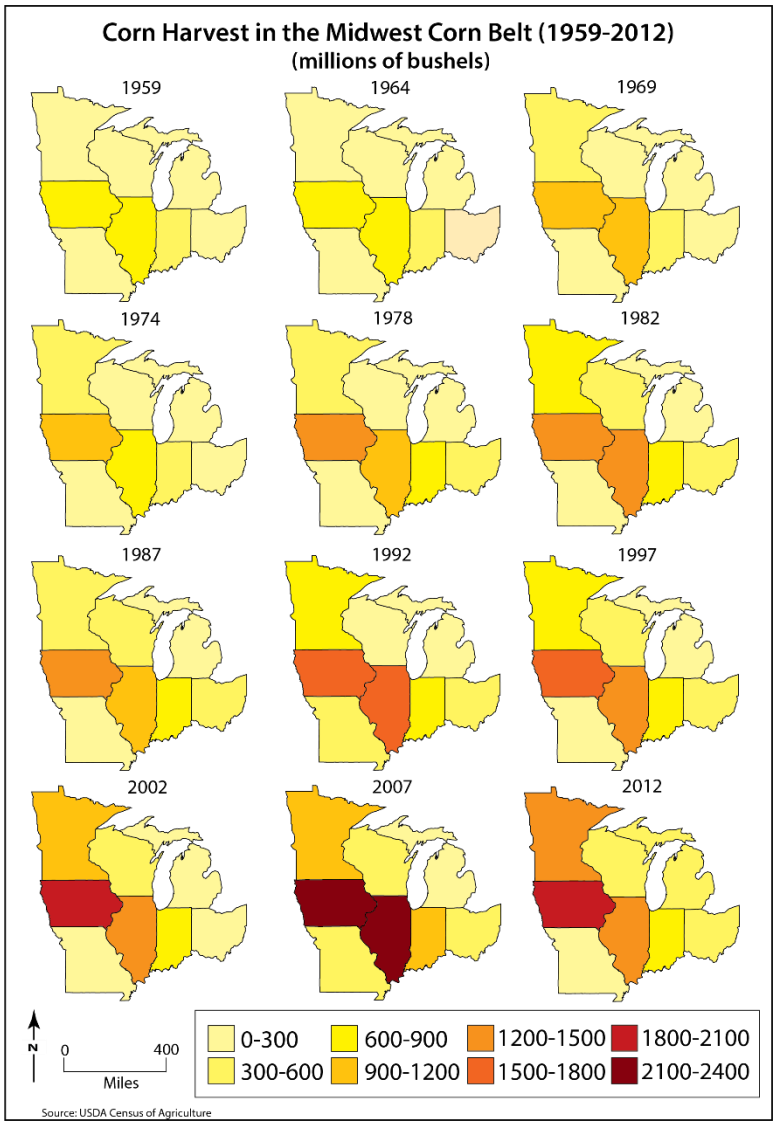

Figure 4.14 Corn harvest within the Midwest Corn Belt states (millions of bushels).

A series of additional choropleth maps have been created to show changes within several other agricultural statistics including: total cropland acres, acres of corn/soybean, and yield per acre to create a visual tool for simple comparative analysis between census years and over the study period as a whole. Since the U.S. *Census of Agriculture* is

released every four to five years, twelve census years which fall within the study period (1956-2016) were included.

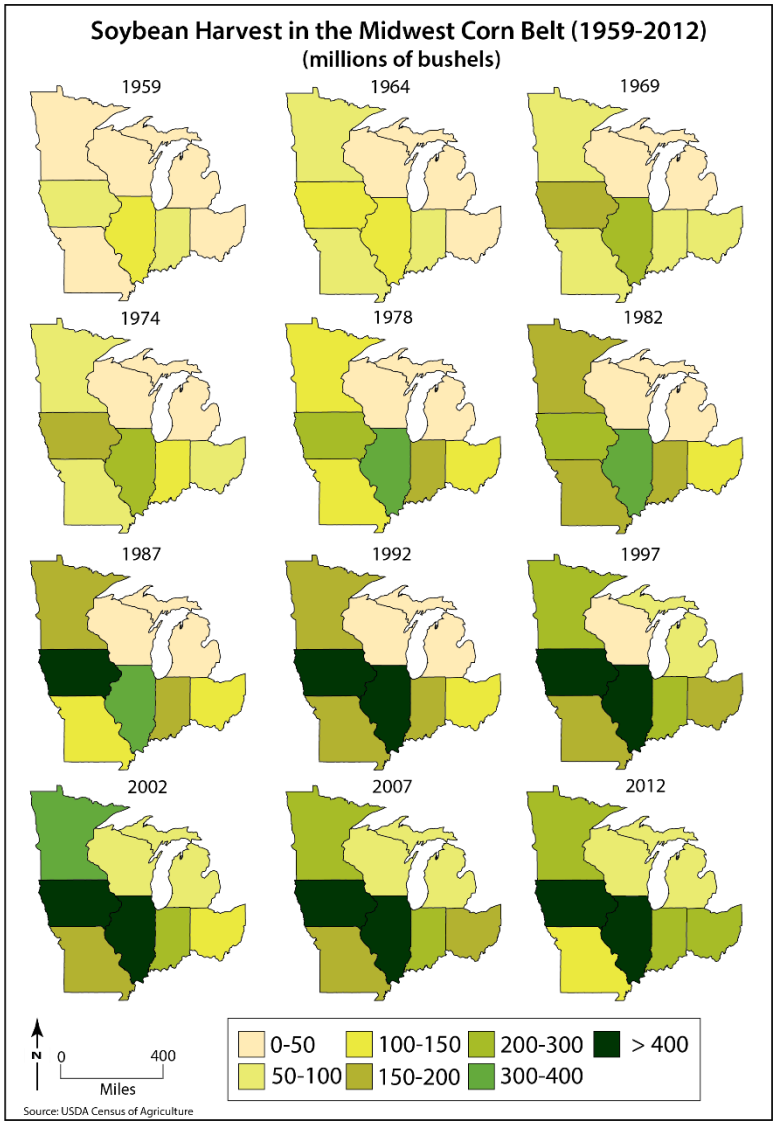

Figure 4.15 Soybean harvest within the Midwest Corn Belt states (millions of bushels).

Further analysis involved running an additional change point detection on state average dew point temperature (compiled from the average of all stations within a state) and corn/soybean production efficiency (yield per acre) to determine if any significant

changes in humidity were associated with increases in production efficiency. The first agricultural census item of interest was determining how much total land area dedicated to cropland use has changed over the study period (Figure 4.16).

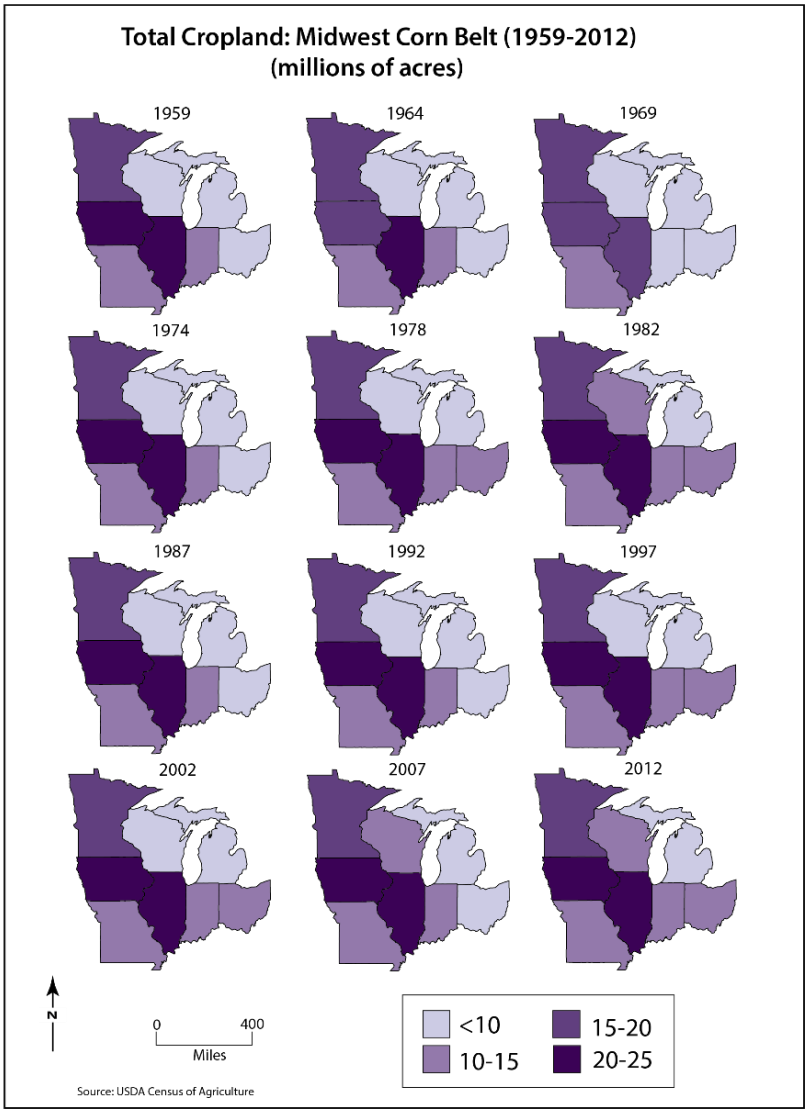

Figure 4.16 Total cropland of all types within the Midwest Corn Belt.

Total cropland within the Corn Belt states has not change dramatically over the study period while crop types have become dominated by corn and soybean with

declining wheat, oat, and forage production (Figures 4.17 and 4.18) (Johnston 2014). Soybeans have seen a larger growth in allocated acres, an occurrence likely due to the crops growing acceptance by producers after its initial importation from Western China and successful replacement of oats as a rotation crop with corn (Hudson 1994). As a

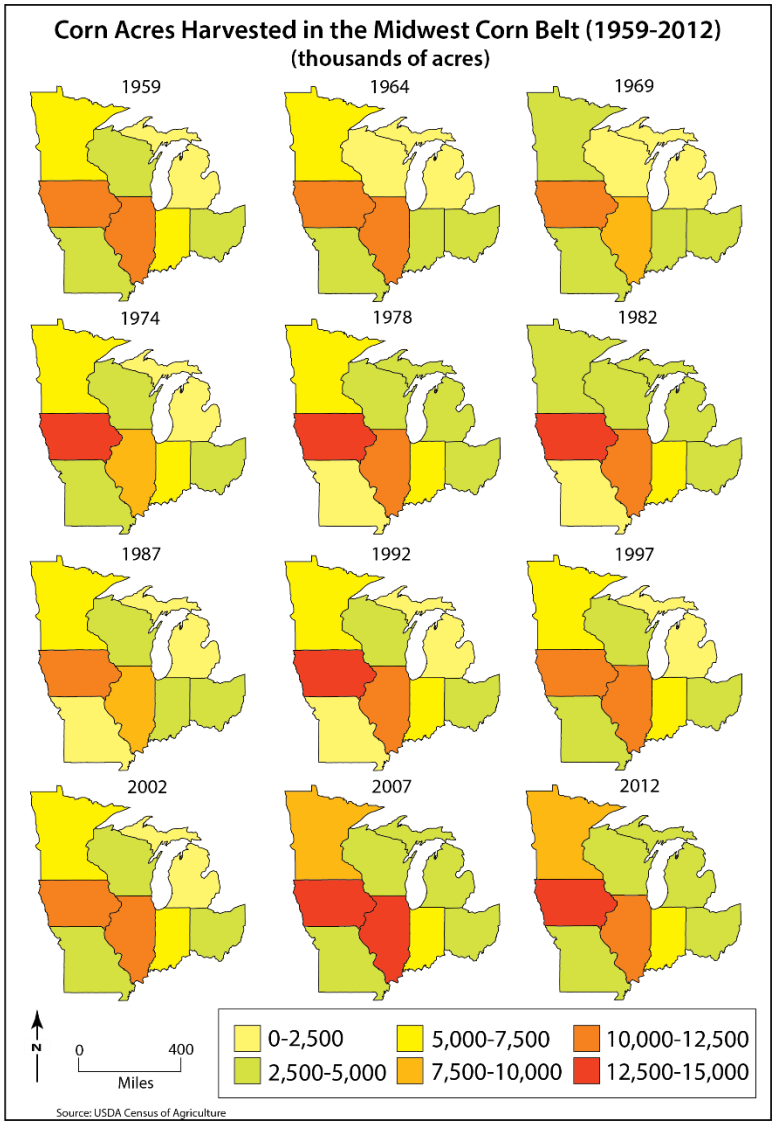

Figure 4.17 Corn acres harvested in the Midwest Corn Belt (thousands of acres).

legume, soybeans also fix nitrogen to the soil. Native to the New World (tropical Mexico), corn was grown as a crop prior to European settlement (Clampitt 2015). The transition to corn and soybean dominated agriculture is likely due to increasing market demand as both crops possess numerous uses and are easily processed into a variety of industrial products. Within the U.S. Great Plains, a shift toward more drought tolerant crops such as wheat and sunflowers has occurred. Nonetheless, irrigation schemes allow for corn/soybeans with Nebraska and Colorado serving a prime examples. With total crop acreage holding more or less steady from 1956-2016, changes occurring on the farm, in crop type, and agricultural intensification (high planting populations) are the probable causes, for an increased regional ABL humidity.

Since the 2007 *Census of Agriculture*, corn acreage has seen an increase in half of the Corn Belt states while soybean has experienced some decreasing acreage which is likely related to increased demand for ethanol production and exported feed grains which underlie higher corn prices. This may be a continued trend with legislative pushes for expanded renewable fuel sources (Mehaffey, Smith, and Van Remortel 2012) or may not persist as previously expected with cheapening natural gas and growing shale extraction technologies (Caporin and Fontini 2017).

One such indicator of changes occurring within Midwest agricultural land use has been a dramatic increase in production efficiencies resulting in higher yield per acre of corn and soybean crops (Figures 4.19 and 4.20). These increases are due to multiple factors, noted earlier in chapter two. These factors include: (1) a transition to high input

agriculture, (2) genetic improvements, biotechnology, and (3) technological developments (Hudson 1994; Clampitt 2005).

The most drastic change from a land use perspective has been the increase in planting density creating much high per acre plant populations. As discussed, this has primarily occurred through breeding selection and genetic improvements, which allow for a reduction of plant stress associated with dense stands. Other notable land use changes have been drastic increases in artificial drainage systems based on field tiling and increased fall tillage which decreases the springtime surface albedo, thereby warming soils for earlier planting.

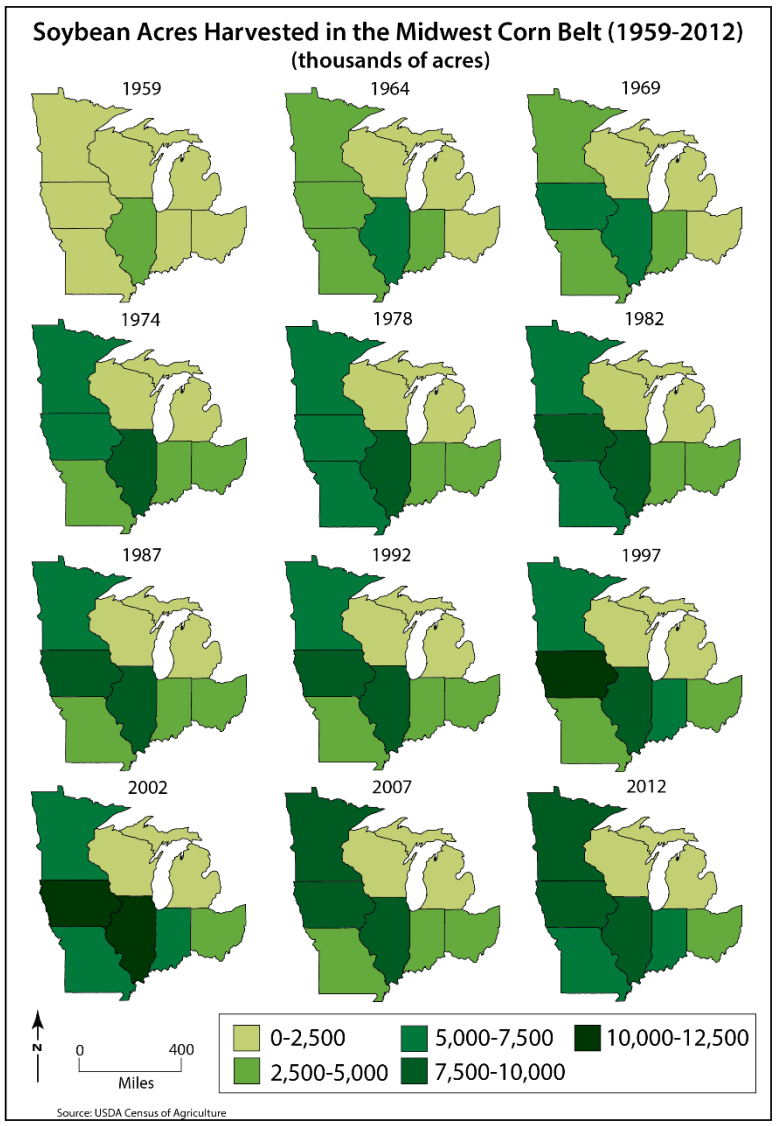

Figure 4.18 Soybean acres harvested in the Midwest Corn Belt (thousands of acres).

The improvement in production efficiency of corn has occurred across the entire Corn Belt. Yields were no greater than 80 bushels per acre prior to the 1969 Agricultural Census with yields reaching over 160 bushels per acre for the core of the region by the 2007 Agricultural Census. Much larger increases in corn yield occurred within most states between the 1974-1978 Census and again in between the 1987-1992 Census with a steady increase to modern day levels. Soybean yield over the study period is similar with

dramatic increases occurring between the 1974-1978 Census, followed by a steady rise to current yields of over 40 bushels per acre.

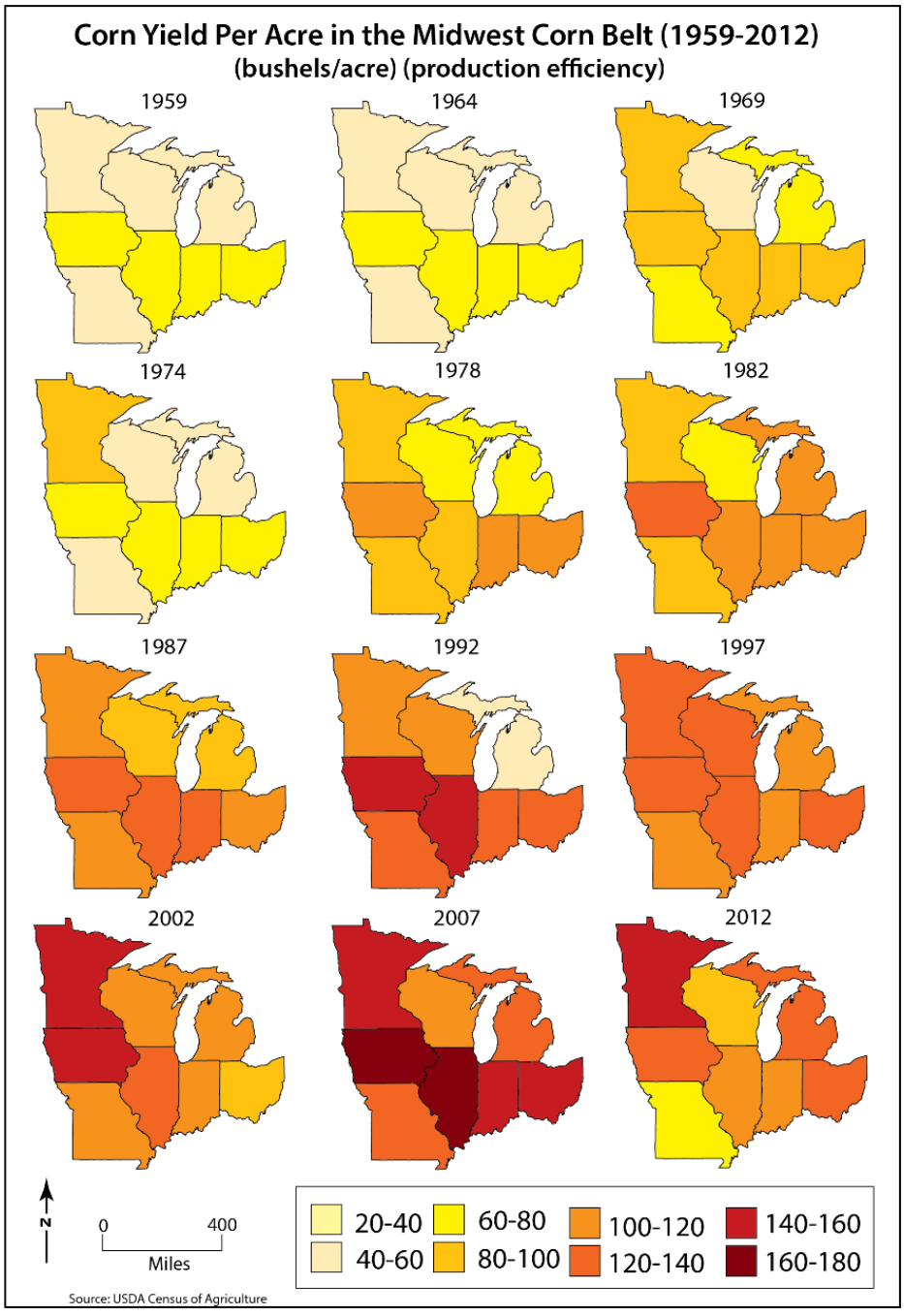

Figure 4.19 Corn yield per acre (production efficiency) within the Midwest Corn Belt.

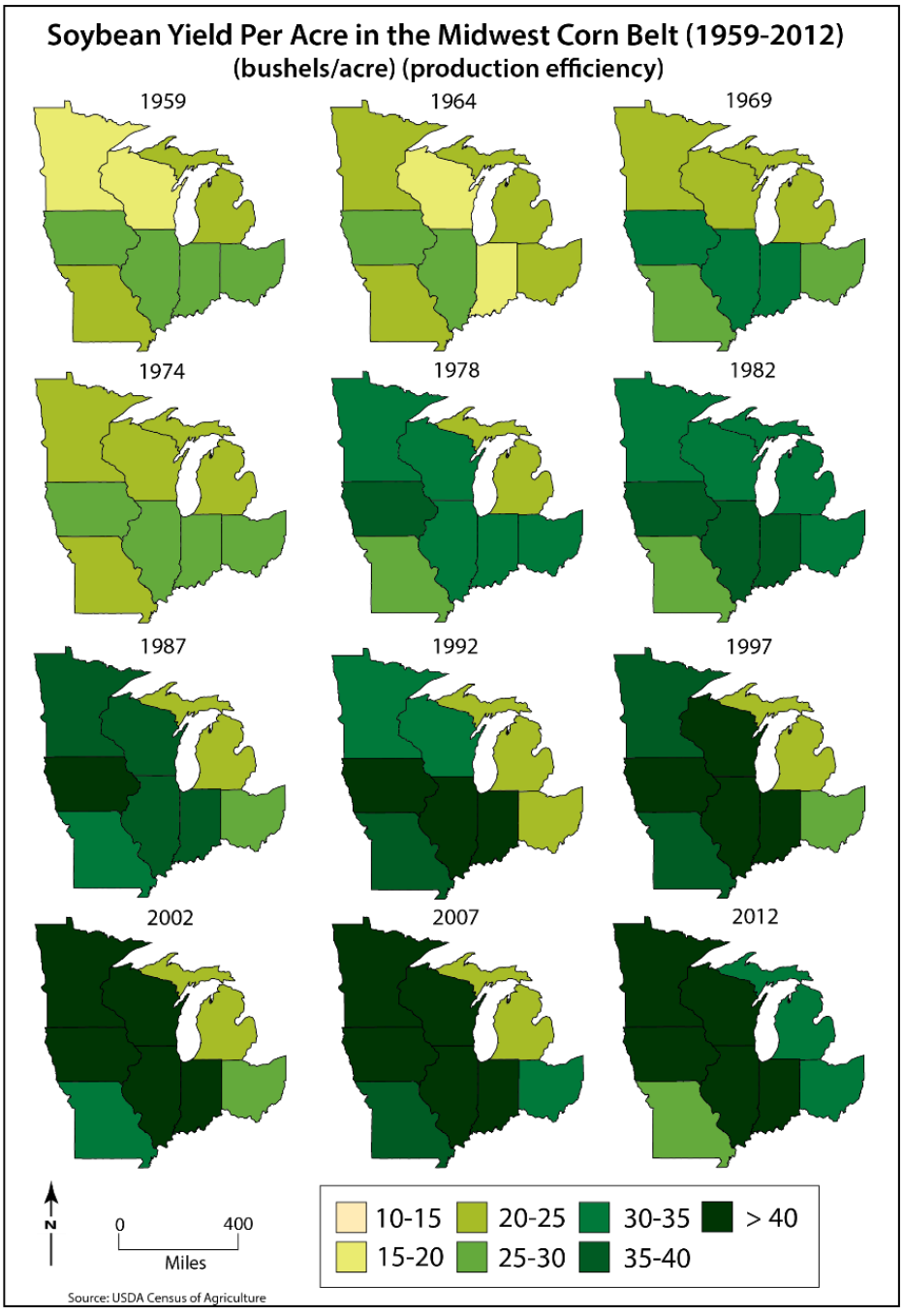

Figure 4.20 Soybean yield per acre (production efficiency) within the Midwest Corn Belt.

The chronology of these increases is further supported by the change point results comparing yield per acre with a state compiled average dew point timeseries. Sample figures are shown for Minnesota and Iowa (Figures 4.21 and 4.22). These charts are listed for each of the eight-primary study area Corn Belt states within Appendix D. This also provides the possibility of comparing significant changes in production efficiency with changes in observed dew point temperature. Results of these change point detections provide overall support for an increase in dew point coinciding with yield increases per area of land. This was especially true for the core of the Corn Belt states (Southern Minnesota, Iowa, Illinois, Indiana) where both corn and soybean yield increases coincided with dew point increases.

In terms of temporal patterns, several years in the late 1970's, particularly 1978 corresponded to the most frequent increase time in dew point temperature (Figure 4.7). Moreover, these Corn Belt states show a sustaining trend (less fluctuation) after significant increases have taken place indicating that intense corn/soybean agriculture is more or less consistent year to year in production and acreage. Consequently, elevated dew points likely buffer any major fluctuations occurring due to other influences such as shifts in summertime airmass transit patterns.

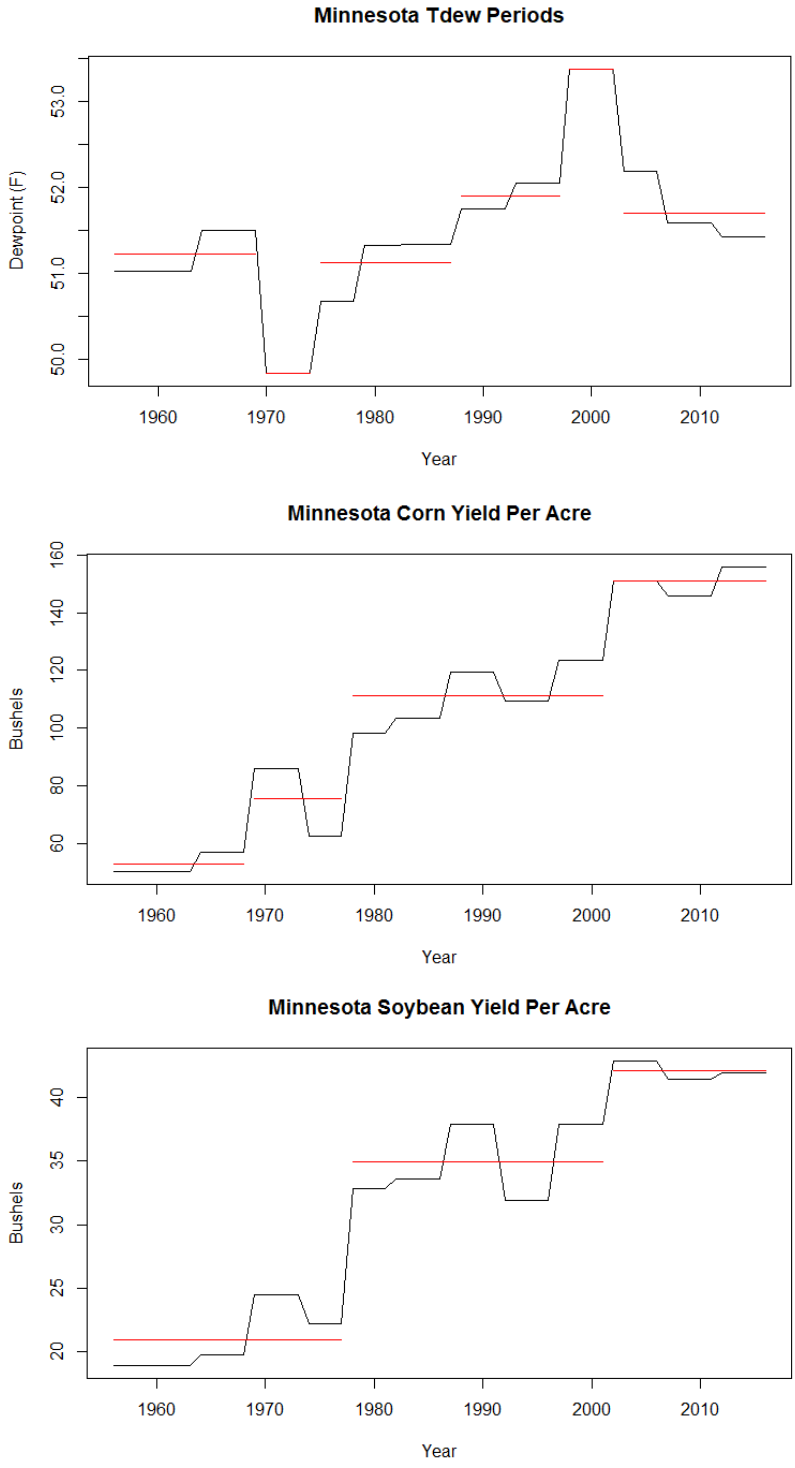

Figure 4.21 Change point results for state compiled dew point temperature aggregated to USDA Census of Agriculture periods with corn and soybean yield per acre for Minnesota.

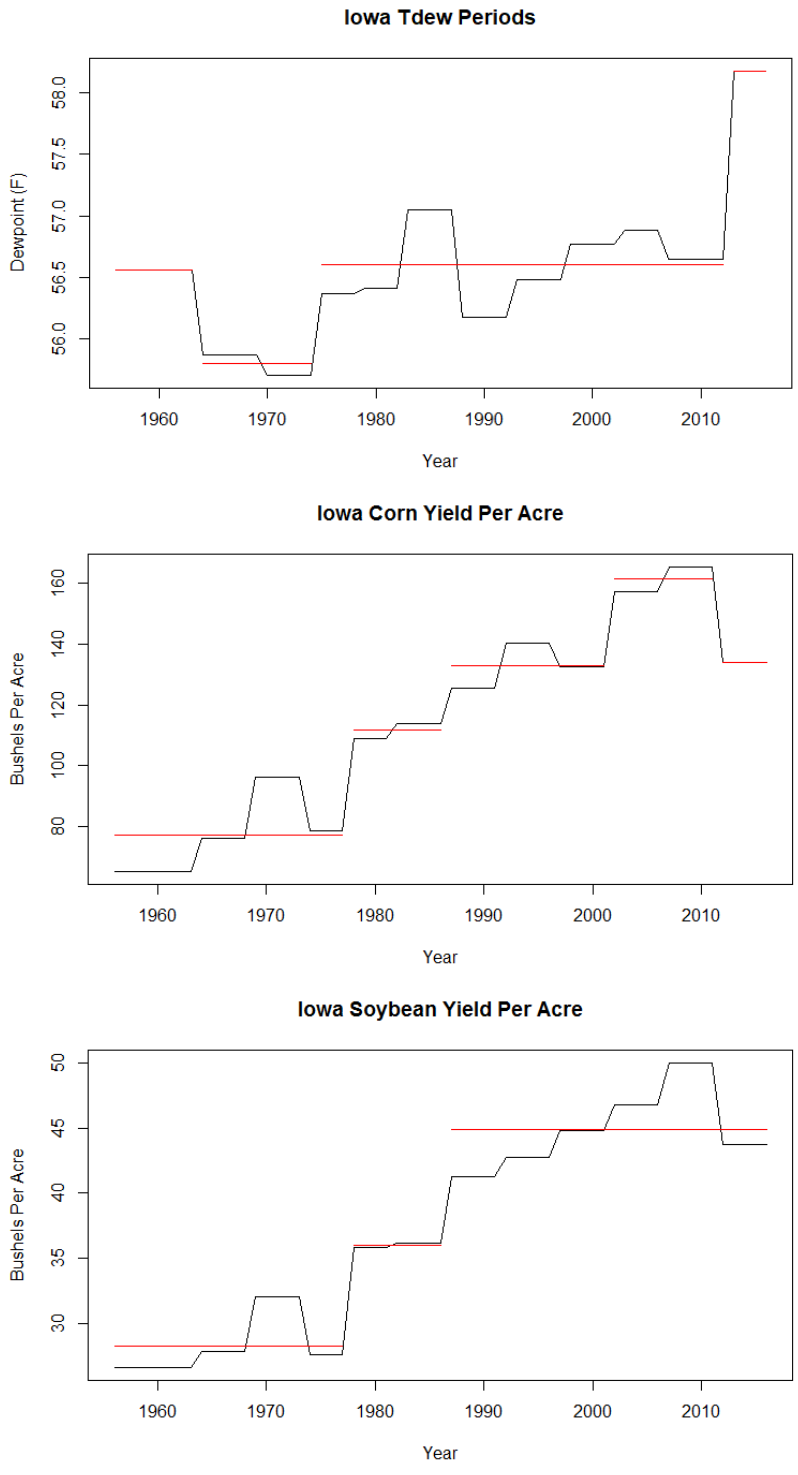

Figure 4.22 Change point results for state compiled dew point temperature aggregated to USDA Census of Agriculture periods with corn and soybean yield per acre for Iowa.

4.4 2017 Growing Season Field Work Results and Discussion (corn and soybean transpiration flux model)

Meteorological data were collected from the same municipal airport reporting station and the research fields were within close proximity to one another so precipitation events are consistent for each of the four fields. Both soybean fields had similar silty-clay soil with field capacity and PWP around 0.45 m^3/m^3 and 0.10 m^3/m^3, respectively. The corn fields consisted of the same silty-clay soil with a similar field capacity of around 0.43 m^3/m^3 and PWP of 0.09 m^3/m^3, which coincided with the soybean fields. Within all four fields, soil moisture levels remained within an acceptable range for plant availability throughout the growing season. This was further supported by the proximity to the Swan Lake wetland area which likely provided a higher water table, allowing crops access to ground water supplies by peak season root development. The highest soil moisture levels occurred on the August 22^{ed} measurement day, five days after the highest precipitation event of the summer on August 17th when 3.33 inches of rain was received. The lowest levels occurred on August 4th, although at this later stage of crop growth, root development has likely allowed for some degree of ground water extraction as above mentioned, thus reducing any associated moisture stress. Volumetric soil moisture was plotted against: (1) field capacity, which was determined prior to spring planting through laboratory analysis, (2) the estimated permanent wilting point (PWP) based of soil types, and (3) all measurable precipitation events that occurred.

This was completed for each of the four research fields that included two corn (Figures 4.23 and 4.24) and two soybean fields (Figures 4.25 and 4.26).

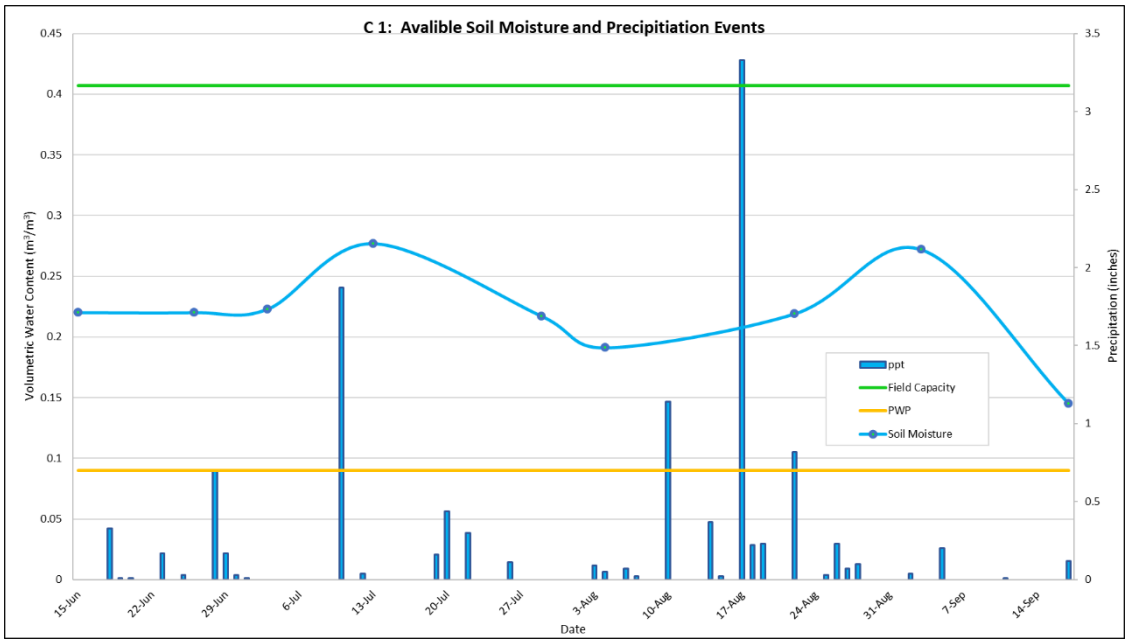

Figure 4.23 Corn field 1: available soil moisture from HH-2 moisture meter and summer precipitation events with calculated field capacity and estimated permanent wilting point based on soil type.

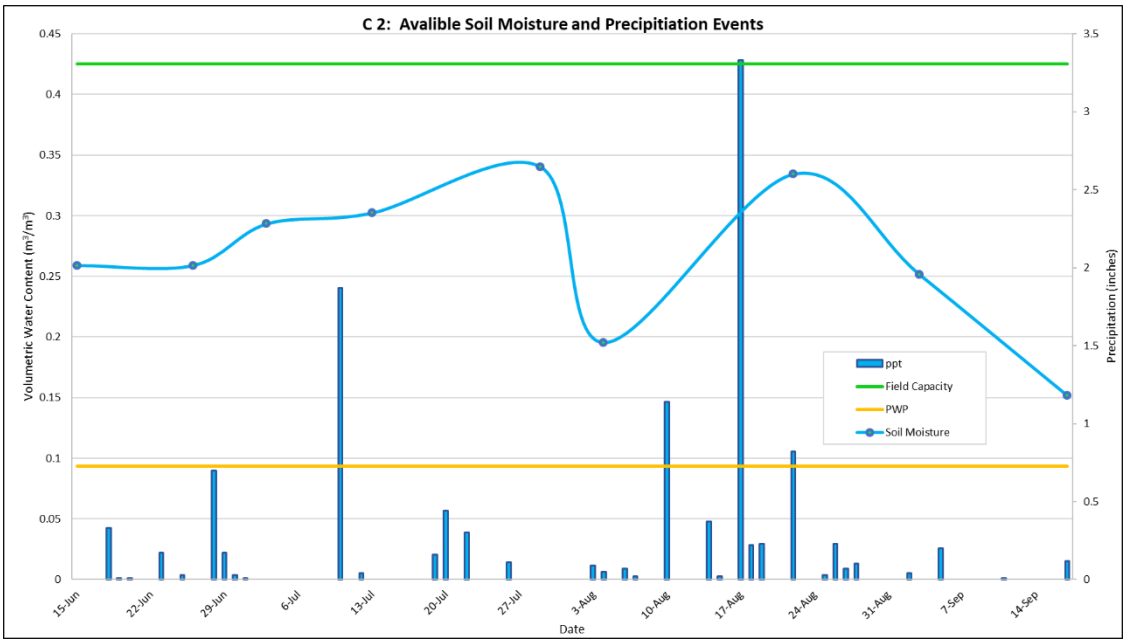

Figure 4.24 Corn field 2: available soil moisture from HH-2 moisture meter and summer precipitation events with calculated field capacity and estimated permanent wilting point based on soil type.

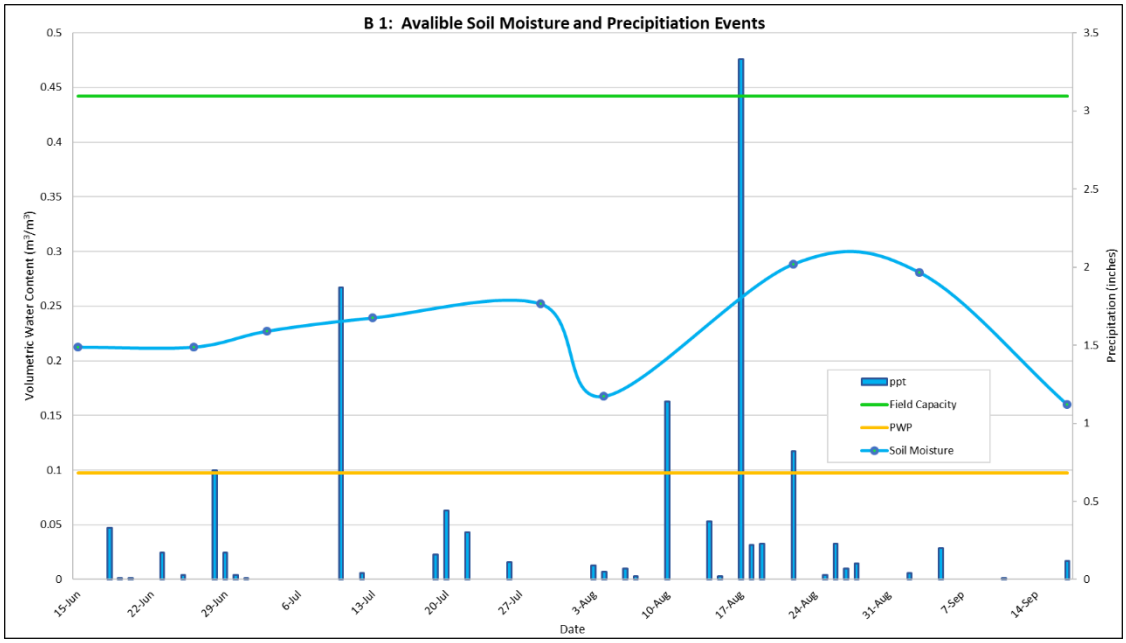

Figure 4.25 Soybean field 1: available soil moisture from HH-2 moisture meter and summer precipitation events with calculated field capacity and estimated permanent wilting point based on soil type.

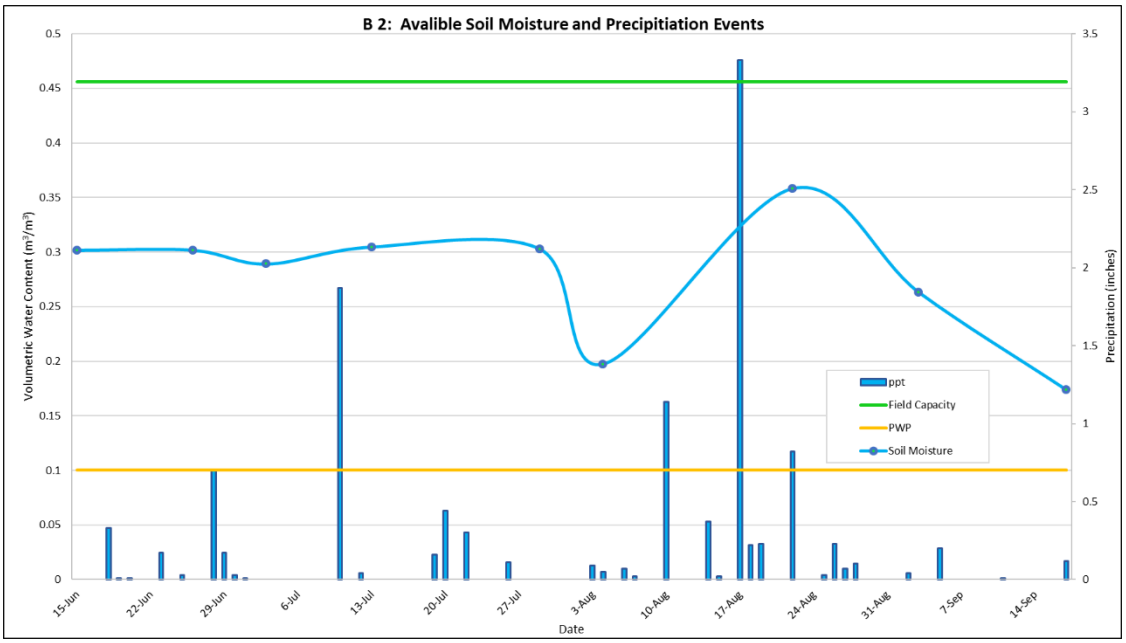

Figure 4.26 Soybean field 2: available soil moisture from HH-2 moisture meter and summer precipitation events with calculated field capacity and estimated permanent wilting point based on soil type.

While precipitation, soil type, root structure, and soil moisture availability are important physical factors influencing potential transpiration rates, other biological factors are equally important when adequate water supplies are available. The main biological factors affecting rates of transpiration which are directly related to crop development and canopy structure are: (1) the plant growth stage or leaf area index (LAI) and (2) the fraction of sunlit vs. shaded leaves within a canopy. These biological factors were key variables in accurately scaling-up leaf level transpiration rates to a canopy or whole field level. Recalling that transpiritive flux potential is directly related to how many stomates are available to preform gas exchange, most plants with a greater overall leaf area will possess more stomates, thus allowing for greater rates of exchange. Since sunlit leaves are more actively photosynthesizing, a greater rate of gas exchange is necessary to supply adequate CO_2 for carbon fixation, thus increasing transpiration rates within this portion of the canopy, with a dramatic reduction in rates associated with shaded canopy portions. The measured LAI's were graphed in Figures 4.27-4.30.

Considering the two corn fields, LAI increases initially at a slow rate when corn plants are small seedlings. During this early growth period soil surface area is often greater than plant leaf area and transpiration amounts are low. At a certain vegetative stage, nearly six weeks after planting, LAI increases at a rapid pace for a three-week period before leveling off as vegetative growth is maximized, and the canopy becomes dense and closed. At this point transpiration becomes the dominate evapotranspirative flux within these highly vegetated environments, thus serving as the main source for atmospheric boundary layer moisture. As the crop reaches maturity, LAI begins to

decrease as lower canopy leaves senesce which occurs about 15 weeks after spring planting (late summer) and continues until full senescence in fall.

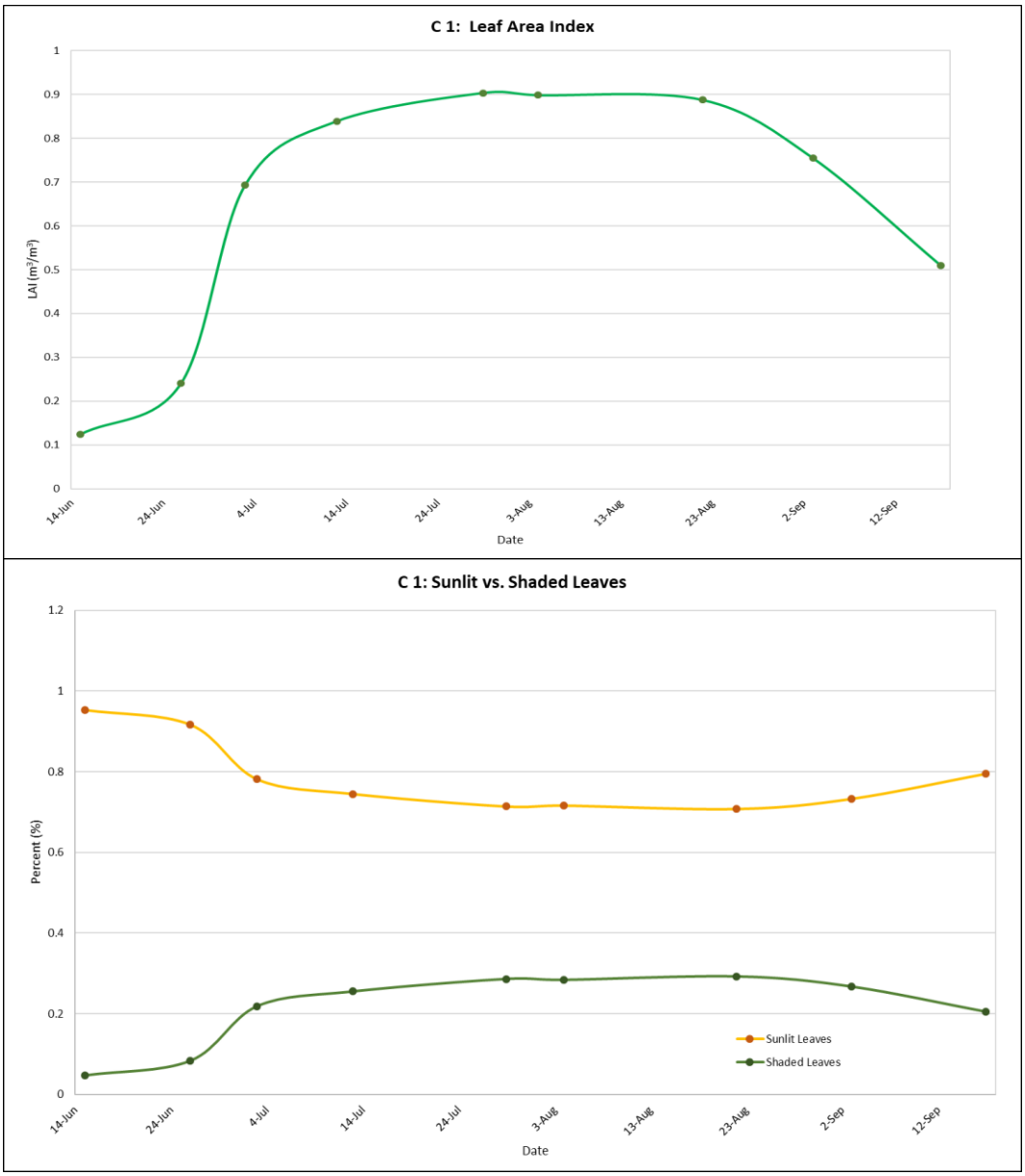

Figure 4.27 Corn field 1: measured leaf area index and calculated sunlit vs. shaded canopy fractions.

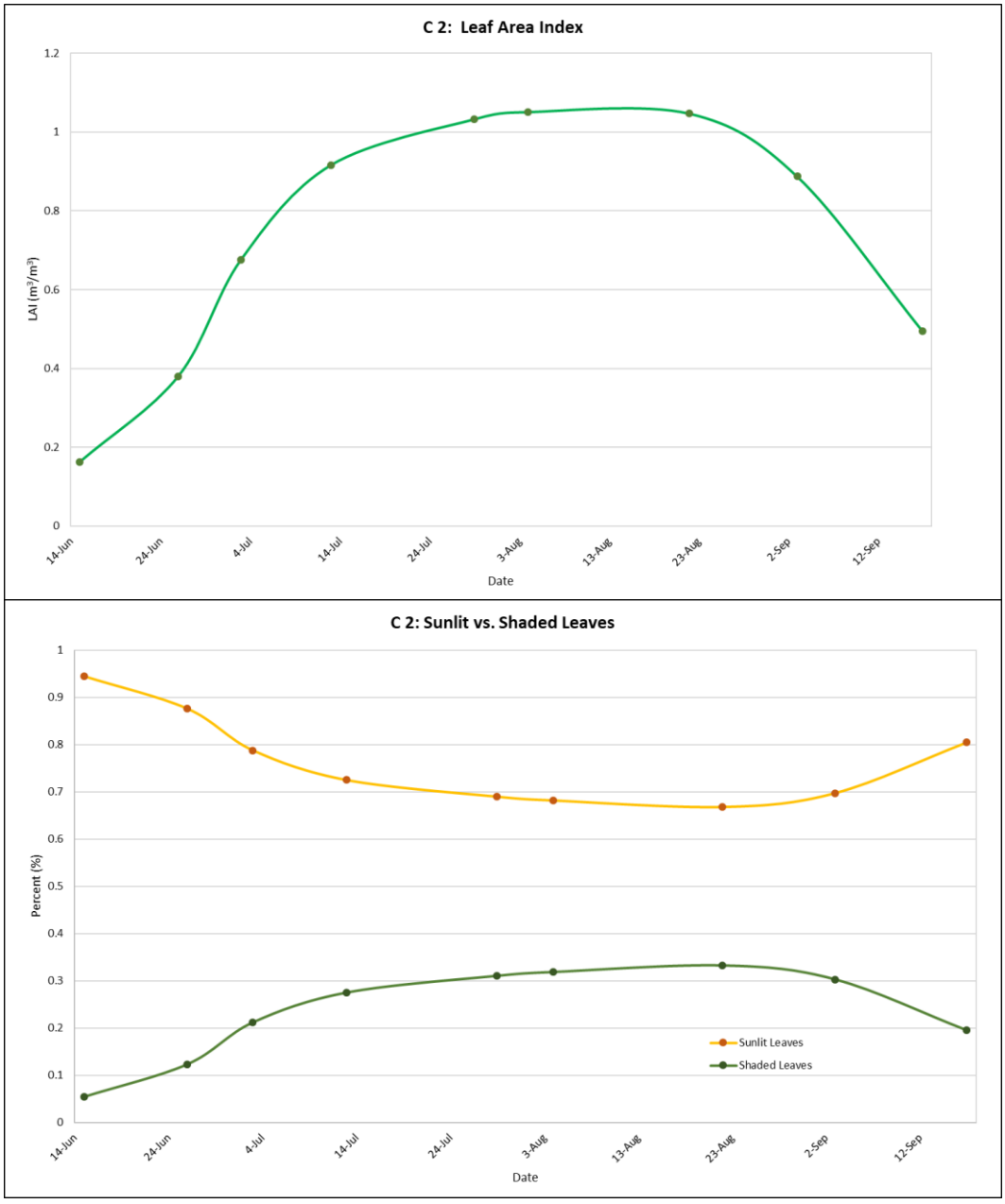

Figure 4.28 Corn field 2: measured leaf area index and calculated sunlit vs. shaded canopy fractions.

The fraction of sunlit leaves within the canopy is inversely related to LAI. During early season, when LAI is low, the fraction of sunlit leaves is much higher. As the season progresses and LAI increases the density of the canopy restricts sunlight penetration resulting in a decreased sunlit leaf fraction. This continues until LAI begins to decrease

which then allows more sunlight to reach lower leaves again. Corn is especially notable in this regard as the tall upright canopy structure of the grass family (*Poaceae*) allows for a greater fraction of sunlit leaves throughout the growing season which corresponds to higher overall transpiration rates.

Figure 4.29 Soybean field 1: measured leaf area index and calculated sunlit vs. shaded canopy fractions

Soybeans, which are more frost sensitive than corn, are planed later in the season and take much longer (around nine weeks after planting) to reach maximum leaf area. This LAI maximum only lasts around four weeks until LAI begins to slowly decrease until full fall senescence. Even more important in regard to reduced transpiritive flux

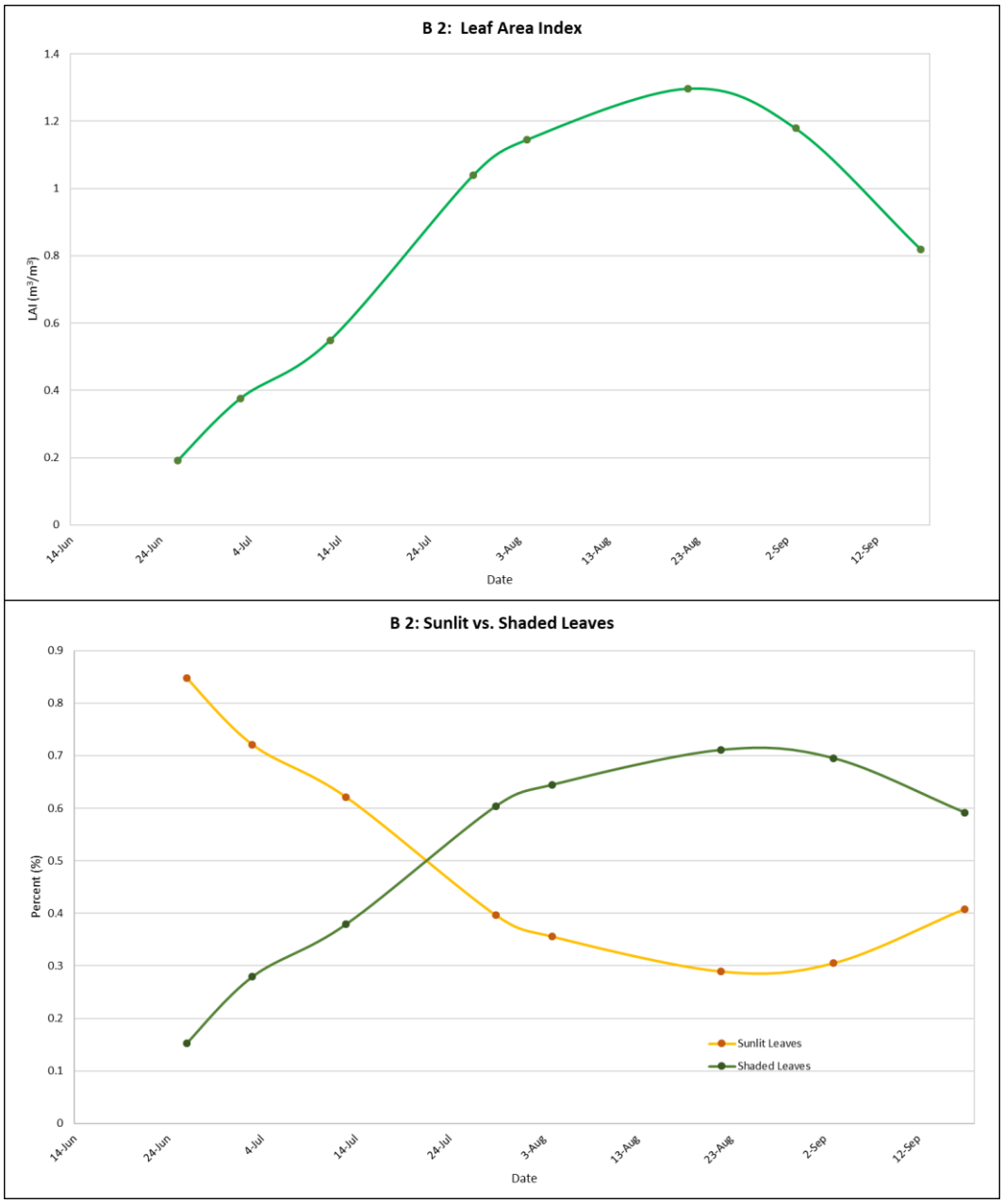

Figure 4.30 Soybean field 2: measured leaf area index and calculated sunlit vs. shaded canopy fractions.

potential, the soybeans possess a dense and short canopy structure, which drastically limits lower canopy light penetration. As the canopy starts rapid development around eight weeks after planting, the fraction of shaded leaves soon becomes greater than the sunlit portion on the canopy. This structural-biological trait typically limits soybean yield potential (Srinivasan, Kumar, and Long 2017).

The final variables of interest include atmospheric vapor pressure deficit (VPD) determined from nearby weather station temperature and humidity data, and actual plant transpiration rates after scaling up to canopy level (Figures 4.31-4.34).
Resulting transpiritive flux rates are especially dependent upon LAI during the early season, prior to peak vegetative development. The actual quantity of water lost to the surrounding environment is directly related to LAI and sunlit/shaded leaf fractions but overall is governed by atmospheric vapor pressure deficit (VPD) which is determined by current near surface air temperature and humidity. There is a large discrepancy between VPD and transpiration rates at the start of the season when crops are still in early development with low LAI. When crops reach peak LAI, VDP becomes the determining factor supporting actual rates of transpiration. Bear in mind this is contingent upon available crop soil moisture at the root zone.

Solar insulation (K↓), which plays a significant role in determining VPD through surface heating, also interacts with plants directly through the photosensitive responses of stomates, determining the degree of stomatal conductance which directly affects potential transpiration rates. The significant impact of reduced solar insulation can be seen on the July 13th measurement day (denoted with a purple star on results figures 4.31-4.34). On

this date, sky conditions were 100 percent overcast which dramatically lowered both VPD and crop transpiration to rates comparable to that of the early season when LAI was much lower.

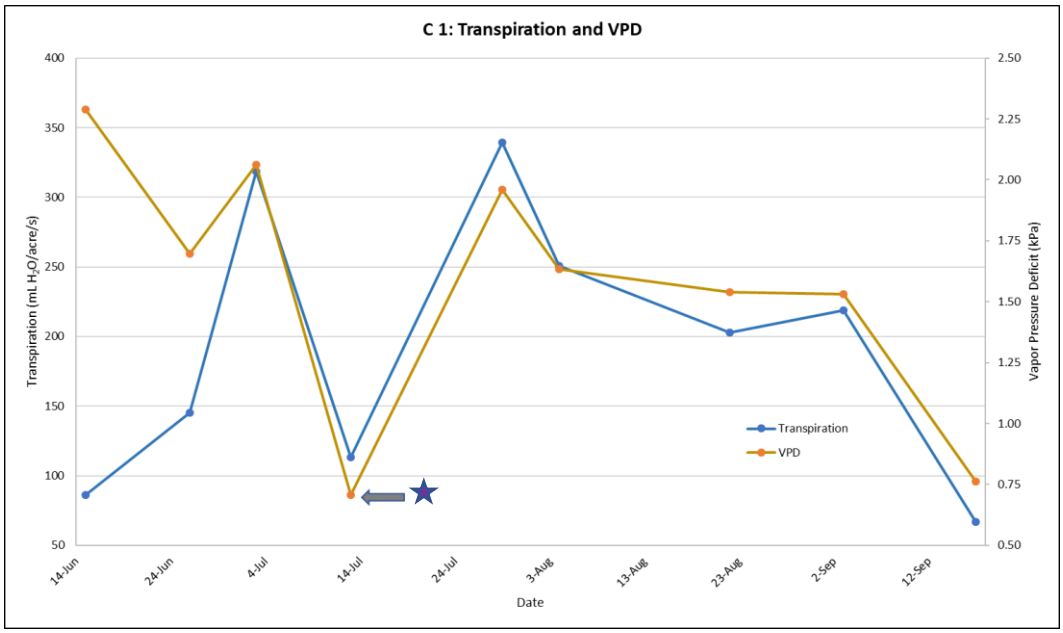

Figure 4.31 Corn field 1: Crop transpiration rates and vapor pressure deficit.

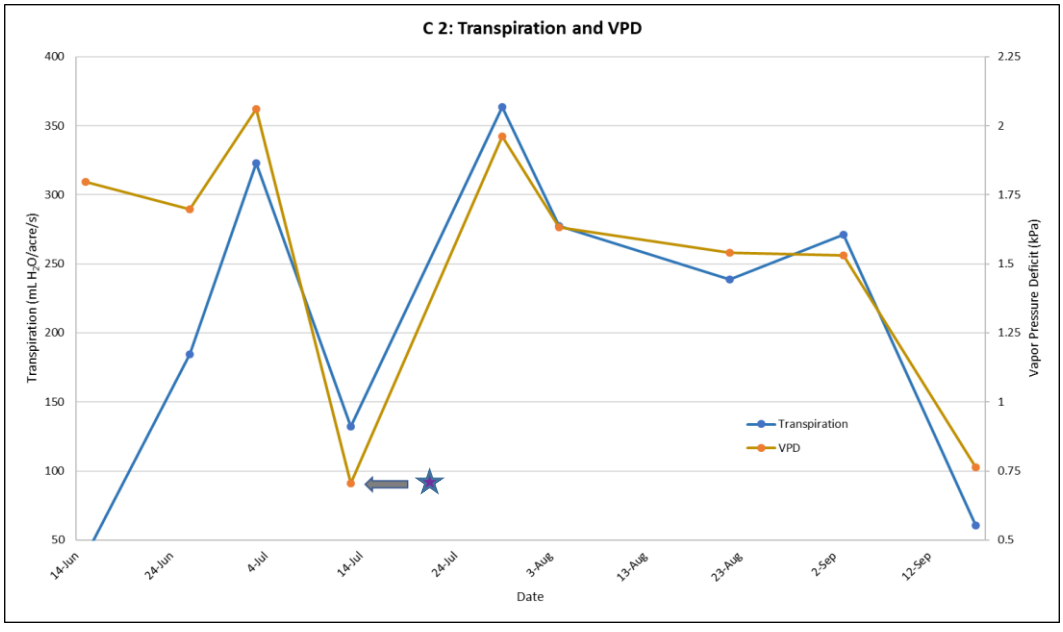

Figure 4.32 Corn field 2: Crop transpiration rates and vapor pressure deficit.

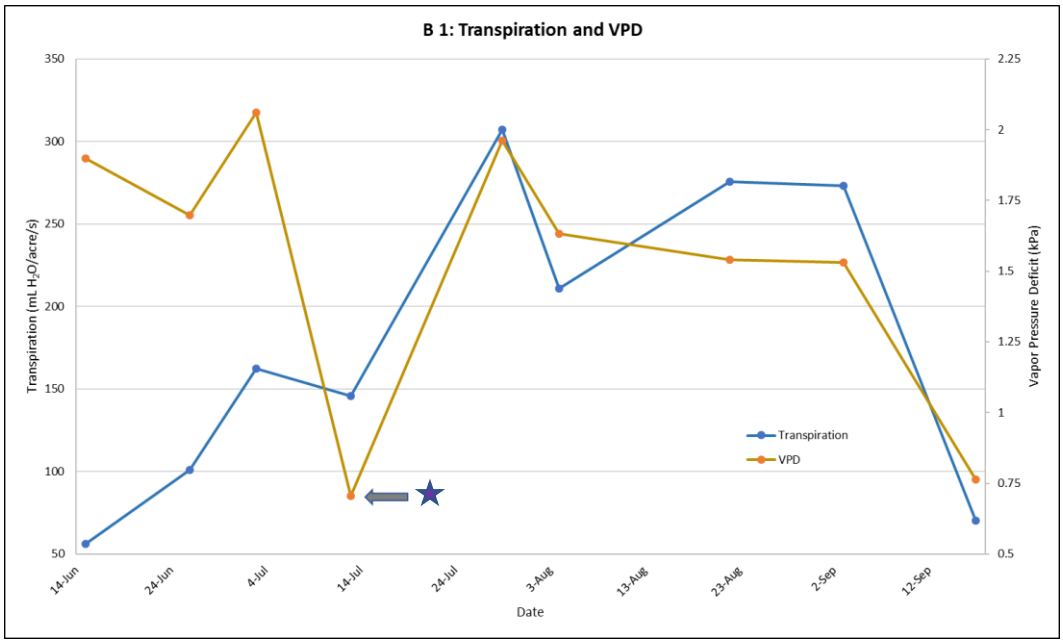

Figure 4.33 Soybean field 1: Crop transpiration rates and vapor pressure deficit.

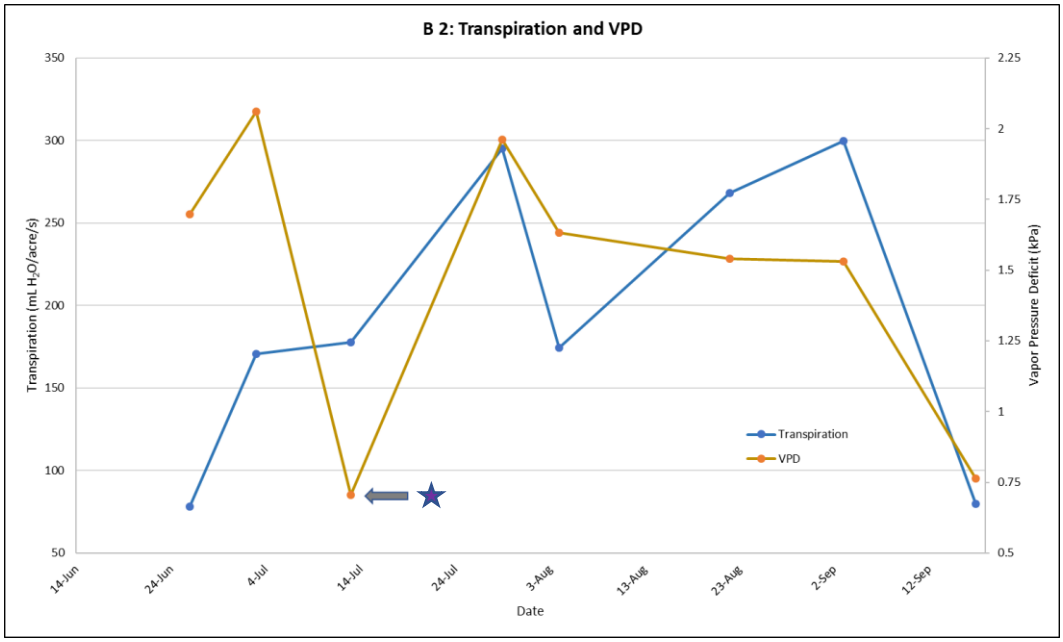

Figure 4.34 Soybean field 2: Crop transpiration rates and vapor pressure deficit.

Transpiration flux rates were converted to mL H_2O/acre/second for intuitive interpretation and comparison. During peak season, flux rates for corn were around 350 mL/acre/second and soybeans were around 300 mL/acre/second. For a typical 80-acre field size these rates translate into twenty-eight liters or just over seven gallons per second for corn and twenty-four liters or just over six gallons per second for soybean. These numbers are on par with previous estimates from the USGS Water-Science school where an acre of corn is estimated to give off between 3,000-4,000 gallons of water each day (USGS 2016). Tabulated results for all calculated and measured variables in the corn/soybean transpiritive flux model can be found within Appendix E.

These rates indeed signify a significant contribution to lower atmospheric moisture sources. If we entertain the idea of up-scaling these field size rates to cover all corn and soybean cropland within the eight state Corn Belt a very rough estimate can be attained for a regional moisture contribution. Considering within these eight states there is roughly 50.5 million acres of corn and 43.8 million acres of soybean, this translates into a combined regional contribution of 7.7 million gallons per second during peak season at midday. This rate can be placed in perspective by comparison with the average discharge rate of the Mississippi River, which is around 4.6 million gallons per second. This estimate has obvious limitations and assumes all crops are preforming similar to the research field sites located in Southern Minnesota with skies free of clouds, nonetheless this provides a starting point for estimating the impact of Midwest corn and soybean contributions relative to regional atmospheric moisture.

Study site fields were compared to surrounding fields through a remote sensing approach using both NDVI (normalized difference vegetation index) and WVC (water volume content) derived from NDWI (normalized difference water index). This resulted in five pseudo color images comparing NDVI and WVC results throughout the growing season, sample images are shown for a peak season and late season period on August 1st and September 11th, respectively for NDVI (Figures 4.35 and 4.36).

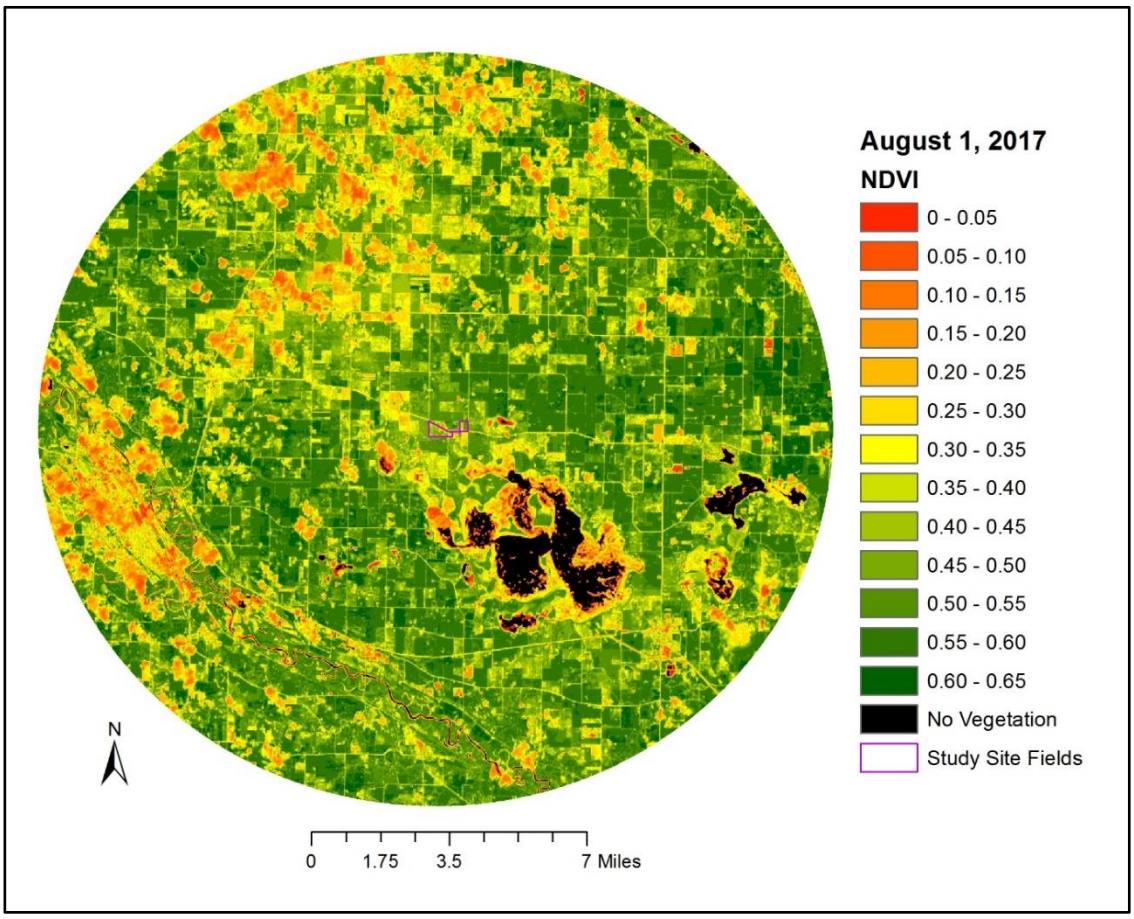

Figure 4.35 Pseudo color normalized difference vegetation index (NDVI) for August 1st, 2017, centered on field study sites.

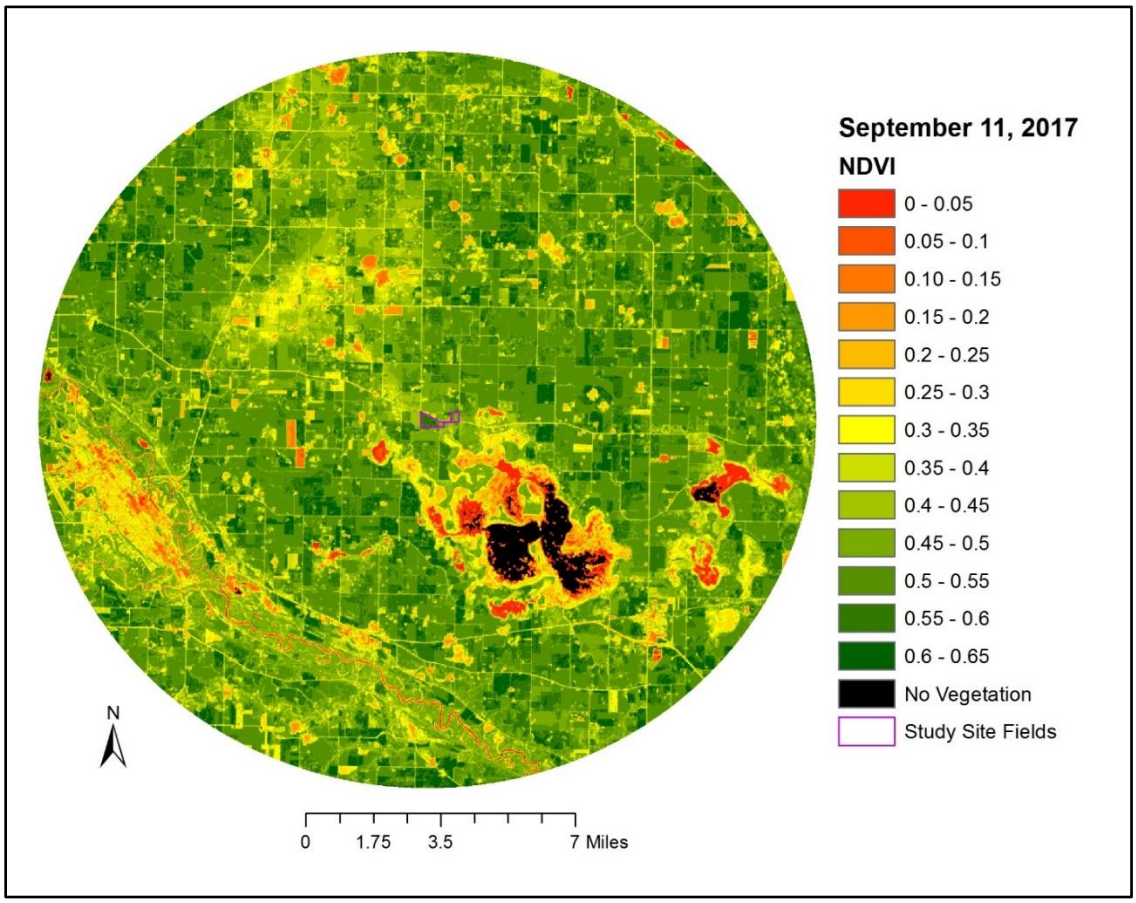

Figure 4.36 Pseudo color normalized difference vegetation index (NDVI) for September 11th, 2017, centered on field study sites.

A general land classification map was produced so crop specific water content equations could be applied (Figure 4.37). Sample images are shown for WVC for the same peak and late season periods on August 1st and September 11th, respectively (Figures 4.38 and 4.39).

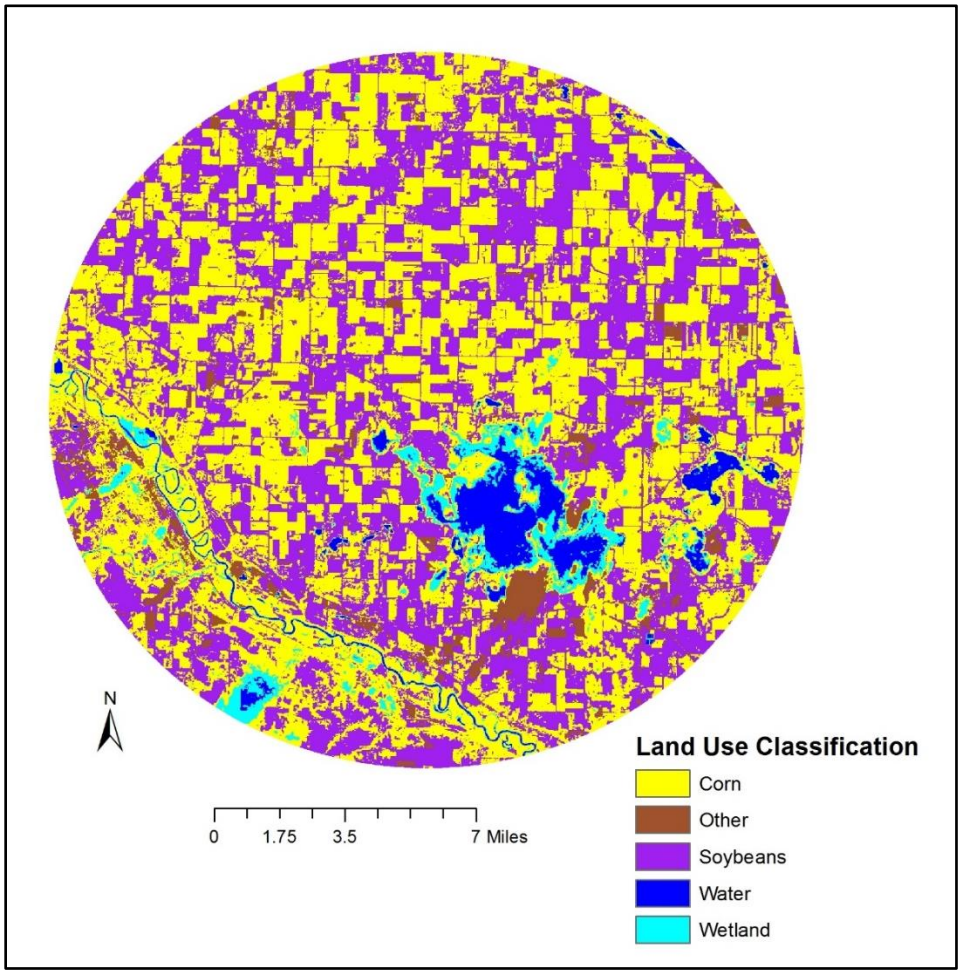

Figure 3.37 Land use classification based on September 11th Landsat-8 image.

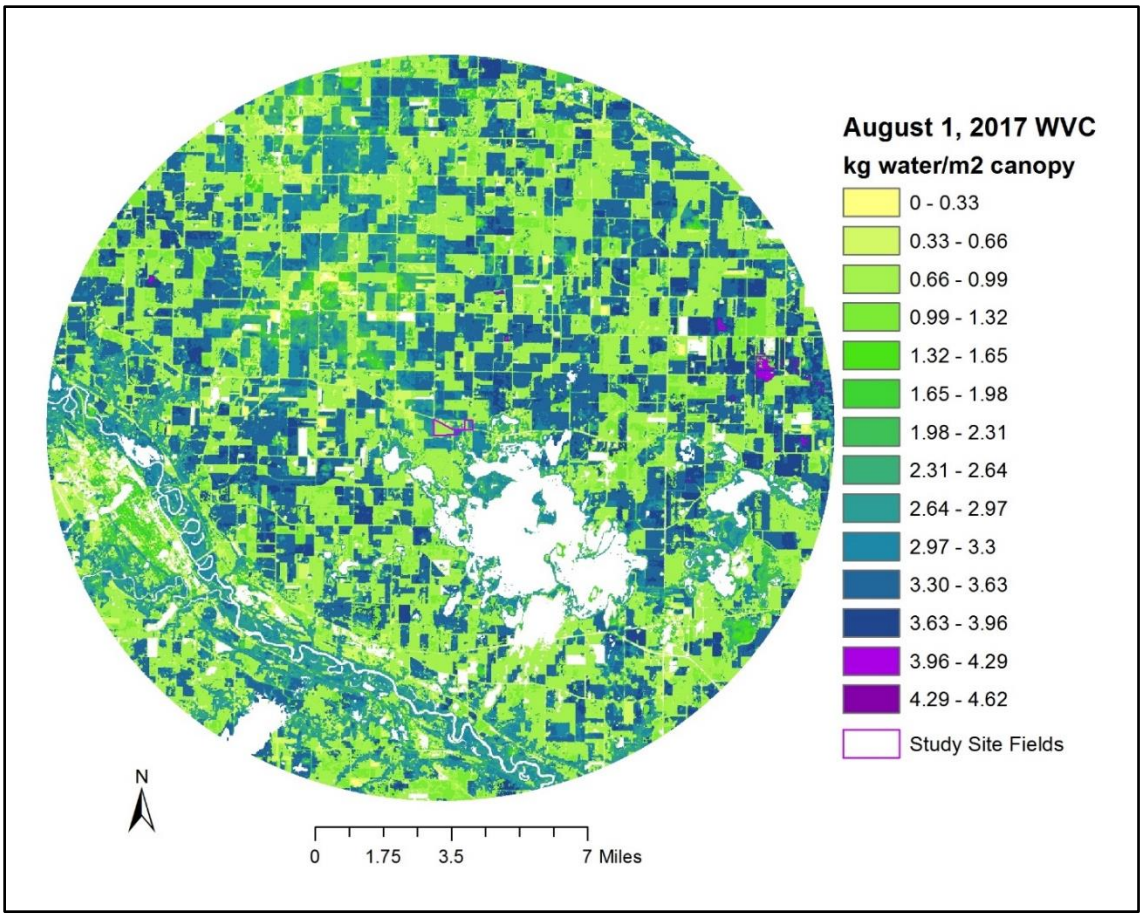

Figure 4.38 Pseudo color vegetation water volume content (WVC) on August 1st, 2017, centered on field study sites.

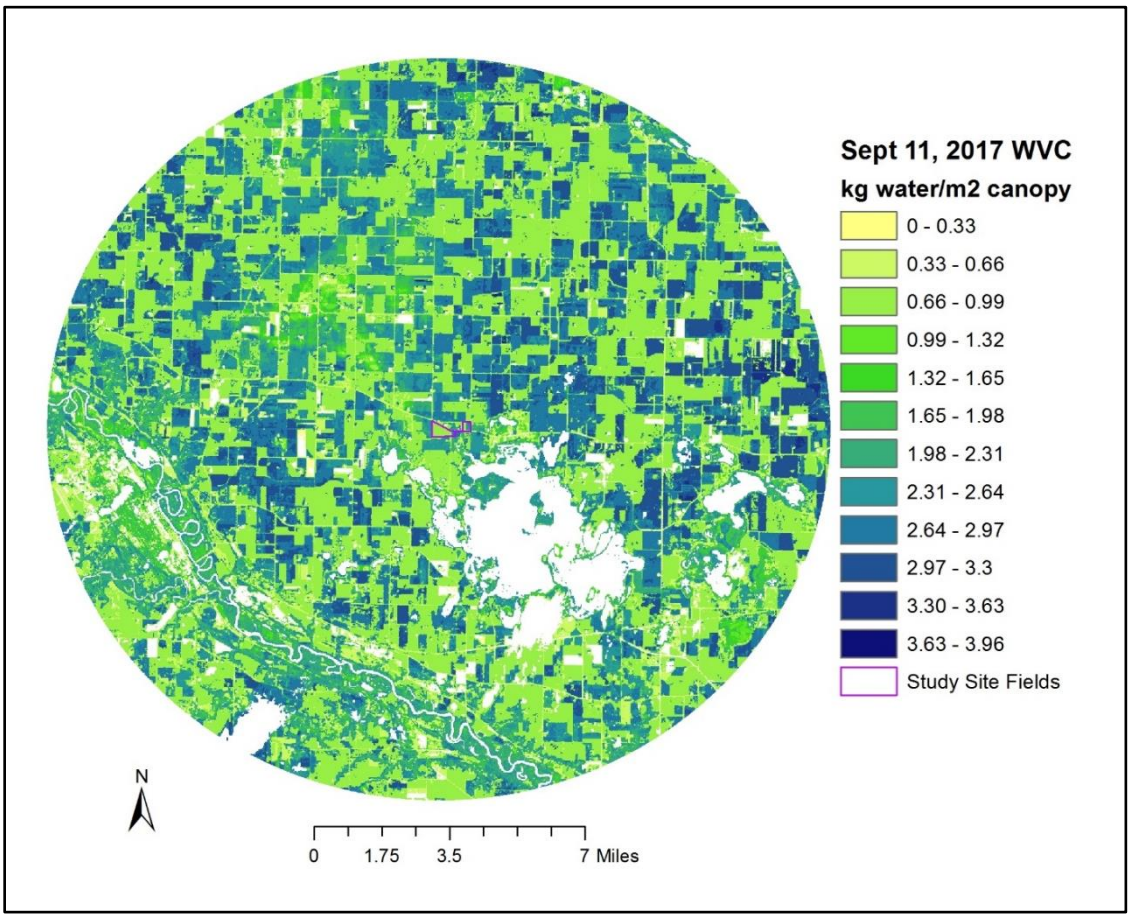

Figure 4.39 Pseudo color vegetation water volume content (WVC) on September 11th, 2017, centered on field study sites.

The first image used for field comparisons was captured on July 16th, exactly one week after a hail event had reduced NDVI values by 0.1 overall compared with unaffected fields. The calculated water volume content on July 16th was also reduced around 0.5-1 kg H_2O/m^2 crop canopy, compared to unaffected fields. Further along in the season, at peak growth stages (August 1st), the NDVI values for the corn study sites were around 0.36-0.50, compared to 0.34-0.44 for soybeans. These figures were again comparably less than surrounding fields, which were not as heavily impacted by the July

9th hail event, possessing values ranging from 0.55-0.65 for corn and 0.35-0.50 for soybeans. Considering WVC at peak season, the study site corn fields ranged from 3.0-3.3 kg H_2O/m^2 crop canopy, while study site soybean fields were around 0.8-1.0 kg H_2O/m^2 crop canopy. The surrounding corn fields contained a higher water volume content with values ranging from 3.5-3.8 kg H_2O/m^2 crop canopy, and soybean fields showing very little change from study sites, ranging from 0.8-1.0 kg H_2O/m^2 crop canopy.

This situation indicates that the hail events experienced on July 9th indeed had an impact on study site fields with NDVI values, which are based off of chlorophyll spectral reflectance and therefore more sensitive to changes in LAI, significantly lower than surrounding field sites. During the peak season (maximum LAI) image analysis on August 1st there was a 40 percent decrease in NDVI values within study site fields for corn compared to surrounding hail free areas and a 9 percent decrease in NDVI within study site fields for soybean compared to surrounding areas. WVC derived from crop specific NDWI showed a less dramatic reduction during this same peak season period with a 16 percent decrease in WVC occurring within corn study site fields and no apparent changes between soybean study site fields and surrounding areas (0 percent decrease). As such, the study site corn fields were more affected by the hail event and did not fully recover for the remainder of the growing season. On the other hand, the soybean fields recovered toward peak and end of season.

Aside from remote sensing indicators of study site crop performance, physical measurements of the LAI within study site fields provided another means of normality

comparison. Since the surrounding field areas were not sampled for LAI because of limited access and permission issues, several studies were used to compare typical LAI ranges for both corn and soybeans. The early-mid season a hail event on July 9th caused damage primarily to the corn plots which acted to reduce LAI with maximum values just over 1.0. Since corn production fields have been observed attaining LAI of around 4.0-6.0 (Nguy-Robertson et al. 2012), the study site fields underestimate actual transpiration rates, therefore providing a conservative estimate of moisture contributions. Likewise, since typical soybean fields are capable of reaching LAI values of around 3.0-5.0 (Nguy-Robertson et al. 2012), the study site plots have also likely underestimated top transpiration rates occurring within the Corn Belt, since soybean LAI maximum only reached to 1.3.

4.5 Conclusions

Examination of growing season averaged meteorological variables has provided an updated regional climatology for dew point temperature, maximum/minimum temperature, and vapor pressure deficit. This has further provided a framework to gauge both spatial and temporal changes in these variables in relation to the U.S. Midwest Corn Belt and changes occurring in agricultural land use practices over a 61-year period.

Results from the student t-test comparing early (1956-1985) and late (1986-2016) climate periods provide evidence of statistically significant increases in dew point temperature occurring within the Midwest with increases of far less magnitude or significance occurring within the U.S. South and Gulf Coast. Related variables of daily minimum temperature showed greater increases focused within the Midwest, while daily

maximum temperature indicated across the board increases, however many of these tested insignificant. Overall, daily temperature patterns support increases in atmospheric moisture. Vapor pressure deficit did not show any patterns of change between study regions, but did indicate an overall significant increase occurring within the eastern portion of both study regions and slight decreases within the core of the Corn Belt.

Moreover, the change point detection provided specific years in which significant changes in dew point occurred over the 61-year historic record for all 59 NWS FOS used in the study, with the years 1977, 1986, and 2010 being most notable. Change point was also used with a compiled state averaged dew point record for the eight state Corn Belt (primary study region) and compared with changes in corn and soybean production efficiency to indicate overall increases in dew point are associated with increases in per acre yield production. The findings included significant coincidence with increases in both dew point temperature and yield per acre during the late 1970's. Subsequently, yield per acre continued to increase within all Corn Belt states while dew point temperature remained augmented post late 1970's increase, not falling to dew point lows characteristic of pre-1970's.

A series of choropleth maps utilizing USDA *Census of Agriculture* survey data provided a means of cartographic visual comparative analysis. Results from this comparison show that overall cropland within these eight states has not substantially changed (corn and soybean acreage has only increased modestly), however, the yield per acre and intensification of crops increased markedly, which in turn links to increases in regional near surface humidity in the atmospheric boundary layer.

Field work completed during the 2017 growing season in the far northwestern boundary of the rain-fed Corn Belt provided a multi-variable mechanistic model for scaling-up leaf level transpiration measurements to canopy or field scale. This calculated per acre transpiration rate was then used to generate a rough estimate of regional moisture contributions for the entire eight-state Corn Belt occurring at midday maximums under cloud free conditions. Considering mid-season hail damage and below average LAI, the estimates from this study are likely conservative and under estimate actual transpiration rates and lower atmospheric moisture contributions from Midwest agriculture. Nonetheless, this regional estimate comprises an important first step or starting point for quantifying the impact of agricultural intensification and specifically, transpiration of water vapor relative to climate change as manifested by dew point and minimum/maximum temperature during the summer growing season.

Chapter 5: Summary

5.1 Introduction

The concluding chapter of this thesis addresses the overall success of the present study in identifying the potential direct impact of U.S. Midwest agricultural land use on local and regional climate factors. Further, 2017 fieldwork is addressed relative to the success of quantifying moisture flux contributions at a canopy level and the significance of Midwest corn and soybean agriculture as a moisture source within the regional lower atmosphere. Research findings will be summarized addressing any study limitations. Further, study implications and future research directions related to achieving an improved understanding of agricultural land use/land cover influences on larger mesoscale and synoptic circulations will be briefly addressed. Finally, the original research questions posed by this study will be re-addressed to validate the overall success of the thesis research.

5.2 Study Limitations and Implications

While this study has provided further evidence of land use impacts on climate factors, several short-comings are apparent. The observing stations chosen for data collection in this study were carefully selected based on consistent and reliable records. Despite this, over the 61-year study period other land use transformations occurring in proximity to these stations may impart influence on the data record, especially in areas which have seen large buildup of urban infrastructure. Even though these stations were previously analyzed for inhomogeneous associated with instrument changes or station

relocations, a reanalysis of these changes should be implemented and then compared to the per station change point results from this study, with consideration for near-station land use changes and observing station metadata records. This situation especially applies to the last observing station humidity sensing instrument update occurring from 1990-2000, when existing HO-83 chilled mirror dew point hygrothermometers were modified with the implementation of the Automated Surface Observing System (ASOS) (Sandstrom, Lauritsen, and Changnon 2004). Further, an improved growing season climatology could be achieved through use of other surface observing networks and integration of this data with existing data sets, although caution will need to be taken to ensure acceptable data records, free from instrumentation bias and recording errors.

Field work completed during the 2017 growing season provided a rough quantification of lower atmospheric moisture contributions from corn and soybean agriculture. Although this portion of the study filled an important gap in present climatology literature, it possesses several limitations and areas for improvement. Firstly, these readings were acquired at midday maximum transpiration rates, only on days with minimally variable cloud cover to avoid dramatic flux rate equilibrium times with the Li-6400 IRGA. To obtain a fuller picture of corn and soybean moisture contributions a method to quantify rates occurring over a 24-hour diurnal period should be implemented with considerations for cloud cover influences on conductance and transpiration rates. Secondly, this portion of the research took place in a spatially limited area (one-two square miles) and only included two corn and two soybean study site fields located within the extreme northwestern boundary of the rain-fed Corn Belt. While these limitations

have likely provided a conservative estimate of moisture contributions occurring throughout the Corn Belt in its entirety, future research should include larger transects coving the entire Midwest for a more definitive look at local variations. Multi-year data sets would also be helpful to gauge impacts associated with year to year variability, chiefly regarding soil moisture availability and precipitation patterns.

Considering the relatively recent concern involving human induced climate change dynamics, this study provides strong supporting evidence of the importance of biophysical factors when addressing such anthropogenic contributions. Concerns over climate alterations have largely focused upon biogeochemical factors acting on a global scale, most notably steadily increasing CO_2 from fossil fuel consumption. While this may be an important piece of the climate change puzzle, it does not paint the whole picture and neglects factors acting on a local and regional scale. This study has shown that dramatic moisture flux rates are occurring within agricultural cropland within the Midwest, which represents a highly modified natural environment, no longer representative of pre-settlement conditions.

5.3 Future Research Directives

Aside from future research recommendations presented in the above sections, larger climate patterns acting on the meso and synoptic scales as influenced by regional land use/land cover need to be addressed. Further research on these topics may improve our understanding of how factors acting on a localized regional scale exert influence on larger climatic processes with the potential for unrealized or not readily apparent teleconnections. While the land use drivers of regional climate impacts may be strongest

within a close spatial proximity, effects may also be manifested within larger global circulation patterns, potentially creating far reaching impacts.

5.5 Final Conclusions

In conclusion of the present study, a reaffirmation of the original research questions should be addressed to evaluate the overall success of the research:

- **What spatial and temporal changes have occurred in observed growing season dew point temperatures across the Midwest to the Gulf Coast over the 61-year study period?** Statistical analysis of growing season dew point temperature has indicated that significant increases are occurring within the Midwest Corn Belt with less significant changes occurring within the U.S. South and Gulf Coast, indicating a regional source of surface moisture, not increased maritime tropical (mT) air mass advection via the low-level jet or changes in regional pressure gradients.

- **How have other associated climate variables changed during this time, including: daily maximum temperature, daily minimum temperature, and atmospheric vapor pressure deficit?** Further statistical analysis of meteorological variables, which often show a direct relationship to lower atmospheric humidity, also indicate a significant focus on increased moisture occurring within the Midwest. Of these variables, growing season daily minimum temperatures showed the most significant increases occurring within the Midwest Corn Belt indicating a regional decrease in nocturnal longwave radiation loss.

Growing season daily maximum temperature showed overall increase across all portions of both study regions, however the majority of these increases tested statistically insignificant. Despite this, some degree of maximum temperature muting was evident within the core of the Corn Belt. Vapor pressure deficit indicated a definitive increase occurring along a north-south transect in the eastern portion of both study periods, but no focused increase was evident within the Midwest where dew point temperatures have increased the greatest.

- **How has agricultural land use changed over the study period, including: overall yields, yields per acre (production efficiency), planting population rates, and technological advancements?** Overall, land allocated to agricultural production has not increased dramatically over the study period, however intensification of farm land use practices and technological advancements have acted to impressively increase yields and production efficiencies throughout the Midwest.

- **Does a potential statistical relationship exist between elevated surface moisture variables and changes in agricultural practices and land use?** While there is inherent difficulty associated with accurately correlating changes in agricultural practices and land use with changes taking place in surface dew point temperatures, this study provides yet another strong support for this phenomenon. Overall, increases in regional dew point temperature are supported by changes occurring in agricultural production. These correlative increases were especially

evident in the late 1970's, after which regional dew point temperature remained augmented relative to the varying fluctuations evident with earlier years.

- **How much moisture are typical corn and soybean fields contributing at midday to surface humidity via stomatal conductance and transpiration processes at different developmental stages (changing leaf area) throughout the 2017 growing season?** Results from the 2017 growing season field survey measures have shown that corn and soybean agriculture within the Midwest represents a significant source for near surface regional moisture contributions. Study site fields, during peak season at midday maximums, are capable of contributing around 6 gallons/80 acres/second and 7 gallons/80 acres/second for soybean and corn, respectively. Extrapolating this mid-season flux rate to all corn and soybean cropland within the eight state Midwest Corn Belt provided a rough regional estimate of moisture contributions on the order of 7.7 million gallons/second at midday under clear-sky conditions. To place this in perspective, the average 85-year flow rate of the U.S. Mississippi River at Baton Rouge, Louisiana is around 4.6 million gallons/second (USGS 2018).

- **What effects do environmental conditions have on overall transpiration rates?** Several important controlling environmental factors were identified which dramatically influenced transpiration rates occurring in agricultural cropland. External non-plant factors included: soil moisture availability (seasonal precipitation patterns, soil type, artificial drainage systems), atmospheric vapor

pressure deficit (ambient air temperature, absolute humidity levels), turbulent air flow, and solar insolation. Internal factors at the plant level include: plant growth stage (leaf area index, rooting depth), canopy architecture (sunlit vs. shaded leaf fractions, leaf angle), and per acre plant populations.

Overall, this study has been successful in addressing all posed research questions through a comprehensive investigation of many crucial factors and review of relevant literature. Additionally, the study has provided an updated regional growing season climatology for dew point, minimum/maximum temperature, and vapor pressure deficit. These findings, combined with analysis of USDA agricultural data, has provided a probable statistical link to changes occurring in near surface atmospheric humidity associated with agricultural intensification. Fieldwork results further support these findings by showing the dramatic moisture flux rates acting as a local/regional atmospheric moisture source.

Figure 5.1 Field work assistant during early-season diurnal flux rate measurements.

References

Aalto, J., P. Pirinen, J. Heikkinen, and A. Venäläinen. 2013. Spatial interpolation of monthly climate data for Finland: comparing the performance of kriging and generalized additive models. *Theoretical and Applied Climatology* 112 (1):99-111.

Adegoke, J. O., R. Pielke Sr, and A. M. Carleton. 2007. Observational and modeling studies of the impacts of agriculture-related land use change on planetary boundary layer processes in the central U.S. *Agricultural and Forest Meteorology* 142 (2–4):203-215.

Alan, M. 2004. *Engineering in a Land-Grant Context : The Past, Present and Future of an Idea*. West Lafayette, US: Purdue University Press.

Alexander, P., M. D. A. Rounsevell, C. Dislich, J. R. Dodson, K. Engström, and D. Moran. 2015. Drivers for global agricultural land use change: The nexus of diet, population, yield and bioenergy. *Global Environmental Change* 35:138-147.

Anderson, H. L. 2011. That Settles It: The Debate and Consequences of the Homestead Act of 1862. *The History Teacher* 45 (1):117-137.

Angelini, I. M., M. Garstang, R. E. Davis, B. Hayden, D. R. Fitzjarrald, D. R. Legates, S. Greco, S. Macko, and V. Connors. 2011. On the coupling between vegetation and the atmosphere. *Theoretical and Applied Climatology* 105 (1):243-261.

Arnfield, A. J. 2003. Two decades of urban climate research: a review of turbulence, exchanges of energy and water, and the urban heat island. *International Journal of Climatology* 23 (1):1-26.

Atlin, G. N., J. E. Cairns, and B. Das. 2017. Rapid breeding and varietal replacement are critical to adaptation of cropping systems in the developing world to climate change. *Global Food Security* 12:31-37.

Beerling, D. J. 2005. Evolutionary Responses of Land Plants to Atmospheric CO2. In *A History of Atmospheric CO2 and Its Effects on Plants, Animals, and Ecosystems*, eds. I. T. Baldwin, M. M. Caldwell, G. Heldmaier, R. B. Jackson, O. L. Lange, H. A. Mooney, E. D. Schulze, U. Sommer, J. R. Ehleringer, M. Denise Dearing and T. E. Cerling, 114-132. New York, NY: Springer New York.

Bentley, M. L., and J. A. Stallins. 2008. Synoptic evolution of Midwestern US extreme dew point events. *International Journal of Climatology* 28 (9):1213-1225.

Betts, R. A. 2001. Biogeophysical impacts of land use on present-day climate: near-surface temperature change and radiative forcing. *Atmospheric Science Letters* 2 (1):39-51.

Bishop-Williams, K. E., O. Berke, D. L. Pearl, and D. F. Kelton. 2015. Mapping dairy cow heat stress in southern Ontario-A common geographic pattern from 2010-2012. *Journal of Epidemiology and Community Health* 69 (1):A4.3-A5.

Bonan, G. B. 1997. Effects of Land Use on the Climate of the United States. *Climatic Change* 37 (3):449-486.

———. 2001. Observational Evidence for Reduction of Daily Maximum Temperature by Croplands in the Midwest United States. *Journal of Climate* 14 (11):2430-2442.

Bornstein, R., and Q. Lin. 2000. Urban heat islands and summertime convective thunderstorms in Atlanta: three case studies. *Atmospheric Environment* 34 (3):507-516.

Bounoua, L., R. DeFries, G. J. Collatz, P. Sellers, and H. Khan. 2002. Effects of Land Cover Conversion on Surface Climate. *Climatic Change* 52 (1):29-64.

Bradshaw, J. E. 2017. Plant breeding: past, present and future. *Euphytica* 213 (3):60.

Brookes, G. 2014. Weed control changes and genetically modified herbicide tolerant crops in the USA 1996–2012. *GM Crops & Food* 5 (4):321-332.

Brooks, C. B., and A. I. Marcus. 2015. The Morrill Mandate and a New Moral Mandate. *Agricultural History* 89 (2):247-262.

Broothaerts, W., H. J. Mitchell, B. Weir, and S. Kaines. 2005. Gene transfer to plants by diverse species of bacteria. *Nature* 433 (7026):629-633.

Brown, P. J., and A. T. DeGaetano. 2013. Trends in U.S. Surface Humidity, 1930-2010. *Journal of Applied Meteorology & Climatology* 52 (1):147-163.

Brubaker, K. L., D. Entekhabi, and P. Eagleson. 1993. Estimation of continental precipitation recycling. *Journal of Climate* 6 (6):1077-1089.

Bunce, J. 1997. Does transpiration control stomatal responses to water vapour pressure deficit? *Plant, Cell & Environment* 20 (1):131-135.

Burrough, P. A. 1986. Principles of geographical information systems for land resources assessment. *Geocarto International* 1(3):54.

Caporin, M., and F. Fontini. 2017. The long-run oil–natural gas price relationship and the shale gas revolution. *Energy Economics* 64 (supplement C):511-519.

Cencus-Bureau, U. S. 2017. *TIGER products* 2017 [cited 12/6/2017]. Available from https://www.census.gov/geo/maps-data/data/tiger.html.

Cess, R. D. 2005. Water Vapor Feedback in Climate Models. *Science* 310 (5749):795-796.

Changnon, D., M. Sandstrom, and M. Bentley. 2006. Midwestern High Dew Point Events 1960-2000. *Physical Geography* 27 (6):494-504.

Changnon, D., M. Sandstrom, and C. Schaffer. 2003. Relating changes in agricultural practices to increasing dew points in extreme Chicago heat waves. *Climate Research* 24 (3):243-254.

Chen, B., Z. Fu, Y. Pan, J. Wang, and Z. Zeng. 2010. Single leaf area measurement using digital camera image. Paper read at International Conference on Computer and Computing Technologies in Agriculture.

Chen, D., J. Huang, and T. J. Jackson. 2005. Vegetation water content estimation for corn and soybeans using spectral indices derived from MODIS near- and short-wave infrared bands. *Remote Sensing of Environment* 98 (2–3):225-236.

Clampitt, C. 2015. *Midwest maize: how corn shaped the U.S. heartland*. Urbana: University of Illinois Press.

Clarkson, J. P., L. Fawcett, S. G. Anthony, and C. Young. 2014. A Model for Sclerotinia sclerotiorum Infection and Disease Development in Lettuce, Based on the Effects of Temperature, Relative Humidity and Ascospore Density. *PLOS ONE* 9 (4):e94049.

Coale, F. J., J. J. Meisinger, and W. J. Wiebold. 1985. Effects of plant breeding and selection on yields and nitrogen fixation in soybeans under two soil nitrogen regimes. *Plant and Soil* 86 (3):357-367.

Cohen, J. E. 2003. Human Population: The Next Half Century. *Science* 302 (5648):1172-1175.

Conkin, P. K. 2008. *A revolution down on the farm : the transformation of American agriculture since 1929*. Lexington, Ky.: University Press of Kentucky.

Cox, W. J., and J. H. Cherney. 2011. Growth and Yield Responses of Soybean to Row Spacing and Seeding Rate *Agronomy Journal* 103 (1):123-128.

Dai, A., and K. E. Trenberth. 1999. Effects of Clouds, Soil Moisture, Precipitation, and Water Vapor on Diurnal Temperature Range. *Journal of Climate* 12 (8):2451-2473.

Dai, Y., R. E. Dickinson, and Y.-P. Wang. 2004. A Two-Big-Leaf Model for Canopy Temperature, Photosynthesis, and Stomatal Conductance. *Journal of Climate* 17 (12):2281-2299.

Davis, R. E., P. C. Knappenberger, P. J. Michaels, and W. M. Novicoff. 2003. Changing heat-related mortality in the United States. *Environmental Health Perspectives* 111 (14):1712-1718.

Defries, R. S., L. Bounoua, and G. J. Collatz. 2002. Human modification of the landscape and surface climate in the next fifty years. *Global Change Biology* 8 (5):438-458.

Desjardins, R. L., M. V. K. Sivakumar, and C. de Kimpe. 2007. The contribution of agriculture to the state of climate: Workshop summary and recommendations. *Agricultural and Forest Meteorology* 142 (2–4):314-324.

Diffenbaugh, N. S. 2009. Influence of modern land cover on the climate of the United States. *Climate Dynamics* 33 (7):945-958.

Dixon, P. G., and T. L. Mote. 2003. Patterns and Causes of Atlanta's Urban Heat Island–Initiated Precipitation. *Journal of Applied Meteorology* 42 (9):1273-1284.

Dodd, A. V., and A. Dodd. 1965. Dew point distribution in the contiguous United States. *Mon. Wea. Rev* 93:113-122.

Duemer, L. S. 2007. The agricultural education origins of the Morrill land grant act of 1862. *American Educational History Journal* 34(1):135-146.

Duvick, D. N. 2005. The contribution of breeding to yield advances in maize (Zea mays L.). *Advances in agronomy* 86:83-145.

Eathington, S., S. Lim, C. Nickell, J. Pataky, and R. Esgar. 1993. Disease pressure on soybean in Illinois. *Plant Disease* 77 (11):1136-1139.

Edgerton, M. D. 2009. Increasing Crop Productivity to Meet Global Needs for Feed, Food, and Fuel. *Plant Physiology* 149 (1):7-13.

Ehleringer, J. R. 2005. The Influence of Atmospheric CO2, Temperature, and Water on the Abundance of C3/C4 Taxa. In *A History of Atmospheric CO2 and Its Effects on Plants, Animals, and Ecosystems*, eds. I. T. Baldwin, M. M. Caldwell, G. Heldmaier, R. B. Jackson, O. L. Lange, H. A. Mooney, E. D. Schulze, U.

Sommer, J. R. Ehleringer, M. Denise Dearing and T. E. Cerling, 214-231. New York, NY: Springer New York.

Ehleringer, J. R., R. F. Sage, L. B. Flanagan, and R. W. Pearcy. 1991. Climate change and the evolution of C4 photosynthesis. *Trends in Ecology & Evolution* 6 (3):95-99.

Eldra P. Solomon, L. R. B., Diana W. Martin. 2005. *Biology*. 7th ed. CA: Thomson Brooks/Cole.

Elliott, W. P., and J. K. Angell. 1997. Variations of cloudiness, precipitable water, and relative humidity over the United States: 1973–1993. *Geophysical Research Letters* 24 (1):41-44.

Ellis, E. C., K. Klein Goldewijk, S. Siebert, D. Lightman, and N. Ramankutty. 2010. Anthropogenic transformation of the biomes, 1700 to 2000. *Global Ecology & Biogeography* 19 (5):589-606.

Escribano-Rocafort, A. G., A. B. Ventre-Lespiaucq, C. Granado-Yela, A. López-Pintor, J. A. Delgado, V. Muñoz, G. A. Dorado, and L. Balaguer. 2014. Simplifying data acquisition in plant canopies-Measurements of leaf angles with a cell phone. *Methods in Ecology and Evolution* 5 (2):132-140.

Feddema, J. J., K. W. Oleson, G. B. Bonan, L. O. Mearns, L. E. Buja, G. A. Meehl, and W. M. Washington. 2005. The Importance of Land-Cover Change in Simulating Future Climates. *Science* 310 (5754):1674-1678.

Fernandez-Cornejo, J., and S. Wechsler. 2012. Revisiting the Impact of Bt Corn Adoption by U.S. Farmers. *Agricultural and Resource Economics Review* 41 (3):377-390.

Field, C. B., R. B. Jackson, and H. A. Mooney. 1995. Stomatal responses to increased CO2: implications from the plant to the global scale. *Plant, Cell & Environment* 18 (10):1214-1225.

Fishback, P. V., W. C. Horrace, and S. Kantor. 2005. Did New Deal Grant Programs Stimulate Local Economies? A Study of Federal Grants and Retail Sales During the Great Depression. *The Journal of Economic History* 65 (1):36-71.

Foley, J. A., M. H. Costa, C. Delire, N. Ramankutty, and P. Snyder. 2003. Green surprise? How terrestrial ecosystems could affect earth's climate. *Frontiers in Ecology and the Environment* 1 (1):38-44.

Frye, J. D., and T. L. Mote. 2010. The synergistic relationship between soil moisture and the low-level jet and its role on the prestorm environment in the southern Great Plains. *Journal of Applied Meteorology and Climatology* 49 (4):775-791.

Gaffen, D. J., and R. J. Ross. 1998. Increased summertime heat stress in the US. *Nature* 396 (6711):529-530.

———. 1999. Climatology and Trends of U.S. Surface Humidity and Temperature. *Journal of Climate* 12 (3):811.

Gao, B.-c. 1996. NDWI—A normalized difference water index for remote sensing of vegetation liquid water from space. *Remote Sensing of Environment* 58 (3):257-266.

Gao, J., Y. Sun, Y. Lu, and L. Li. 2014. Impact of Ambient Humidity on Child Health: A Systematic Review. *PLOS ONE* 9 (12):e112508.

Gerhart, L. M., and J. K. Ward. 2010. Plant responses to low [CO2] of the past. *New Phytologist* 188 (3):674-695.

Granke, L., and M. Hausbeck. 2010. Effects of temperature, humidity, and wounding on development of Phytophthora rot of cucumber fruit. *Plant Disease* 94 (12):1417-1424.

Grassini, P., J. E. Specht, M. Tollenaar, I. Ciampitti, and K. G. Cassman. 2014. High-yield maize-soybean cropping systems in the US Corn Belt. *Crop Physiology: Applications for Genetic Improvement and Agronomy. Amsterdam: Elsevier*:17-41.

Grassini, P., H. Yang, and K. G. Cassman. 2009. Limits to maize productivity in Western Corn-Belt: A simulation analysis for fully irrigated and rainfed conditions. *Agricultural and Forest Meteorology* 149 (8):1254-1265.

Grimmond, C., and T. R. Oke. 1986. Urban water balance: 2. Results from a suburb of Vancouver, British Columbia. *Water Resources Research* 22 (10):1404-1412.

Guerra, E., F. Ventura, and R. L. Snyder. 2016. Crop Coefficients: A Literature Review. *Journal of Irrigation and Drainage Engineering* 142 (3):06015006.

Guo, M., X. Bian, X. Wu, and M. Wu. 2011. Agrobacterium-mediated genetic transformation: history and progress. In *Genetic Transformation*: InTech:1-28.

Halford, N. G. 2011. *Genetically Modified Crops (2)*. London, US: Imperial College Press.

Hancock, P. A., and M. F. Hutchinson. 2006. Spatial interpolation of large climate data sets using bivariate thin plate smoothing splines. *Environmental Modelling & Software* 21 (12):1684-1694.

Hao, B., Q. Xue, T. H. Marek, K. E. Jessup, X. Hou, W. Xu, E. D. Bynum, and B. W. Bean. 2015. Soil water extraction, water use, and grain yield by drought-tolerant maize on the Texas High Plains. *Agricultural Water Management* 155:11-21.

Hart, J. F., and S. S. Ziegler. 2008. *Landscapes of Minnesota: a geography*: Minnesota Historical Society.

Held, I. M., and B. J. Soden. 2000. Water vapor feedback and global warming. *Annual Review of Energy & the Environment* 25 (1):441-475.

Hest, D. 2014. Rainy future for the Corn Belt. *Corn and Soybean Digest*.

Hetherington, A. M., and F. I. Woodward. 2003. The role of stomata in sensing and driving environmental change. *Nature* 424 (6951):901-908.

Homestead Act. (1862). Statutes at Large 12:392.

Hopkins, W. G., and N. P. Huner. 2004. *Introduction to Plant Physiology*. 3 ed. USA: John Wiley and Sons.

Huang, J., D. Chen, and M. H. Cosh. 2009. Sub-pixel reflectance unmixing in estimating vegetation water content and dry biomass of corn and soybeans cropland using normalized difference water index (NDWI) from satellites. *International Journal of Remote Sensing* 30 (8):2075-2104.

Hudson, J. C. 1994. *Making the corn belt: A geographical history of middle-western agriculture*. Indiana: Bloomington: Indiana University Press. .

Ingebritsen, S. E. 2000. Delta subsidence in California: the sinking heart of the state. Sacramento, CA. Government Document: U.S. Dept. of the Interior, U.S. Geological Survey.

Jackson, T. J., D. Chen, M. Cosh, F. Li, M. Anderson, C. Walthall, P. Doriaswamy, and E. R. Hunt. 2004. Vegetation water content mapping using Landsat data derived normalized difference water index for corn and soybeans. *Remote Sensing of Environment* 92 (4):475-482.

Jasechko, S., Z. D. Sharp, J. J. Gibson, S. J. Birks, Y. Yi, and P. J. Fawcett. 2013. Terrestrial water fluxes dominated by transpiration. *Nature* 496 (7445):347-350.

Jentsch, A., and C. Beierkuhnlein. 2008. Research frontiers in climate change: Effects of extreme meteorological events on ecosystems. *Comptes Rendus Geoscience* 340 (9):621-628.

Johnson, T. 2016. Nitrogen Nation: The Legacy of World War I and the Politics of Chemical Agriculture in the United States, 1916-1933. *Agricultural History* 90 (2):209-229.

Johnston, C. A. 2014. Agricultural expansion: land use shell game in the U.S. Northern Plains. *Landscape Ecology* 29 (1):81-95.

Jones, H. G. 2014. *Plants and microclimate: a quantitative approach to environmental plant physiology*. Third ed. New York; Cambridge University Press.

Kalnay, E., and M. Cai. 2003. Impact of urbanization and land-use change on climate. *Nature* 423(6939):528-531.

Karl, T. R., R. W. Knight, K. P. Gallo, T. C. Peterson, P. D. Jones, G. Kukla, N. Plummer, V. Razuvayev, J. Lindseay, and R. J. Charlson. 1993. A new perspective on recent global warming: Asymmetric trends of daily maximum and minimum temperature. *Bulletin of the American Meterological Society* 74 (6):1007-1023.

Keyser, H. H., and F. Li. 1992. Potential for increasing biological nitrogen fixation in soybean. *Plant and Soil* 141:119-135.

Khush, G. S. 2012. Genetically modified crop: the fastest adopted crop technology in the history of modern agriculture. *Agriculture & Food Security* 1:14.

Killick, R., and I. A. Eckley. 2014. changepoint: An R Package for Changepoint Analysis. *Journal of Statistical Software* 58 (3):19.

Knappenberger, P. C., P. J. Michaels, and P. D. Schwartzman. 1996. Observed changes in the diurnal temperature and dewpoint cycles across the United States. *Geophysical Research Letters* 23 (19):2637-2640.

Kunkel, K. E., and S. A. Changnon. 1996. The July 1995 heat wave in the Midwest: A climactic perspective and critical weather factors. *Bulletin of the American Meteorological Society* 77 (7):1507-1518.

Lange, O. L., R. Lösch, E.-D. Schulze, and L. Kappen. 1971. Responses of stomata to changes in humidity. *Planta* 100 (1):76-86.

Leakey, A., C. Bernacchi, F. Dohleman, D. Ort, and S. Long. 2004. Will photosynthesis of maize (zea mays) in the US corn belt increase in future [CO2] rich atmospheres? An analysis of diurnal courses of CO2 uptake under free-air concentration enrichment (face). *Global Change Biology* 10 (6):951-962.

Lebergott, S. 1966. Labor force and employment, 1800–1960. In *Output, employment, and productivity in the United States after 1800*, 117-204: NBER.

Li-Cor. 1999. Using the Li-6400 Portable Photosynthesis System, ed. L.-C. Biosciences, 1-7, 1-8.

Li, J., and A. D. Heap. 2014. Spatial interpolation methods applied in the environmental sciences: A review. *Environmental Modelling & Software* 53 (supplement C):173-189.

Lobell, D. B., G. Bala, and P. B. Duffy. 2006. Biogeophysical impacts of cropland management changes on climate. *Geophysical Research Letters* 33 (6):L06708.

Loss, C. P. 2012. Why the Morrill Act Still Matters. *The Chronicle of Higher Education* 58 (41):A17.

Mahmood, R., K. G. Hubbard, R. D. Leeper, and S. A. Foster. 2008. Increase in Near-Surface Atmospheric Moisture Content due to Land Use Changes: Evidence from the Observed Dewpoint Temperature Data. *Monthly Weather Review* 136 (4):1554-1561.

Mahmood, R., R. A. Pielke, K. G. Hubbard, D. Niyogi, P. A. Dirmeyer, C. McAlpine, A. M. Carleton, R. Hale, S. Gameda, A. Beltrán-Przekurat, B. Baker, R. McNider, D. R. Legates, M. Shepherd, J. Du, P. D. Blanken, O. W. Frauenfeld, U. S. Nair, and S. Fall. 2014. Land cover changes and their biogeophysical effects on climate. *International Journal of Climatology* 34 (4):929-953.

Mannion, A. M., and S. Morse. 2012. Biotechnology in agriculture. *Progress in Physical Geography* 36 (6):747-763.

McAdam, S. A. M., and T. J. Brodribb. 2015. The Evolution of Mechanisms Driving the Stomatal Response to Vapor Pressure Deficit. *Plant Physiology* 167 (3):833-843.

McAusland, L., S. Vialet-Chabrand, P. Davey, N. R. Baker, O. Brendel, and T. Lawson. 2016. Effects of kinetics of light-induced stomatal responses on photosynthesis and water-use efficiency. *New Phytologist* 211 (4):1209-1220.

McPherson, R. A., and D. J. Stensrud. 2005. Influences of a Winter Wheat Belt on the Evolution of the Boundary Layer. *Monthly Weather Review* 133 (8):2178-2199.

McPherson, R. A., D. J. Stensrud, and K. C. Crawford. 2004. The Impact of Oklahoma's Winter Wheat Belt on the Mesoscale Environment. *Monthly Weather Review* 132 (2):405-421.

Mehaffey, M., E. Smith, and R. Van Remortel. 2012. Midwest U.S. landscape change to 2020 driven by biofuel mandates. *Ecological Applications* 22 (1):8-19.

Morril College Act. (1862). Statutes at Large 12:503.

Murray, F. W. 1966. On the computation of saturation vapor pressure: US Department of Defense. Rand Corperation Santa Monica CA.

National Defense Act of 1916. (1916). Statutes at Large 39:116.

United Nations. 2017. *World Population Prospects 2017*. United Nations Population Division 2017 [cited 10/12/2017]. Available from https://esa.un.org/unpd/wpp/Download/Standard/Population/.

Nguy-Robertson, A., A. Gitelson, Y. Peng, A. Viña, T. Arkebauer, and D. Rundquist. 2012. Green leaf area index estimation in maize and soybean: Combining vegetation indices to achieve maximal sensitivity. *Agronomy Journal* 104 (5):1336-1347.

Nienkamp, P. 2010. Land-grant colleges and American engineers: redefining professional and vocational engineering education in the American Midwest, 1862-1917. *American Educational History Journal* 37:313-330.

NOAA. 2017a. *National Climate Report - August 2016 Summer Dew Point Tempurature Maps* [cited 9/13/2017]. Available from https://www.ncdc.noaa.gov/sotc/national/2016/8/supplemental/page-6.

———. 2017b. *NOAA Solar Posistion Calculator*. [cited 9/19/2017]. Available from https://www.esrl.noaa.gov/gmd/grad/solcalc/azel.html.

———. 2017c. *Sea Surface Tempurature-Map Viewer*. [cited 10/14/2017]. Available from https://www.climate.gov/maps-data/dataset/sea-surface-temperature-map-viewer.

Oke, T. R. 1978. *Bountry Layer Climates*. Great Britin: William Clowes and Sons Limitied.

Ortiz-Monasterio, J. I., N. Palacios-Rojas, E. Meng, K. Pixley, R. Trethowan, and R. J. Peña. 2007. Enhancing the mineral and vitamin content of wheat and maize through plant breeding. *Journal of Cereal Science* 46 (3):293-307.

Pereira, P., M. Oliva, and I. Misiune. 2016. Spatial interpolation of precipitation indexes in Sierra Nevada (Spain): comparing the performance of some interpolation methods. *Theoretical and Applied Climatology* 126 (3):683-698.

Pielke, R. A. 2001. Influence of the spatial distribution of vegetation and soils on the prediction of cumulus convective rainfall. *Reviews of Geophysics* 39 (2):151-177.

Pielke, R. A., Sr, R. Avissar, M. Raupach, A. J. Dolman, X. Zeng, and A. S. Denning. 1998. Interactions between the atmosphere and terrestrial ecosystems: influence on weather and climate. *Global Change Biology* 4 (5):461-475.

Prentice, I. C., W. Cramer, S. P. Harrison, R. Leemans, R. A. Monserud, and A. M. Solomon. 1992. Special Paper: A Global Biome Model Based on Plant Physiology and Dominance, Soil Properties and Climate. *Journal of Biogeography* 19 (2):117-134.

Raddatz, R. L. 2007. Evidence for the influence of agriculture on weather and climate through the transformation and management of vegetation: Illustrated by examples from the Canadian Prairies. *Agricultural and Forest Meteorology* 142 (2–4):186-202.

Ramankutty, N., and J. A. Foley. 1999. Estimating historical changes in global land cover: Croplands from 1700 to 1992. *Global Biogeochemical Cycles* 13 (4):997-1027.

Rao, I. M., R. S. Zeigler, R. Vera, and S. Sarkarung. 1993. Selection and Breeding for Acid-Soil Tolerance in Crops. *BioScience* 43 (7):454-465.

Reicosky, D., T. Kaspar, and H. Taylor. 1982. Diurnal relationship between evapotranspiration and leaf water potential of field-grown soybeans. *Agronomy Journal* 74 (4):667-673.

Robinson, P. J. 1998. Monthly variations of dew point temperature in the coterminous United States. *International Journal of Climatology* 18 (14):1539-1556.

———. 2000. Temporal trends in United States dew point temperatures. *International Journal of Climatology* 20 (9):985-1002.

Ross, R. J., and W. P. Elliott. 1996. Tropospheric water vapor climatology and trends over North America: 1973–93. *Journal of Climate* 9 (12):3561-3574.

Ross, R. J., and W. P. Elliott. 2001. Radiosonde-Based Northern Hemisphere Tropospheric Water Vapor Trends. *Journal of Climate* 14 (7):1602-1612.

Rouse Jr, J. W., R. Haas, J. Schell, and D. Deering. 1974. Monitoring vegetation systems in the Great Plains with ERTS. NASA. Goldenrod space flight center 3d ERTS-1 symposium 1 (sec A):309-317.

Rowe, W. C. 2011. Turning the Soviet Union into Iowa: The Virgin Lands Program in the Soviet Union. In *Engineering Earth: The Impacts of Megaengineering Projects*, ed. S. D. Brunn, 237-256. Dordrecht: Springer Netherlands.

Sage, R. F., T. L. Sage, and F. Kocacinar. 2012. Photorespiration and the Evolution of C4 Photosynthesis. *Annual Review of Plant Biology* 63 (1):19-47.

Samanta, S., D. K. Pal, D. Lohar, and B. Pal. 2012. Interpolation of climate variables and temperature modeling. *Theoretical and Applied Climatology* 107 (1):35-45.

Sandstrom, M. A., R. G. Lauritsen, and D. Changnon. 2004. A Central-U.S. Summer Extreme Dew-Point Climatology (1949-2000). *Physical Geography* 25 (3):191-207.

Schlesinger, W. H., and S. Jasechko. 2014. Transpiration in the global water cycle. *Agricultural and Forest Meteorology* 189–190:115-117.

Schwartz, J., J. M. Samet, and J. A. Patz. 2004. Hospital Admissions for Heart Disease: The Effects of Temperature and Humidity. *Epidemiology* 15 (6):755-761.

Schwartzman, P. D., P. J. Michaels, and P. C. Knappenberger. 1998. Observed changes in the diurnal dewpoint cycles across North America. *Geophysical Research Letters* 25 (13):2265-2268.

Secchi, S., P. W. Gassman, J. R. Williams, and B. A. Babcock. 2009. Corn-Based Ethanol Production and Environmental Quality: A Case of Iowa and the Conservation Reserve Program. *Environmental Management* 44 (4):732-44.

Seddon, A. W. R., M. Macias-Fauria, P. R. Long, D. Benz, and K. J. Willis. 2016. Sensitivity of global terrestrial ecosystems to climate variability. *Nature* 531 (7593):229-232.

Seinfeld, J. H. 2011. Insights on global warming. *AIChE Journal* 57 (12):3259-3284.

Sharma, K. P., C. D. Dybing, and C. Lay. 1990. Soybean Flower Abortion: Genetics and Impact of Selection on Seed Yield. *Crop Science* 30 (5):1017-1022.

Shih, P. M. 2013. Letters from the past: Molecular time travel to the origins of photosynthesis, RuBisCO, and the cyanobacterial phylum. Ph.D., University of California, Berkeley, Ann Arbor.

Shimazaki, K.-i., M. Doi, S. M. Assmann, and T. Kinoshita. 2007. Light regulation of stomatal movement. *Annu. Rev. Plant Biol.* 58 (1):219-247.

Singh, R. J., and T. Hymowitz. 1999. Soybean genetic resources and crop improvement. *Genome* 42 (4):605-616.

Sparks, J., D. Changnon, and J. Starke. 2002. Changes in the Frequency of Extreme Warm-Season Surface Dewpoints in Northeastern Illinois: Implications for Cooling-System Design and Operation. *Journal of Applied Meteorology* 41 (8):890-898.

Srinivasan, V., P. Kumar, and S. P. Long. 2017. Decreasing, not increasing, leaf area will raise crop yields under global atmospheric change. *Global Change Biology* 23 (4):1626-1635.

Staskawicz, B. J., F. M. Ausubel, B. J. Baker, J. G. Ellis, and D. G. J. Jonathan. 1995. Molecular Genetics of Plant Disease Resistance. *Science* 268 (5211):661-667.

Still, C. J., J. A. Berry, G. J. Collatz, and R. S. DeFries. 2003. Global distribution of C3 and C4 vegetation: Carbon cycle implications. *Global Biogeochemical Cycles* 17 (1):6-1-6-14.

Tanır Kayıkçı, E., and S. Zengin Kazancı. 2016. Comparison of regression-based and combined versions of Inverse Distance Weighted methods for spatial interpolation of daily mean temperature data. *Arabian Journal of Geosciences* 9 (17):690.

Thien, S. J. 1979. A flow diagram for teaching texture-by-feel analysis. *Journal of Agronomic Education* 8 (2).

Tokatlidis, I., and S. Koutroubas. 2004. A review of maize hybrids' dependence on high plant populations and its implications for crop yield stability. *Field Crops Research* 88 (2):103-114.

Trenberth, K. E. 2004. Rural land-use change and climate. *Nature* 427 (6971):213.

Tsvetsinskaya, E. A., L. O. Mearns, and W. E. Easterling. 2001. Investigating the Effect of Seasonal Plant Growth and Development in Three-Dimensional Atmospheric Simulations. Part I: Simulation of Surface Fluxes over the Growing Season. *Journal of Climate* 14 (5):692-709.

Turner, B. L. 1990. *The Earth as transformed by human action: Global and regional changes in the biosphere over the past 300 years*. New York: Cambridge University Press with Clark University.

USDA-NRCS. 2017a. USDA Guide to Texture by Feel. [cited 10/16/2017]. Avalible from https://www.nrcs.usda.gov/wps/portal/nrcs/detail/soils/edu/?cid=nrcs142p2_054311.

———. 2017b. *WETS Tables Growing Season Dates and Length.* [cited 10/16/2017]. Available from https://www.wcc.nrcs.usda.gov/climate/wets_dates.html.

USDA. 2012. *Census of Agriculture*. [cited 11/14/2016]. Available from https://www.agcensus.usda.gov/Publications/2012/Full_Report/Volume_1,_Chapter_1_State_Level/California/.

———. 2013. *World Agricultural Production*. [cited 10/16/2017]. Available from http://usda.mannlib.cornell.edu/MannUsda/viewDocumentInfo.do?documentID=1860.

———. 2017. Crop Productivity Annual Summary. [cited 2/28/2018]. Available from http://usda.mannlib.cornell.edu/MannUsda/viewDocumentInfo.do?documentID=1047.

USGS. 2016. *Transpiration- The Water Cycle*. USGS 2016 [cited 1/3/2018 2018]. Available from https://water.usgs.gov/edu/watercycletranspiration.html.

———. 2017. *Attributes for NHDPlus Catchments (Version 1.1) for the Conterminous United States: 30-Year Average Annual Precipitation, 1971-2000*. United States Geological Survey. [cited 7/7/2017]. Available from https://water.usgs.gov/GIS/browse/nhd_ppt30yr_mrb.jpg.

———. 2018. *National Water Information System: USGS 07374000 Mississippi River at Baton Rouge, LA.* [cited 2/7/2018 2018]. Available from https://waterdata.usgs.gov/usa/nwis/uv?site_no=07374000.

Vanos, J., L. Kalkstein, and T. Sanford. 2015. Detecting synoptic warming trends across the US Midwest and implications to human health and heat-related mortality. *International Journal of Climatology* 35 (1):85-96.

VanToai, T., A. Beuerlein, S. Schmitthenner, and S. St Martin. 1994. Genetic variability for flooding tolerance in soybeans. *Crop Science* 34 (4):1112-1115.

Wallander, S., R. Claassen, and C. Nickerson. 2011. The ethanol decade: an expansion of US corn production, 2000-09. *USDA-ERS Economic Information Bulletin* (79):1-22.

Wang, Y., and Z. Wang. 2015. Contribution of surface roughness to simulations of historical deforestation. *Physics and Chemistry of the Earth, Parts A/B/C* 87:119-125.

Weber, C., R. Shibles, and D. Byth. 1966. Effect of plant population and row spacing on soybean development and production. *Agronomy Journal* 58 (1):99-102.

Wegner, K., C. Lambertz, G. Das, G. Reiner, and M. Gauly. 2016. Effects of temperature and temperature-humidity index on the reproductive performance of sows during summer months under a temperate climate. *Animal Science Journal* 87 (11):1334-1339.

Widdicombe, W. D., and K. D. Thelen. 2002. Row width and plant density effects on corn grain production in the northern Corn Belt. *Agronomy Journal* 94 (5):1020-1023.

Willett, K. M., N. P. Gillett, P. D. Jones, and P. W. Thorne. 2007. Attribution of observed surface humidity changes to human influence. *Nature* 449 (7163):710-712.

Xin, X.-F., K. Nomura, K. Aung, A. C. Velásquez, J. Yao, F. Boutrot, J. H. Chang, C. Zipfel, and S. Y. He. 2016. Bacteria establish an aqueous living space in plants crucial for virulence. *Nature* 539 (7630):524-529.

Yilmaz, M. T., E. R. Hunt, and T. J. Jackson. 2008. Remote sensing of vegetation water content from equivalent water thickness using satellite imagery. *Remote Sensing of Environment* 112 (5):2514-2522.

Yuan, F., and M. Mitchell. 2014. Long-Term Climate Change at Four Rural Stations in Minnesota, 1920-2010. *Journal of Geography and Geology* 6 (3):228-241.

Zhou, S., R. A. Duursma, B. E. Medlyn, J. W. G. Kelly, and I. C. Prentice. 2013. How should we model plant responses to drought? An analysis of stomatal and non-stomatal responses to water stress. *Agricultural and Forest Meteorology* 182:204-214.

Zhou, Z., Y. Jiang, Z. Wang, Z. Gou, J. Lyu, W. Li, Y. Yu, L. Shu, Y. Zhao, Y. Ma, C. Fang, Y. Shen, T. Liu, C. Li, Q. Li, M. Wu, M. Wang, Y. Wu, Y. Dong, W. Wan, X. Wang, Z. Ding, Y. Gao, H. Xiang, B. Zhu, S.-H. Lee, W. Wang, and Z. Tian. 2015. Resequencing 302 wild and cultivated accessions identifies genes related to domestication and improvement in soybean. *Nature Biotechnology* 33 (4):408-414.

Appendix A- *Independent t-test statistics results summary comparing early (1956-1985), and late (1986-2016), seasonal (May-Sept) climate periods for dew point temperature, maximum temperature, minimum temperature, and vapor pressure deficit. Stations listed in bold tested significant α<.05 (95%) level.*

Dew Point Temperature

Station	Period	n	μ	SD	Δμ	df	t	p	T-Test Summary	Δ°F
	1956-1985	30	55.2	1.42						
Akron	1986-2016	31	55.7	1.26	0.50	59	4.44	**<.001**	t(59)=4.44,p=<.001	**0.50**
	1956-1985	30	63.5	1.32						
Atlanta	1986-2016	31	64.1	1.35	0.60	59	1.54	0.129	t(59)=1.54,p=.129	0.60
	1956-1985	30	66.7	1.44						
Austin	1986-2016	31	67.4	1.73	0.70	59	1.81	0.076	t(59)=1.81,p=.076	0.70
	1956-1985	30	69	1.25						
Baton Rouge	1986-2016	31	70.2	0.961	1.20	59	4.17	**<.001**	t(59)=4.17,p=<.001	**1.20**
	1956-1985	30	64.9	1.23						
Birmingham	1986-2016	31	63.5	5.46	-1.40	33	1.45	0.156	t(33)=1.45,p=.156	-1.40
	1956-1985	30	63.6	1.44						
Chattanooga	1986-2016	31	64.3	1.21	0.70	59	2.17	**0.034**	t(59)=2.17,p=.034	**0.70**
	1956-1985	30	55.6	1.6						
Cleveland	1986-2016	31	57.1	1.35	1.50	59	3.93	**<.001**	t(59)=3.93,p=<.001	**1.50**
	1956-1985	30	57.2	1.73						
Columbus	1986-2016	31	58.3	1.38	1.10	59	2.73	**0.008**	t(59)=2.73,p=.008	**1.10**
	1956-1985	30	59.9	1.51						
Covington	1986-2016	31	61.1	1.35	1.20	59	3.07	**0.003**	t(59)=3.07,p=.003	**1.20**
	1956-1985	30	56.9	1.75						
Dayton	1986-2016	31	58	1.4	1.10	59	2.82	**0.006**	t(59)=2.82,p=.006	**1.10**
	1956-1985	30	57.1	1.63						
Des Moines	1986-2016	31	58.3	1.59	1.20	59	3	**0.004**	t(59)=3.00,p=.004	**1.20**
	1956-1985	30	47.6	1.43						
Duluth	1986-2016	31	49.6	1.51	2.00	59	5.38	**<.001**	t(59)=5.38,p=<.001	**2.00**
	1956-1985	30	50.8	2						
Fargo	1986-2016	31	52.2	1.5	1.40	59	3.16	**0.003**	t(59)=3.16,p=.003	**1.40**
	1956-1985	30	53.7	1.59						
Flint	1986-2016	31	55.1	1.48	1.40	59	3.61	**0.001**	t(59)=3.61,p=.001	**1.40**
	1956-1985	30	64.2	1.61						
Fort Smith	1986-2016	31	65.4	1.43	1.20	59	3.04	**0.004**	t(59)=3.04,p=.004	**1.20**
	1956-1985	30	56.2	1.72						
Fort Wayne	1986-2016	31	57.8	1.37	1.60	59	4.1	**<.001**	t(59)=4.10,p=<.001	**1.60**
	1956-1985	30	53.2	1.66						
Green Bay	1986-2016	31	54.8	1.65	1.60	59	3.79	**<.001**	t(59)=3.79,p=<.001	**1.60**

	1956-1985	30	53.3	2.07						
Huron	1986-2016	31	55	1.56	1.70	59	3.58	**0.001**	t(59)=3.58,p=.001	**1.70**
	1956-1985	30	59.2	1.66						
Indianapolis	1986-2016	31	59.3	1.47	0.10	59	0.415	0.679	t(59)=.415,p=.679	0.10
	1956-1985	30	48.3	1.72						
International Falls	1986-2016	31	49.7	1.35	1.40	59	3.49	**0.001**	t(59)=3.49,p=.001	**1.40**
	1956-1985	30	60.4	1.86						
Kansas City	1986-2016	31	61.3	1.86	0.90	59	2.16	**0.035**	t(59)=2.16,p=.035	**0.90**
	1956-1985	30	62.7	1.58						
Knoxville	1986-2016	31	63.2	1.21	0.50	59	1.41	0.164	t(59)=1.41,p=.164	0.50
	1956-1985	30	59.6	1.43						
Lexington	1986-2016	31	60.9	1.41	1.30	59	3.58	**0.001**	t(59)=3.58,p=.001	**1.30**
	1956-1985	30	65.4	1.41						
Little Rock	1986-2016	31	66.2	1.26	0.80	59	2.46	**0.017**	t(59)=2.46,p=.017	**0.80**
	1956-1985	30	61.1	1.45						
Louisville	1986-2016	31	61.8	1.31	0.70	59	1.9	0.063	t(59)=1.90,p=.063	0.70
	1956-1985	30	68.5	1.37						
Lufkin	1986-2016	31	69	1.49	0.50	59	1.33	0.188	t(59)=1.33,p=.188	0.50
	1956-1985	30	54.2	1.69						
Madison	1986-2016	31	55.7	1.58	1.50	59	3.6	**0.001**	t(59)=3.60,p=.001	**1.50**
	1956-1985	30	55.2	1.78						
Mason City	1986-2016	31	55	3.12	-0.20	48	0.234	0.816	t(48)=.234,p=.816	-0.20
	1956-1985	30	66.7	1.49						
Meridian	1986-2016	31	67.4	1.13	0.70	59	2.19	**0.033**	t(59)=2.19,p=.033	**0.70**
	1956-1985	30	54.3	1.44						
Milwaukee	1986-2016	31	55.3	1.68	1.00	59	2.47	**0.016**	t(59)=2.47,p=.016	**1.00**
	1956-1985	30	53.2	1.75						
Minneapolis	1986-2016	31	54.2	1.49	1.00	59	2.61	**0.012**	t(59)=2.61,p=.012	**1.00**
	1956-1985	30	68.5	1.44						
Mobile	1986-2016	31	69.3	1.2	0.80	59	2.56	**0.013**	t(59)=2.56,p=.013	**0.80**
	1956-1985	30	57.3	1.39						
Moline	1986-2016	31	58.6	1.66	1.30	59	3.31	**0.002**	t(59)=3.31,p=.002	**1.30**
	1956-1985	30	66.7	1.25						
Montgomery	1986-2016	31	67.3	1.18	0.60	59	1.75	0.086	t(59)=1.75,p=.086	0.60
	1956-1985	30	53.7	1.4						
Muskegon	1986-2016	31	55.1	1.51	1.40	59	3.66	**0.001**	t(59)=3.66,p=.001	**1.40**
	1956-1985	30	63.3	1.29						
Nashville	1986-2016	31	63.2	1.45	-0.10	59	0.366	0.716	t(59)=.366,p=.716	-0.10
	1956-1985	30	70.4	70.4						
New Orleans	1986-2016	31	71.2	71.2	0.80	48	2.32	**0.025**	t(48)=2.32,p=.025	**0.80**

	1956-1985	30	61.8	1.92						
Oklahoma City	1986-2016	31	63	1.65	1.20	59	2.63	**0.011**	t(59)=2.63,p=.011	**1.20**
	1956-1985	30	57.9	1.47						
Peoria	1986-2016	31	59.3	1.78	1.40	59	3.38	**0.001**	t(59)=3.38,p=.001	**1.40**
	1956-1985	30	71.6	1.15						
Port Arthur	1986-2016	31	71.8	1.12	0.20	59	0.711	0.48	t(59)=.711,p=.480	0.20
	1956-1985	30	53.7	1.81						
Rochester	1986-2016	31	55.2	1.71	1.50	59	3.36	**0.001**	t(59)=3.36,p=.001	**1.50**
	1956-1985	30	49	1.56						
Sault Ste Marie	1986-2016	31	50.4	1.47	1.40	59	3.61	**0.001**	t(59)=3.61,p=.001	**1.40**
	1956-1985	30	67.2	1.19						
Shreveport	1986-2016	31	67.7	1.52	0.50	59	1.4	0.168	t(59)=1.40,p=.168	0.50
	1956-1985	30	56.3	1.83						
Sioux City	1986-2016	31	57.5	1.58	1.20	59	2.64	**0.011**	t(59)=2.64,p=.011	**1.20**
	1956-1985	30	53.4	2.08						
Sioux Falls	1986-2016	31	55.5	1.59	2.10	59	4.34	**<.001**	t(59)=4.34,p=<.001	**2.10**
	1956-1985	30	56	1.89						
South Bend	1986-2016	31	56.7	1.4	0.70	59	1.74	0.087	t(59)=1.74,P=.087	0.70
	1956-1985	30	59.3	1.68						
Springfield IL	1986-2016	31	60.2	1.76	0.90	59	2.06	**0.043**	t(59)=2.01,p=.043	**0.90**
	1956-1985	30	60.7	1.95						
Springfield MO	1986-2016	31	61.8	1.59	1.10	59	2.33	**0.023**	t(59)=2.33,p=.023	**1.10**
	1956-1985	30	52.1	1.65						
St Cloud	1986-2016	31	53.4	1.57	1.30	59	3.03	**0.004**	t(59)=3.03,p=.004	**1.30**
	1956-1985	30	61.1	1.81						
St Louis	1986-2016	31	61.4	1.77	0.30	59	0.625	0.534	t(59)=.625,p=.534	0.30
	1956-1985	30	69	1.14						
Tallahassee	1986-2016	31	68.8	1.11	-0.20	59	0.529	0.599	t(59)=.529,p=.599	-0.20
	1956-1985	30	60.7	1.62						
Topeka	1986-2016	31	61.5	1.42	0.80	59	1.97	0.053	t(59)=1.97,p=.053	0.80
	1956-1985	30	51.7	1.69						
Traverse City	1986-2016	31	52.8	1.45	1.10	59	2.61	**0.012**	t(59)=2.61,p=.012	**1.10**
	1956-1985	30	63.7	1.66						
Tulsa	1986-2016	31	64.2	1.68	0.50	59	0.984	0.329	t(59)=.984,p=.329	0.50
	1956-1985	30	70.6	0.888						
Victoria	1986-2016	31	71.5	1.02	0.90	59	3.68	**0.001**	t(59)=3.68,p=.001	**0.90**
	1956-1985	30	66	1.49						
Waco	1986-2016	31	66.7	1.78	0.70	59	1.88	0.066	t(59)=1.88,p=.066	0.70
	1956-1985	30	59.3	2.06						
Wichita	1986-2016	31	61.2	1.49	1.90	59	4.05	**<.001**	t(59)=4.05,p=<.001	**1.90**

	1956-1985	30	62.2	1.7						
Wichita Falls	1986-2016	31	62.9	2.13	0.70	59	1.48	0.145	t(59)=1.48,p=.145	0.70
	1956-1985	30	54.6	1.61						
Youngstown	1986-2016	31	56.1	1.35	1.50	59	3.95	**<.001**	t(59)=3.95,p=<.001	**1.50**

Maximum Temperature

Station	Period	n	μ	SD	Δμ	df	t	p	T-Test Summary	Δ°F
	1956-1985	30	84.2	1.80						
Akron	1986-2016	31	85.8	1.94	1.60	59	3.33	**<.001**	t(59)= 3.33,p=<.001	**1.60**
	1956-1985	30	84.2	1.80						
Atlanta	1986-2016	31	85.8	1.94	1.60	59	3.33	**<.001**	t(59)= 3.33,p=<.001	**1.60**
	1956-1985	30	88.8	1.29						
Baton Rouge	1986-2016	31	89.9	1.17	1.05	59	3.34	**<.001**	t(59)= 3.34,p=<.001	**1.05**
	1956-1985	30	86.4	1.79						
Birmingham	1986-2016	31	87.5	1.91	1.06	59	2.24	**0.03**	t(59)= 2.24,p=.030	**1.06**
	1956-1985	30	84.8	1.86						
Chattanooga	1986-2016	31	86.5	2.26	1.64	59	3.09	**<.001**	t(59)= 3.09,p=<.001	**1.64**
	1956-1985	30	79.4	1.69						
Columbus	1986-2016	31	80.5	2.08	1.11	59	2.29	**0.03**	t(59)= 2.29,p=.030	**1.11**
	1956-1985	30	79.5	1.54						
Dayton	1986-2016	31	79.7	2.02	0.18	59	0.4	0.69	t(59)= .400,p=.690	0.18
	1956-1985	30	80.0	1.54						
Des Moines	1986-2016	31	80.2	2.15	0.25	59	0.52	0.61	t(59)= .520,p=.610	0.25
	1956-1985	30	69.0	1.44						
Duluth	1986-2016	31	70.2	1.88	1.18	59	2.74	**0.01**	t(59)= 2.74,p=.010	**1.18**
	1956-1986	30	84.8	1.49						
Evansville	1986-2016	31	85.9	1.90	0.98	59	2.55	**0.01**	t(59)= 2.55,p=.010	**1.12**
	1956-1985	30	75.6	1.72						
Fargo	1986-2016	31	76.5	2.01	0.96	59	1.99	**0.05**	t(59)= 1.99,p=.050	**0.96**
	1956-1985	30	75.2	1.29						
Flint	1986-2016	31	77.2	2.15	2.02	49	4.45	**<.001**	t(49)=4.45,p=<.001	**2.03**
	1956-1985	30	87.7	2.22						
Fort Smith	1986-2016	31	88.6	2.30	0.91	59	1.57	0.12	t(59)= 1.57,p=.120	0.90
	1956-1985	30	78.6	1.60						
Fort Wayne	1986-2016	31	79.3	2.15	0.65	55	1.34	0.18	t(55)= 1.34,p=.180	0.65
	1956-1985	30	74.2	1.33						
Green Bay	1986-2016	31	75.2	1.90	0.95	59	2.27	**0.03**	t(59)= 2.27,p=.030	**0.96**

	1956-1985	30	79.5	1.98						
Huron	1986-2016	31	79.2	2.22	-0.29	59	0.53	0.6	t(59)= .530,p=.600	-0.29
	1956-1985	30	80.2	1.47						
Indianapolis	1986-2016	31	80.7	2.14	0.49	53	1.03	0.3	t(53)= 1.03,p=.300	0.49
	1956-1985	30	71.0	1.65						
International Falls	1986-2016	31	71.7	1.86	0.72	59	1.61	0.11	t(59)= 1.61,p=.110	0.72
	1956-1985	30	83.3	1.78						
Knoxville	1986-2016	31	84.6	1.98	1.24	59	2.57	**0.01**	t(59)= 2.57,p=.010	**1.24**
	1956-1985	30	80.9	1.67						
Lexington	1986-2016	31	81.8	2.05	0.90	59	1.89	0.06	t(59)= 1.89,p=.060	0.91
	1956-1985	30	87.6	1.75						
Little Rock	1986-2016	31	88.6	1.99	0.86	59	1.96	**0.05**	t(59)= 1.96,p=.050	**0.94**
	1956-1985	30	82.6	1.71						
Louisville	1986-2016	31	84.1	2.08	1.48	59	3.02	**<.001**	t(59)= 3.02,p=<.001	**1.48**
	1956-1985	30	90.1	1.74						
Lufkin	1986-2016	31	91.0	1.92	0.97	59	2.06	**0.04**	t(59)= 2.06,p=.040	**0.97**
	1956-1985	30	76.8	1.53						
Madison	1986-2016	31	76.9	2.02	0.09	59	0.2	0.84	t(59)= .200,p=.840	0.09
	1956-1985	30	77.1	1.42						
Mason City	1986-2016	31	77.6	1.96	0.46	59	1.04	0.3	t(59)= 1.04,p=.300	0.46
	1956-1985	30	88.9	1.75						
Meridian	1986-2016	31	89.3	1.58	0.42	59	0.98	0.33	t(59)= .980,p=.330	0.42
	1956-1985	30	73.7	1.40						
Milwaukee	1986-2016	31	74.8	2.05	1.08	53	2.4	**0.02**	t(53)= 2.40,p=.020	**1.08**
	1956-1985	30	76.4	1.61						
Minneapolis	1986-2016	31	77.1	1.95	0.86	59	1.55	0.13	t(59)= 1.55,p=.130	0.71
	1956-1985	30	88.4	1.28						
Mobile	1986-2016	31	88.8	1.03	0.33	59	1.12	0.27	t(59)= 1.12,p=.270	0.34
	1956-1985	30	79.8	1.34						
Moline	1986-2016	31	80.6	1.93	0.74	59	1.72	0.09	t(59)= .090,p=.090	0.74
	1956-1985	30	88.2	1.57						
Montgomery	1986-2016	31	89.9	1.73	1.61	59	3.79	**<.001**	t(59)= 3.79,p=<.001	**1.61**
	1956-1985	30	74.4	1.13						
Muskegon	1986-2016	31	75.1	1.79	0.70	51	1.82	0.07	t(51)= 1.82,p=.070	0.70
	1956-1985	30	85.0	1.70						
Nashville	1986-2016	31	85.8	1.93	0.77	59	1.65	0.1	t(59)= 1.65,p=.100	0.77
	1956-1985	30	88.1	1.35						
New Orleans	1986-2016	31	89.2	1.05	1.09	59	3.52	**<.001**	t(59)= 3.52,p=<.001	**1.08**
	1956-1985	30	87.2	1.98						
Oklahoma City	1986-2016	31	87.8	2.37	0.68	59	1.21	0.23	t(59)= 1.21,p=.230	0.68

	1956-1985	30	79.8	1.49						
Peoria	1986-2016	31	80.7	2.09	0.94	59	1.85	0.07	t(59)= 1.85,p=.070	0.86
	1956-1985	30	88.9	1.66						
Port Arthur	1986-2016	31	89.8	1.08	0.93	59	2.6	**0.01**	t(59)= 2.60,p=.010	**0.93**
	1956-1985	30	75.1	1.59						
Rochester	1986-2016	31	75.2	2.05	0.07	59	0.14	0.89	t(59)= .140,p=.890	0.07
	1956-1985	30	68.9	1.58						
Sault Ste Marie	1986-2016	31	70.4	1.95	1.49	59	3.26	**<.001**	t(59)= 3.26,p=<.001	**1.49**
	1956-1985	30	89.2	1.94						
Shreveport	1986-2016	31	90.4	2.04	1.28	59	2.52	**0.01**	t(59)= 2.52,p=.010	**1.28**
	1956-1985	30	80.0	1.41						
Sioux City	1986-2016	31	80.5	2.08	0.47	59	1.04	0.3	t(59)= 1.04,p=.300	0.47
	1956-1985	30	78.7	1.82						
Sioux Falls	1986-2016	31	78.2	2.19	-0.45	59	0.87	0.39	t(59)= .870,p=.390	-0.45
	1956-1985	30	77.3	1.56						
South Bend	1986-2016	31	78.1	2.04	0.77	59	1.64	0.1	t(59)= 1.64,p=.100	0.76
	1956-1985	30	81.8	1.49						
Springfield IL	1986-2016	31	81.9	1.95	0.14	59	0.3	0.76	t(59)= .300,p=.760	0.13
	1956-1985	30	75.0	1.46						
St Cloud	1986-2016	31	76.0	1.91	0.99	59	2.27	**0.03**	t(59)= 2.27,p=.030	**0.99**
	1956-1985	30	83.2	1.58						
St Louis	1986-2016	31	84.2	1.83	1.02	59	2.31	**0.02**	t(59)= 2.31,p=.020	**1.01**
	1956-1985	30	89.0	1.01						
Tallahassee	1986-2016	31	90.7	1.42	1.72	59	5.43	**<.001**	t(59)= 5.43,p=<.001	**1.72**
	1956-1985	30	83.3	2.10						
Topeka	1986-2016	31	84.4	2.12	1.06	59	1.96	**0.05**	t(59)= 1.96,p=.050	**1.06**
	1956-1985	30	74.0	1.44						
Traverse City	1986-2016	31	75.0	1.86	1.12	59	2.3	**0.03**	t(59)= 2.30,p=.030	**0.98**
	1956-1985	30	87.7	2.25						
Tulsa	1986-2016	31	87.7	2.09	0.02	59	0.04	0.97	t(59)= .040,p=.970	0.02
	1956-1985	30	91.8	2.01						
Waco	1986-2016	31	92.6	1.87	0.71	59	1.72	0.09	t(59)= .090,p=.090	0.86
	1956-1985	30	85.9	1.64						
Wichita	1986-2016	31	86.4	2.52	0.26	59	0.48	0.64	t(59)= .480,p=.640	0.50
	1956-1985	30	91.9	2.01						
Wichita Falls	1986-2016	31	91.7	2.38	0.49	59	0.87	0.39	t(59)= .870,p=.390	-0.26
	1956-1985	30	75.8	1.29						
Youngstown	1986-2016	31	77.0	1.93	1.18	52	2.81	**0.01**	t(52)= 2.81,p=.010	**1.18**

Minimum Temperature

Station	Period	n	μ	SD	Δμ	df	t	p	T-Test Summary	Δ°F
	1956-1985	30	55.9	1.52						
Akron	1986-2016	31	57.0	1.49	1.03	59	2.84	**0.01**	t(59)= 2.84,p=.010	**1.09**
	1956-1985	30	65.2	1.55						
Atlanta	1986-2016	31	67.4	1.19	2.16	59	6.12	**<.001**	t(59)= 6.12,p=<.001	**2.16**
	1956-1985	30	69.6	1.11						
Baton Rouge	1986-2016	31	70.4	1.05	0.81	59	2.91	**0.01**	t(59)= 2.91,p=.010	**0.81**
	1956-1985	30	65.1	1.54						
Birmingham	1986-2016	31	66.7	1.54	1.48	59	3.99	**<.001**	t(59)= 3.99,p=<.001	**1.57**
	1956-1985	30	63.2	1.72						
Chattanooga	1986-2016	31	65.4	1.44	2.39	59	5.44	**<.001**	t(59)= 5.44,p=<.001	**2.21**
	1956-1985	30	57.6	1.53						
Columbus	1986-2016	31	60.0	1.56	1.97	59	6.08	**<.001**	t(59)= 6.08,p=<.001	**2.40**
	1956-1985	30	58.5	1.51						
Dayton	1986-2016	31	59.4	1.25	0.95	59	2.46	**0.02**	t(59)= 2.46,p=.020	**0.87**
	1956-1985	30	59.3	1.45						
Des Moines	1986-2016	31	60.3	1.65	0.96	59	2.54	**0.01**	t(59)= 2.54,p=.010	**1.01**
	1956-1985	30	47.7	1.34						
Duluth	1986-2016	31	49.7	1.56	2.07	59	5.28	**<.001**	t(59)= 5.28,p=<.001	**1.97**
	1956-1986	30	61.2	1.42						
Evansville	1986-2016	31	63.2	1.82	1.53	59	4.64	**<.001**	t(59)= 4.64,p=<.001	**1.93**
	1956-1985	30	51.6	1.42						
Fargo	1986-2016	31	53.3	1.58	1.94	59	4.46	**<.001**	t(59)= 4.46,p=<.001	**1.71**
	1956-1985	30	53.5	1.52						
Flint	1986-2016	31	54.4	1.52	0.88	59	2.45	**0.02**	t(59)= 2.45,p=.020	**0.95**
	1956-1985	30	65.0	1.50						
Fort Smith	1986-2016	31	66.8	1.55	1.50	59	4.5	**<.001**	t(59)= 4.50,p=.<001	**1.76**
	1956-1985	30	56.9	1.52						
Fort Wayne	1986-2016	31	57.4	1.36	0.47	59	1.28	0.2	t(59)= 1.28,p=.200	0.47
	1956-1985	30	51.9	1.45						
Green Bay	1986-2016	31	53.4	1.54	1.62	59	3.79	**<.001**	t(59)= 3.79,p=<.001	**1.46**
	1956-1985	30	53.1	1.55						
Huron	1986-2016	31	54.6	1.54	1.50	59	3.86	**<.001**	t(59)= 3.86,p=<.001	**1.53**
	1956-1985	30	59.1	1.47						
Indianapolis	1986-2016	31	60.8	1.63	1.76	59	4.08	**<.001**	t(59)= 4.08,p=<.001	**1.62**
	1956-1985	30	47.0	1.59						
International Falls	1986-2016	31	47.1	1.68	0.09	59	0.21	0.83	t(59)= 0.21,p=.830	0.09

	1956-1985	30	63.1	1.90						
Knoxville	1986-2016	31	63.8	1.27	0.66	51	1.61	0.11	t(51)= 1.61,p=.110	0.67
	1956-1985	30	60.7	1.38						
Lexington	1986-2016	31	61.5	1.17	0.86	59	2.45	**0.02**	t(59)= 2.45,p=.020	**0.81**
	1956-1985	30	66.3	1.57						
Little Rock	1986-2016	31	67.8	1.52	1.20	59	3.74	**<.001**	t(59)= 3.74,p=<.001	**1.48**
	1956-1985	30	62.1	1.58						
Louisville	1986-2016	31	64.8	1.63	2.41	59	6.46	**<.001**	t(59)= 6.46,p=<.001	**2.65**
	1956-1985	30	68.6	1.17						
Lufkin	1986-2016	31	69.1	1.35	0.53	59	1.64	0.11	t(59)= 1.64,p=.110	0.53
	1956-1985	30	52.2	1.69						
Madison	1986-2016	31	55.0	1.58	2.79	59	6.66	**<.001**	t(59)= 6.66,p=<.001	**2.79**
	1956-1985	30	54.5	1.40						
Mason City	1986-2016	31	54.5	1.43	0.03	59	0.09	0.92	t(59)= 0.09,p=.920	0.03
	1956-1985	30	65.7	1.57						
Meridian	1986-2016	31	66.3	1.11	0.67	59	1.94	0.06	t(59)= 1.94,p=.060	0.68
	1956-1985	30	54.7	1.43						
Milwaukee	1986-2016	31	57.6	1.76	2.88	59	6.99	**<.001**	t(59)= 6.99,p=<.001	**2.88**
	1956-1985	30	55.5	1.55						
Minneapolis	1986-2016	31	57.7	1.86	2.21	59	5.03	**<.001**	t(59)= 5.03,p=<.001	**2.21**
	1956-1985	30	70.0	1.36						
Mobile	1986-2016	31	69.7	0.84	-0.26	48	0.9	0.37	t(48)= 0.90,p=.370	-0.26
	1956-1985	30	57.8	1.36						
Moline	1986-2016	31	58.6	1.65	0.69	59	1.9	0.06	t(59)= 1.90,p=.060	0.74
	1956-1985	30	67.6	1.35						
Montgomery	1986-2016	31	67.8	1.21	0.19	59	0.59	0.56	t(59)= 0.59,p=.560	0.19
	1956-1985	30	54.1	1.22						
Muskegon	1986-2016	31	55.3	1.86	1.39	59	2.97	**<.001**	t(59)= 2.97,p=<.001	**1.20**
	1956-1985	30	63.7	1.37						
Nashville	1986-2016	31	65.1	1.10	1.25	59	4.38	**<.001**	t(59)= 4.38,p=<.001	**1.39**
	1956-1985	30	70.4	1.55						
New Orleans	1986-2016	31	72.8	1.68	1.71	59	5.77	**<.001**	t(59)= 5.77,p=<.001	**2.39**
	1956-1985	30	65.1	1.52						
Oklahoma City	1986-2016	31	66.1	1.48	0.80	59	2.48	**0.02**	t(59)= 2.48,p=.020	**0.95**
	1956-1985	30	58.4	1.48						
Peoria	1986-2016	31	59.9	1.66	1.57	59	3.71	**<.001**	t(59)= 3.71,p=<.001	**1.50**
	1956-1985	30	71.1	1.36						
Port Arthur	1986-2016	31	71.9	0.84	0.78	48	2.7	**0.01**	t(48)= 2.70,p=.010	**0.78**
	1956-1985	30	53.2	1.43						
Rochester	1986-2016	31	54.7	1.54	1.45	59	3.94	**<.001**	t(59)= 3.94,p=<.001	**1.50**

	1956-1985	30	46.6	1.45						
Sault Ste Marie	1986-2016	31	49.3	2.22	2.72	52	5.65	**<.001**	t(52)= 5.65,p=<.001	**2.73**
	1956-1985	30	68.2	1.44						
Shreveport	1986-2016	31	69.5	1.35	0.95	59	3.47	**<.001**	t(59)= 3.47,p=<.001	**1.24**
	1956-1985	30	57.6	1.10						
Sioux City	1986-2016	31	57.1	1.49	-0.53	59	1.57	0.12	t(59)= 1.57,p=.120	-0.53
	1956-1985	30	54.4	1.50						
Sioux Falls	1986-2016	31	55.5	1.45	1.24	59	2.72	**0.01**	t(59)= 2.72,p=.010	**1.03**
	1956-1985	30	57.0	1.50						
South Bend	1986-2016	31	57.3	1.40	0.39	59	1.04	0.3	t(59)= 1.04,p=.300	0.39
	1956-1985	30	59.9	1.41						
Springfield IL	1986-2016	31	60.2	1.66	0.36	59	0.92	0.36	t(59)= 0.92,p=.360	0.36
	1956-1985	30	51.4	1.33						
St Cloud	1986-2016	31	52.3	1.67	1.01	59	2.27	**0.03**	t(59)= 2.27,p=.030	**0.88**
	1956-1985	30	62.7	1.77						
St Louis	1986-2016	31	65.5	1.44	2.65	59	6.63	**<.001**	t(59)= 6.63,p=<.001	**2.73**
	1956-1985	30	68.3	1.10						
Tallahassee	1986-2016	31	69.1	1.48	0.83	59	2.49	**0.02**	t(59)= 2.49,p=.020	**0.83**
	1956-1985	30	60.9	1.40						
Topeka	1986-2016	31	62.2	1.65	1.09	59	3.19	**<.001**	t(59)= 3.19,p=<.001	**1.24**
	1956-1985	30	50.7	1.66						
Traverse City	1986-2016	31	52.8	1.69	2.22	59	4.84	**<.001**	t(59)= 4.84,p=<.001	**2.08**
	1956-1985	30	66.3	2.02						
Tulsa	1986-2016	31	67.2	1.42	0.74	59	1.92	0.06	t(59)= 1.92,p=.060	0.86
	1956-1985	30	70.7	1.48						
Waco	1986-2016	31	70.3	1.28	-0.38	59	1.08	0.29	t(59)= 1.08,p=.290	-0.38
	1956-1985	30	63.1	1.59						
Wichita	1986-2016	31	64.0	1.42	0.87	59	2.86	**0.01**	t(59)= 2.86,p=.010	**0.96**
	1956-1985	30	66.7	1.79						
Wichita Falls	1986-2016	31	67.9	1.40	1.11	59	2.34	**0.02**	t(59)= 2.34,p=.020	**1.11**
	1956-1985	30	53.9	1.34						
Youngstown	1986-2016	31	54.6	1.29	2.74	59	2.04	**0.05**	t(59)= 2.04,p=.050	**0.68**

Vapor Pressure Deficit

Station	Period	n	μ	SD	Δμ	df	t	p	T-Test Summary	%Δ
	1956-1985	30	0.85	0.09						
Akron	1986-2016	31	0.84	0.15	-0.02	49.176	0.53	0.60	t(49)=.531,p=.600	-1.97
	1956-1985	30	0.94	0.12						
Atlanta	1986-2016	31	1.10	0.20	0.16	59	3.65	**<.001**	t(59)=3.65,p=<.001	**16.55**
	1956-1985	30	1.13	0.10						
Baton Rouge	1986-2016	31	1.15	0.14	0.01	53.881	0.42	0.68	t(54)=.415,p=.680	1.13
	1956-1985	30	1.11	0.17						
Birmingham	1986-2016	31	1.21	0.21	0.11	59	2.15	**0.04**	t(59)=2.15,p=.040	**9.48**
	1956-1985	30	1.03	0.14						
Chattanooga	1986-2016	31	1.17	0.21	0.14	59	3.15	**0.00**	t(59)=3.15,p=.000	**13.80**
	1956-1985	30	0.92	0.10						
Columbus	1986-2016	31	1.00	0.16	0.08	59	2.30	**0.03**	t(59)=2.30,p=.030	**8.47**
	1956-1985	30	0.97	0.10						
Dayton	1986-2016	31	0.95	0.14	-0.03	52.795	0.82	0.42	t(53)=.821,p=.420	-2.65
	1956-1985	30	1.02	0.13						
Des Moines	1986-2016	31	0.99	0.18	-0.02	54.541	0.62	0.54	t(55)=.621,p=.540	-2.40
	1956-1985	30	0.65	0.08						
Duluth	1986-2016	31	0.66	0.08	0.01	58.976	0.42	0.68	t(59)=.420,p=.680	1.27
	1956-1985	30	0.90	0.13						
Fargo	1986-2016	31	0.92	0.13	0.02	58.91	0.72	0.47	t(59)=.724,p=.470	2.63
	1956-1985	30	0.78	0.07						
Flint	1986-2016	31	0.84	0.13	0.06	59	2.14	**0.04**	t(59)=2.14,p=.040	**7.59**
	1956-1985	30	1.25	0.19						
Fort Smith	1986-2016	31	1.30	0.25	0.05	55.599	0.89	0.38	t(56)=.894,p=.380	3.98
	1956-1985	30	0.92	0.09						
Fort Wayne	1986-2016	31	0.88	0.16	-0.04	48.104	1.16	0.25	t(48)=1.16,p=.250	-4.11
	1956-1985	30	0.72	0.08						
Green Bay	1986-2016	31	0.72	0.11	0.00	52.243	0.04	0.97	t(52)=.037,p=.970	0.12
	1956-1985	30	1.02	0.16						
Huron	1986-2016	31	0.96	0.15	-0.06	58.147	1.59	0.12	t(58)=1.59,p=.120	-6.26
	1956-1985	30	0.90	0.12						
Indianapolis	1986-2016	31	0.98	0.18	0.08	52.106	1.97	**0.05**	t(52)=1.97,p=.050	**8.36**
	1956-1985	30	0.69	0.09						
International Falls	1986-2016	31	0.66	0.08	-0.03	56.114	1.20	0.24	t(56)=1.20,p=.240	-3.74
	1956-1985	30	0.99	0.13						
Knoxville	1986-2016	31	1.06	0.17	0.07	56.241	1.85	0.07	t(56)=1.85,p=.070	7.24

	1956-1985	30	0.96	0.13						
Lexington	1986-2016	31	0.97	0.17	0.00	55.789	0.06	0.95	t(56)=.058,p=.950	0.23
	1956-1985	30	1.20	0.14						
Little Rock	1986-2016	31	1.27	0.20	0.07	54.973	1.49	0.14	t(55)=1.49,p=.140	5.43
	1956-1985	30	1.02	0.11						
Louisville	1986-2016	31	1.17	0.20	0.15	59	3.53	<.001	t(59)=3.53,p=<.001	14.42
	1956-1985	30	1.23	0.15						
Lufkin	1986-2016	31	1.28	0.24	0.06	50.864	1.12	0.27	t(51)=1.12,p=.270	4.60
	1956-1985	30	0.81	0.11						
Madison	1986-2016	31	0.81	0.13	0.00	57.759	0.02	0.98	t(58)=.021,p=.980	0.09
	1956-1985	30	0.83	0.10						
Mason City	1986-2016	31	0.86	0.20	0.03	43.978	0.75	0.46	t(44)=.749,p=.460	3.59
	1956-1985	30	1.17	0.14						
Meridian	1986-2016	31	1.17	0.15	0.01	58.495	0.18	0.86	t(59)=.184,p=.860	0.59
	1956-1985	30	0.71	0.08						
Milwaukee	1986-2016	31	0.79	0.12	0.09	59	3.24	**<.001**	t(59)=3.24,p=.000	**12.05**
	1956-1985	30	0.93	0.12						
Minneapolis	1986-2016	31	0.97	0.15	0.05	56.788	1.32	0.19	t(57)=1.32,p=.190	4.95
	1956-1985	30	1.17	0.11						
Mobile	1986-2016	31	1.11	0.12	-0.06	58.84	2.00	**0.05**	t(59)=2.00,p=.050	**-5.10**
	1956-1985	30	0.95	0.09						
Moline	1986-2016	31	0.94	0.15	-0.01	48.395	0.36	0.72	t(48)=.363,p=.720	-1.19
	1956-1985	30	1.20	0.15						
Montgomery	1986-2016	31	1.28	0.20	0.08	55.209	1.89	0.06	t(55)=1.89,p=.060	7.03
	1956-1985	30	0.76	0.07						
Muskegon	1986-2016	31	0.76	0.11	0.00	52.519	0.00	1.00	t(53)=.002,p=1.00	0.01
	1956-1985	30	1.07	0.13						
Nashville	1986-2016	31	1.19	0.19	0.11	59	2.68	**0.01**	t(59)=2.68,p=.010	**10.50**
	1956-1985	30	1.00	0.10						
New Orleans	1986-2016	31	1.12	0.15	0.12	59	3.69	**<.001**	t(59)=3.69,p=<.001	**12.16**
	1956-1985	30	1.38	0.24						
Oklahoma City	1986-2016	31	1.38	0.27	0.00	58.585	0.07	0.95	t(59)=.067,p=.950	0.31
	1956-1985	30	0.94	0.10						
Peoria	1986-2016	31	0.95	0.18	0.01	47.334	0.31	0.76	t(47)=.305,p=.760	1.20
	1956-1985	30	0.99	0.14						
Port Arthur	1986-2016	31	1.08	0.14	0.09	59	2.42	**0.02**	t(59)=2.42,p=.020	**8.84**
	1956-1985	30	0.78	0.09						
Rochester	1986-2016	31	0.74	0.13	-0.03	54.066	1.09	0.28	t(54)=1.09,p=.280	-4.13
	1956-1985	30	0.56	0.08						
Sault Ste Marie	1986-2016	31	0.62	0.09	0.06	59	2.80	**0.01**	t(59)=2.80,p=.010	**10.62**

	1956-1985	30	1.25	0.18						
Shreveport	1986-2016	31	1.36	0.26	0.11	53.975	1.94	0.06	t(54)=1.94,p=.060	8.94
	1956-1985	30	1.01	0.14						
Sioux City	1986-2016	31	0.96	0.14	-0.05	58.993	1.27	0.21	t(59)=1.27,p=.210	-4.51
	1956-1985	30	1.00	0.16						
Sioux Falls	1986-2016	31	0.90	0.16	-0.10	58.586	2.47	**0.02**	t(59)=2.47,p=.020	**-10.12**
	1956-1985	30	0.86	0.11						
South Bend	1986-2016	31	0.88	0.13	0.02	57.462	0.56	0.58	t(58)=.562,p=.580	1.97
	1956-1985	30	1.01	0.11						
Springfield IL	1986-2016	31	0.98	0.17	-0.03	52.29	0.88	0.38	t(52)=.883,p=.380	-3.14
	1956-1985	30	0.80	0.10						
St Cloud	1986-2016	31	0.82	0.12	0.01	56.543	0.48	0.63	t(57)=.484,p=.630	1.69
	1956-1985	30	1.08	0.15						
St Louis	1986-2016	31	1.22	0.19	0.15	59	3.33	**0.00**	t(59)=3.33,p=.000	**13.70**
	1956-1985	30	1.09	0.10						
Tallahassee	1986-2016	31	1.27	0.15	0.18	59	5.53	**0.00**	t(59)=5.53,p=.000	**16.22**
	1956-1985	30	1.05	0.17						
Topeka	1986-2016	31	1.11	0.17	0.06	58.859	1.34	0.19	t(59)=1.34,p=.190	5.68
	1956-1985	30	0.76	0.08						
Traverse City	1986-2016	31	0.81	0.10	0.05	59	2.17	**0.03**	t(59)=2.17,p=.030	**6.77**
	1956-1985	30	1.33	0.23						
Tulsa	1986-2016	31	1.33	0.23	0.00	58.957	0.05	0.96	t(59)=.051,p=.960	0.23
	1956-1985	30	1.65	0.24						
Waco	1986-2016	31	1.64	0.28	-0.01	58.378	0.10	0.92	t(58)=.099,p=.920	-0.39
	1956-1985	30	1.77	0.24						
Wichita	1986-2016	31	1.75	0.37	-0.02	51.353	0.26	0.80	t(51)=.256,p=.800	-1.15
	1956-1985	30	1.38	0.22						
Wichita Falls	1986-2016	31	1.33	0.24	-0.05	58.793	0.83	0.41	t(59)=.825,p=.410	-3.47
	1956-1985	30	0.78	0.08						
Youngstown	1986-2016	31	0.78	0.12	0.00	52.031	0.12	0.90	t(52)=.124,p=.900	0.41

Appendix B- *Dew point record change point analysis for all NWS FOS.*

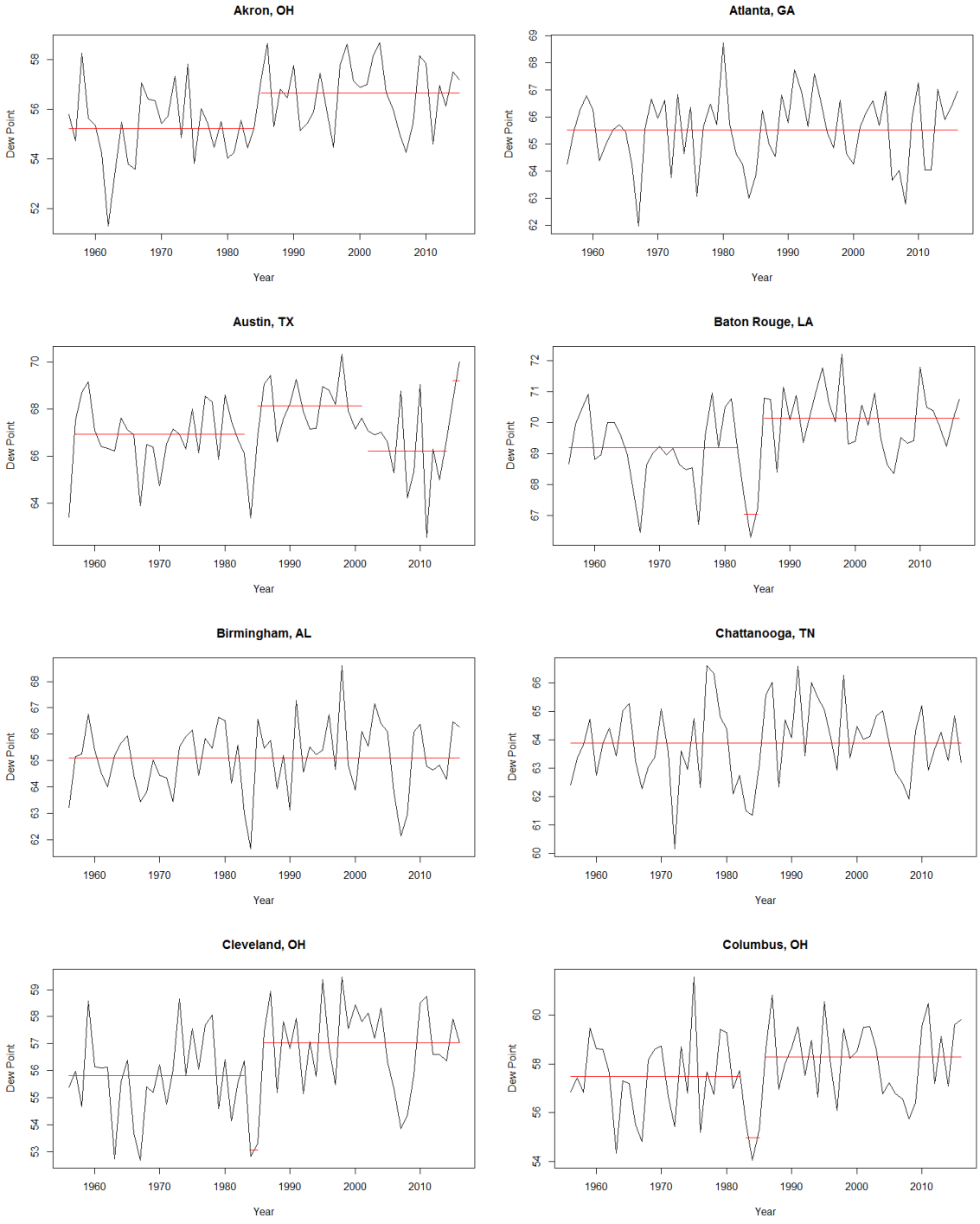

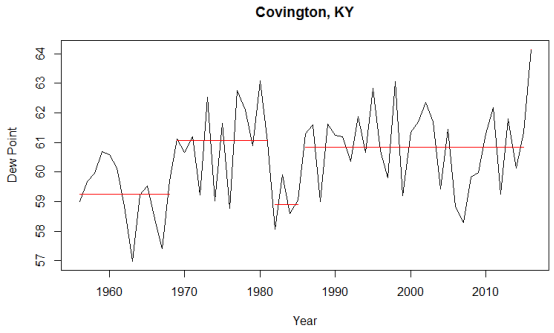
Covington, KY
Dew Point
Year

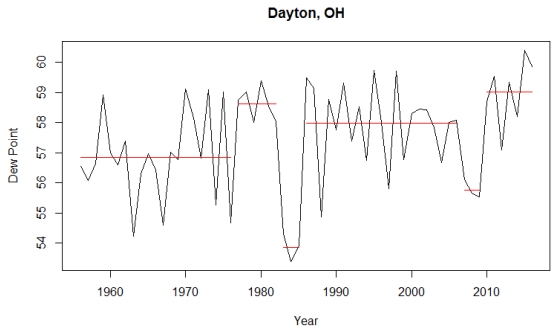
Dayton, OH
Dew Point
Year

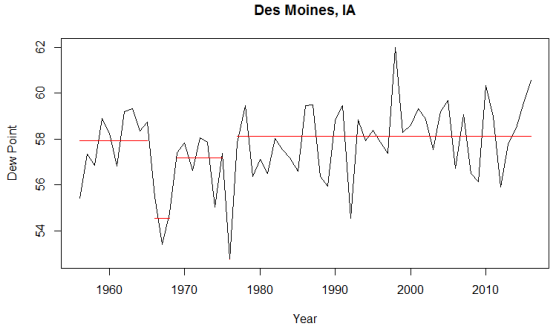
Des Moines, IA
Dew Point
Year

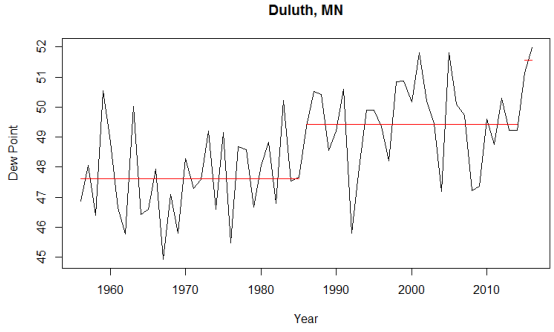
Duluth, MN
Dew Point
Year

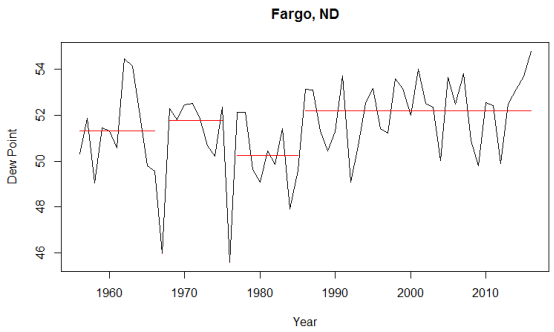
Fargo, ND
Dew Point
Year

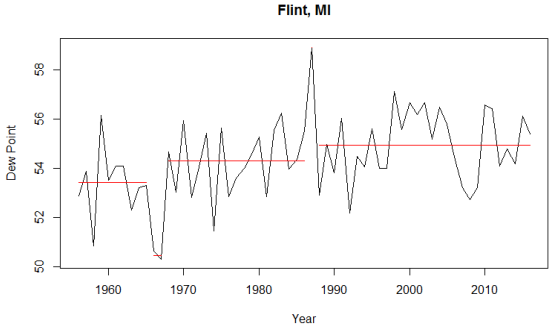
Flint, MI
Dew Point
Year

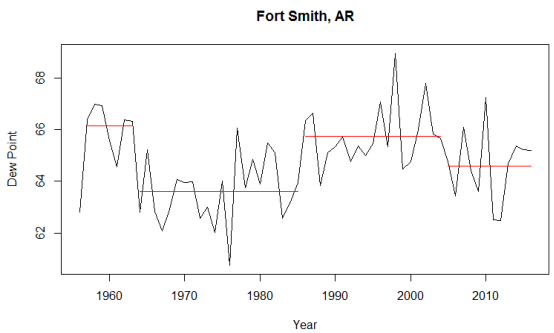
Fort Smith, AR
Dew Point
Year

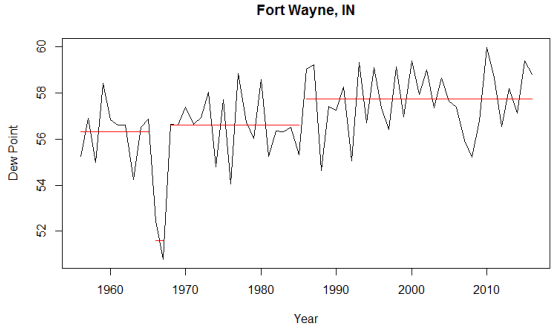
Fort Wayne, IN
Dew Point
Year

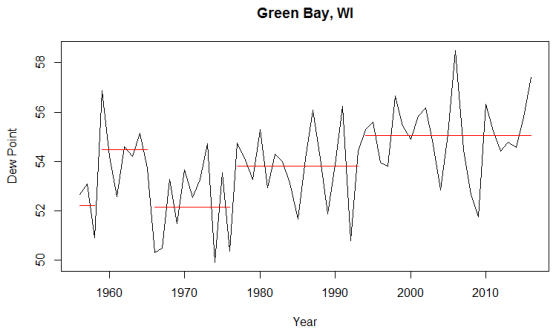
Green Bay, WI
Dew Point
Year

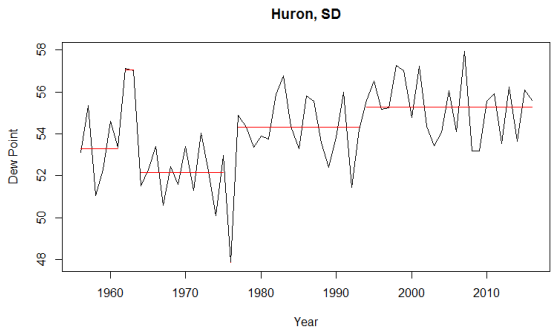
Huron, SD
Dew Point
Year

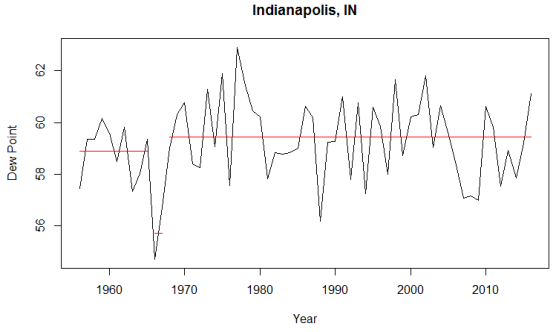
Indianapolis, IN
Dew Point
Year

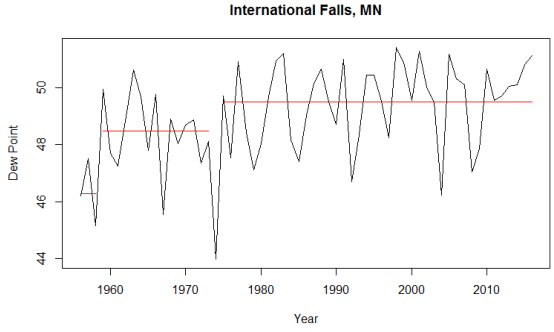
International Falls, MN
Dew Point
Year

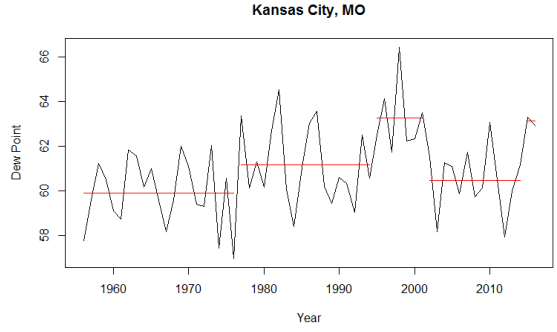
Kansas City, MO
Dew Point
Year

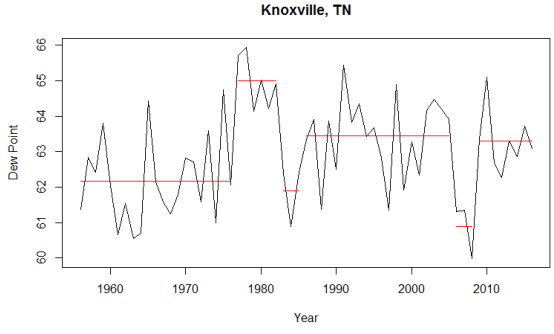
Knoxville, TN
Dew Point
Year

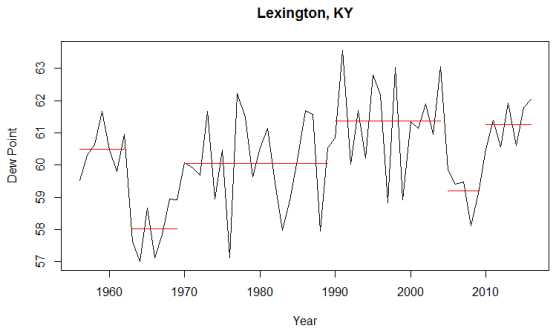
Lexington, KY
Dew Point
Year

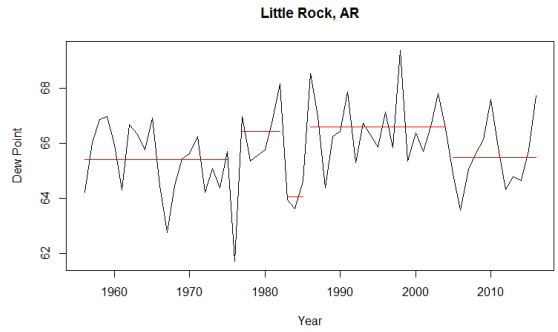
Little Rock, AR
Dew Point
Year

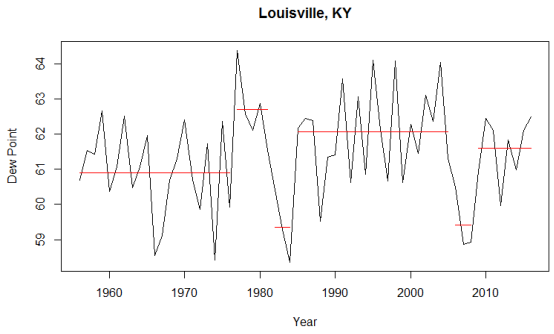
Louisville, KY
Dew Point
Year

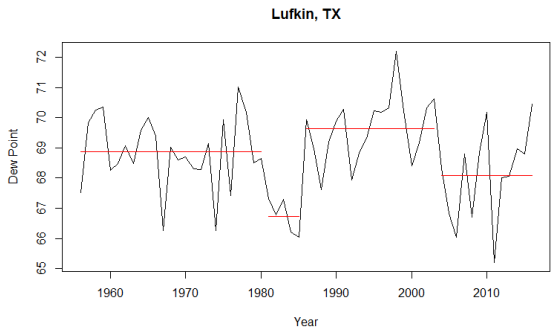
Lufkin, TX
Dew Point
Year

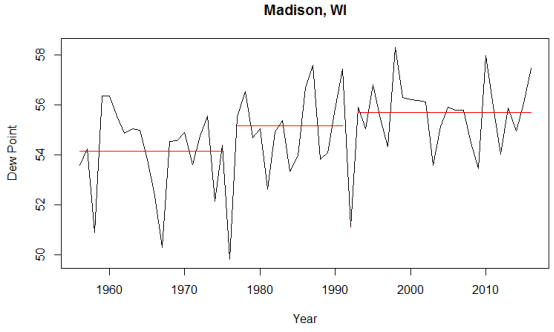
Madison, WI
Dew Point
Year

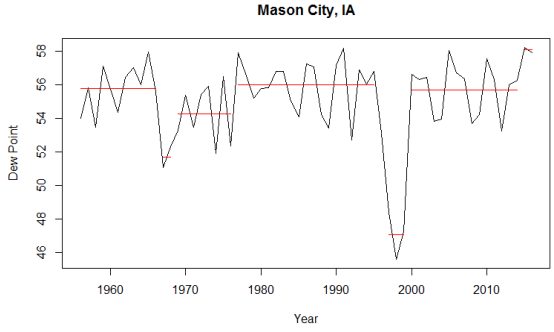
Mason City, IA
Dew Point
Year

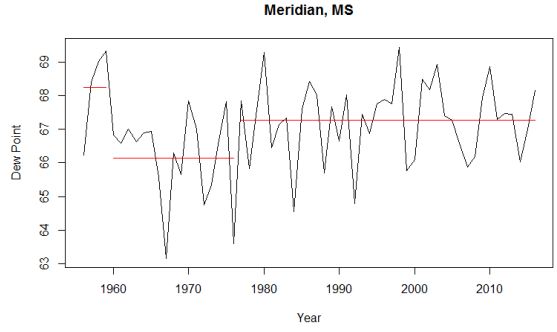
Meridian, MS
Dew Point
Year

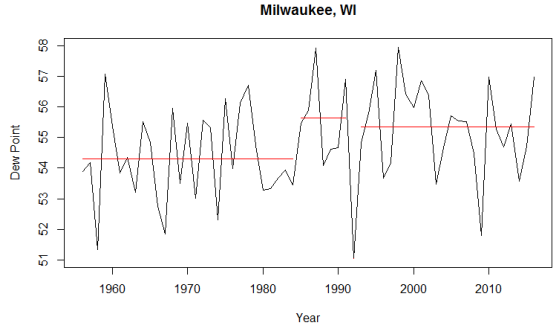
Milwaukee, WI
Dew Point
Year

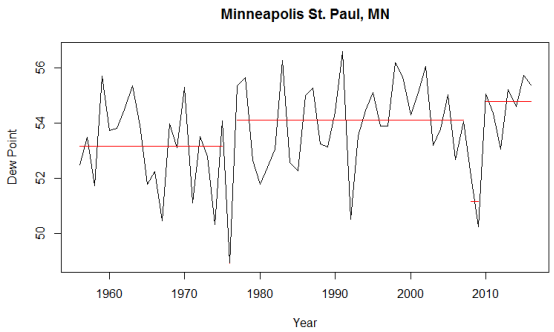
Minneapolis St. Paul, MN
Dew Point
Year

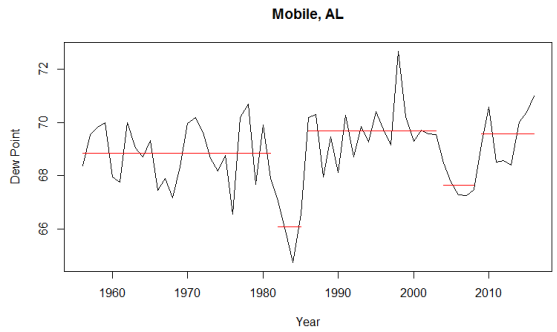
Mobile, AL
Dew Point
Year

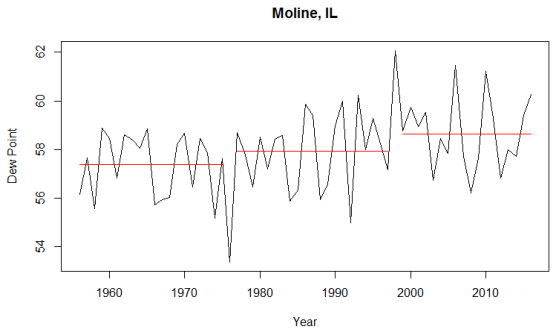
Moline, IL
Dew Point
Year

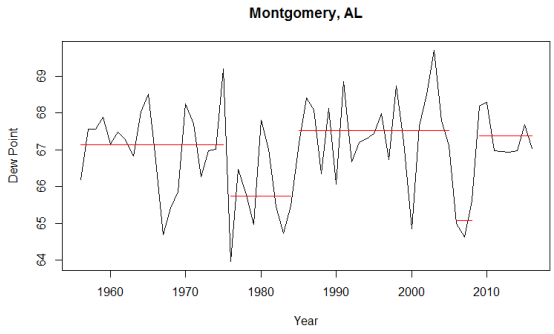
Montgomery, AL
Dew Point
Year

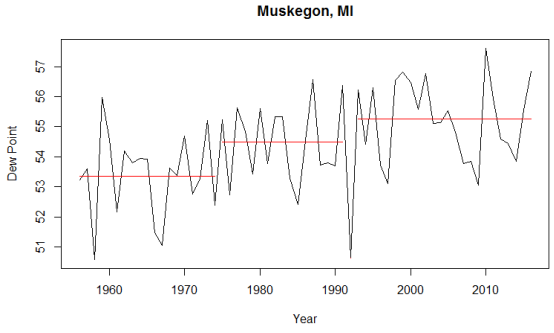
Muskegon, MI
Dew Point
Year

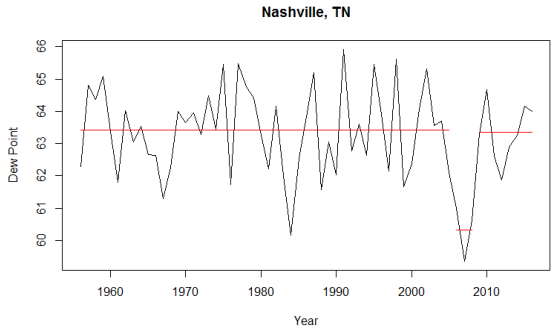
Nashville, TN
Dew Point
Year

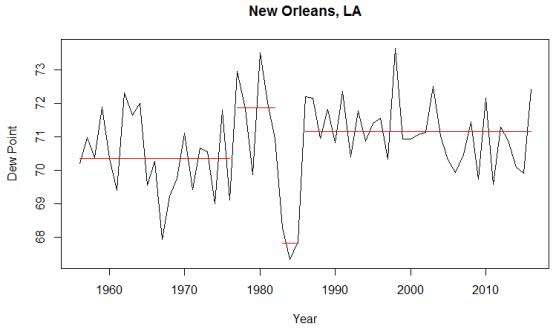
New Orleans, LA
Dew Point
Year

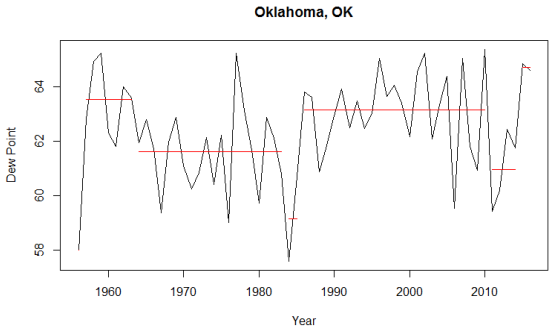
Oklahoma, OK
Dew Point
Year

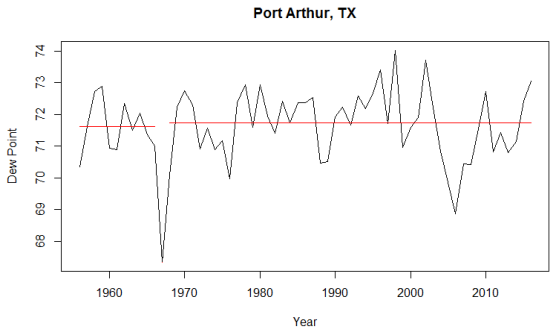
Port Arthur, TX
Dew Point
Year

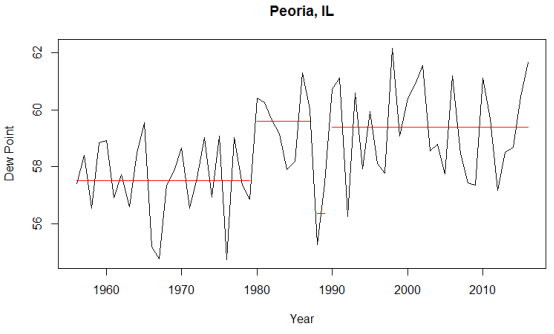
Peoria, IL
Dew Point
Year

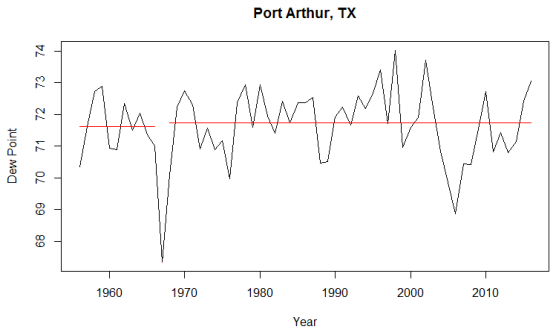
Port Arthur, TX
Dew Point
Year

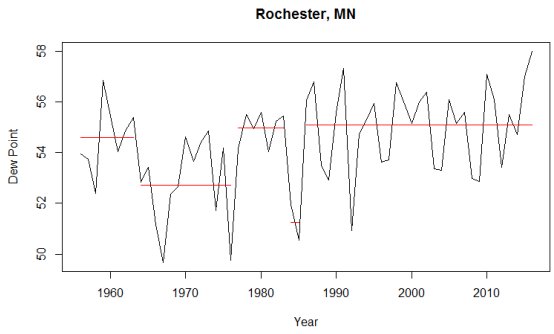
Rochester, MN
Dew Point
Year

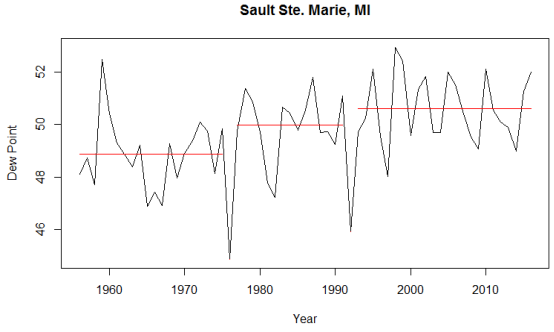
Sault Ste. Marie, MI
Dew Point
Year

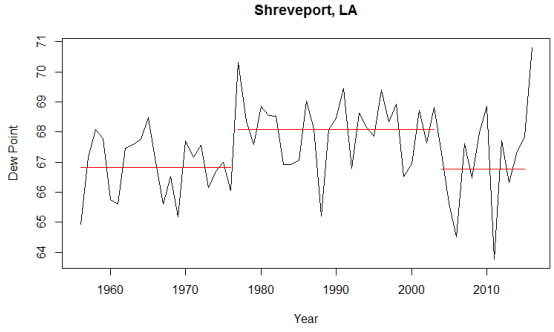
Shreveport, LA
Dew Point
Year

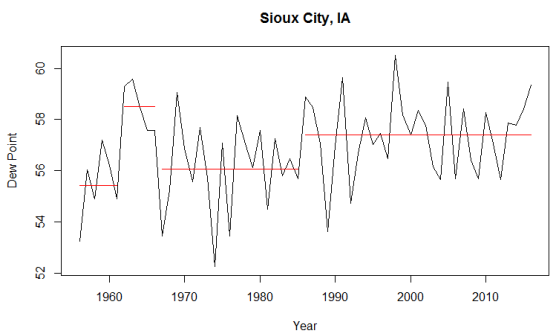
Sioux City, IA
Dew Point
Year

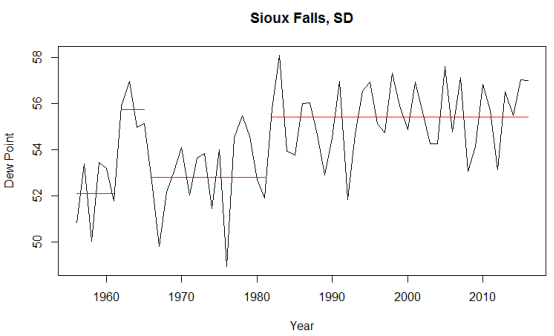
Sioux Falls, SD
Dew Point
Year

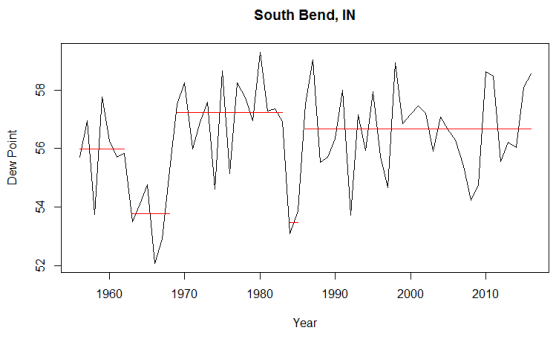
South Bend, IN
Dew Point
Year

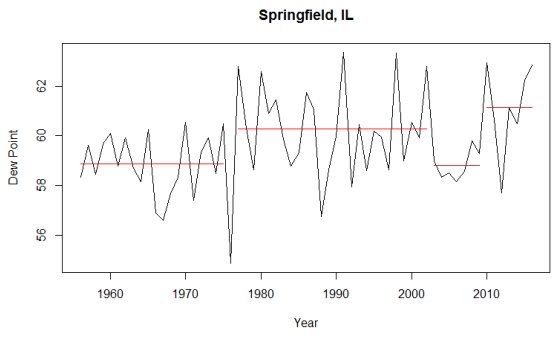
Springfield, IL
Dew Point
Year

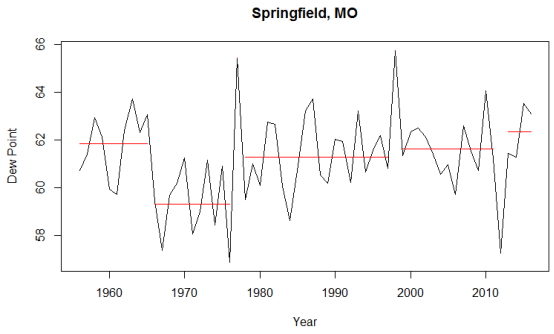
Springfield, MO
Dew Point
Year

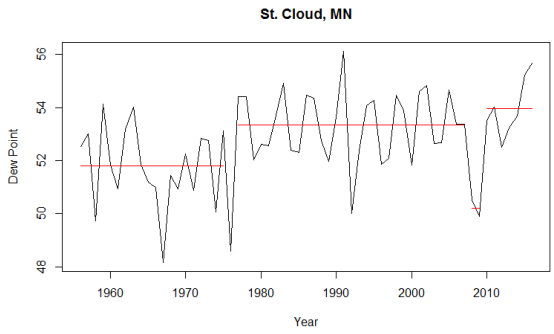
St. Cloud, MN
Dew Point
Year

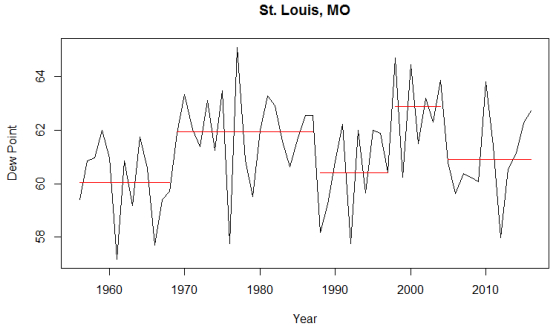
St. Louis, MO
Dew Point
Year

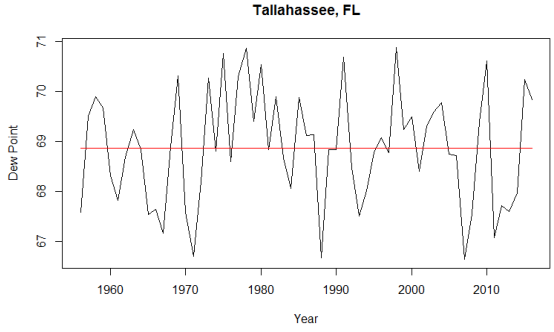
Tallahassee, FL
Dew Point
Year

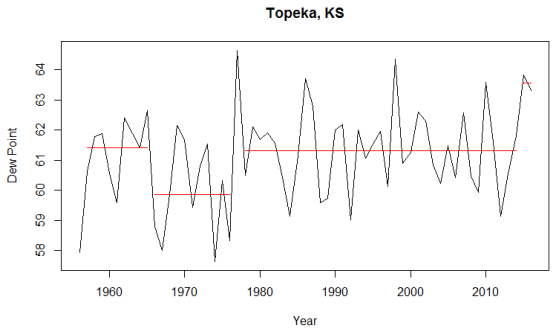
Topeka, KS
Dew Point
Year

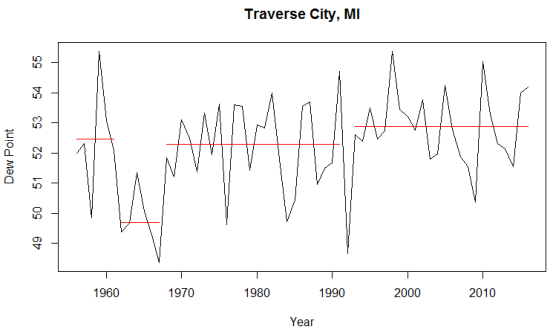
Traverse City, MI
Dew Point
Year

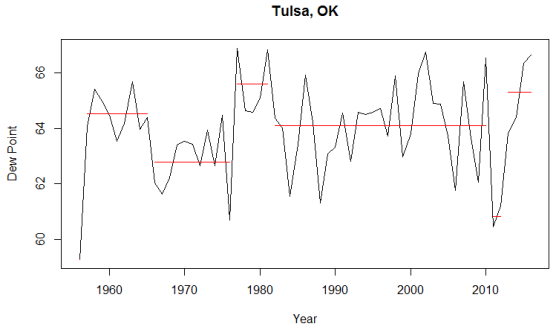
Tulsa, OK
Dew Point
Year

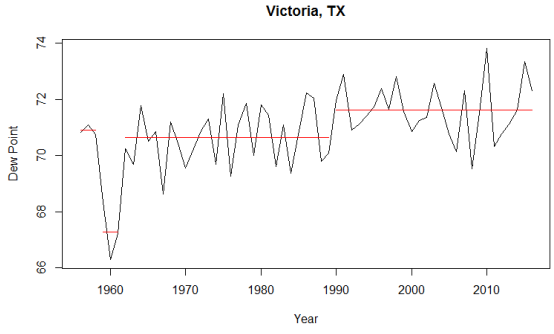
Victoria, TX
Dew Point
Year

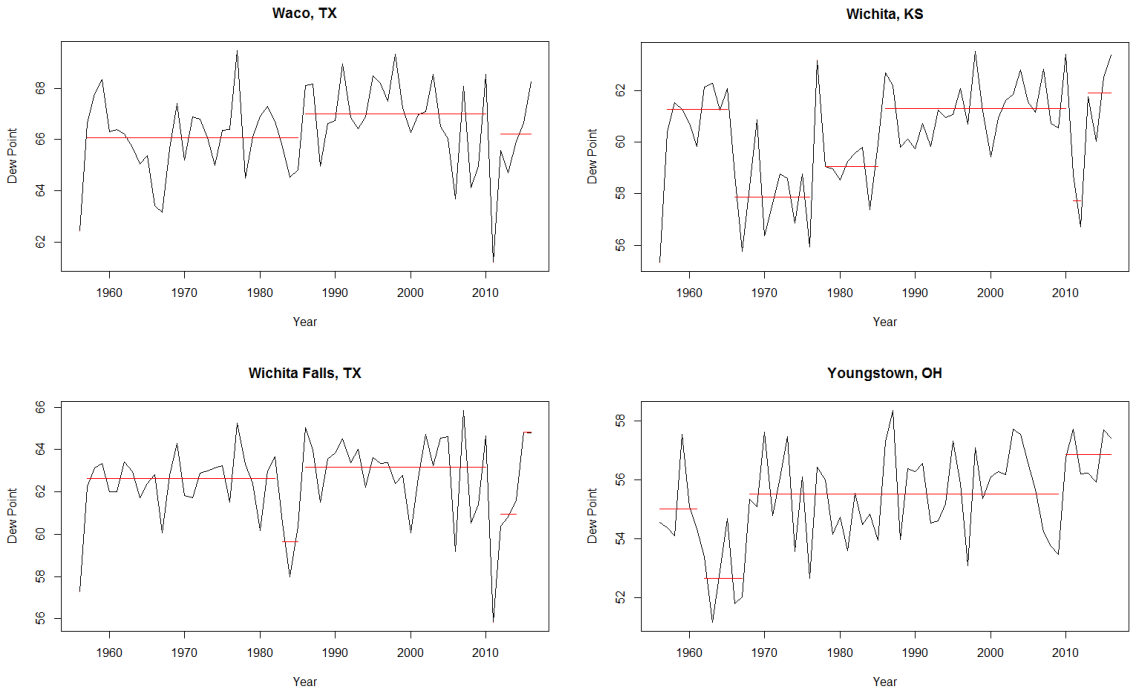
Waco, TX
Dew Point
Year
62
64
66
68
1960
1970
1980
1990
2000
2010
Wichita, KS
Dew Point
Year
56
58
60
62
1960
1970
1980
1990
2000
2010
Wichita Falls, TX
Dew Point
Year
56
58
60
62
64
66
1960
1970
1980
1990
2000
2010
Youngstown, OH
Dew Point
Year
52
54
56
58
1960
1970
1980
1990
2000
2010

Appendix C- *Interpolated images showing dew point, maximum/minimum temperature, and vapor pressure deficit from NWS FOS point location station data.*

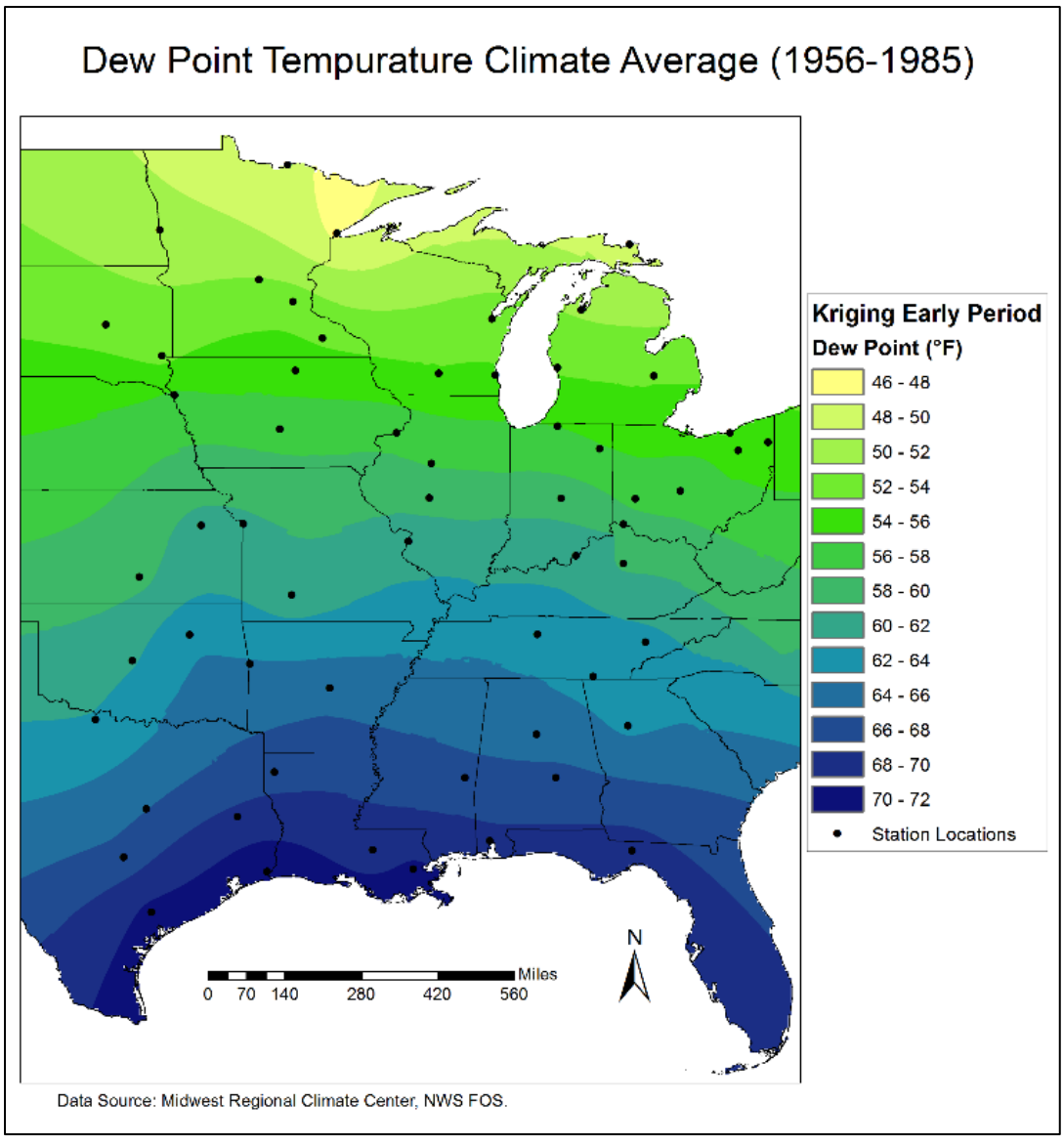

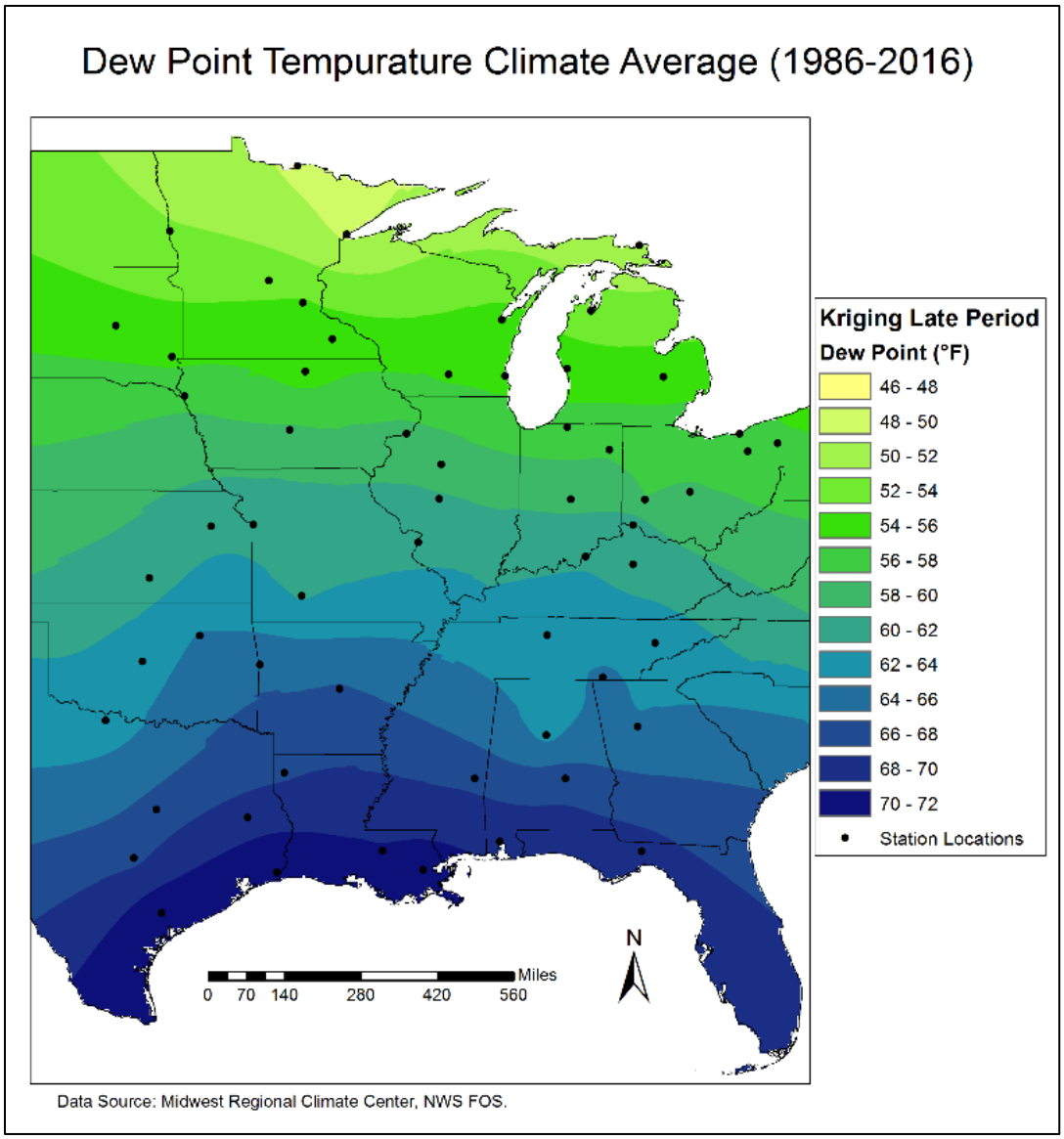
Dew Point Tempurature Climate Average (1986-2016)
Kriging Late Period
Dew Point (°F)
46 - 48
48 - 50
50 - 52
52 - 54
54 - 56
56 - 58
58 - 60
60 - 62
62 - 64
64 - 66
66 - 68
68 - 70
70 - 72
Station Locations
N
Miles
0 70 140 280 420 560
Data Source: Midwest Regional Climate Center, NWS FOS.

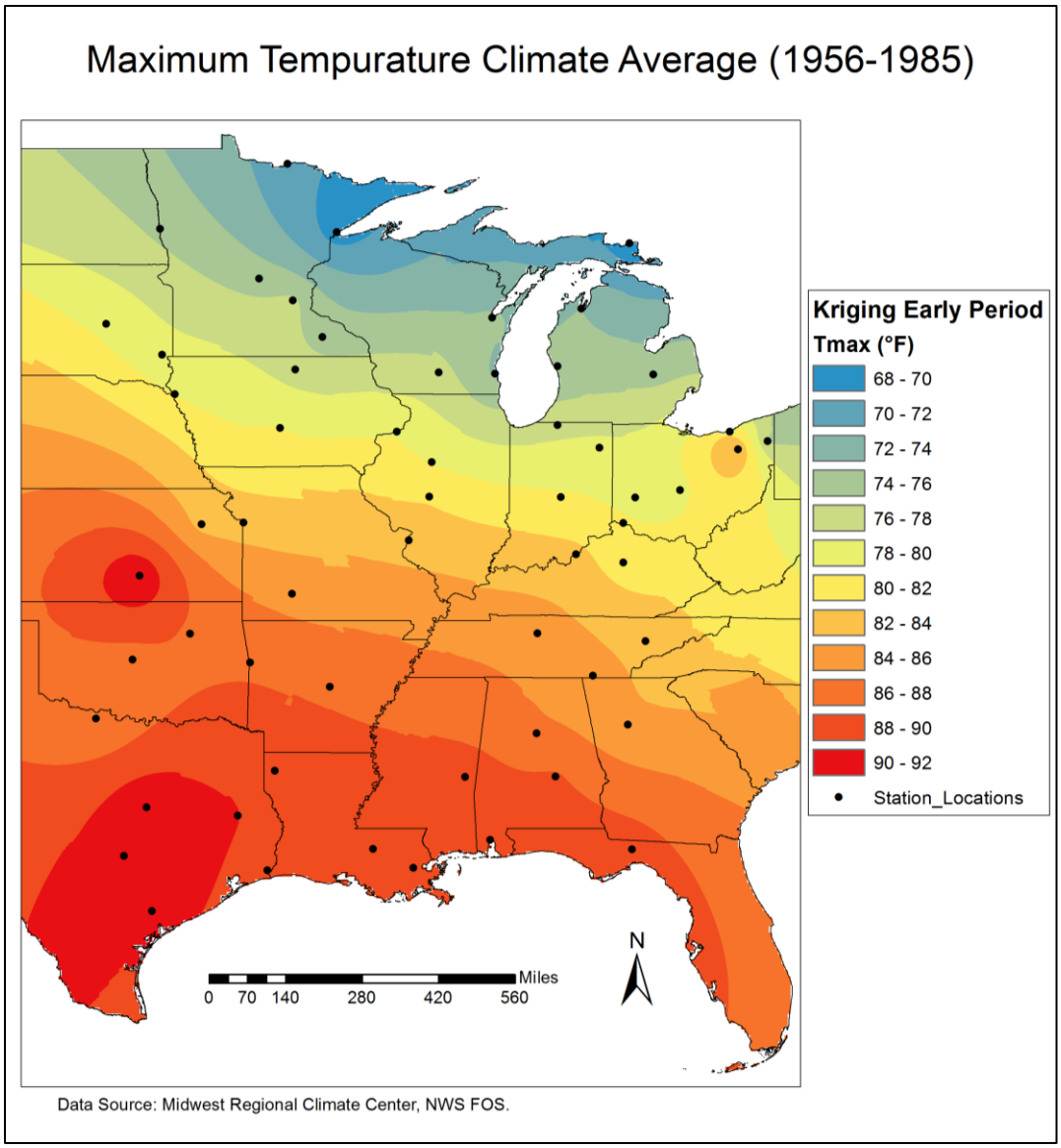
Maximum Tempurature Climate Average (1956-1985)
Kriging Early Period
Tmax (°F)
68 - 70
70 - 72
72 - 74
74 - 76
76 - 78
78 - 80
80 - 82
82 - 84
84 - 86
86 - 88
88 - 90
90 - 92
Station_Locations
Miles
0 70 140 280 420 560
N
Data Source: Midwest Regional Climate Center, NWS FOS.

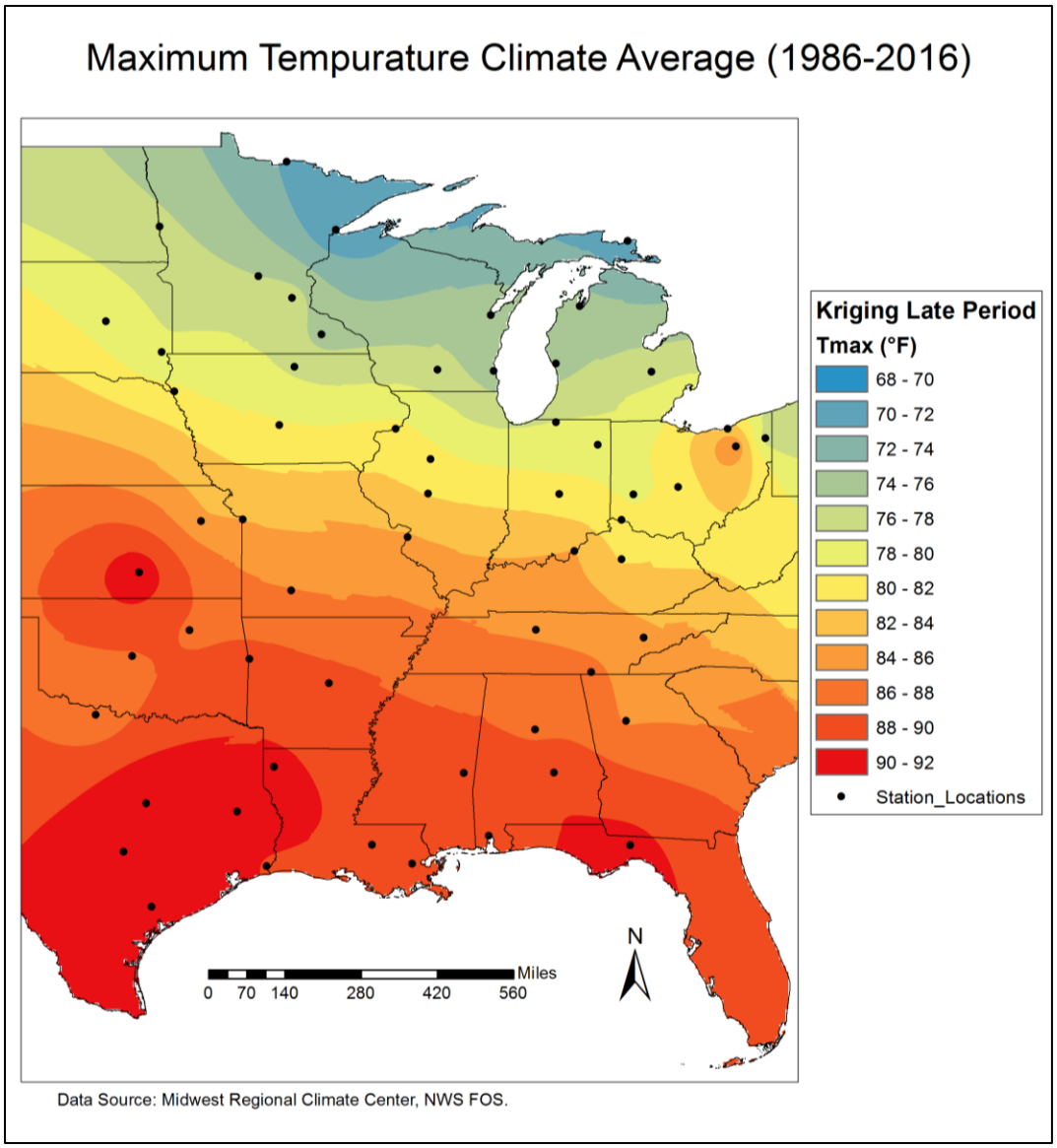
Maximum Tempurature Climate Average (1986-2016)
Kriging Late Period
Tmax (°F)
68 - 70
70 - 72
72 - 74
74 - 76
76 - 78
78 - 80
80 - 82
82 - 84
84 - 86
86 - 88
88 - 90
90 - 92
Station_Locations
Miles
0 70 140 280 420 560
N
Data Source: Midwest Regional Climate Center, NWS FOS.

Minimum Tempurature Climate Average (1956-1985)

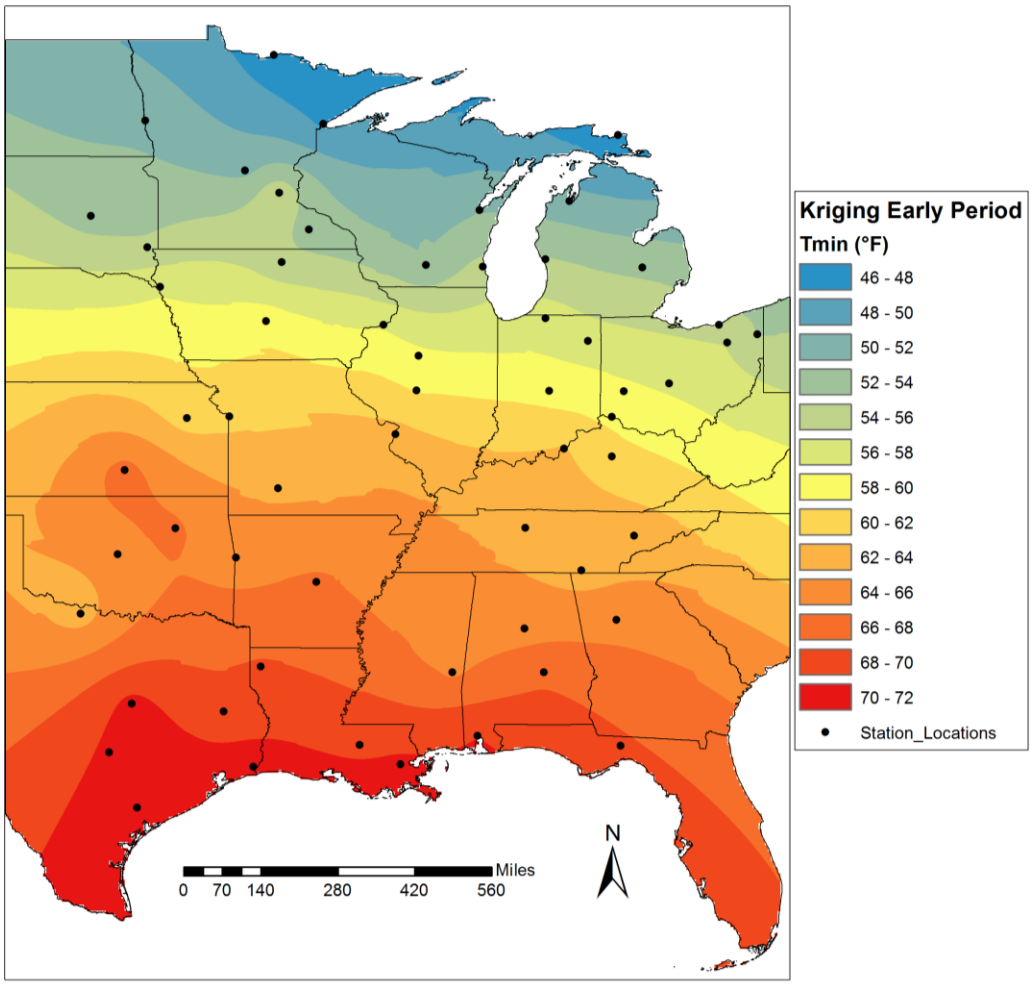

Data Source: Midwest Regional Climate Center, NWS FOS.

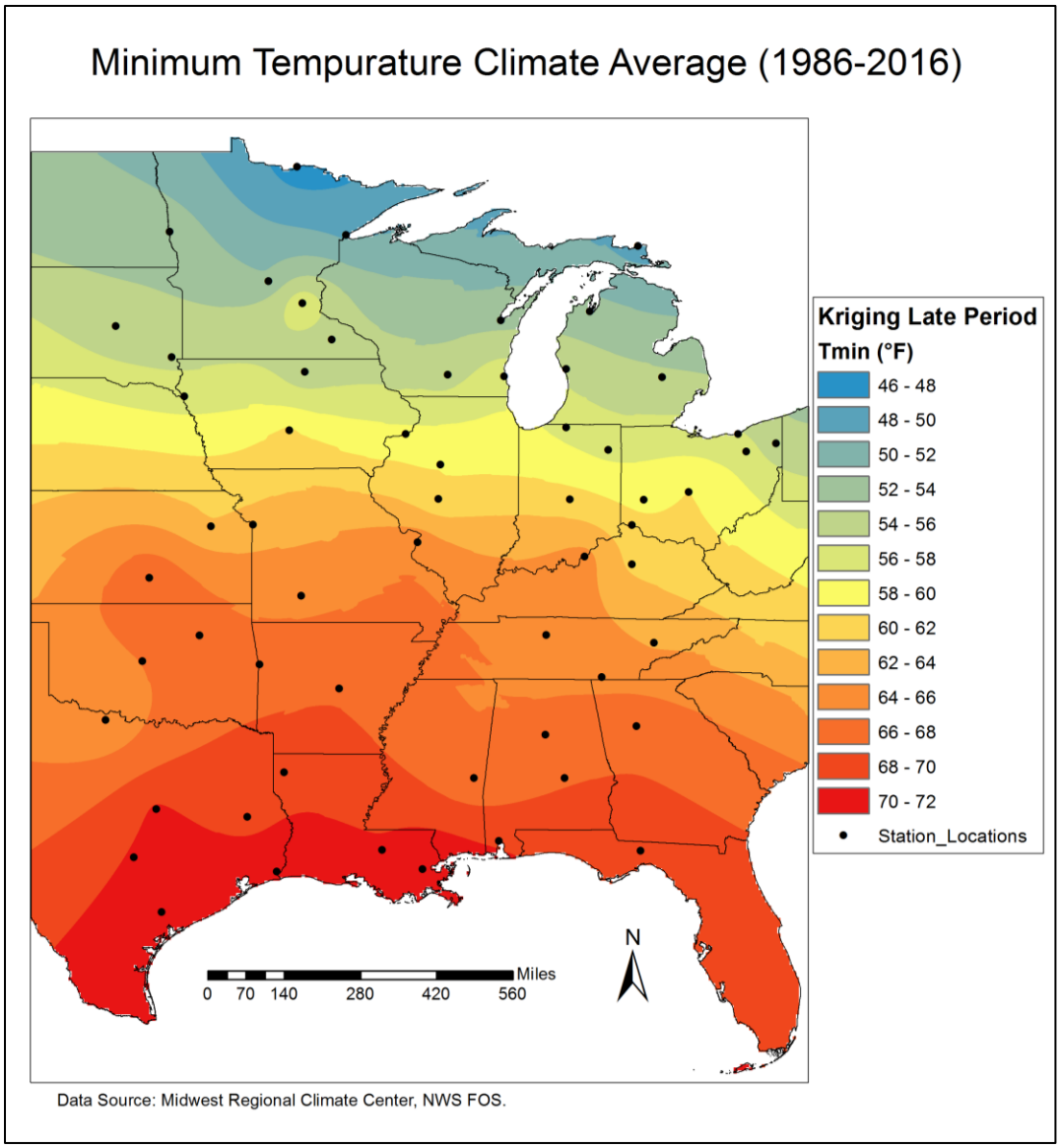
Minimum Tempurature Climate Average (1986-2016)
Kriging Late Period
Tmin (°F)
46 - 48
48 - 50
50 - 52
52 - 54
54 - 56
56 - 58
58 - 60
60 - 62
62 - 64
64 - 66
66 - 68
68 - 70
70 - 72
Station_Locations
Miles
0 70 140 280 420 560
N
Data Source: Midwest Regional Climate Center, NWS FOS.

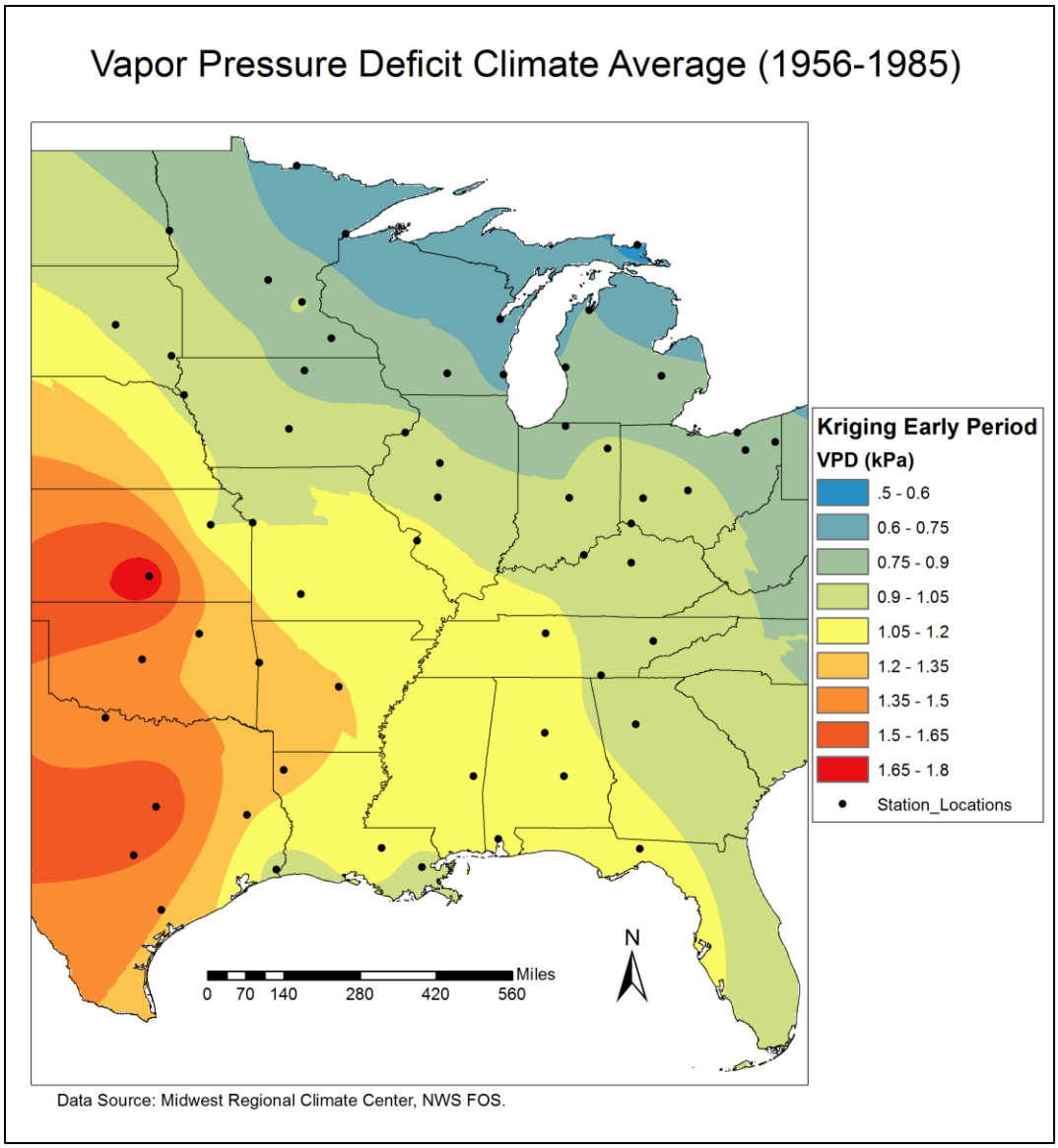
Vapor Pressure Deficit Climate Average (1956-1985)
Kriging Early Period
VPD (kPa)
.5 - 0.6
0.6 - 0.75
0.75 - 0.9
0.9 - 1.05
1.05 - 1.2
1.2 - 1.35
1.35 - 1.5
1.5 - 1.65
1.65 - 1.8
Station_Locations
Miles
0 70 140 280 420 560
N
Data Source: Midwest Regional Climate Center, NWS FOS.

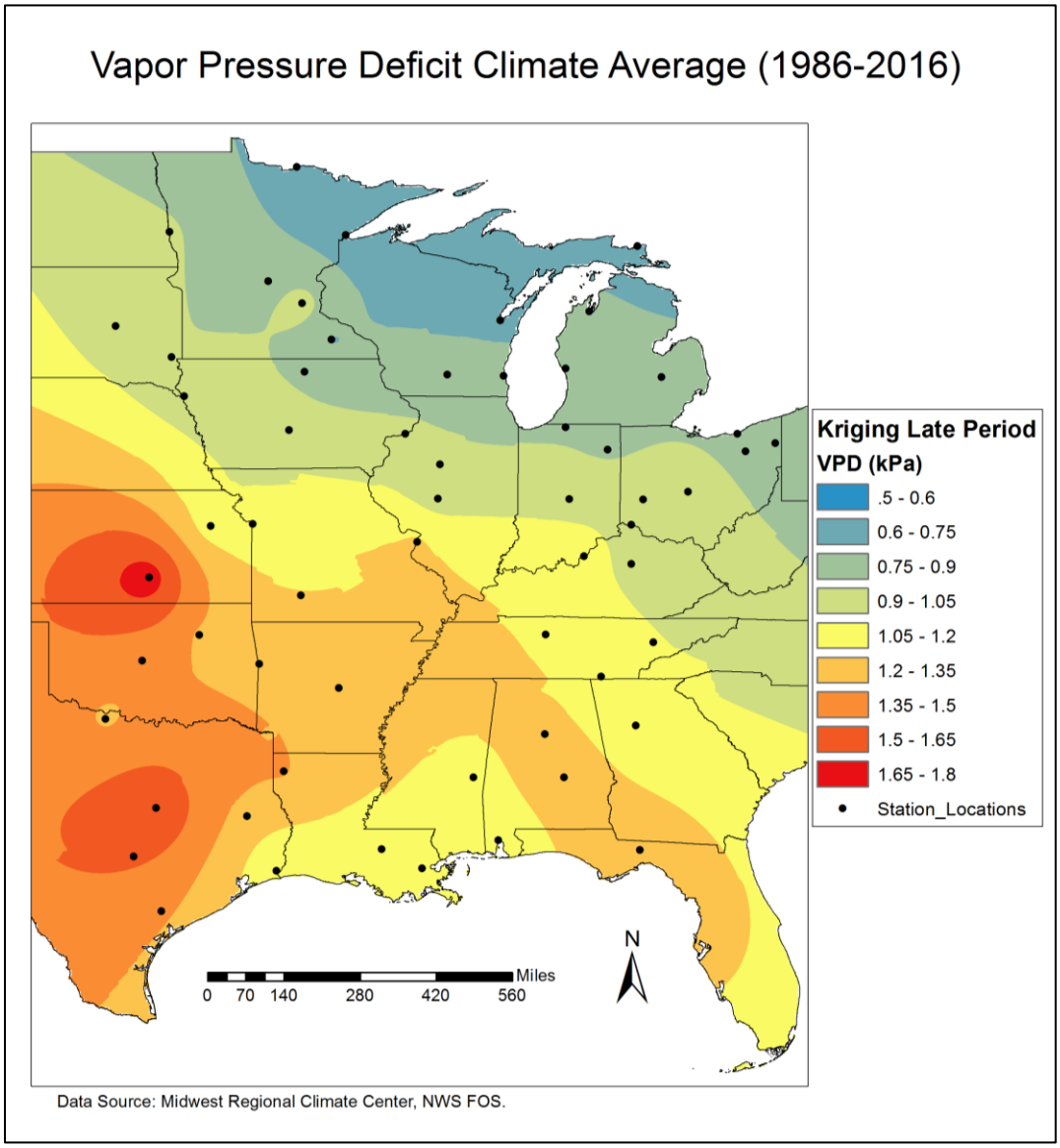
Vapor Pressure Deficit Climate Average (1986-2016)
Kriging Late Period
VPD (kPa)
.5 - 0.6
0.6 - 0.75
0.75 - 0.9
0.9 - 1.05
1.05 - 1.2
1.2 - 1.35
1.35 - 1.5
1.5 - 1.65
1.65 - 1.8
Station_Locations
N
Miles
0 70 140 280 420 560
Data Source: Midwest Regional Climate Center, NWS FOS.

Appendix D- *State compiled dew point temperature change points (aggregated to USDA Census of Agriculture periods) with corn and soybean yield per acre change points.*

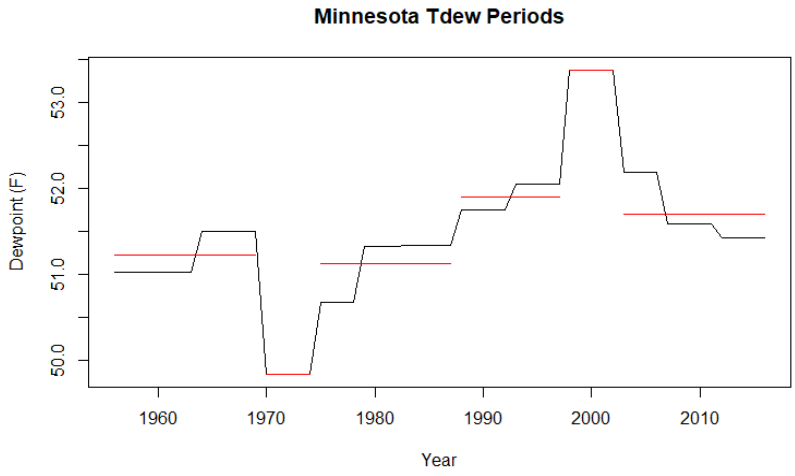

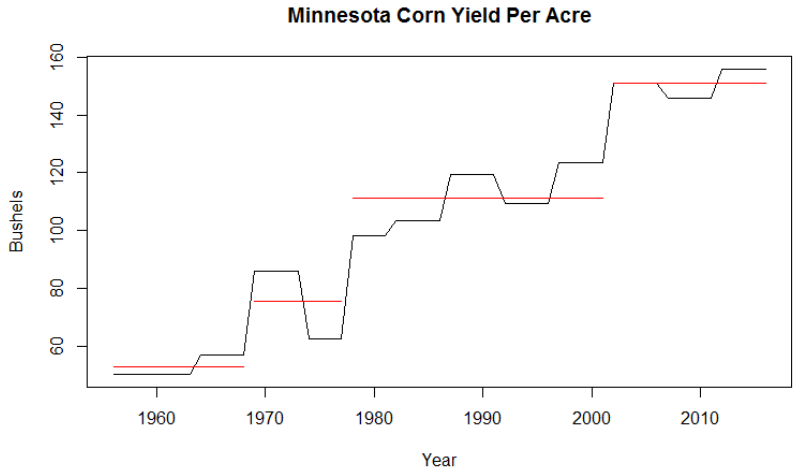

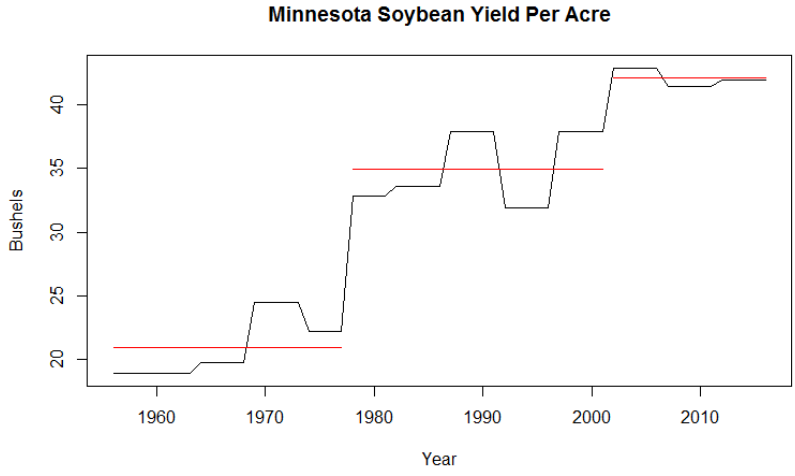

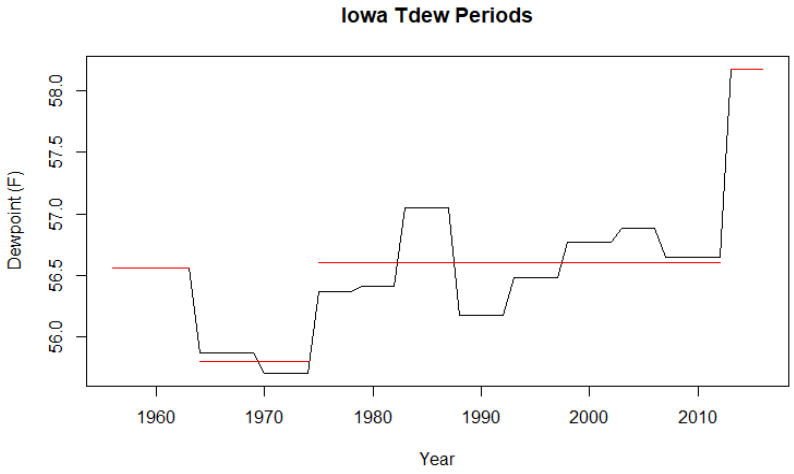
Iowa Tdew Periods
Dewpoint (F)
56.0
56.5
57.0
57.5
58.0
1960
1970
1980
1990
2000
2010
Year

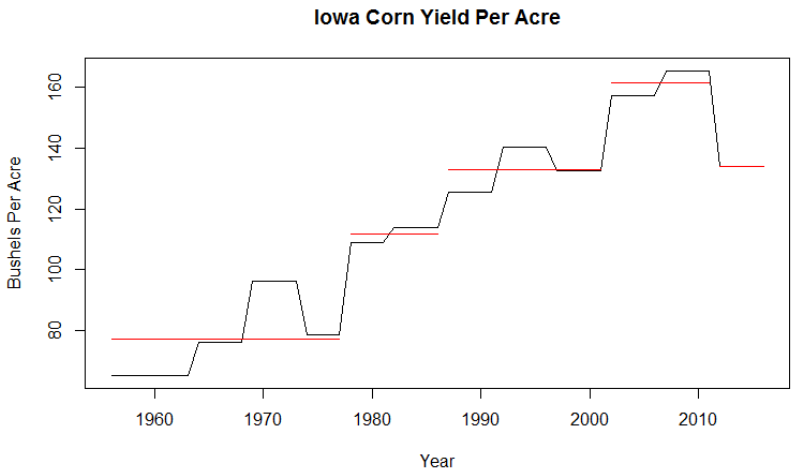
Iowa Corn Yield Per Acre
Bushels Per Acre
80
100
120
140
160
1960
1970
1980
1990
2000
2010
Year

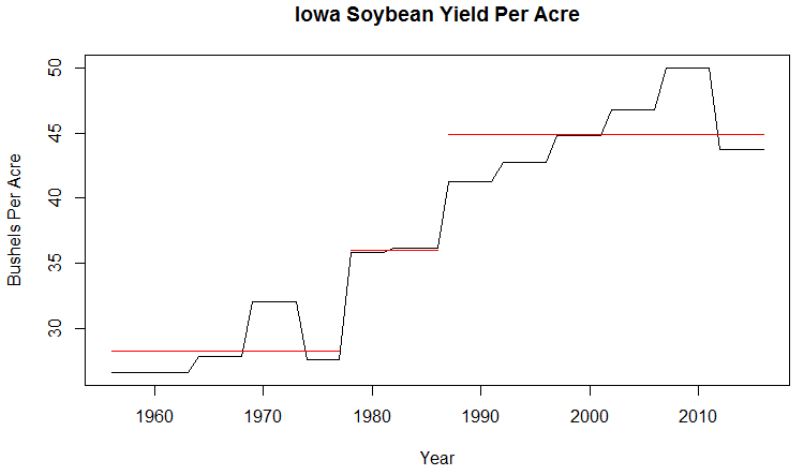
Iowa Soybean Yield Per Acre
Bushels Per Acre
30
35
40
45
50
1960
1970
1980
1990
2000
2010
Year

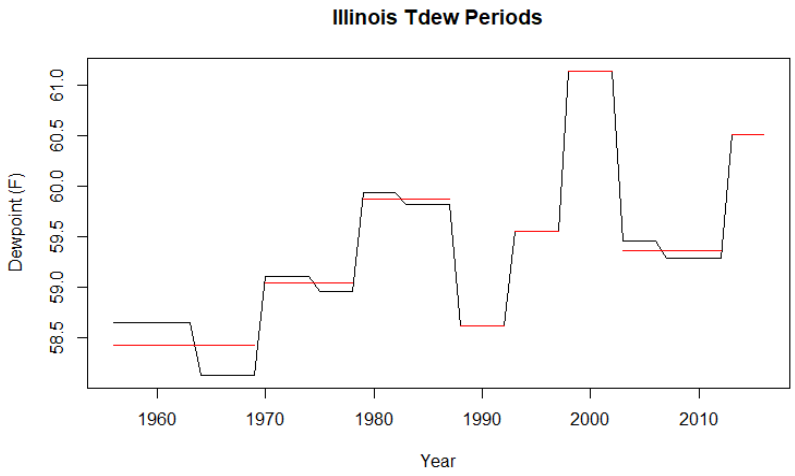
Illinois Tdew Periods
Dewpoint (F)
58.5
59.0
59.5
60.0
60.5
61.0
1960
1970
1980
1990
2000
2010
Year

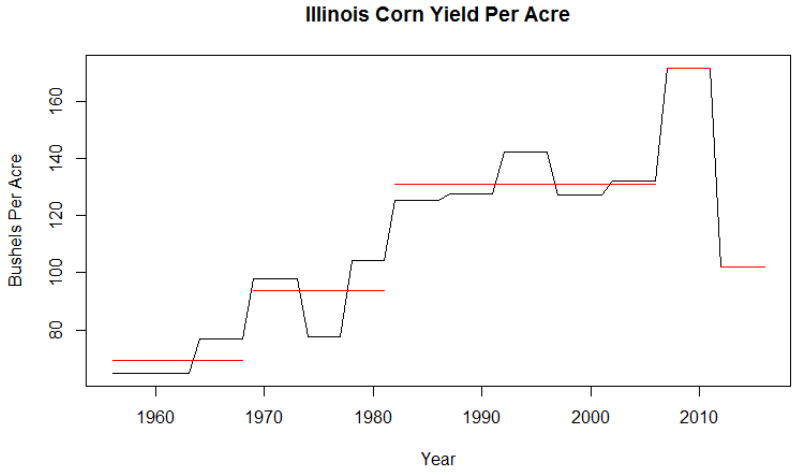
Illinois Corn Yield Per Acre
Bushels Per Acre
80
100
120
140
160
1960
1970
1980
1990
2000
2010
Year

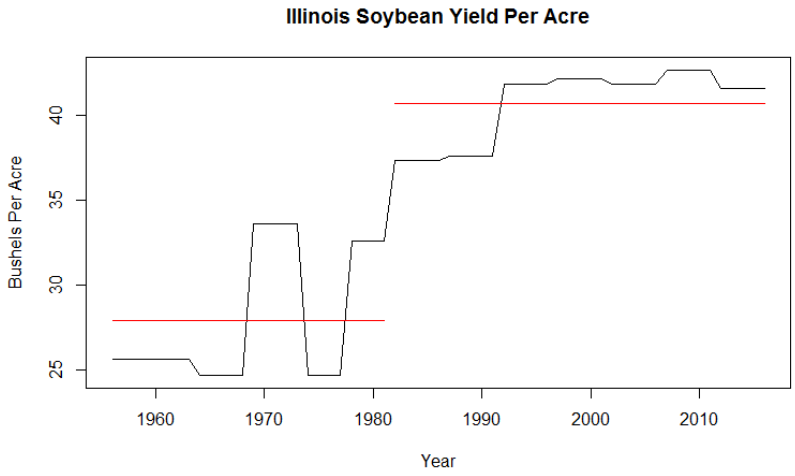
Illinois Soybean Yield Per Acre
Bushels Per Acre
25
30
35
40
1960
1970
1980
1990
2000
2010
Year

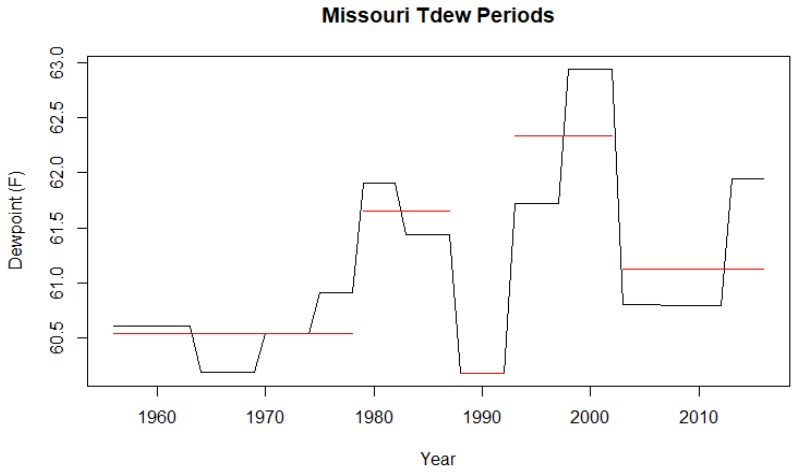
Missouri Tdew Periods
Dewpoint (F)
60.5
61.0
61.5
62.0
62.5
63.0
1960
1970
1980
1990
2000
2010
Year

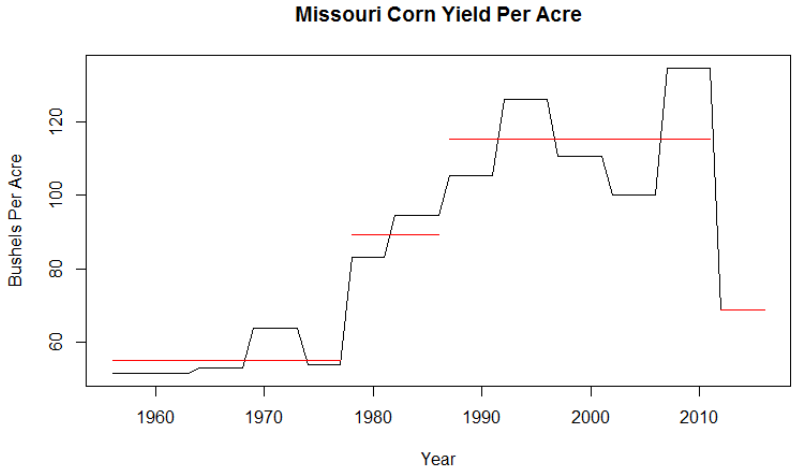
Missouri Corn Yield Per Acre
Bushels Per Acre
60
80
100
120
1960
1970
1980
1990
2000
2010
Year

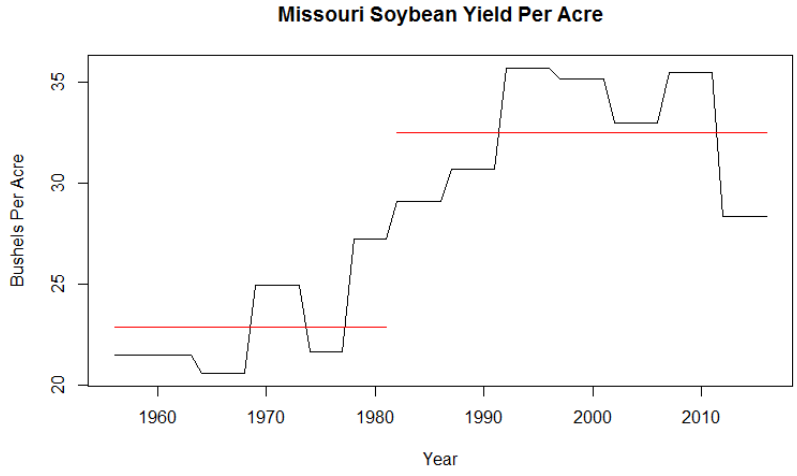
Missouri Soybean Yield Per Acre
Bushels Per Acre
20
25
30
35
1960
1970
1980
1990
2000
2010
Year

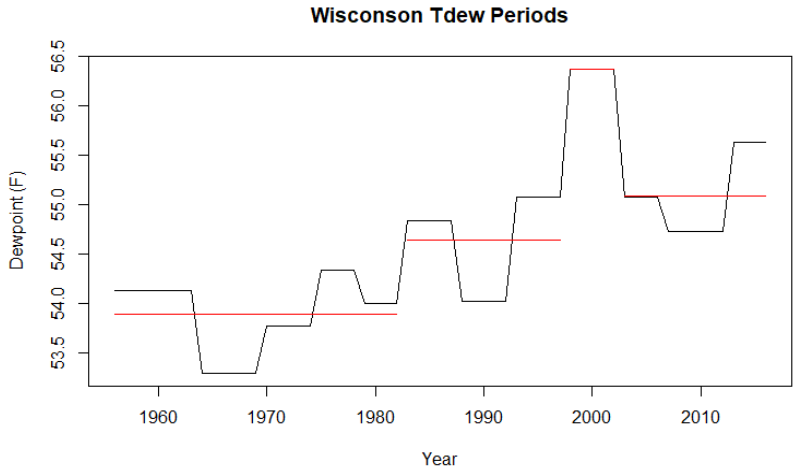
Wisconson Tdew Periods
Dewpoint (F)
53.5
54.0
54.5
55.0
55.5
56.0
56.5
1960
1970
1980
1990
2000
2010
Year

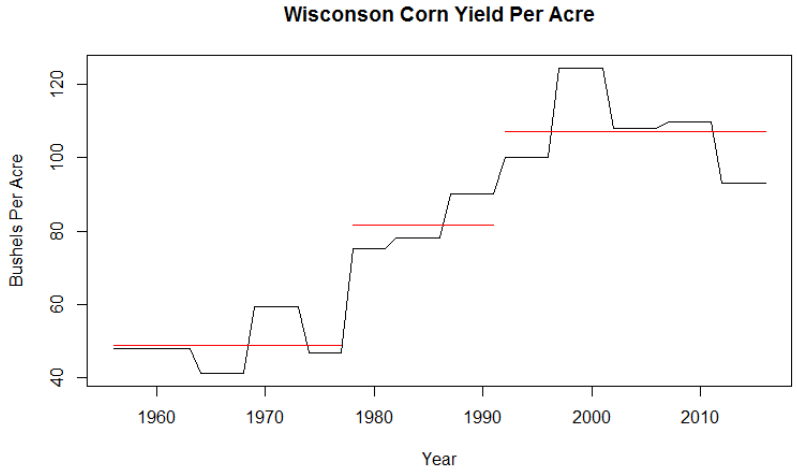
Wisconson Corn Yield Per Acre
Bushels Per Acre
40
60
80
100
120
1960
1970
1980
1990
2000
2010
Year

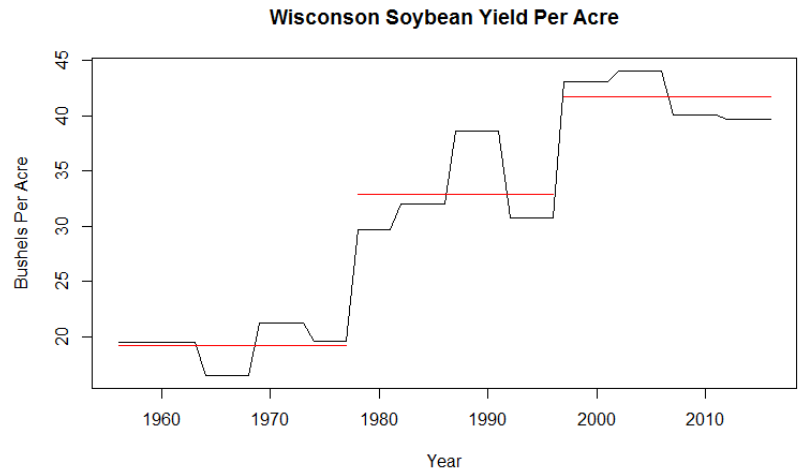
Wisconson Soybean Yield Per Acre
Bushels Per Acre
20
25
30
35
40
45
1960
1970
1980
1990
2000
2010
Year

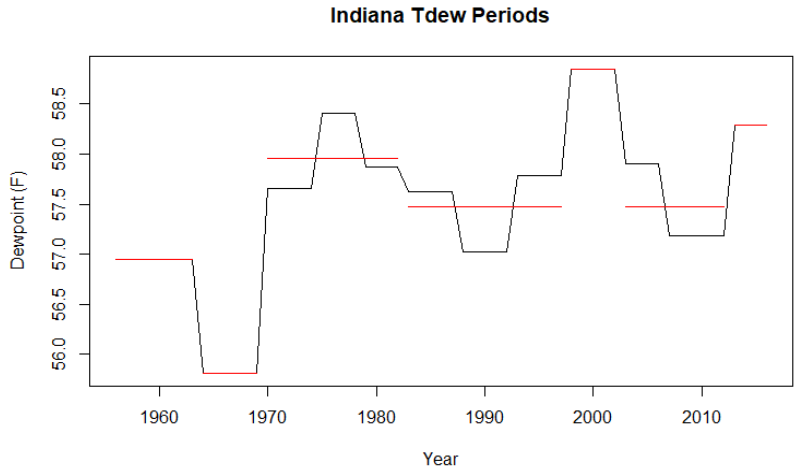
Indiana Tdew Periods
Dewpoint (F)
56.0
56.5
57.0
57.5
58.0
58.5
1960
1970
1980
1990
2000
2010
Year

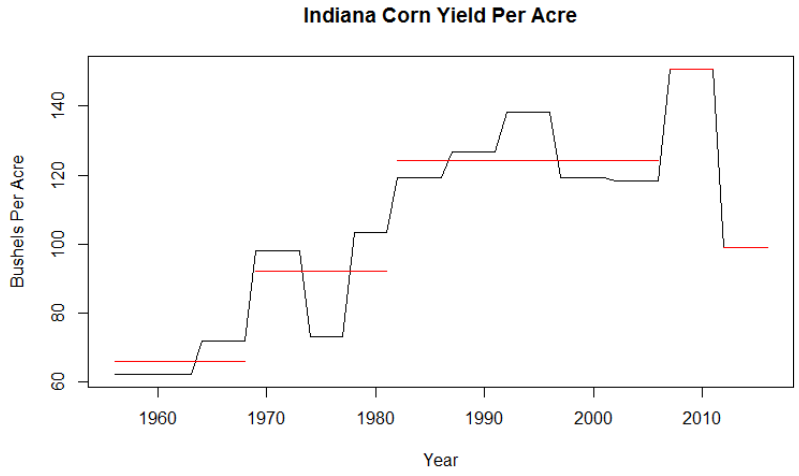
Indiana Corn Yield Per Acre
Bushels Per Acre
60
80
100
120
140
1960
1970
1980
1990
2000
2010
Year

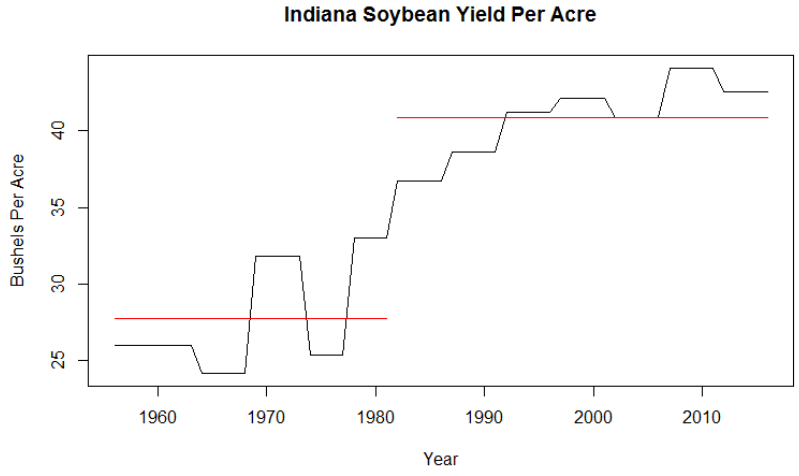
Indiana Soybean Yield Per Acre
Bushels Per Acre
25
30
35
40
1960
1970
1980
1990
2000
2010
Year

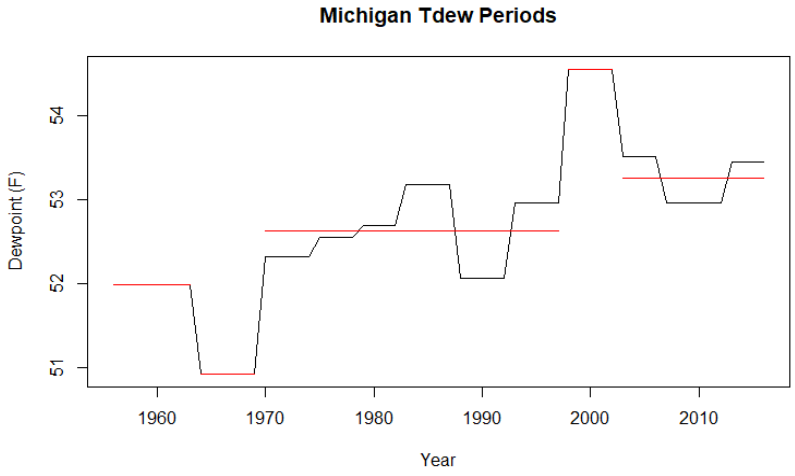
Michigan Tdew Periods
Dewpoint (F)
51
52
53
54
1960
1970
1980
1990
2000
2010
Year

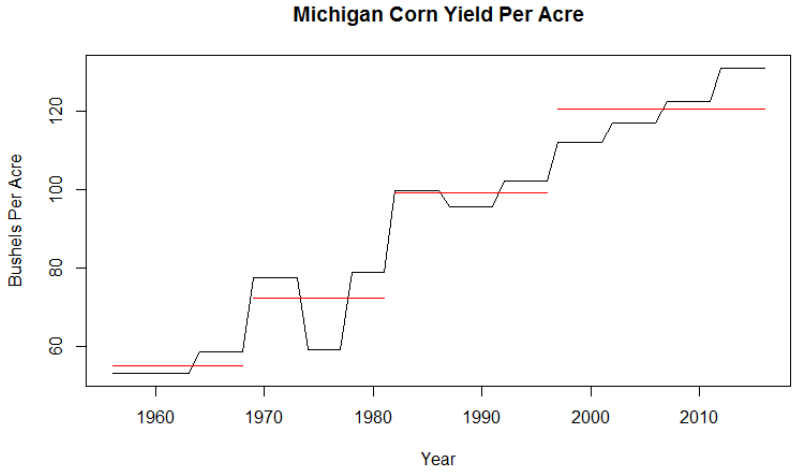
Michigan Corn Yield Per Acre
Bushels Per Acre
60
80
100
120
1960
1970
1980
1990
2000
2010
Year

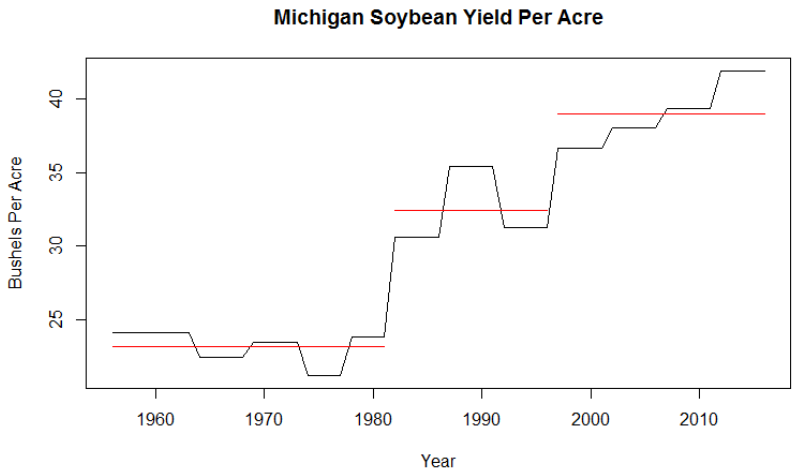
Michigan Soybean Yield Per Acre
Bushels Per Acre
25
30
35
40
1960
1970
1980
1990
2000
2010
Year

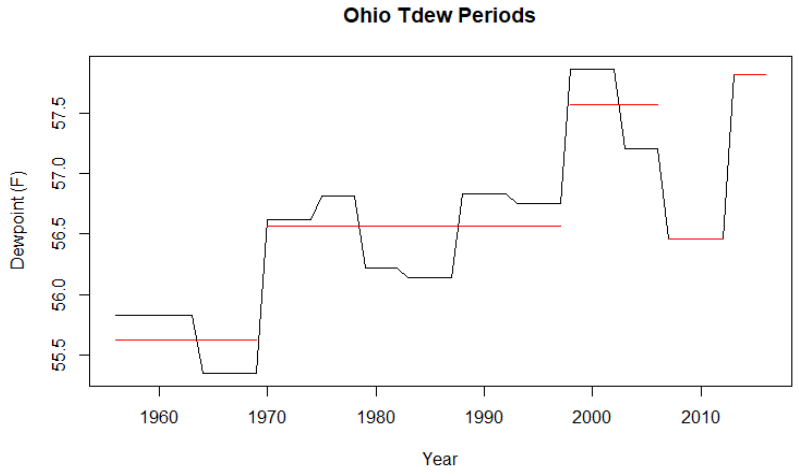
Ohio Tdew Periods
Dewpoint (F)
55.5
56.0
56.5
57.0
57.5
1960
1970
1980
1990
2000
2010
Year

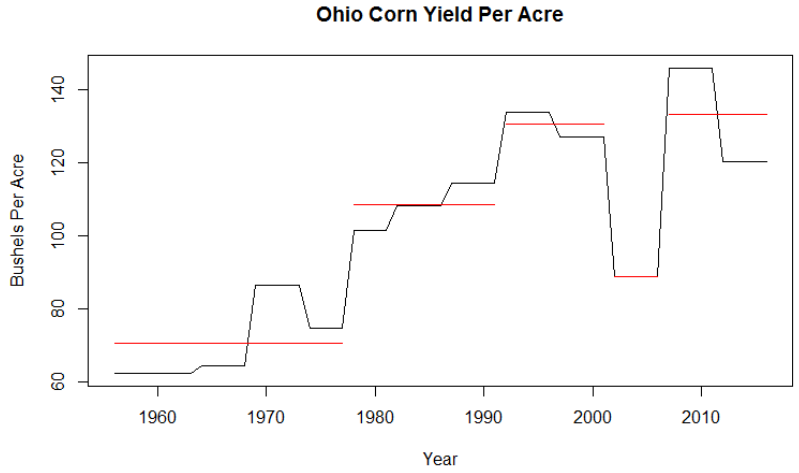
Ohio Corn Yield Per Acre
Bushels Per Acre
60
80
100
120
140
1960
1970
1980
1990
2000
2010
Year

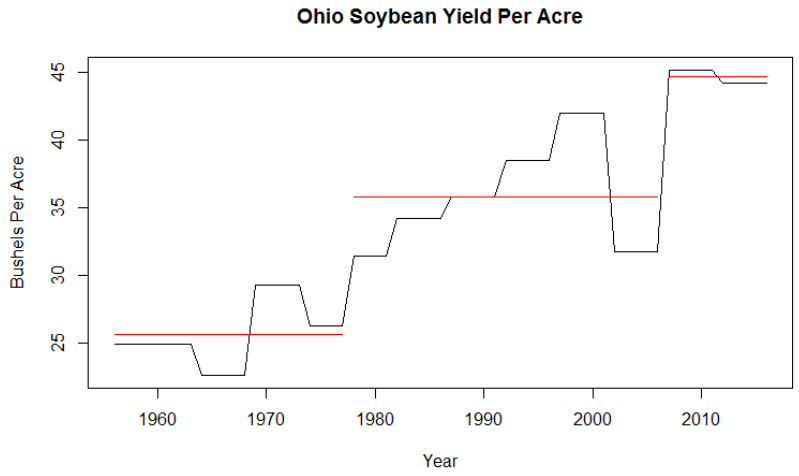
Ohio Soybean Yield Per Acre
Bushels Per Acre
25
30
35
40
45
1960
1970
1980
1990
2000
2010
Year

Appendix E- *2017 field work results, multivariable transpiritive flux, leaf to canopy model.*

Corn Field 1

Date	6/15/17	6/26/17	7/3/17	7/13/17	7/29/17	8/4/17	8/22/17	9/3/17	9/17/17
Time	2:22pm	1:38pm	1:21pm	12:39pm	1:35pm	1:15pm	12:57pm	12:56pm	1:04pm
Growth Stage	V4	V8	V11	V13	R2	R3	R4	R5	late R5
Ambient Conditions									
Ambient Temp (F)	81.00	70.00	79.00	66.00	79.00	73.00	72.00	80.00	59.00
Ambient Temp (C)	27.22	21.11	26.11	18.89	26.11	22.78	22.22	26.67	15.00
Dew Point Temp (F)	52.00	39.00	52.00	55.00	54.00	48.00	48.00	63.00	43.00
Dew Point Temp (C)	11.11	3.89	11.11	12.78	12.22	8.89	8.89	17.22	6.11
Relative Humidity (%)	52.00	33.00	39.00	68.00	42.00	41.00	43.00	54.00	57.00
Atm Pressure (kPa)	97.46	98.67	98.23	98.50	98.65	98.32	98.45	97.90	98.66
Percent Sky Cover (%)	0.00	20.00	5.00	100.00	0.00	15.00	0.00	0 hazy	0.00
Wind Speed (mph)	12.00	7.00	9.00	10.00	14.00	9.00	14.00	12.00	12.00
Wind Direction	NW	N	E	NNW	SSE	N	NW	SSW	WNW
Vapor Pressure									
es air (kPa)	3.61	2.50	3.38	2.18	3.38	2.77	2.68	3.50	1.71
ea air (kPa)	1.32	0.81	1.32	1.48	1.42	1.14	1.14	1.96	0.94
Calculated Atmospheric VPD (kPa)	**2.29**	**1.70**	**2.06**	**0.71**	**1.96**	**1.63**	**1.54**	**1.53**	**0.76**
Measured Values									
Soil Moisture 1 (m3/m3)	X	0.263	0.248	0.282	0.213	0.213	0.134	0.262	0.121
Soil Moisture 2 (m3/m3)	X	0.182	0.216	0.281	0.210	0.158	0.242	0.271	0.164
Soil Moisture 3 (m3/m3)	X	0.214	0.204	0.269	0.229	0.203	0.280	0.283	0.149
Average Soil Moisture (m3/m3)	**X**	**0.220**	**0.223**	**0.277**	**0.217**	**0.191**	**0.219**	**0.272**	**0.145**
IRGA Readings									
Upper Photo 1	46.20	41.10	48.80	17.50	33.60	29.90	27.80	34.10	13.90
Upper Photo 2	43.20	44.10	49.00	16.20	43.70	36.70	32.20	27.30	22.80
Upper Photo 3	45.40	44.40	52.90	22.10	43.50	33.70	30.20	32.80	19.10
Upper Photo 4	45.90	47.10	47.10	17.90	40.90	36.30	31.30	29.60	25.00
Upper Photo 5	45.50	49.30	49.60	17.90	33.00	36.70	34.20	30.80	15.20
Upper Photo 6	43.20	41.90	53.10	17.00	39.40	34.40	33.00	36.40	18.50
Upper Photo 7	40.00	44.50	52.00	19.60	41.70	31.80	37.80	32.00	24.70
Upper Photo 8	40.90	47.40	51.20	16.40	38.80	32.90	32.10	29.90	20.50
Avg Upper Photo (umol CO2/m2/s)	**43.79**	**44.98**	**50.46**	**18.08**	**39.33**	**34.05**	**32.33**	**31.61**	**19.96**
Upper Plant Photo (umol CO2 plant/s)	**0.710**	**1.411**	**3.566**	**1.474**	**3.310**	**2.859**	**2.649**	**2.284**	**1.055**
Upper Cond 1	1.730	0.930	0.364	0.141	0.229	0.180	0.148	0.253	0.077

Upper Cond 2	1.180	0.903	0.347	0.118	0.371	0.229	0.191	0.183	0.118
Upper Cond 3	1.620	1.060	0.432	0.165	0.349	0.189	0.215	0.219	0.091
Upper Cond 4	1.830	1.030	0.322	0.158	0.258	0.210	0.187	0.180	0.119
Upper Cond 5	1.590	1.120	0.348	0.155	0.218	0.217	0.257	0.209	0.126
Upper Cond 6	1.130	1.050	0.423	0.131	0.292	0.188	0.214	0.238	0.094
Upper Cond 7	1.050	0.926	0.372	0.166	0.296	0.226	0.276	0.246	0.122
Upper Cond 8	1.100	1.320	0.418	0.140	0.287	0.205	0.203	0.215	0.102
Avg Upper Cond (mol H2O/m2/s)	**1.404**	**1.042**	**0.378**	**0.147**	**0.288**	**0.206**	**0.211**	**0.218**	**0.106**
Upper Plant Cond (mol H2O plant/s)	**0.023**	**0.033**	**0.027**	**0.012**	**0.024**	**0.017**	**0.017**	**0.016**	**0.006**
Upper Transpiration 1	9.12	7.59	7.16	1.97	5.34	4.42	2.93	5.24	1.44
Upper Transpiration 2	8.73	7.78	6.99	1.72	7.24	5.27	3.70	4.24	2.23
Upper Transpiration 3	9.42	8.24	7.93	2.25	7.10	4.66	3.91	4.88	1.89
Upper Transpiration 4	9.56	8.57	6.84	2.12	6.20	5.33	3.42	4.37	2.28
Upper Transpiration 5	9.53	8.87	7.16	2.05	5.72	5.34	4.53	4.78	1.98
Upper Transpiration 6	9.31	7.70	7.85	1.93	7.17	4.85	4.15	5.16	1.97
Upper Transpiration 7	8.83	7.38	7.62	2.21	7.26	5.23	4.95	5.27	2.43
Upper Transpiration 8	9.38	8.13	7.67	2.00	7.06	4.66	4.18	4.98	1.87
Avg Upper Trans (mmol H2O/m2/s)	**9.24**	**8.03**	**7.40**	**2.03**	**6.64**	**4.97**	**3.97**	**4.87**	**2.01**
Upper Plant Trans (mmol H2O plant/s)	**0.150**	**0.252**	**0.523**	**0.166**	**0.559**	**0.417**	**0.325**	**0.351**	**0.106**
Lower Photo 1	N/A	N/A	3.31	3.15	2.39	3.87	8.08	3.98	4.19
Lower Photo 2	N/A	N/A	4.53	3.88	0.08	2.78	6.43	6.14	2.75
Lower Photo 3	N/A	N/A	5.92	5.36	2.21	1.74	4.42	3.40	5.03
Lower Photo 4	N/A	N/A	0.93	5.61	1.32	0.19	4.15	2.91	4.92
Lower Photo 5	N/A	N/A	5.56	7.21	4.62	2.50	2.44	7.57	6.07
Lower Photo 6	N/A	N/A	1.92	3.42	3.42	2.95	1.74	3.62	6.60
Lower Photo 7	N/A	N/A	2.34	5.43	2.42	2.76	3.18	2.33	3.97
Lower Photo 8	N/A	N/A	0.11	10.00	1.49	2.91	5.12	5.91	7.01
Avg Lower Photo (umol CO2/m2/s)	**N/A**	**N/A**	**3.08**	**5.51**	**2.24**	**2.46**	**4.45**	**4.48**	**5.07**
Lower Plant Photo (umol CO2 plant/s)	**N/A**	**N/A**	**0.06**	**0.15**	**0.08**	**0.08**	**0.15**	**0.12**	**0.07**
Lower Cond 1	N/A	N/A	0.05	0.12	0.049	0.036	0.04	0.03	0.03
Lower Cond 2	N/A	N/A	0.04	0.03	0.016	0.016	0.07	0.06	0.02
Lower Cond 3	N/A	N/A	0.06	0.06	0.026	0.012	0.05	0.03	0.03
Lower Cond 4	N/A	N/A	0.04	0.10	0.017	0.003	0.02	0.05	0.02
Lower Cond 5	N/A	N/A	0.04	0.09	0.039	0.013	0.02	0.08	0.11
Lower Cond 6	N/A	N/A	0.13	0.10	0.045	0.045	0.03	0.03	0.05
Lower Cond 7	N/A	N/A	0.05	0.05	0.024	0.010	0.03	0.04	0.05
Lower Cond 8	N/A	N/A	0.05	0.06	0.037	0.032	0.06	0.05	0.06
Avg Lower Cond (mol H2O/m2/s)	**N/A**	**N/A**	**0.06**	**0.08**	**0.032**	**0.021**	**0.039**	**0.046**	**0.045**

Lower Cond (mol H2O plant/s)	**N/A**	**N/A**	**0.00**	**0.00**	**0.001**	**0.001**	**0.001**	**0.001**	**0.001**
Lower Transpiration 1	N/A	N/A	1.38	0.55	1.45	0.91	1.36	0.79	0.46
Lower Transpiration 2	N/A	N/A	1.20	0.95	0.51	0.46	0.83	1.40	0.37
Lower Transpiration 3	N/A	N/A	1.41	1.41	0.81	0.34	0.44	0.71	0.43
Lower Transpiration 4	N/A	N/A	1.05	1.31	0.52	0.08	0.77	1.31	0.29
Lower Transpiration 5	N/A	N/A	1.05	1.35	1.09	0.43	0.45	1.37	1.68
Lower Transpiration 6	N/A	N/A	2.94	0.80	1.15	1.13	0.57	0.67	0.84
Lower Transpiration 7	N/A	N/A	1.45	0.96	0.64	0.28	0.58	1.02	0.78
Lower Transpiration 8	N/A	N/A	1.38	1.61	0.92	0.65	1.15	1.18	0.99
Avg Lower Trans (mmol H2O m2/s)	**N/A**	**N/A**	**1.48**	**1.12**	**0.89**	**0.53**	**0.77**	**1.06**	**0.73**
Lower Trans (mmol H2O plant/s)	**N/A**	**N/A**	**0.03**	**0.03**	**0.03**	**0.02**	**0.03**	**0.03**	**0.01**
Leaf Area Upper (m2)	0.01622	0.03138	0.07066	0.08154	0.08418	0.08397	0.08196	0.07224	0.05287
Leaf Area Lower (m2)	N/A	N/A	0.01979	0.02795	0.03375	0.03329	0.03387	0.02634	0.01363
Total Leave Area per Plant	**0.01622**	**0.03138**	**0.09045**	**0.10949**	**0.11793**	**0.11726**	**0.11583**	**0.09858**	**0.06650**
Leaf Area Index (LAI)	0.12425	0.24038	0.69287	0.83872	0.90337	0.89824	0.88726	0.75515	0.50941
Cosine of Zenth Solar Angle (u)	0.83910	0.89540	0.90800	0.92060	0.86710	0.87020	0.83010	0.78580	0.71840
G(u) at 67.5° Leaf Angle	0.32356	0.32356	0.32356	0.32356	0.32356	0.32356	0.32356	0.32356	0.32356
Kb	0.38561	0.36136	0.35635	0.35147	0.37316	0.37183	0.38979	0.41176	0.45040
Sunlit Leaf Fraction	0.95	0.92	0.78	0.74	0.71	0.72	0.71	0.73	0.79
Shaded Leaf Fraction	0.05	0.08	0.22	0.26	0.29	0.28	0.29	0.27	0.21
Total Plant Photo (umol CO2 plant/s)	0.710	1.411	3.627	1.628	3.386	2.941	2.800	2.402	1.124
Total Plant Cond (mol H2O plant/s)	0.023	0.033	0.028	0.014	0.025	0.018	0.019	0.017	0.006
Total Plant Trans (mmol H2O plant/s)	0.150	0.252	0.552	0.197	0.589	0.435	0.352	0.379	0.116
Population/Acre	32000	32000	32000	32000	32000	32000	32000	32000	32000
Total Photo/Acre (umol CO2 acre/s)	22727	45162	116052	52087	108359	94112	89598	76852	35982
Total Cond/Acre (mol H2O acre/s)	728.60	1046.71	892.37	451.87	808.58	574.29	596.72	542.57	199.08
Total Trans/Acre (mmol H2O acre/s)	4793	8066	17677	6300	18835	13922	11249	12135	3721
Total Trans (mL/acre/s)	**86.35**	**145.31**	**318.45**	**113.50**	**339.32**	**250.81**	**202.65**	**218.62**	**67.04**
Total Trans (mL/acre/min)	5181	8718	19107	6810	20359	15048	12159	13117	4022
Total Trans (mL/acre/hour)	310867	523107	1146422	408605	1221548	902904	729546	787014	241337
Total Trans (mL/m2/hour)	76.82	129.26	283.29	100.97	301.85	223.11	180.27	194.48	59.64

Total Cond (mL/acre/s)	13126	18857	16076	8140	14567	10346	10750	9774	3586
Total Cond (mL/acre/min)	787546	1131390	964567	488429	873994	620747	644995	586465	215181
Total Cond (mL/acre/hour)	47252780	67883413	57873992	29305757	52439667	37244816	38699697	35187915	12910868
Total Cond (mL/m2/hour)	11676	16774	14301	7242	12958	9203	9563	8695	3190
CO2 (mol/acre/s)	0.02273	0.04516	0.11605	0.05209	0.10836	0.09411	0.08960	0.07685	0.03598
Air Temp in K	300.37	294.26	299.26	292.04	299.26	295.93	295.37	299.82	288.15
CO2 (L/acre/s)	0.58241	1.11988	2.93973	1.28405	2.73317	2.35525	2.23512	1.95693	0.87379
Pressure (atm)	0.96	0.97	0.97	0.97	0.97	0.97	0.97	0.97	0.97

Corn Field 2

Date	6/16/17	6/26/17	7/3/17	7/13/17	7/29/17	8/4/17	8/22/17	9/3/17	9/17/2017
Time	12:35pm	12:35pm	12:50pm	12:12pm	12:23pm	12:20pm	12:25pm	12:21pm	12:27pm
Growth Stage	V4	V9	V10	V12	R2	R3	R4	R5	R6
Ambient Conditions									
Ambient Temp (F)	79.00	70.00	79.00	66.00	79.00	73.00	72.00	80.00	59.00
Ambient Temp (C)	26.11	21.11	26.11	18.89	26.11	22.78	22.22	26.67	15.00
Dew Point Temp (F)	57.00	39.00	52.00	55.00	54.00	48.00	48.00	63.00	43.00
Dew Point Temp (C)	13.89	3.89	11.11	12.78	12.22	8.89	8.89	17.22	6.11
Relative Humidity (%)	47.00	33.00	39.00	68.00	42.00	41.00	43.00	54.00	57.00
Atm Pressure (kPa)	97.90	98.67	98.30	98.50	98.65	98.32	98.45	97.90	98.66
Percent Sky Cover (%)	100.00	20.00	5.00	100.00	0.00	15.00	0.00	0 hazy	0.00
Wind Speed (mph)	6.00	7.00	9.00	10.00	14.00	9.00	14.00	12.00	12.00
Wind Direction	SW	N	E	NNW	SSE	N	NW	SSW	WNW
Vapor Pressure									
es air (kPa)	3.38	2.50	3.38	2.18	3.38	2.77	2.68	3.50	1.71
ea air (kPa)	1.59	0.81	1.32	1.48	1.42	1.14	1.14	1.96	0.94
Calculated Atmospheric VPD (kPa)	**1.80**	**1.70**	**2.06**	**0.71**	**1.96**	**1.63**	**1.54**	**1.53**	**0.76**
Measured Values									
Soil Moisture 1 (m3/m3)	X	0.250	0.314	0.328	0.353	0.180	0.334	0.232	0.124
Soil Moisture 2 (m3/m3)	X	0.274	0.244	0.298	0.339	0.175	0.330	0.278	0.163
Soil Moisture 3 (m3/m3)	X	0.253	0.322	0.281	0.329	0.231	0.339	0.244	0.168
Average Soil Moisture (m3/m3)	**X**	**0.259**	**0.293**	**0.302**	**0.340**	**0.195**	**0.334**	**0.251**	**0.152**
IRGA Readings									
Upper Photo 1	17.90	40.00	47.30	19.80	44.70	36.60	36.10	33.10	17.00
Upper Photo 2	16.00	40.10	48.70	14.60	41.90	38.30	32.70	29.70	16.90
Upper Photo 3	21.70	33.50	49.60	22.60	45.60	39.30	37.70	37.30	18.30
Upper Photo 4	22.40	36.50	50.50	17.20	48.00	40.40	32.20	53.90	20.20
Upper Photo 5	11.70	35.70	46.80	19.70	47.40	38.70	33.70	34.40	17.90
Upper Photo 6	6.16	34.40	48.40	14.40	46.50	41.00	35.00	33.90	9.80
Upper Photo 7	6.05	36.80	53.30	18.20	41.80	39.40	33.60	32.40	16.70
Upper Photo 8	5.05	39.10	51.20	20.00	48.60	35.30	30.50	33.90	13.10
Avg Upper Photo (umol CO2/m2/s)	**13.37**	**37.01**	**49.48**	**18.31**	**45.56**	**38.63**	**33.94**	**36.08**	**16.24**
Upper Plant Photo (umol CO2 plant/s)	**0.274**	**1.778**	**4.229**	**1.537**	**4.103**	**3.499**	**3.000**	**2.823**	**0.817**
Upper Cond 1	0.654	0.977	0.364	0.176	0.282	0.253	0.244	0.212	0.091
Upper Cond 2	0.622	1.050	0.372	0.136	0.268	0.233	0.213	0.202	0.092
Upper Cond 3	0.633	0.962	0.456	0.146	0.303	0.227	0.274	0.320	0.134

Upper Cond 4	0.959	0.958	0.433	0.113	0.335	0.238	0.198	0.306	0.116
Upper Cond 5	0.375	0.864	0.346	0.170	0.322	0.227	0.245	0.282	0.050
Upper Cond 6	0.195	0.752	0.381	0.119	0.323	0.281	0.239	0.289	0.104
Upper Cond 7	0.203	0.799	0.489	0.166	0.310	0.224	0.246	0.229	0.050
Upper Cond 8	0.170	0.701	0.541	0.176	0.384	0.213	0.210	0.226	0.102
Avg Upper Cond (mol H2O/m2/s)	**0.476**	**0.883**	**0.423**	**0.150**	**0.316**	**0.237**	**0.234**	**0.258**	**0.092**
Upper Plant Cond (mol H2O plant/s)	**0.010**	**0.042**	**0.036**	**0.013**	**0.028**	**0.021**	**0.021**	**0.020**	**0.005**
Upper Transpiration 1	4.04	5.02	5.76	2.27	5.44	4.36	2.24	4.52	1.87
Upper Transpiration 2	4.01	7.47	6.17	1.84	5.75	4.36	3.88	4.23	1.90
Upper Transpiration 3	4.16	7.20	6.72	1.90	6.04	4.59	4.82	5.77	2.35
Upper Transpiration 4	4.90	7.03	6.63	1.68	6.35	4.67	3.94	5.33	2.34
Upper Transpiration 5	3.12	6.36	6.00	2.24	6.58	4.66	4.29	5.49	2.15
Upper Transpiration 6	2.09	6.65	6.39	1.76	6.82	5.40	4.56	5.01	1.14
Upper Transpiration 7	2.06	6.70	7.09	2.38	6.65	4.93	4.73	5.07	1.95
Upper Transpiration 8	1.84	6.91	7.62	2.46	7.97	4.71	4.52	5.64	1.89
Avg Upper Trans (mmol H2O/m2/s)	**3.28**	**6.67**	**6.55**	**2.07**	**6.45**	**4.71**	**4.12**	**5.13**	**1.95**
Upper Plant Trans (mmol H2O plant/s)	**0.067**	**0.320**	**0.560**	**0.173**	**0.581**	**0.427**	**0.364**	**0.402**	**0.098**
Lower Photo 1	N/A	N/A	N/A	7.77	2.44	5.45	2.12	6.76	2.17
Lower Photo 2	N/A	N/A	N/A	9.59	3.11	5.18	3.18	10.60	4.33
Lower Photo 3	N/A	N/A	N/A	11.10	6.63	1.64	2.80	6.60	2.72
Lower Photo 4	N/A	N/A	N/A	7.06	2.84	3.93	3.34	3.84	3.15
Lower Photo 5	N/A	N/A	N/A	11.20	3.57	6.77	5.02	6.14	2.97
Lower Photo 6	N/A	N/A	N/A	9.21	5.28	7.90	4.04	4.62	1.54
Lower Photo 7	N/A	N/A	N/A	9.67	3.56	4.40	3.85	2.03	0.78
Lower Photo 8	N/A	N/A	N/A	10.80	5.50	3.10	2.52	2.68	4.15
Avg Lower Photo (umol CO2/m2/s)	**N/A**	**N/A**	**N/A**	**9.55**	**4.12**	**4.80**	**3.36**	**5.41**	**2.73**
Lower Plant Photo (umol CO2 plant/s)	**N/A**	**N/A**	**N/A**	**0.30**	**0.17**	**0.20**	**0.15**	**0.18**	**0.03**
Lower Cond 1	N/A	N/A	N/A	0.12	0.057	0.048	0.06	0.12	0.052
Lower Cond 2	N/A	N/A	N/A	0.10	0.021	0.064	0.04	0.12	0.021
Lower Cond 3	N/A	N/A	N/A	0.16	0.036	0.106	0.05	0.07	0.047
Lower Cond 4	N/A	N/A	N/A	0.11	0.019	0.056	0.05	0.07	0.013
Lower Cond 5	N/A	N/A	N/A	0.15	0.038	0.050	0.06	0.09	0.028
Lower Cond 6	N/A	N/A	N/A	0.16	0.111	0.049	0.07	0.06	0.042
Lower Cond 7	N/A	N/A	N/A	0.09	0.046	0.050	0.13	0.15	0.035
Lower Cond 8	N/A	N/A	N/A	0.13	0.065	0.060	0.05	0.06	0.045
Avg Lower Cond (mol H2O/m2/s)	**N/A**	**N/A**	**N/A**	**0.13**	**0.049**	**0.060**	**0.066**	**0.091**	**0.035**

Lower Cond (mol H2O plant/s)	**N/A**	**N/A**	**N/A**	**0.00**	**0.002**	**0.003**	**0.003**	**0.003**	**0.000**
Lower Transpiration 1	N/A	N/A	N/A	1.68	1.46	1.00	1.24	2.37	0.82
Lower Transpiration 2	N/A	N/A	N/A	1.54	0.55	1.37	0.81	2.32	0.33
Lower Transpiration 3	N/A	N/A	N/A	2.06	1.02	2.14	0.86	1.50	0.73
Lower Transpiration 4	N/A	N/A	N/A	1.56	0.52	1.21	1.01	1.60	0.18
Lower Transpiration 5	N/A	N/A	N/A	2.06	0.98	1.05	1.30	1.94	0.47
Lower Transpiration 6	N/A	N/A	N/A	2.12	2.48	1.05	0.82	2.05	0.67
Lower Transpiration 7	N/A	N/A	N/A	1.28	1.20	1.13	2.05	2.87	0.59
Lower Transpiration 8	N/A	N/A	N/A	1.70	1.63	1.32	0.92	1.44	0.75
Avg Lower Trans (mmol H2O m2/s)	**N/A**	**N/A**	**N/A**	**1.75**	**1.23**	**1.28**	**1.13**	**2.01**	**0.57**
Lower Trans (mmol H2O plant/s)	**N/A**	**N/A**	**N/A**	**0.06**	**0.05**	**0.05**	**0.05**	**0.07**	**0.01**
Leaf Area Upper (m2)	0.02051	0.04805	0.08548	0.08396	0.09005	0.09058	0.08840	0.07825	0.05029
Leaf Area Lower (m2)	N/A	N/A	N/A	0.03184	0.04049	0.04227	0.04394	0.03395	0.01221
Total Leave Area per Plant	**0.02051**	**0.04805**	**0.08548**	**0.11580**	**0.13054**	**0.13285**	**0.13234**	**0.11220**	**0.06250**
Leaf Area Index (LAI)	0.16218	0.37995	0.67592	0.91567	1.03223	1.05049	1.04646	0.88721	0.49421
Cosine of Zenth Solar Angle (u)	0.93270	0.93260	0.91760	0.92140	0.89960	0.88750	0.83910	0.79660	0.73570
G(u) at 67.5° Leaf Angle	0.32356	0.32356	0.32356	0.32356	0.32356	0.32356	0.32356	0.32356	0.32356
Kb	0.34691	0.34695	0.35262	0.35117	0.35968	0.36458	0.38561	0.40618	0.43980
Sunlit Leaf Fraction	0.95	0.88	0.79	0.73	0.69	0.68	0.67	0.70	0.80
Shaded Leaf Fraction	0.05	0.12	0.21	0.27	0.31	0.32	0.33	0.30	0.20
Total Plant Photo (umol CO2 plant/s)	0.067	0.320	0.560	11.087	4.270	3.701	3.148	3.007	0.850
Total Plant Cond (mol H2O plant/s)	0.010	0.042	0.036	0.278	0.030	0.024	0.024	0.023	0.005
Total Plant Trans (mmol H2O plant/s)	0.067	0.320	0.560	0.229	0.631	0.481	0.414	0.470	0.105
Population/Acre	32000	32000	32000	32000	32000	32000	32000	32000	32000.00
Total Photo/Acre (umol CO2 acre/s)	2151	10252	17910	354799	136632	118444	100723	96208	27195.88
Total Cond/Acre (mol H2O acre/s)	312.65	1357.51	1156.37	8902.00	974.04	768.29	753.07	745.96	162.41
Total Trans/Acre (mmol H2O acre/s)	2151	10252	17910	7334	20180	15389	13245	15037	3357.29
Total Trans (mL/acre/s)	**38.75**	**184.69**	**322.64**	**132.13**	**363.54**	**277.23**	**238.61**	**270.89**	**60.48**
Total Trans (mL/acre/min)	2325	11081	19359	7928	21813	16634	14317	16253	3628.90
Total Trans (mL/acre/hour)	139507	664880	1161520	475668	1308759	998016	859012	975201	217733.74
Total Trans (mL/m2/hour)	34.47	164.30	287.02	117.54	323.40	246.61	212.27	240.98	53.80

Total Cond (mL/acre/s)	5632	24456	20832	160370	17547	13841	13567	13438	2925.79
Total Cond (mL/acre/min)	337948	1467331	1249924	9622172	1052842	830440	813995	806306	175547.54
Total Cond (mL/acre/hour)	20276891	88039863	74995443	5.77E+08	63170518	49826407	48839719	48378368	10532852.26
Total Cond (mL/m2/hour)	5011	21755	18532	142661	15610	12312	12069	11955	2602.72
CO2 (mol/acre/s)	0.00215	0.01025	0.01791	0.35480	0.13663	0.11844	0.10072	0.09621	0.02719588
Air Temp in K	299.26	294.26	299.26	292.04	299.26	295.93	295.37	299.82	288.15
CO2 (L/acre/s)	0.05467	0.25422	0.45335	8.74652	3.44630	2.96419	2.51265	2.44982	0.6604331
Pressure (atm)	0.97	0.97	0.97	0.97	0.97	0.97	0.97	0.97	0.97

Soybean Field 1

Date	6/20/17	6/26/17	7/3/17	7/13/17	7/29/17	8/4/17	8/22/17	9/3/17	9/17/17
Time	12:49pm	1:14pm	1:11pm	12:30pm	1:22pm	12:55pm	1:10pm	12:46pm	12:53pm
Growth Stage	V3	V7	V8	V10/R1	R2	R3	R4	R5	R6
Ambient Conditions									
Ambient Temp (F)	73.00	70.00	79.00	66.00	79.00	73.00	72.00	80.00	59.00
Ambient Temp (C)	22.78	21.11	26.11	18.89	26.11	22.78	22.22	26.67	15.00
Dew Point Temp (F)	41.00	39.00	52.00	55.00	54.00	48.00	48.00	63.00	43.00
Dew Point Temp (C)	5.00	3.89	11.11	12.78	12.22	8.89	8.89	17.22	6.11
Relative Humidity (%)	31.00	33.00	39.00	68.00	42.00	41.00	43.00	54.00	57.00
Atm Pressure (kPa)	97.86	98.67	98.30	98.50	98.65	98.32	98.45	97.90	98.66
Percent Sky Cover (%)	0.00	20.00	5.00	100.00	0.00	15.00	0.00	0 hazy	0.00
Wind Speed (mph)	14.00	7.00	9.00	10.00	14.00	9.00	14.00	12.00	12.00
Wind Direction	N	N	E	NNW	SSE	N	NW	SSW	WNW
Vapor Pressure									
es air (kPa)	2.77	2.50	3.38	2.18	3.38	2.77	2.68	3.50	1.71
ea air (kPa)	0.87	0.81	1.32	1.48	1.42	1.14	1.14	1.96	0.94
Calculated Atmospheric VPD (kPa)	**1.90**	**1.70**	**2.06**	**0.71**	**1.96**	**1.63**	**1.54**	**1.53**	**0.76**
Measured Values									
Soil Moisture 1 (m3/m3)	X	0.188	0.247	0.291	0.229	0.179	0.286	0.287	0.147
Soil Moisture 2 (m3/m3)	X	0.243	0.204	0.216	0.244	0.169	0.272	0.279	0.185
Soil Moisture 3 (m3/m3)	X	0.206	0.230	0.210	0.282	0.154	0.307	0.275	0.147
Average Soil Moisture (m3/m3)	**X**	**0.212**	**0.227**	**0.239**	**0.252**	**0.167**	**0.288**	**0.280**	**0.160**
IRGA Readings									
Upper Photo 1	10.70	10.10	17.20	15.30	19.20	21.60	24.50	26.80	7.55
Upper Photo 2	10.40	13.00	20.50	13.80	24.10	18.90	26.30	22.50	6.13
Upper Photo 3	8.79	13.90	17.90	17.10	16.80	13.30	29.60	26.70	6.54
Upper Photo 4	8.02	10.20	19.20	14.60	25.90	17.20	29.70	21.90	8.66
Upper Photo 5	15.70	12.60	17.00	14.50	17.40	19.70	26.90	22.70	10.40
Upper Photo 6	11.70	10.80	17.90	11.10	16.60	20.10	24.50	23.10	9.84
Upper Photo 7	10.50	12.00	15.20	12.20	17.60	22.70	24.80	21.20	9.39
Upper Photo 8	9.22	15.20	19.90	15.00	15.80	17.20	28.00	20.00	9.67
Avg Upper Photo (umol CO2/m2/s)	**10.63**	**12.23**	**18.10**	**14.20**	**19.18**	**18.84**	**26.79**	**23.11**	**8.52**
Upper Plant Photo (umol CO2 plant/s)	**0.050**	**0.099**	**0.210**	**0.241**	**0.299**	**0.288**	**0.384**	**0.326**	**0.110**
Upper Cond 1	0.570	0.701	0.324	0.648	0.274	0.240	0.490	0.666	0.154
Upper Cond 2	0.499	0.613	0.432	0.498	0.430	0.191	0.646	0.429	0.053
Upper Cond 3	0.725	0.600	0.390	0.701	0.241	0.131	0.661	0.651	0.043
Upper Cond 4	0.435	0.504	0.380	0.590	0.430	0.317	0.674	0.373	0.082

Upper Cond 5	1.080	0.429	0.367	0.691	0.232	0.228	0.530	0.546	0.120
Upper Cond 6	0.561	0.496	0.401	0.478	0.311	0.229	0.404	0.462	0.093
Upper Cond 7	1.090	0.500	0.359	0.565	0.304	0.304	0.493	0.437	0.067
Upper Cond 8	0.814	0.912	0.393	0.590	0.306	0.169	0.137	0.444	0.092
Avg Upper Cond (mol H2O/m2/s)	**0.722**	**0.594**	**0.381**	**0.595**	**0.316**	**0.226**	**0.504**	**0.501**	**0.088**
Upper Plant Cond (mol H2O plant/s)	**0.003**	**0.005**	**0.004**	**0.010**	**0.005**	**0.003**	**0.007**	**0.007**	**0.001**
Upper Transpiration 1	5.75	6.69	6.71	4.74	5.99	5.19	6.74	8.36	2.48
Upper Transpiration 2	5.72	6.50	7.88	4.41	7.56	4.73	7.74	7.06	1.15
Upper Transpiration 3	6.32	7.31	7.49	4.95	5.73	3.64	7.52	7.89	0.88
Upper Transpiration 4	5.19	7.51	7.80	4.70	7.77	4.75	7.61	6.52	1.86
Upper Transpiration 5	7.49	6.48	7.28	4.87	5.64	4.86	6.87	7.73	2.03
Upper Transpiration 6	6.62	6.39	7.61	4.01	6.32	5.03	6.10	7.15	1.83
Upper Transpiration 7	7.01	5.62	7.41	4.27	6.25	6.15	6.58	7.16	1.40
Upper Transpiration 8	6.49	6.88	7.65	4.76	6.30	4.49	6.66	6.97	2.01
Avg Upper Trans (mmol H2O/m2/s)	**6.32**	**6.67**	**7.48**	**4.59**	**6.45**	**4.86**	**6.98**	**7.36**	**1.70**
Upper Plant Trans (mmol H2O plant/s)	**0.030**	**0.054**	**0.087**	**0.078**	**0.101**	**0.074**	**0.100**	**0.104**	**0.022**
Lower Photo 1	N/A	N/A	N/A	N/A	1.72	2.62	3.84	4.27	1.28
Lower Photo 2	N/A	N/A	N/A	N/A	0.89	1.36	2.91	1.60	1.46
Lower Photo 3	N/A	N/A	N/A	N/A	1.41	1.59	3.25	1.82	3.61
Lower Photo 4	N/A	N/A	N/A	N/A	1.50	3.65	3.13	2.63	3.27
Lower Photo 5	N/A	N/A	N/A	N/A	0.00	1.63	3.11	2.99	1.62
Lower Photo 6	N/A	N/A	N/A	N/A	1.69	1.69	2.59	3.02	1.69
Lower Photo 7	N/A	N/A	N/A	N/A	0.00	0.00	2.27	1.97	1.71
Lower Photo 8	N/A	N/A	N/A	N/A	1.79	0.92	1.92	2.72	1.49
Avg Lower Photo (umol CO2/m2/s)	**N/A**	**N/A**	**N/A**	**N/A**	**1.12**	**1.68**	**2.88**	**2.63**	**2.02**
Lower Plant Photo (umol CO2 plant/s)	**N/A**	**N/A**	**N/A**	**N/A**	**0.04**	**0.05**	**0.10**	**0.06**	**0.04**
Lower Cond 1	N/A	N/A	N/A	N/A	0.168	0.052	0.11	0.25	0.08
Lower Cond 2	N/A	N/A	N/A	N/A	0.173	0.091	0.11	0.04	0.02
Lower Cond 3	N/A	N/A	N/A	N/A	0.082	0.046	0.11	0.10	0.08
Lower Cond 4	N/A	N/A	N/A	N/A	0.098	0.055	0.18	0.32	0.12
Lower Cond 5	N/A	N/A	N/A	N/A	0.044	0.060	0.06	0.18	0.03
Lower Cond 6	N/A	N/A	N/A	N/A	0.042	0.098	0.12	0.25	0.03
Lower Cond 7	N/A	N/A	N/A	N/A	0.026	0.036	0.21	0.09	0.01
Lower Cond 8	N/A	N/A	N/A	N/A	0.189	0.044	0.05	0.08	0.02
Avg Lower Cond (mol H2O/m2/s)	**N/A**	**N/A**	**N/A**	**N/A**	**0.103**	**0.060**	**0.119**	**0.164**	**0.388**
Lower Cond (mol H2O plant/s)	**N/A**	**N/A**	**N/A**	**N/A**	**0.003**	**0.002**	**0.004**	**0.004**	**0.008**
Lower Transpiration 1	N/A	N/A	N/A	N/A	3.14	1.11	1.33	2.97	1.40
Lower Transpiration 2	N/A	N/A	N/A	N/A	3.29	1.67	1.27	0.93	0.34

Lower Transpiration 3	N/A	N/A	N/A	N/A	1.85	1.03	1.13	2.04	1.08
Lower Transpiration 4	N/A	N/A	N/A	N/A	1.99	1.00	1.82	1.31	1.43
Lower Transpiration 5	N/A	N/A	N/A	N/A	1.06	1.31	0.80	2.78	0.44
Lower Transpiration 6	N/A	N/A	N/A	N/A	0.97	1.88	1.40	1.26	0.59
Lower Transpiration 7	N/A	N/A	N/A	N/A	0.64	0.79	2.11	1.65	0.17
Lower Transpiration 8	N/A	N/A	N/A	N/A	3.16	0.92	0.79	1.61	0.42
Avg Lower Trans (mmol H2O m2/s)	**N/A**	**N/A**	**N/A**	**N/A**	**2.01**	**1.21**	**1.33**	**1.82**	**0.73**
Lower Trans (mmol H2O plant/s)	**N/A**	**N/A**	**N/A**	**N/A**	**0.06**	**0.04**	**0.05**	**0.04**	**0.02**
Leaf Area Upper (m2)	0.00473	0.00809	0.01159	0.01695	0.01561	0.01529	0.01433	0.01412	0.01296
Leaf Area Lower (m2)	N/A	N/A	N/A	N/A	0.03148	0.03159	0.03537	0.02305	0.02104
Total Leave Area per Plant	**0.00473**	**0.00809**	**0.01159**	**0.01695**	**0.04709**	**0.04688**	**0.04970**	**0.03717**	**0.03400**
Leaf Area Index (LAI)	0.12156	0.20790	0.29785	0.43560	1.21016	1.20477	1.27721	0.95523	0.87376
Cosine of Zenth Solar Angle (u)	0.92780	0.91480	0.91470	0.92190	0.87780	0.86130	0.82260	0.79050	0.72540
G(u) at 67.5° Leaf Angle	0.80085	0.80085	0.80085	0.80085	0.80085	0.80085	0.80085	0.80085	0.80085
Kb	0.86317	0.87543	0.87553	0.86869	0.91233	0.92981	0.97355	1.01309	1.10401
Sunlit Leaf Fraction	0.90	0.83	0.77	0.68	0.33	0.33	0.29	0.38	0.38
Shaded Leaf Fraction	0.10	0.17	0.23	0.32	0.67	0.67	0.71	0.62	0.62
Total Plant Photo (umol CO2 plant/s)	0.050	0.099	0.210	0.241	0.335	0.341	0.486	0.387	0.153
Total Plant Cond (mol H2O plant/s)	0.003	0.005	0.004	0.010	0.008	0.005	0.011	0.011	0.009
Total Plant Trans (mmol H2O plant/s)	0.030	0.054	0.087	0.078	0.164	0.113	0.147	0.146	0.038
Population/Acre	104000	104000	104000	104000	104000	104000	104000	104000	104000
Total Photo/Acre (umol CO2 acre/s)	5228	10286	21817	25032	34814	35488	50513	40244	15898
Total Cond/Acre (mol H2O acre/s)	355.04	500.08	458.94	1049.09	849.72	557.24	1189.47	1129.36	967.56
Total Trans/Acre (mmol H2O acre/s)	3111	5614	9015	8089	17049	11709	15294	15162	3902
Total Trans (mL/acre/s)	**56.04**	**101.14**	**162.40**	**145.72**	**307.13**	**210.94**	**275.53**	**273.14**	**70.30**
Total Trans (mL/acre/min)	3362	6068	9744	8743	18428	12656	16532	16388	4218
Total Trans (mL/acre/hour)	201746	364089	584632	524607	1105677	759370	991905	983299	253067
Total Trans (mL/m2/hour)	49.85	89.97	144.47	129.63	273.22	187.64	245.10	242.98	62.53
Total Cond (mL/acre/s)	6396	9009	8268	18899	15308	10039	21428	20345	17431
Total Cond (mL/acre/min)	383766	540540	496069	1133957	918457	602319	1285701	1220722	1045835

Total Cond (mL/acre/hour)	23025976	32432406	29764148	68037446	55107450	36139168	77142058	73243318	62750107
Total Cond (mL/m2/hour)	5690	8014	7355	16812	13617	8930	19062	18099	15506
CO2 (mol/acre/s)	0.00523	0.01029	0.02182	0.02503	0.03481	0.03549	0.05051	0.04024	0.01590
Air Temp in K	295.93	294.26	299.26	292.04	299.26	295.93	295.37	299.82	288.15
CO2 (L/acre/s)	0.13146	0.25505	0.55226	0.61708	0.87813	0.88812	1.26011	1.02477	0.38606
Pressure (atm)	0.97	0.97	0.97	0.97	0.97	0.97	0.97	0.97	0.97

Soybean Field 2

Date	6/26/17	7/3/17	7/13/17	7/29/17	8/4/17	8/22/17	9/3/17	9/17/17
Time	12:47pm	12:59pm	12:21pm	12:37pm	12:36pm	12:38pm	12:32pm	12:39pm
Growth Stage	V6	V8	V10/R1	R2	R2	R4	R5	R6
Ambient Conditions								
Ambient Temp (F)	70.00	79.00	66.00	79.00	73.00	72.00	80.00	59.00
Ambient Temp (C)	21.11	26.11	18.89	26.11	22.78	22.22	26.67	15.00
Dew Point Temp (F)	39.00	52.00	55.00	54.00	48.00	48.00	63.00	43.00
Dew Point Temp (C)	3.89	11.11	12.78	12.22	8.89	8.89	17.22	6.11
Relative Humidity (%)	33.00	39.00	68.00	42.00	41.00	43.00	54.00	57.00
Atm Pressure (kPa)	98.67	98.30	98.50	98.65	98.32	98.45	97.90	98.66
Percent Sky Cover (%)	20.00	5.00	100.00	0.00	15.00	0.00	0 hazy	0.00
Wind Speed (mph)	7.00	9.00	10.00	14.00	9.00	14.00	12.00	12.00
Wind Direction	N	E	NNW	SSE	N	NW	SSW	WNW
Vapor Pressure (kPa)								
es air (kPa)	2.50	3.38	2.18	3.38	2.77	2.68	3.50	1.71
ea air (kPa)	0.81	1.32	1.48	1.42	1.14	1.14	1.96	0.94
Calculated Atmospheric VPD (kPa)	**1.70**	**2.06**	**0.71**	**1.96**	**1.63**	**1.54**	**1.53**	**0.76**
Measured Values								
Soil Moisture 1 (m3/m3)	0.27	0.282	0.291	0.287	0.188	0.353	0.222	0.128
Soil Moisture 2 (m3/m3)	0.32	0.293	0.316	0.297	0.195	0.333	0.293	0.230
Soil Moisture 3 (m3/m3)	0.31	0.292	0.307	0.324	0.209	0.389	0.274	0.163
Average Soil Moisture (m3/m3)	**0.30**	**0.289**	**0.305**	**0.303**	**0.197**	**0.358**	**0.263**	**0.174**
IRGA Readings								
Upper Photo 1	8.99	14.00	12.20	17.60	15.60	23.70	23.20	7.11
Upper Photo 2	14.50	20.20	9.93	23.10	16.10	22.50	21.40	10.10
Upper Photo 3	11.90	19.50	11.70	25.00	14.80	30.40	20.20	10.40
Upper Photo 4	10.20	15.90	11.00	15.90	12.80	24.20	23.40	9.19
Upper Photo 5	10.10	19.90	10.20	16.40	21.60	31.40	20.70	4.12
Upper Photo 6	8.52	14.60	10.90	18.50	11.20	24.00	24.60	9.39
Upper Photo 7	7.76	15.70	13.60	15.40	18.40	25.30	17.60	7.67
Upper Photo 8	7.00	17.10	9.77	22.30	15.50	25.90	23.60	8.55
Avg Upper Photo (umol CO2/m2/s)	**9.87**	**17.11**	**11.16**	**19.28**	**15.75**	**25.93**	**21.84**	**8.32**
Upper Plant Photo (umol CO2 plant/s)	**0.051**	**0.174**	**0.165**	**0.214**	**0.173**	**0.262**	**0.212**	**0.075**
Upper Cond 1	0.429	0.314	0.564	0.487	0.180	0.643	0.591	0.128
Upper Cond 2	0.620	0.460	0.573	0.433	0.184	0.549	0.636	0.138
Upper Cond 3	0.499	0.325	0.599	0.273	0.194	0.648	0.593	0.140

Upper Cond 4	0.388	0.266	0.553	0.316	0.137	0.489	0.521	0.135
Upper Cond 5	0.554	0.343	0.532	0.251	0.328	0.456	0.694	0.078
Upper Cond 6	0.697	0.312	0.481	0.248	0.116	0.444	0.570	0.158
Upper Cond 7	0.377	0.280	0.530	0.405	0.178	0.514	0.571	0.127
Upper Cond 8	0.235	0.363	0.376	0.391	0.180	0.631	0.582	0.109
Avg Upper Cond (mol H2O/m2/s)	**0.475**	**0.333**	**0.526**	**0.351**	**0.187**	**0.547**	**0.595**	**0.127**
Upper Plant Cond (mol H2O plant/s)	**0.002**	**0.003**	**0.008**	**0.004**	**0.002**	**0.006**	**0.006**	**0.001**
Upper Transpiration 1	5.05	5.83	4.67	6.35	4.38	6.69	8.14	2.41
Upper Transpiration 2	6.59	7.33	4.42	8.19	4.05	6.13	7.63	2.54
Upper Transpiration 3	5.82	6.01	4.65	8.25	3.97	6.92	7.37	2.61
Upper Transpiration 4	4.87	5.50	4.72	6.13	3.40	6.74	7.65	2.51
Upper Transpiration 5	6.79	6.55	4.59	6.38	5.70	7.43	8.06	1.72
Upper Transpiration 6	6.24	5.83	4.26	6.49	2.80	5.21	8.28	2.77
Upper Transpiration 7	5.11	5.71	4.51	6.27	4.27	5.44	7.87	2.29
Upper Transpiration 8	4.25	6.99	3.76	8.29	3.92	5.82	7.99	2.12
Avg Upper Trans (mmol H2O/m2/s)	**5.59**	**6.22**	**4.45**	**7.04**	**4.06**	**6.30**	**7.87**	**2.37**
Upper Plant Trans (mmol H2O plant/s)	**0.029**	**0.063**	**0.066**	**0.078**	**0.045**	**0.064**	**0.076**	**0.021**
Lower Photo 1	N/A	N/A	N/A	0.67	0.15	0.00	2.79	0.31
Lower Photo 2	N/A	N/A	N/A	2.03	0.55	2.87	2.54	0.00
Lower Photo 3	N/A	N/A	N/A	1.78	1.07	2.72	0.84	0.70
Lower Photo 4	N/A	N/A	N/A	1.39	1.12	0.19	3.26	0.69
Lower Photo 5	N/A	N/A	N/A	2.21	1.41	0.84	1.93	0.37
Lower Photo 6	N/A	N/A	N/A	2.14	1.44	1.29	2.61	0.00
Lower Photo 7	N/A	N/A	N/A	1.89	1.12	0.13	0.99	0.17
Lower Photo 8	N/A	N/A	N/A	1.32	0.94	0.60	0.66	0.00
Avg Lower Photo (umol CO2/m2/s)	**N/A**	**N/A**	**N/A**	**1.68**	**0.98**	**1.08**	**1.95**	**0.28**
Lower Plant Photo (umol CO2 plant/s)	**N/A**	**N/A**	**N/A**	**0.03**	**0.02**	**0.03**	**0.04**	**0.00**
Lower Cond 1	N/A	N/A	N/A	0.12	0.027	0.212	0.30	0.05
Lower Cond 2	N/A	N/A	N/A	0.06	0.108	0.099	0.24	0.04
Lower Cond 3	N/A	N/A	N/A	0.06	0.036	0.101	0.16	0.01
Lower Cond 4	N/A	N/A	N/A	0.06	0.042	0.150	0.31	0.02
Lower Cond 5	N/A	N/A	N/A	0.10	0.099	0.168	0.13	0.05
Lower Cond 6	N/A	N/A	N/A	0.03	0.029	0.077	0.15	0.03
Lower Cond 7	N/A	N/A	N/A	0.05	0.024	0.076	0.24	0.05
Lower Cond 8	N/A	N/A	N/A	0.05	0.053	0.127	0.14	0.04
Avg Lower Cond (mol H2O/m2/s)	**N/A**	**N/A**	**N/A**	**0.07**	**0.052**	**0.126**	**0.208**	**0.036**
Lower Cond (mol H2O plant/s)	**N/A**	**N/A**	**N/A**	**0.00**	**0.001**	**0.003**	**0.005**	**0.000**
Lower Transpiration 1	N/A	N/A	N/A	0.53	0.55	2.10	1.38	0.80

Lower Transpiration 2	N/A	N/A	N/A	1.61	1.91	1.24	1.99	0.65
Lower Transpiration 3	N/A	N/A	N/A	1.49	0.77	1.21	2.09	0.17
Lower Transpiration 4	N/A	N/A	N/A	1.56	0.85	1.66	1.02	0.38
Lower Transpiration 5	N/A	N/A	N/A	2.53	1.83	1.81	1.77	0.41
Lower Transpiration 6	N/A	N/A	N/A	4.14	0.58	0.97	1.82	0.90
Lower Transpiration 7	N/A	N/A	N/A	1.34	0.49	0.96	0.45	0.74
Lower Transpiration 8	N/A	N/A	N/A	1.44	1.01	1.45	1.98	0.92
Avg Lower Trans (mmol H2O m2/s)	**N/A**	**N/A**	**N/A**	**1.83**	**1.00**	**1.43**	**1.56**	**0.62**
Lower Trans (mmol H2O plant/s)	**N/A**	**N/A**	**N/A**	**0.03**	**0.02**	**0.04**	**0.03**	**0.01**
Leaf Area Upper (m2)	0.00517	0.01015	0.01480	0.01110	0.01098	0.01012	0.00970	0.00902
Leaf Area Lower (m2)	N/A	N/A	N/A	0.01693	0.01990	0.02486	0.02210	0.01308
Total Leave Area per Plant	**0.00517**	**0.01015**	**0.01480**	**0.02803**	**0.03088**	**0.03498**	**0.03180**	**0.02210**
Leaf Area Index (LAI)	0.19163	0.37622	0.54857	1.03895	1.14459	1.29667	1.17869	0.81915
Cosine of Zenth Solar Angle (u)	0.92720	0.92070	0.92210	0.89840	0.88650	0.83710	0.79500	0.73210
G(u) at 67.5° Leaf Angle	0.80085	0.80085	0.80085	0.80085	0.80085	0.80085	0.80085	0.80085
Kb	0.86373	0.86982	0.86850	0.89141	0.90338	0.95669	1.00735	1.09390
Sunlit Leaf Fraction	0.85	0.72	0.62	0.40	0.36	0.29	0.31	0.41
Shaded Leaf Fraction	0.15	0.28	0.38	0.60	0.64	0.71	0.69	0.59
Total Plant Photo (umol CO2 plant/s)	0.029	0.063	0.066	0.242	0.192	0.289	0.255	0.079
Total Plant Cond (mol H2O plant/s)	0.002	0.003	0.008	0.005	0.003	0.009	0.010	0.002
Total Plant Trans (mmol H2O plant/s)	0.029	0.063	0.066	0.109	0.064	0.099	0.111	0.030
Population/Acre	150000	150000	150000	150000	150000	150000	150000	150000
Total Photo/Acre (umol CO2 acre/s)	4335	9468	9873	36363	28852	43373	38245	11802
Total Cond/Acre (mol H2O acre/s)	368.27	506.80	1167.72	753.82	463.76	1300.56	1554.46	242.45
Total Trans/Acre (mmol H2O acre/s)	4335	9468	9873	16377	9672	14875	16636	4429
Total Trans (mL/acre/s)	**78.10**	**170.57**	**177.87**	**295.03**	**174.24**	**267.98**	**299.69**	**79.78**
Total Trans (mL/acre/min)	4686	10234	10672	17702	10455	16079	17982	4787
Total Trans (mL/acre/hour)	281145	614041	640333	1062101	627280	964715	1078900	287226
Total Trans (mL/m2/hour)	69.47	151.73	158.23	262.45	155.00	238.39	266.60	70.97
Total Cond (mL/acre/s)	6634	9130	21036	13580	8355	23430	28004	4368
Total Cond (mL/acre/min)	398058	547802	1262189	814804	501276	1405779	1680212	262062

Total Cond (mL/acre/hour)	23883495	32868149	75731313	48888244	30076564	84346770	1.008E+08	15723702
Total Cond (mL/m2/hour)	5902	8122	18714	12081	7432	20843	24911	3885
CO2 (mol/acre/s)	0.00434	0.00947	0.00987	0.03636	0.02885	0.04337	0.03824	0.01180
Air Temp in K	294.26	299.26	292.04	299.26	295.93	295.37	299.82	288.15
CO2 (L/acre/s)	0.10750	0.23967	0.24340	0.91719	0.72206	1.08199	0.97385	0.28661
Pressure (atm)	0.97	0.97	0.97	0.97	0.97	0.97	0.97	0.97